ECHINOCOCCUS GRANULOSUS: STUDIES ON THE DEVELOPMENT OF THE METACESTODE TEGUMENT

by

MICHAEL THOMAS ROGAN (BSc)

A thesis submitted to the
University of Keele
for the degree of
Doctor of Philosophy
September 1987

Volume Two
part A

CHAPTER ONE

GENERAL INTRODUCTION.

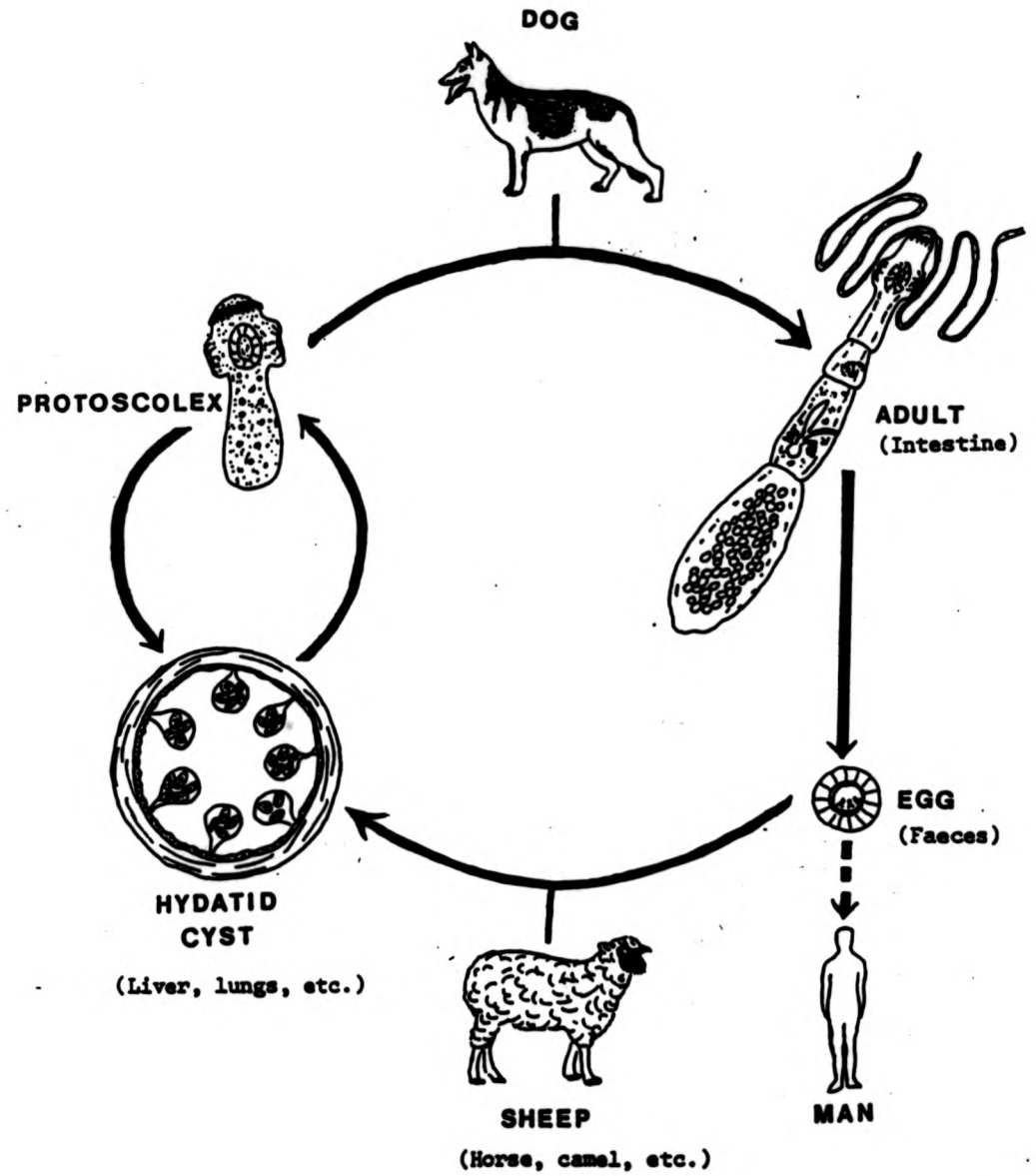

Fig. 1.1 Life cycle of Echinococcus granulosus.

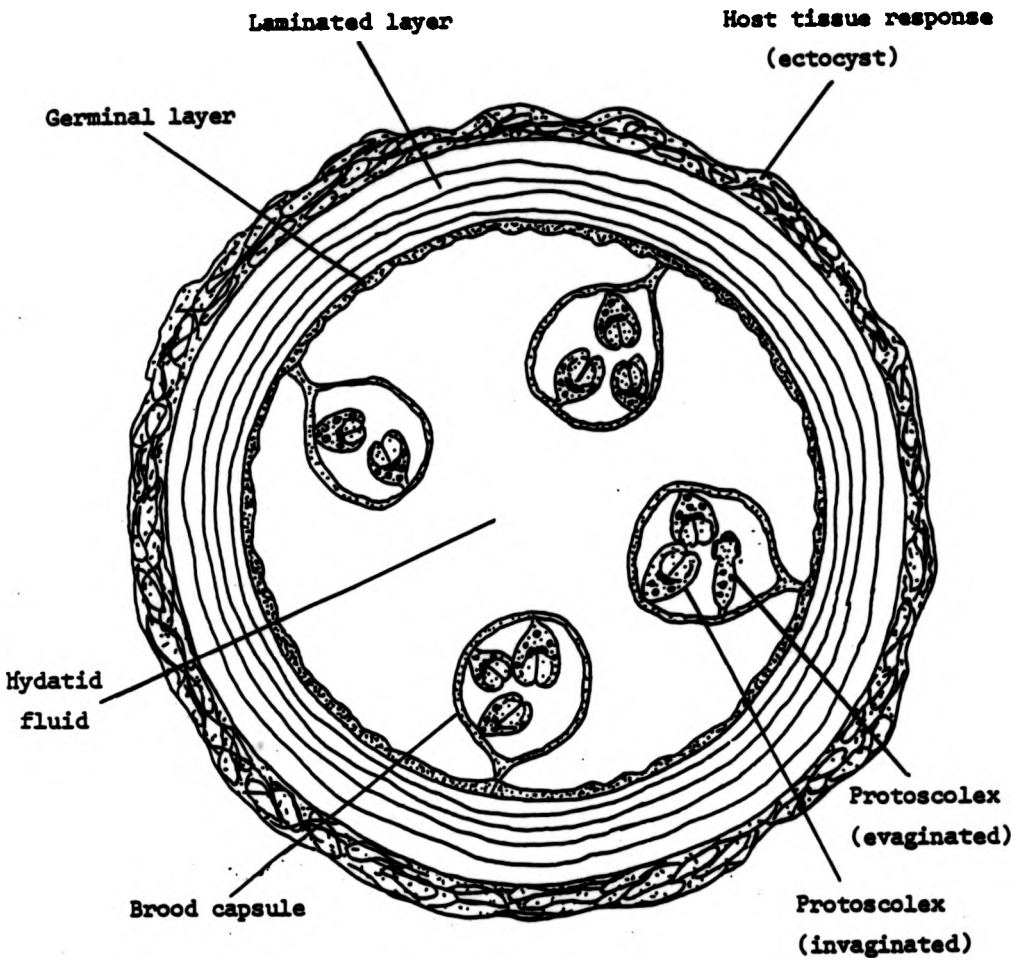

Fig. 1.2 Diagram showing the tissue relationships within a hydatid cyst of Echinococcus granulosus.

CHAPTER TWO

MATERIALS AND METHODS.

Fig. 2.1 A large number of hydatid cysts are present in a horse liver obtained from the abbattoir. (Coin = 10 pence piece).

Fig. 2.2 A horse liver possessing two very large hydatid cysts of approximately 15cm in diameter.

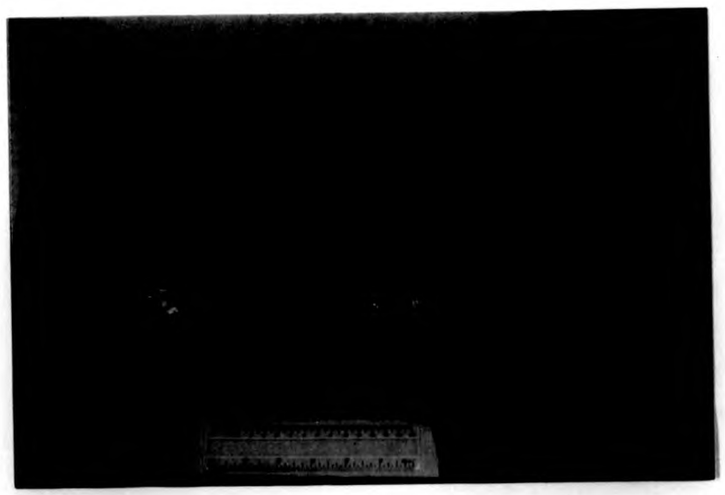

Fig. 2.3 A diffusion chamber after construction and prior to filling M; membrane, R; Plexiglass ring, arrow; position of filling hole.

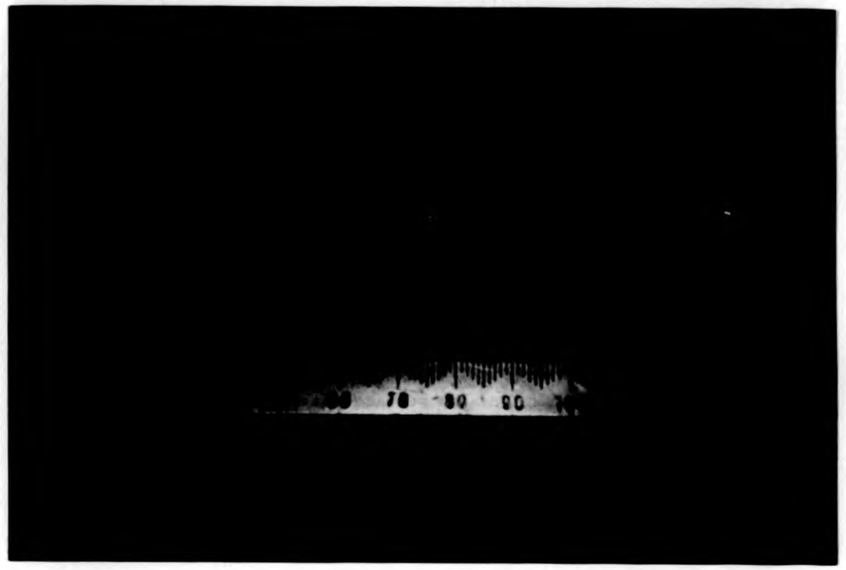

Fig. 2.4 Stage 1 in the implantation of diffusion chambers. The mouse is anaesthetized and its abdomen shaved.

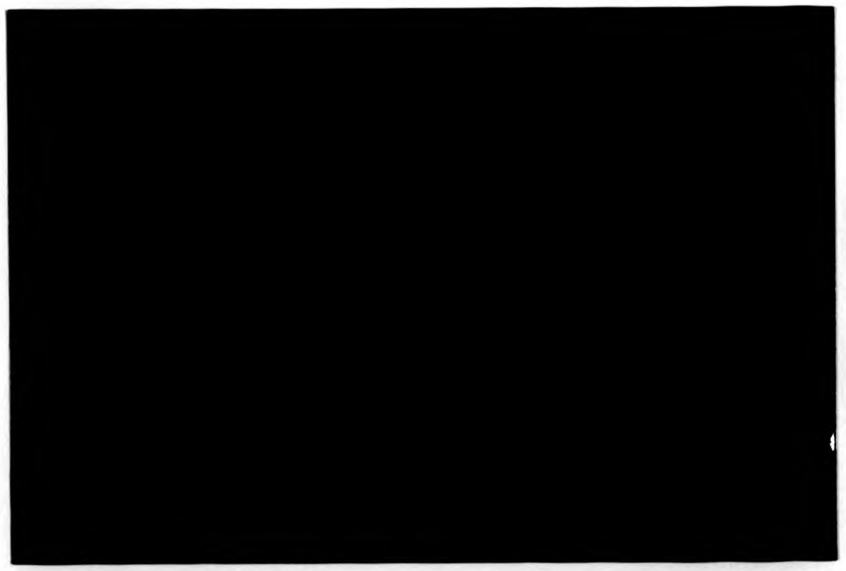

Fig. 2.5 Stage 2 in the implantation of diffusion chambers. A lateral incision is made in the skin and body wall.

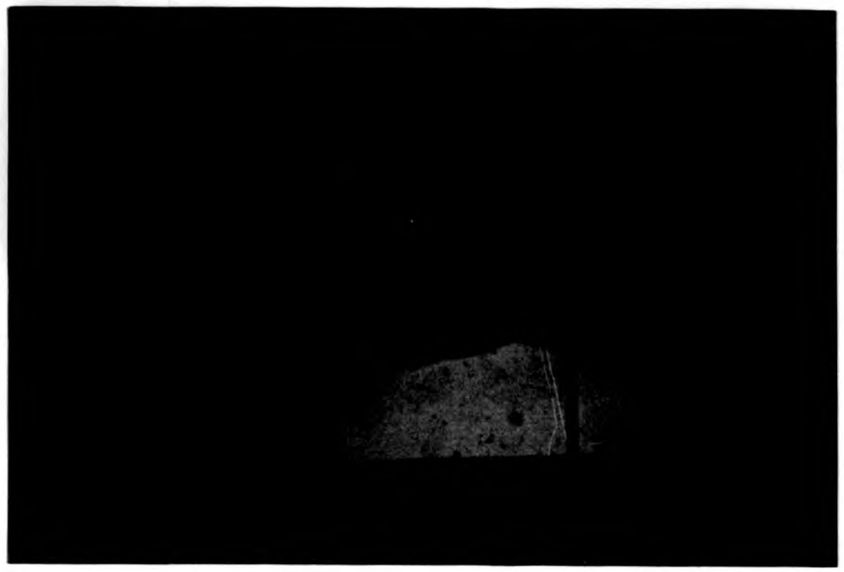

Fig. 2.6 Stage 3 in the implantation of diffusion chambers. The chamber is inserted through the incision into the peritoneal cavity.

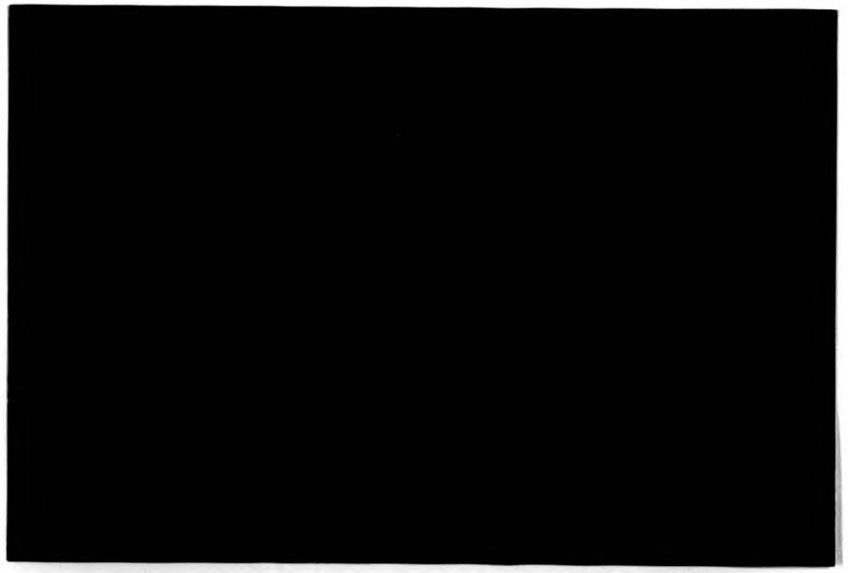

Fig. 2.7 Stage 4 in the implantation of diffusion chambers. The peritoneum is closed with two stitches.

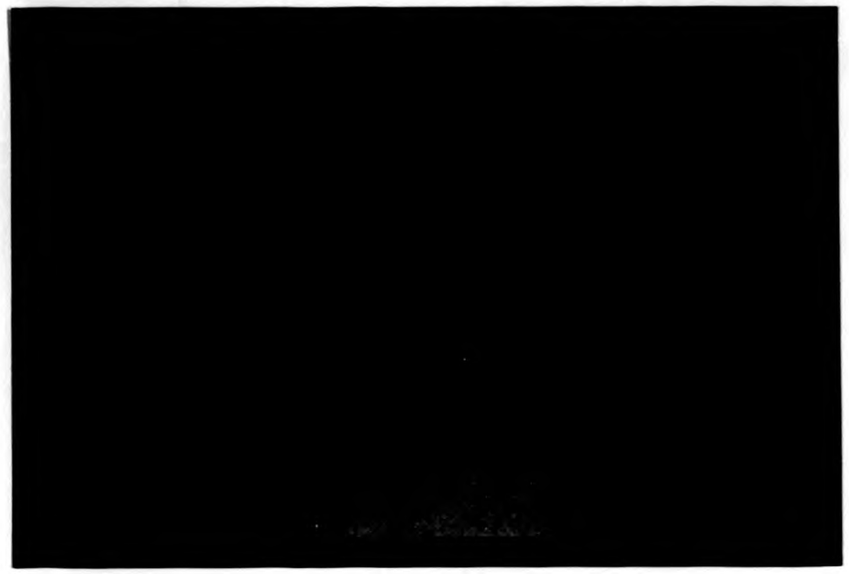

Fig. 2.8 Stage 5 in the implantation of diffusion chambers. The skin is closed with three stitches and sealed with Histoacryl Blue

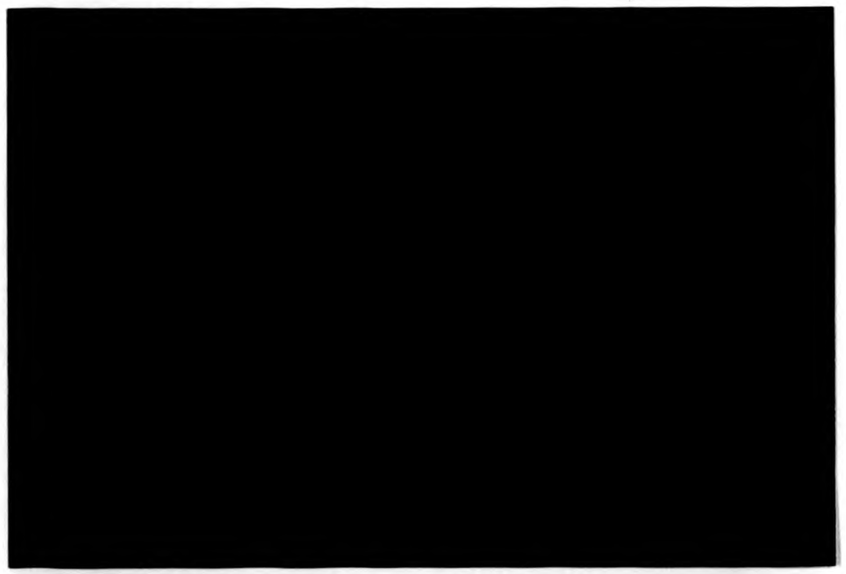

CHAPTER THREE

MORPHOLOGICAL DEVELOPMENT OF HYDATID CYSTS IN VITRO.

Fig. 3.1 LM whole mount of invaginated protoscoleces liberated from equine hydatid cysts. H; hooks, S; suckers, CC; calcareous corpuscles. X195.

Fig. 3.2 LM whole mount of evaginated protoscoleces liberated from equine hydatid cysts. H; hooks, S; suckers, CC; calcareous corpuscles, So; soma. X310.

Fig. 3.3 LM whole mount of early vesiculating protoscoleces after 3 days in culture. Note that the rostellar region (Ro) is still invaginated into the soma. The suckers (Sk) have partially emerged. X310.

Fig. 3.4 LM whole mount of a fully vesicular protoscolex after 30 days in culture. The scolex is still invaginated and a column of supporting tissue (S) runs from anterior to posterior. The calcareous corpuscles (CC) are reduced in number. Sk; suckers. X310.

3.1

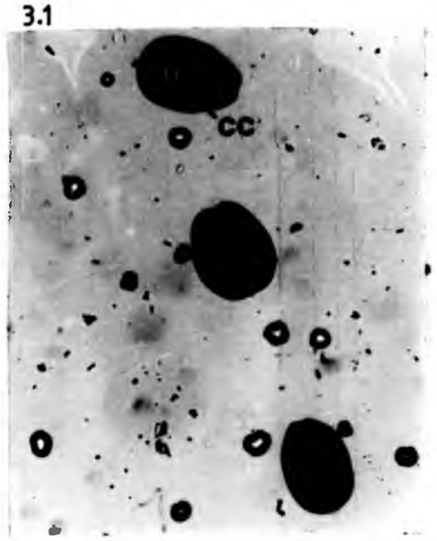

3.2

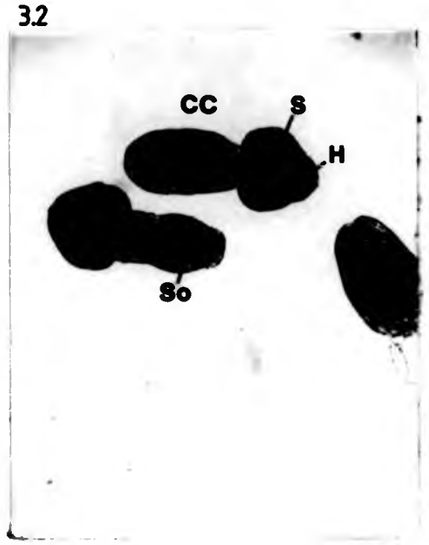

3.3

3.4

Fig. 3.5 LM whole mount of a fully vesicular protoscolex after 30 days in culture. The scolex is still invaginated and strands of supporting tissue (S) radiate from the central region. The calcareous corpuscles (CC) are reduced in number. H; hooks, Sk; suckers. X310.

Fig. 3.6 LM whole mount of an evaginated protoscolex which has shown overall vesiculation of both the scolex and soma. 30 days in culture. H; hooks, Sk; suckers. X310.

Fig. 3.7 LM whole mount of a fully vesicular, evaginated protoscolex after 28 days in culture. The rostellar hooks (H) are present at the apex and the suckers (Sk) are located towards the mid line of the globular structure. X195.

3.5

3.6

3.7

Fig. 3.8 LM whole mount of an evaginated protoscolex showing initial vesiculation of the posterior part of the soma region (So). 30 days in culture. Sc; scolex. X310

Fig. 3.9 LM whole mount of an evaginated protoscolex showing vesiculation of the entire soma region (So) whilst the scolex (Sc) remains unchanged. 30 days in culture. X310.

Fig. 3.10 LM whole mount of an evaginated protoscolex undergoing vesiculation of the scolex after vesiculation of the soma. The swelling process has now spread to the region immediately posterior to the suckers (Sk). 30 days in culture. H; hooks, S; supporting tissue. X310.

Fig. 3.11 LM whole mount of an evaginated protoscolex showing further vesiculation of the scolex up to the level of the rostellum (R). 30 days in culture. Sk; suckers, CC; calcareous corpuscles, S; supporting tissue. X310.

3.8

3.9

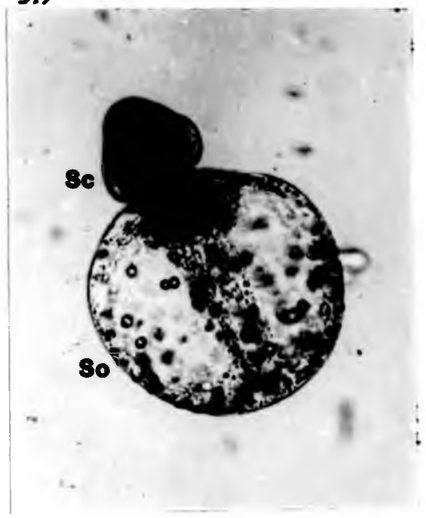

3.10

3.11

Fig. 3.12 LM whole mount of an evaginated protoscolex undergoing vesiculation of the scolex region (Sc) before the soma region (So). 15 days in culture. H; hooks. X310.

Fig. 3.13 LM whole mount of a vesicular protoscolex which has started to produce a laminated layer. The surface of the parasite is sticky and attracts any debris within the culture media. 28 days in culture. X195.

Fig. 3.14 LM whole mount of a developing cyst after the initial formation of the laminated layer (LL). The layer appears as a thin, colourless zone around the parasite. 30 days in culture. X310.

Fig. 3.15 LM whole mount of a developing cyst possessing a thicker laminated layer (LL). The layer is still colourless and lacks laminations. 54 days in culture. X195.

3.12

3.13

3.14

3.15

Fig. 3.16 LM whole mount of a developing cyst after 70 days in culture. The laminated layer (LL) has now taken on a tanned appearance and possesses some laminations (arrow). H; hooks. X195.

3.16

Fig. 3.17 LM whole mount of a developing cyst after 110 days in culture. The laminated layer (LL) appears tanned except in the outermost region which is still colourless (arrows). X275.

3.17

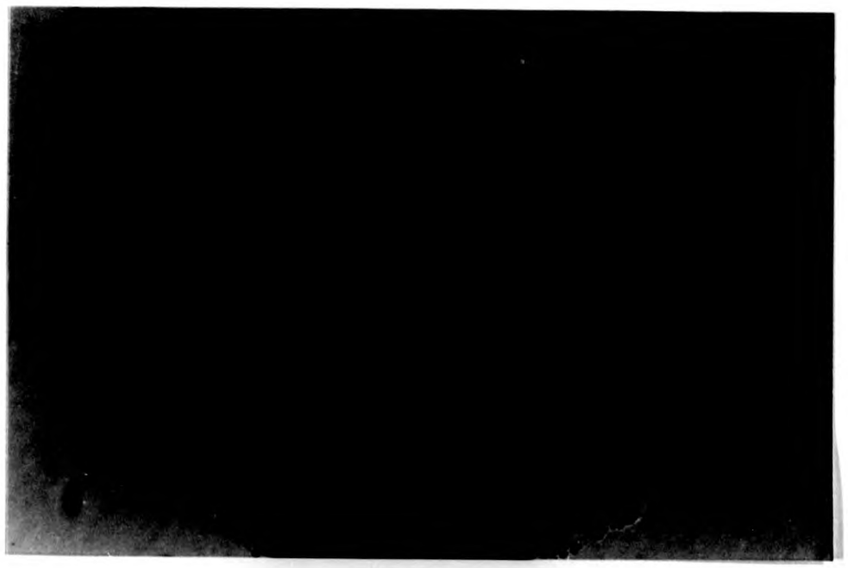

Fig. 3.18 LM whole mount of a developing cyst after 120 days in culture. The laminated layer (LL) is now well developed and possesses approximately 20 laminations. X430.

3.18

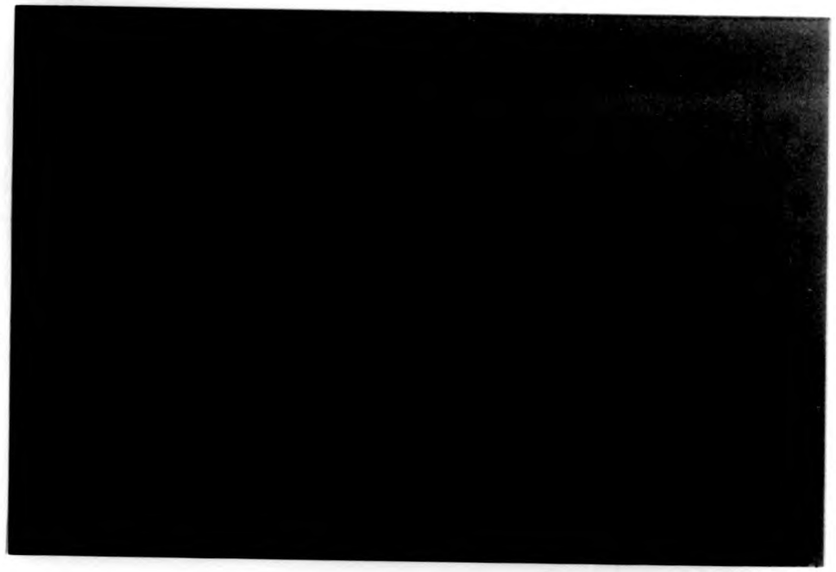

Fig. 3.19 LM whole mount of a developing cyst after 60 days in culture. A well developed laminated layer (LL) is present although the hooks (H) and suckers (Sk) of the scolex are still evident. X195.

Fig. 3.20 LM whole mount of a developing cyst after 96 days in culture. The rostellar region has become elongated into a 'neck' region (N) which contains the hooks at the apex (arrow). LL; laminated layer. X195.

Fig. 3.21 LM whole mount of a developing cyst after 120 days in culture. Small clusters of hooks (H) have become budded off from the 'neck' region (N) into the laminated layer (LL). X310.

Fig. 3.22 LM whole mount of a developing cyst after 110 days in culture. The cytoplasm surrounding the hooks has pulled away (arrow) thus freeing the hooks (H) to fall into the cyst cavity. X195.

3.19

3.20

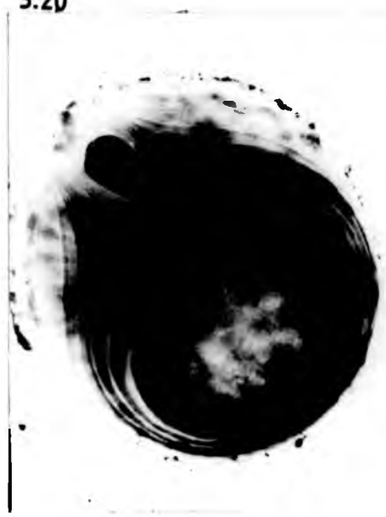

3.21

3.22

Fig. 3.23 LM whole mount of a developing cyst after 25 days in culture. The entire scolex region appears to have been lost and an accumulation of tissue at the distal (arrow) end may represent a healed zone. X310.

3.23

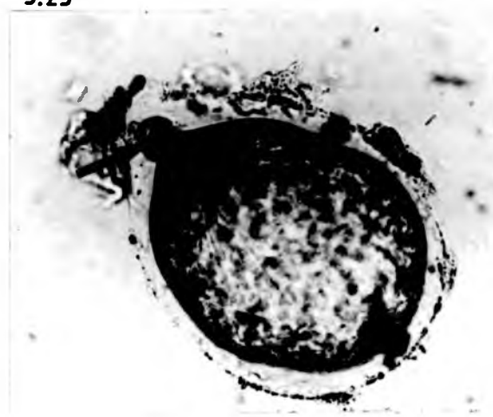

Fig. 3.24 LM whole mount of a developing cyst after 33 days in culture. The cells of the germinal layer appear stellate (arrow) with long processes extending from a central region. X1240.

3.24

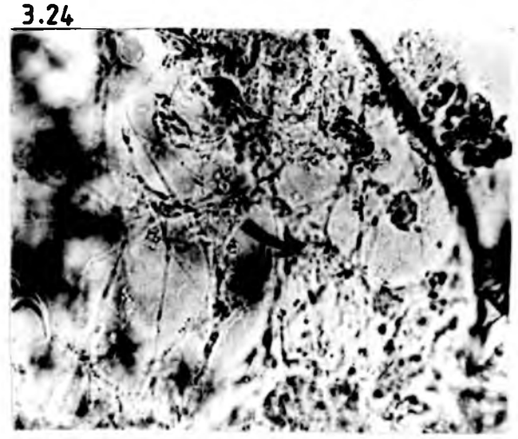

Fig. 3.25 LM whole mount of a number of cysts after 6 months in culture. A well developed laminated layer (LL) is present but the germinal layer appears irregular and very dense. X110.

Fig. 3.26 LM whole mount of a cyst after 6 months in culture. The cells of the germinal layer still appear stellate (arrow) but the radiating processes are shorter and compacted. X430.

3.25

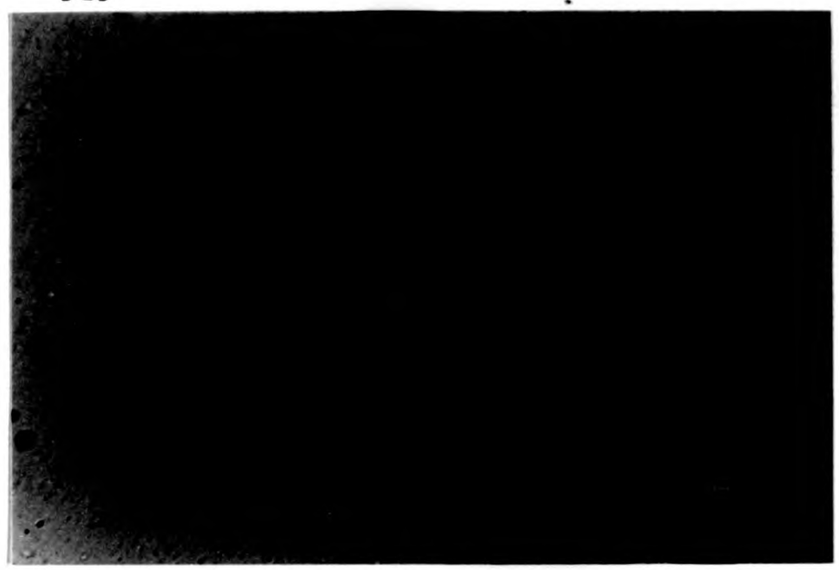

3.26

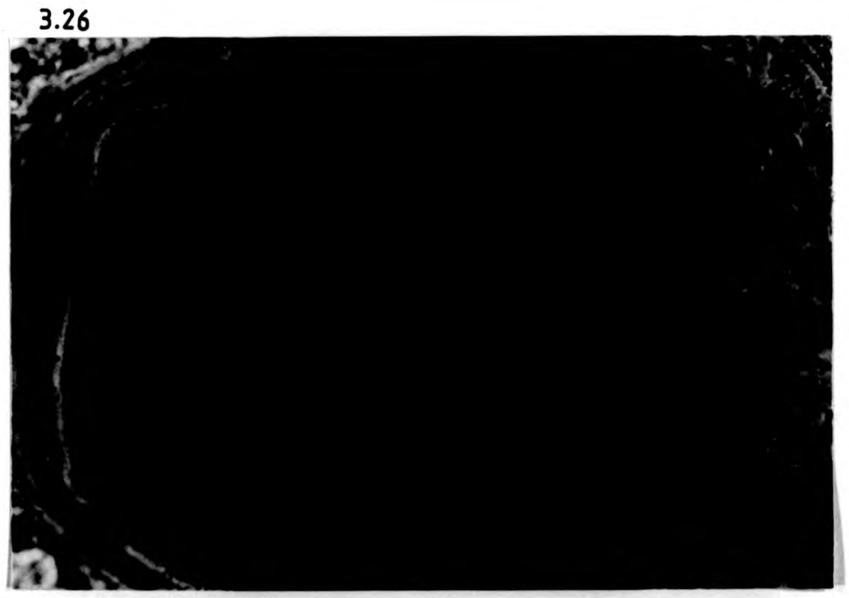

Fig. 3.27 LM whole mount of a dead cyst after 110 days in culture. Note that the germinal layer (GL) is degenerate and has collapsed into the centre of the cyst. X195.

Fig. 3.28 LM whole mount of an invaginated protoscolex with a small posterior bladder (PB) after 2 days in culture. H; hooks. X390.

Fig. 3.29 LM whole mount of a cyst with a posterior swelling (arrow) after 40 days in culture. The swelling appears to have arisen from vesiculation of the soma rather than from a posterior bladder. X365.

Fig. 3.30 LM whole mount of a ruptured brood capsule from an equine hydatid. 3 invaginated protoscoleces are attached to the collapsed brood capsule wall (BC). X310.

3.27

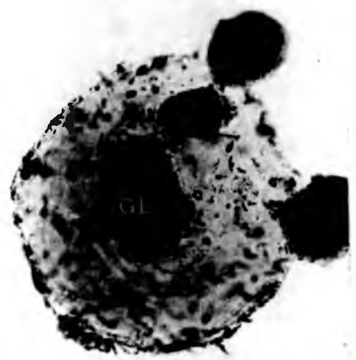

3.28

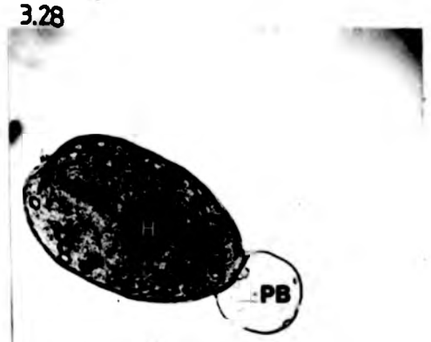

3.29

3.30

Fig. 3.31 LM whole mount of protoscoleces liberated from an equine hydatid. The protoscoleces retain, to varying degrees a proportion of the attachment stalk (St) and in some cases a portion of the brood capsule wall (B) also. X310.

Fig. 3.32 LM whole mount of a protoscolex which is showing initial swelling of the attachment stalk (St). X310.

Fig. 3.33 LM whole mount of a protoscolex where the attachment stalk has swollen to produce a small posterior bladder (PB). X310.

Fig. 3.34 LM whole mount of a number of small free vesicles, devoid of protoscoleces, occurring in the culture medium. X310.

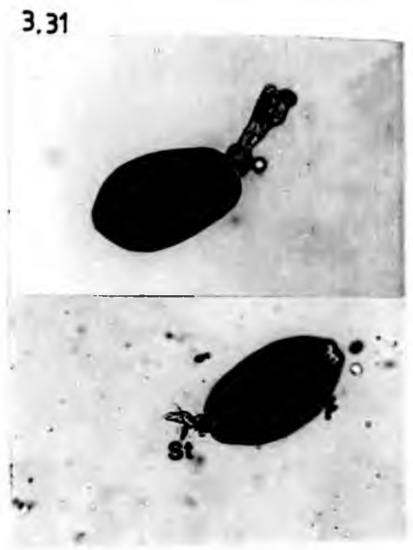

Fig. 3.35 LM whole mount of a detached posterior bladder which has developed a laminated layer (LL) after 21 days in culture. X780.

Fig. 3.36 LM whole mount of a ruptured, everted brood capsule after 9 days in culture. The protoscoleces (P) are now attached to the outside of the vesicular brood capsule wall (BC). X195.

Fig. 3.37 LM whole mount of two protoscoleces (P) attached to a vesicle derived from a portion of brood capsule wall (BC) 15 days in culture. X195.

Fig. 3.38 LM whole mount of a ruptured everted brood capsule (BC) bearing both invaginated protoscoleces (I) and active evaginated protoscoleces (E). 22 days in culture. X195.

3.35

3.36

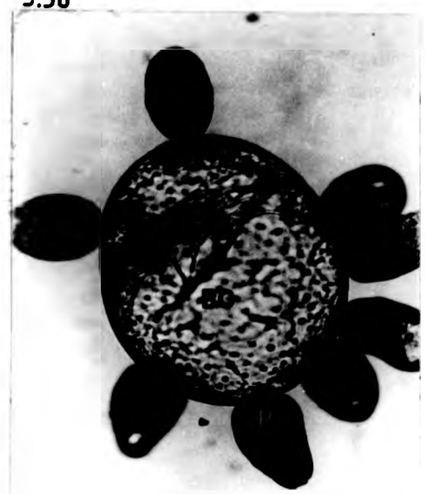

3.37

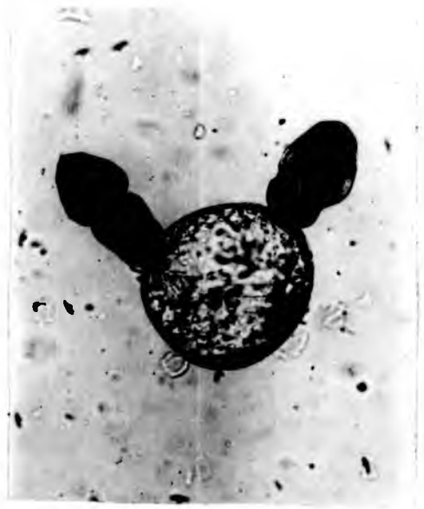

3.38

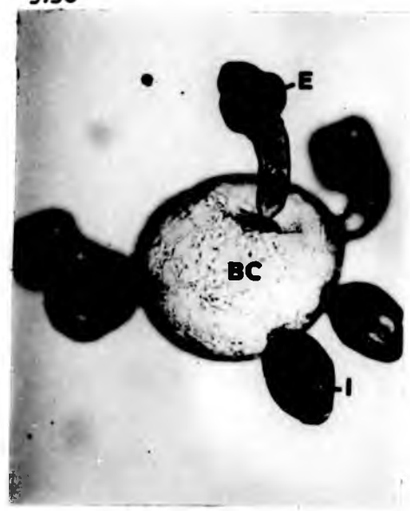

Fig. 3.39 LM whole mount of a small ruptured everted brood capsule (BC) which has developed a laminated layer (arrow) after 110 days in culture. The attached protoscoleces (P) appear degenerated and have lost their integrity. X124.

3.39

Fig. 3.40 LM whole mount of a large ruptured, everted brood capsule (BC) which has developed a laminated layer (LL) after 110 days in culture. The many protoscoleces (P) appear to have become absorbed into the brood capsule tissue and only the scolex region of some protoscoleces is recognisable (arrow). X78

3.40

Fig. 3.41 LM whole mount of a large free vesicle (V) occurring in culture after 28 days. The vesicle is devoid of any protoscoleces and is clearly derived from a ruptured everted brood capsule (BC) similar to that shown. X195.

Fig. 3.42 LM whole mount of a large free vesicle (V) derived from a ruptured brood capsule which has produced a laminated layer (LL). 28 days in culture. X195.

Fig. 3.43 LM whole mount of a single protoscolex (P) attached to a ruptured everted brood capsule (BC) which has produced a laminated layer (LL) 22 days in culture. X195.

3.41

3.42

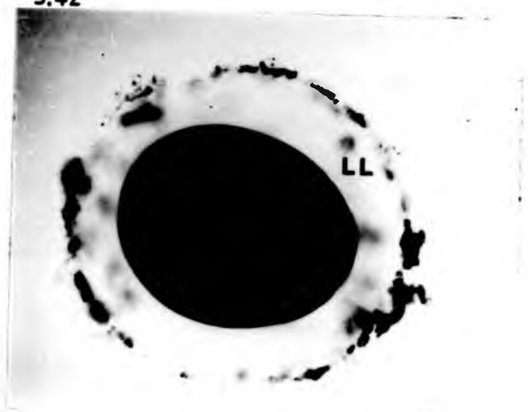

3.43

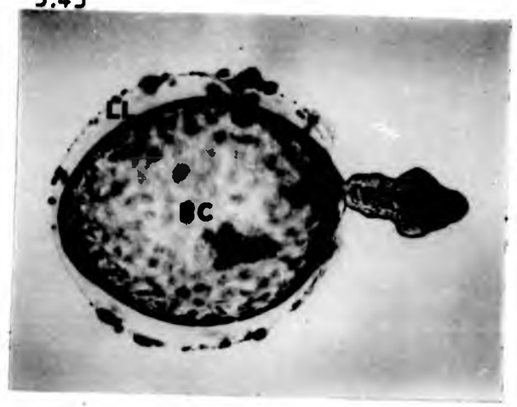

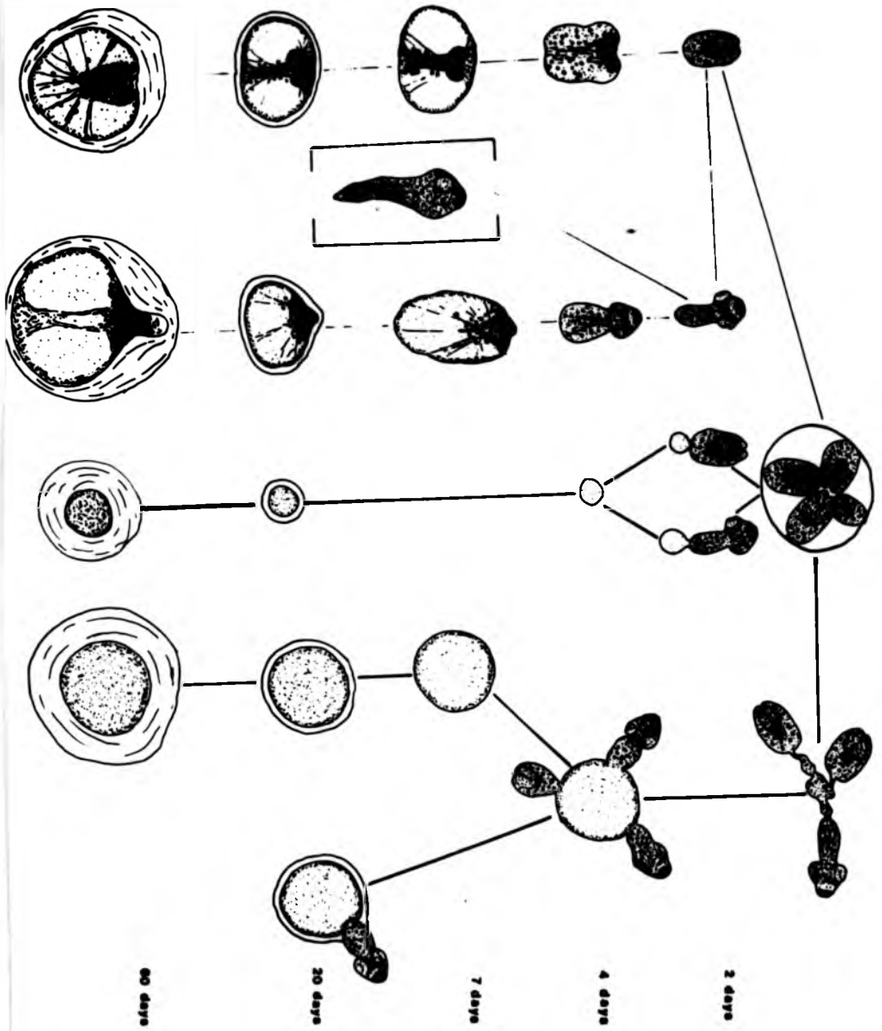

Fig. 3.44 Diagrammatic summary of the pathways involved in cystic development during *in vitro* culture. Partial development of protoscoleces in an adult direction is shown in brackets.

Fig. 3.45 LM whole mount of a protoscolex which has commenced development in an adult direction. The parasite has become elongated and highly active and excretory canals (EC) are now evident. Calcareous corpuscles are much reduced in number. 60 days in culture. X310.

Fig. 3.46 LM whole mount of 4 adult-type individuals which have apparently become fused together. 77 days in culture. X310.

Fig. 3.47 LM whole mount of an adult-type individual which has apparently become vesicular after 60 days in monophasic culture and 17 days in diphasic culture (77 days total). H; hooks, Sk; suckers. X310.

3.45

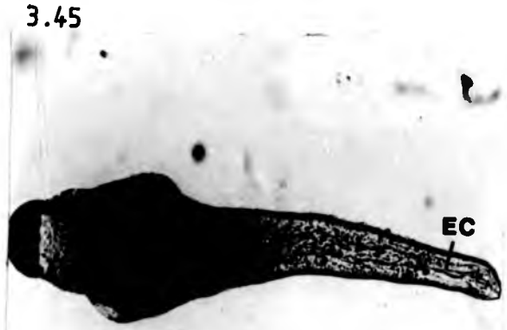

3.46

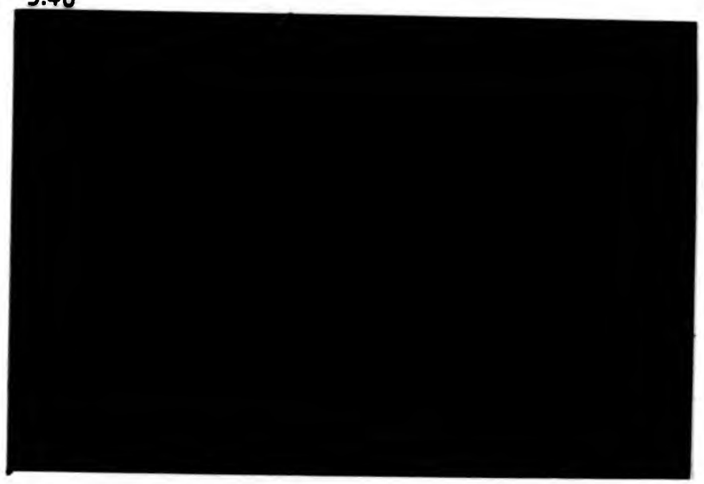

3.47

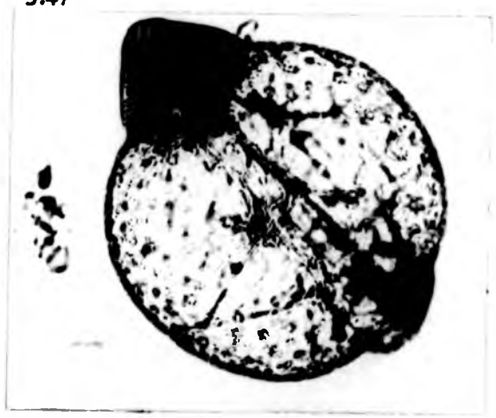

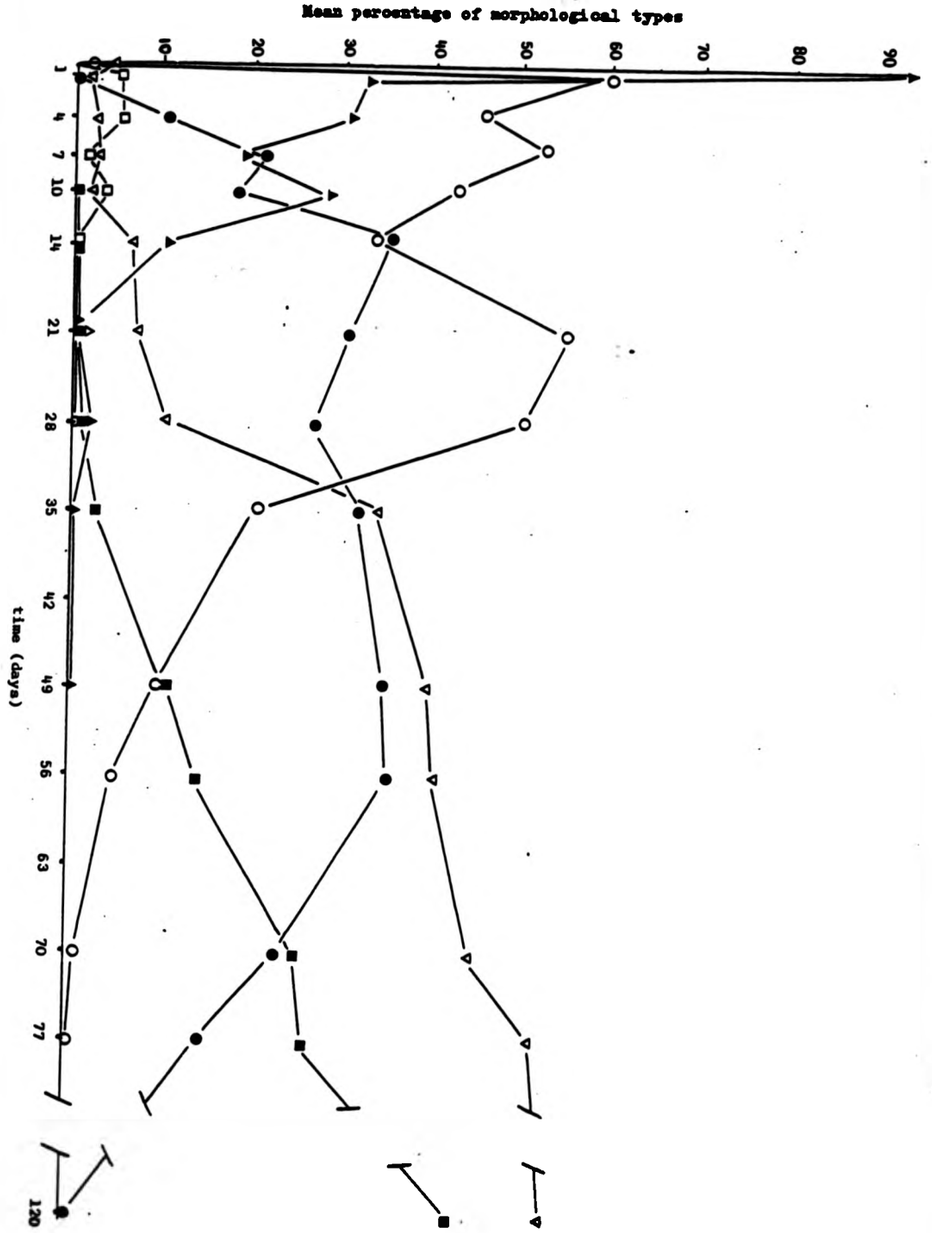

Fig. 3.48 Graphical representation of the mean percentage of morphological types occurring at various times during *in vitro* culture under standard conditions.

Invaginated —▲—

Evaginated —○—

Vesicular —●—

Posterior bladders —□—

Laminated layers —■—

Dead —▽—

Fig. 3.49 Photograph of a primary cyst in a horse liver, containing numerous daughter cysts (D). Note that the primary cyst is degenerate and its laminated layer (LL) has collapsed into the' cyst cavity. Note also that some of the daughter cysts are fertile and contain protoscoleces (arrows).

3.49

Fig. 3.50 LM of a developing cyst cultured in vitro for 60 days, showing binding of WGA to the laminated layer (LL). X 152.

3.50

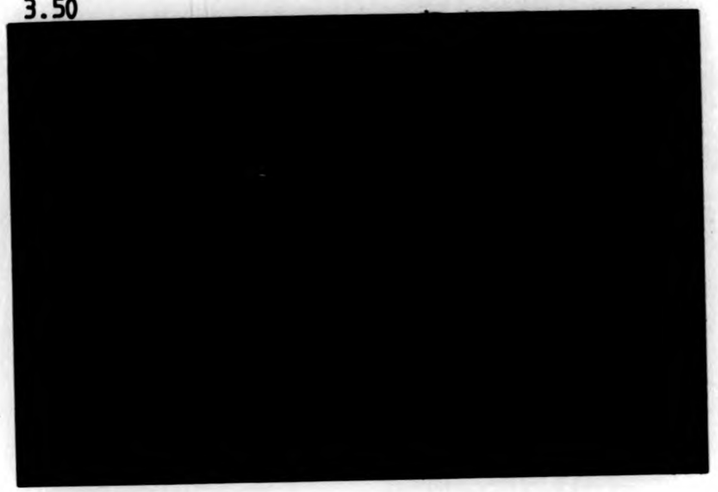

Fig. 3.51. Higher power LM of a 60 day in vitro cyst showing WGA binding to the laminated layer (LL) and a portion of germinal layer (GL) X 760.

3.51

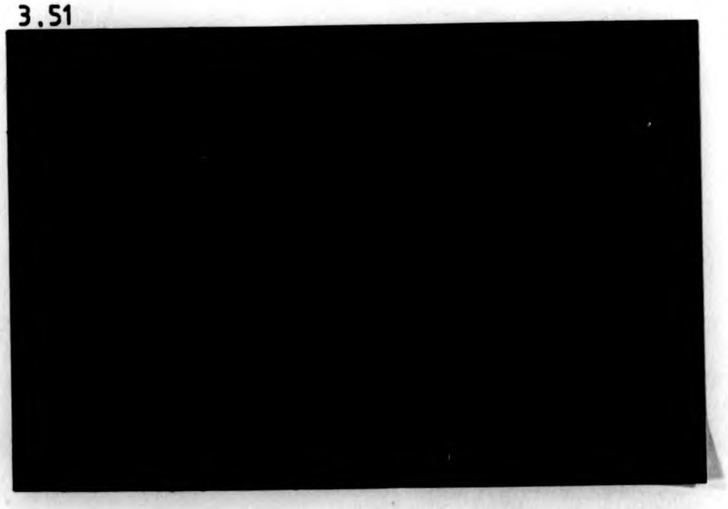

Fig. 3.50 LM of a developing cyst cultured in vitro for 60 days, showing binding of WGA to the laminated layer (LL). X 152.

3.50

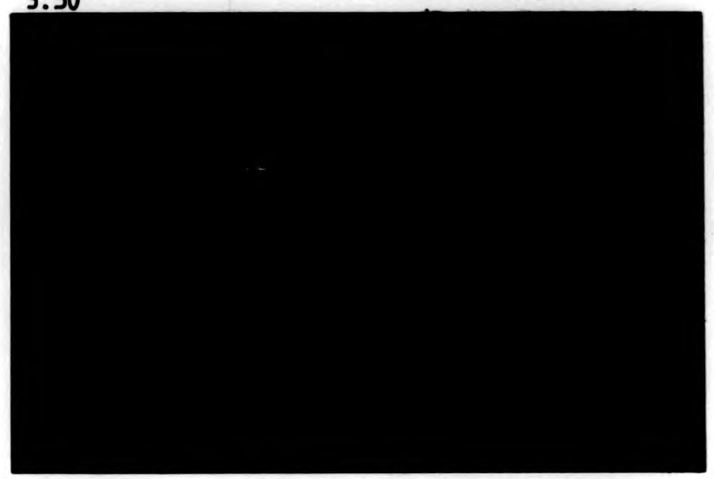

Fig. 3.51. Higher power LM of a 60 day in vitro cyst showing WGA binding to the laminated layer (LL) and a portion of germinal layer (GL). X 760.

3.51

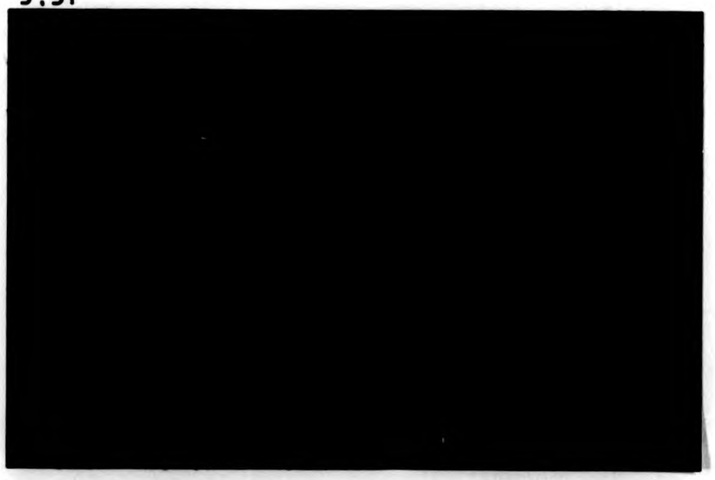

Fig. 3.52. LM of a developing cyst cultured in vitro for 60 days, showing binding of SBA to the laminated layer (LL). X 152.

3.52

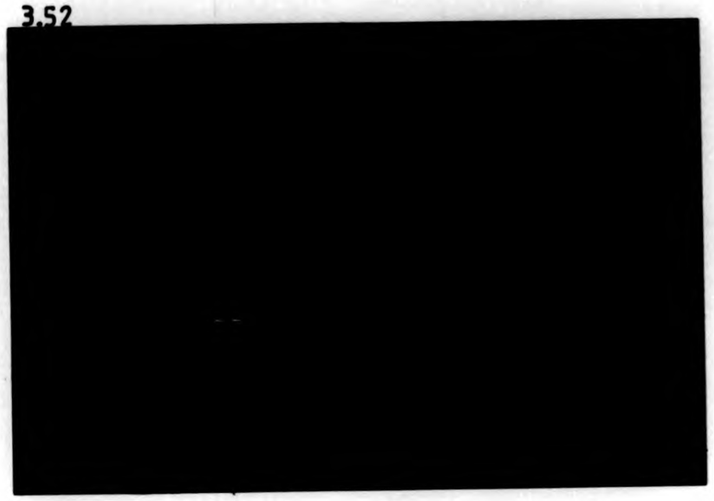

Fig. 3.53. Higher power LM of a 60 day in vitro cyst showing SBA binding to the laminated layer (LL). The germinal layer is not identifiable. X 760.

3.53

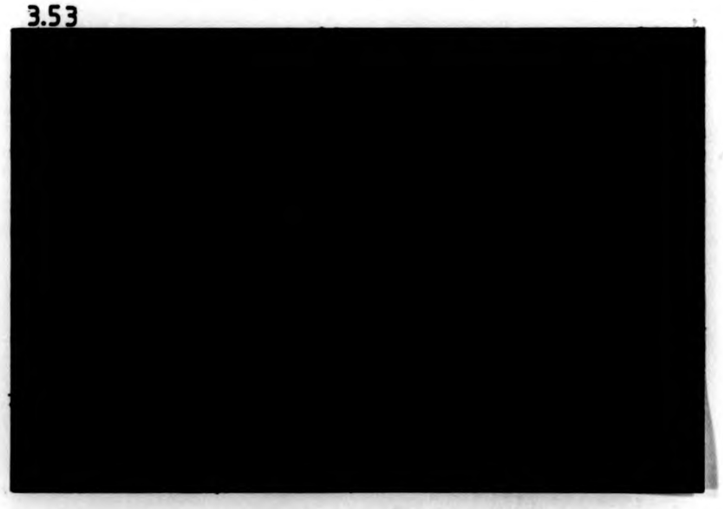

Fig. 3.54. LM of a developing cyst cultured in vitro for 60 days, showing binding of PNA to the laminated layer (LL). X 152.

Fig. 3.55. LM of a developing cyst cultured in vitro for 60 days showing that Con A does not bind to the laminated layer (LL) but does bind slightly to the germinal layer (GL). X 760.

Fig. 3.56. LM of a developing cyst cultured in vitro for 60 days, showing that binding of APA does not occur. X 760.

3.54

3.55

3.56

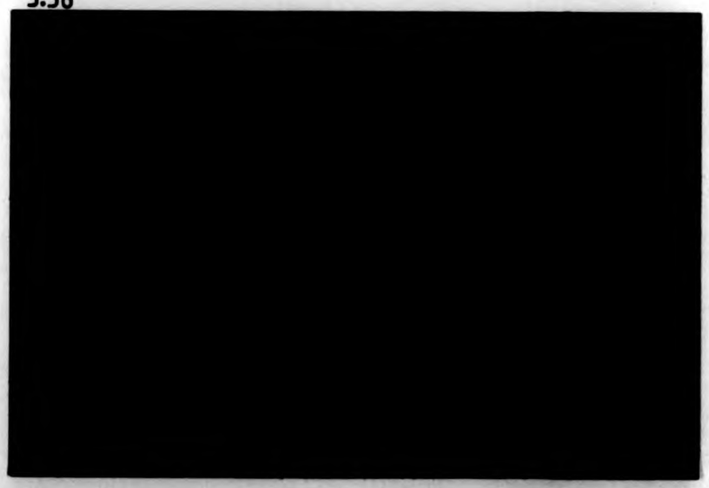

Fig. 3.57 Diagrammatic representation of the initial variation in size of posterior bladders (PB) occuring during *in vitro* culture. The broken lines represent hypothetical break off points. S; stalk, B; ruptured, everted brood capsule wall.

3.57

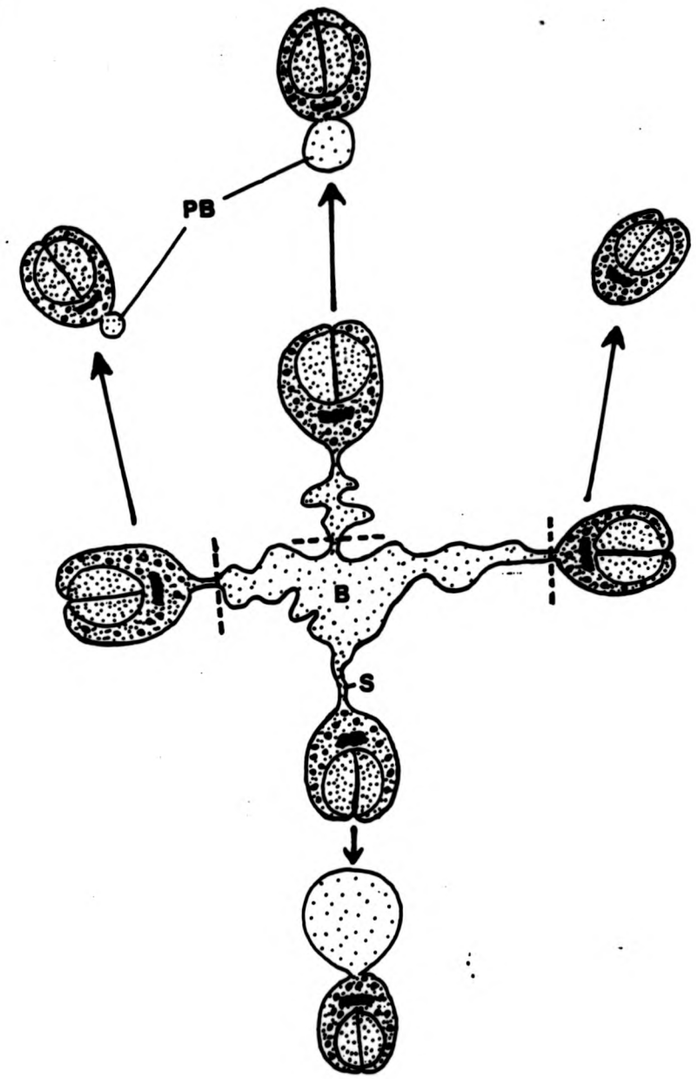

CHAPTER FOUR

MORPHOLOGICAL DEVELOPMENT OF SECONDARY HYDATID CYSTS IN VIVO.

Fig. 4.1 LM section of a clump of protoscoleces (P) encapsulated by host leucocytes, 2 days p.i. H; hooks, Sk; suckers. (Toluidine blue staining). X310.

Fig. 4.2 LM whole mount of an invaginated misshapen protoscolex 14 days p.i. H; hooks, CC; calcareous corpuscles. X310.

Fig. 4.3 LM whole mount of an evaginated misshapen protoscolex, 14 days p.i. H; hooks, CC; calcareous corpuscles. X310.

Fig. 4.4 LM whole mount of a protoscolex starting to undergo vesiculation 14 days p.i. X310.

Fig. 4.5 LM whole mount of a fully vesicular protoscolex which has produced a laminated layer (LL), 30 days p.i. Note that the laminated layer has a clear appearance and that the hooks (H) and suckers (Sk) are still present. X310.

Fig. 4.6 LM whole mount of an invaginated, non-vesicular protoscolex which has produced a laminated layer (LL), 40 days p.i. H; hooks, Sk; sucker, HC; host cells. X310.

Fig. 4.7 LM whole mount of a protoscolex with very irregular outline which has produced a laminted layer (LL), 54 days p.i. H; hooks. X195.

Fig. 4.8 LM whole mount of three irregular shaped cysts possessing a thickened though clear laminated layer (LL). X195.

4.5

4.6

4.7

4.8

Fig. 4.9 LM whole mount of a fully vesicular protoscolex possessing a laminated layer (LL), 30 days p.i. Note that the suckers (Sk) are less well defined and showing signs of degeneration. X310.

Fig. 4.10 LM whole mount of a vesicular protoscolex with a laminated layer (LL) 54 days p.i. Abundant calcareous corpuscles (CC) are present in this parasite though absent from others. X310.

Fig. 4.11 LM whole mount of a developing cyst 40 days p.i. The parasite has undergone posterior vesiculation and the hooks (H) have been condensed into a small bud. LL; laminated layer. X310.

Fig. 4.12 LM whole mount of a developing cyst 42 days p.i. The cyst has now developed a 'neck' region (arrow) at the end of which is the hook bud (B). The laminated layer (LL) has now become thicker and more opaque. X310.

4.9

4.10

4.11

4.12

Fig. 4.13 LM whole mount of developing cysts 132 days p.i. The cysts are still irregular in shape although the laminated layer (LL) has become tanned and possesses laminations. X124.

Fig. 4.14 Photograph illustrating the size differences of cysts occurring *in situ* at 12 months p.i. Some cysts are large (straight arrow) whilst others occurring in cyst masses are comparatively smaller (curved arrow).

4.13

4.14

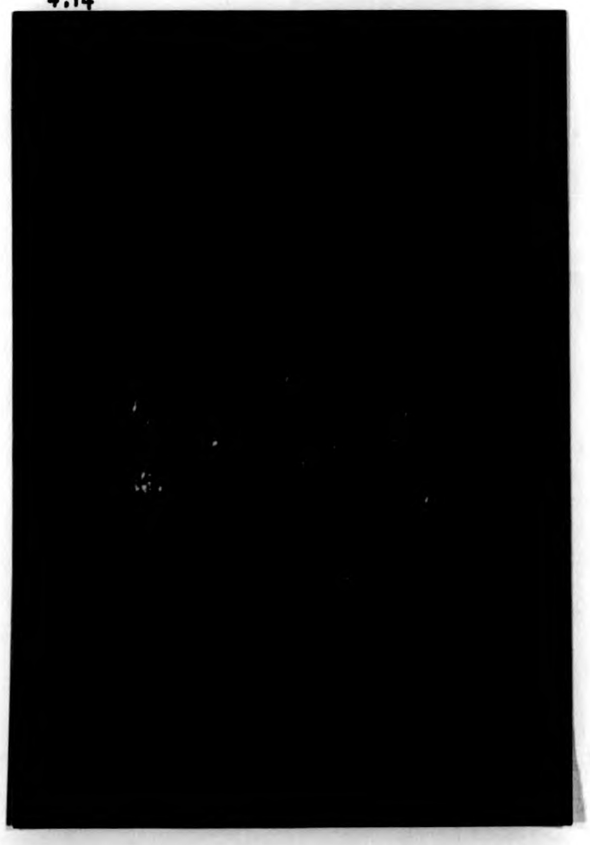

Fig. 4.15 LM whole mount of two cysts 7 months p.i. The cysts differ considerably in size but the thickness of the laminated layer (LL) is greater on the smaller one. X124.

4.15

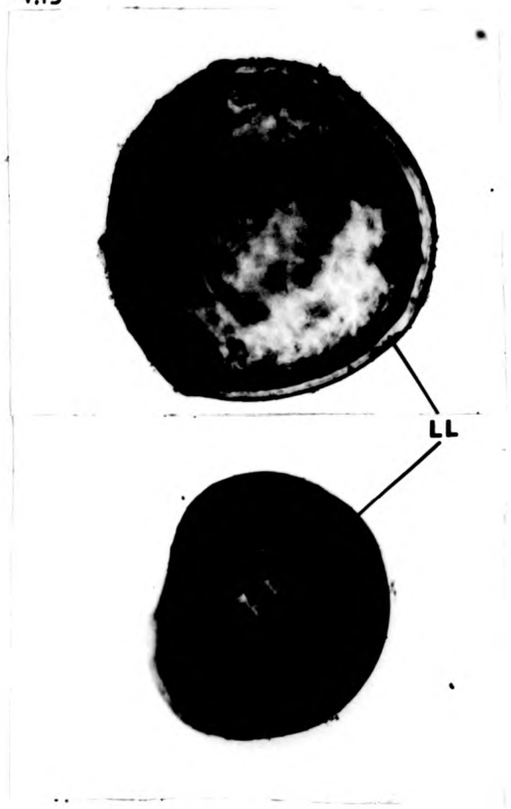

Fig. 4.16 Graph of the mean cyst diameter (with standrad errors) of hydatid cysts retrieved from mice at various times post-infection.

4.16

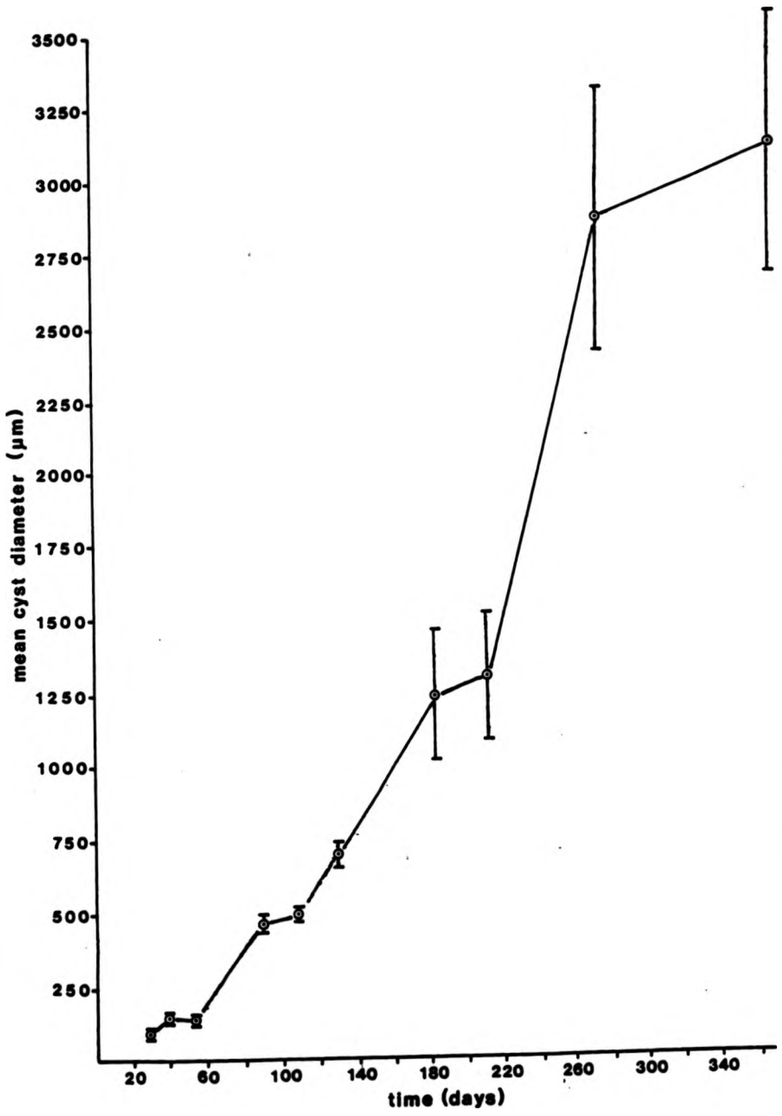

Fig. 4.17 Graph of the mean laminated layer thickness (with standard errors) of cysts retrieved from mice at various times post-infection.

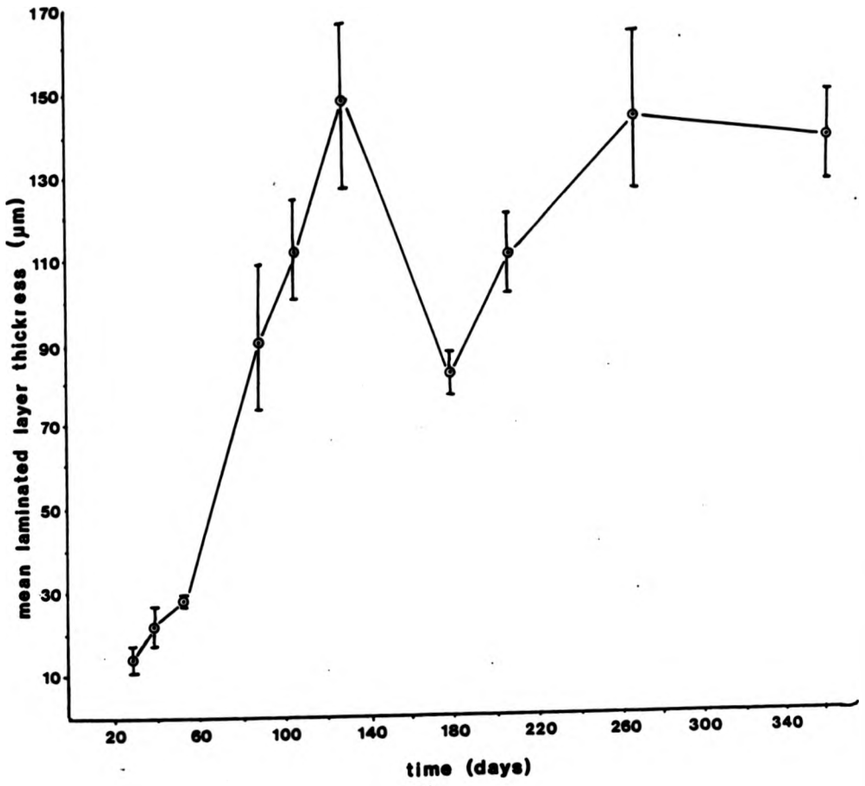

Fig. 4.18 LM whole mount of a protoscolex showing adult-like development recovered from a diffusion chamber 35 days p.i. H; hooks, Sk; suckers. X310.

Fig. 4.19 LM whole mount of developing cyst recovered from a diffusion chamber, 90 days p.i. The cysts possess a laminated layer (LL) which lucent in appearance and generally lacking in laminations. A 'neck' and hook bud (B) are also present. X78.

Fig. 4.20 LM whole mount of a cyst recovered from a diffusion chamber 90 days p.i. The laminated layer (LL) has a 'tanned' appearance and possesses several laminations. X78.

Fig. 4.21 LM whole mount of a cyst recovered from a diffusion chamber 90 days p.i. The cyst has a relatively thick laminated layer (LL) and a hook bud (B). X124.

4.18

4.19

4.20

4.21

Fig. 4.22 LM whole mount of a cyst taken from a diffusion chamber 7 months p.i. The laminated layer is well developed and possesses several laminations. X124.

4.22

CHAPTER FIVE

STRUCTURE OF THE GERMINAL LAYER, BROOD CAPSULE WALL AND PROTOSCOLEX TEGUMENT.

Fig. 5.1 Diagrammatic representation of the structure of the cestode tegument showing features of both adults and metacestodes. The terminology used in the present study is given with alternative terms in brackets.

5.1

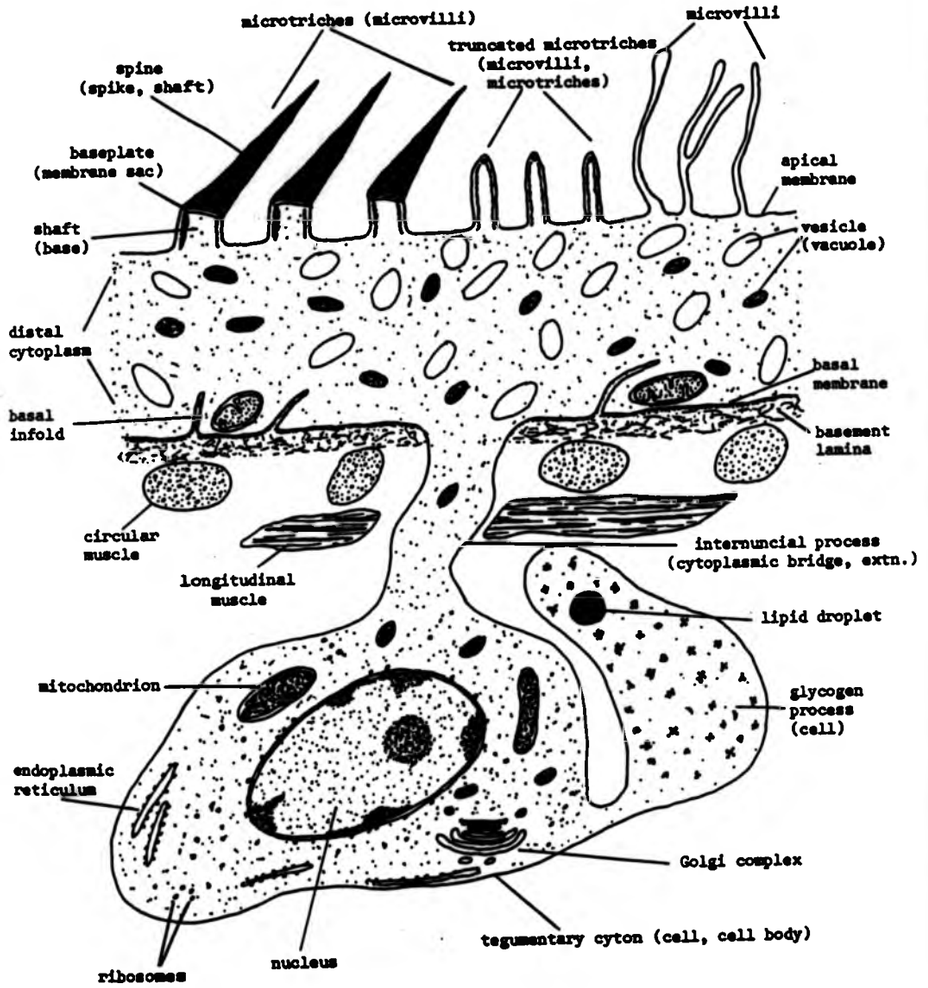

Fig. 5.2 TEM of the cyst wall of a murine hydatid cyst 9 months p.i. The tegumentary distal cytoplasm (DC) possesses truncated microtriches (TM) extending into the laminated layer (LL) which is composed of aggregates of electron-dense granules (G) in a microfibrillate matrix. X20,000.

5.2

Fig. 5.3 TEM of the tegumentary distal cytoplasm of a murine cyst, 4 months p.i. The truncated microtriches (TM) are cylindrical in shape and have an inner, electron-dense shaft support (SS). A spherical base plate (BP) is present above which there is sometimes an accumulation of electron dense material (arrow). Microfilamentous structures (MF) are present within the core of the projections. Vesicles within the distal cytoplasm frequently contain electron-dense granules (G). X66,860.

5.3

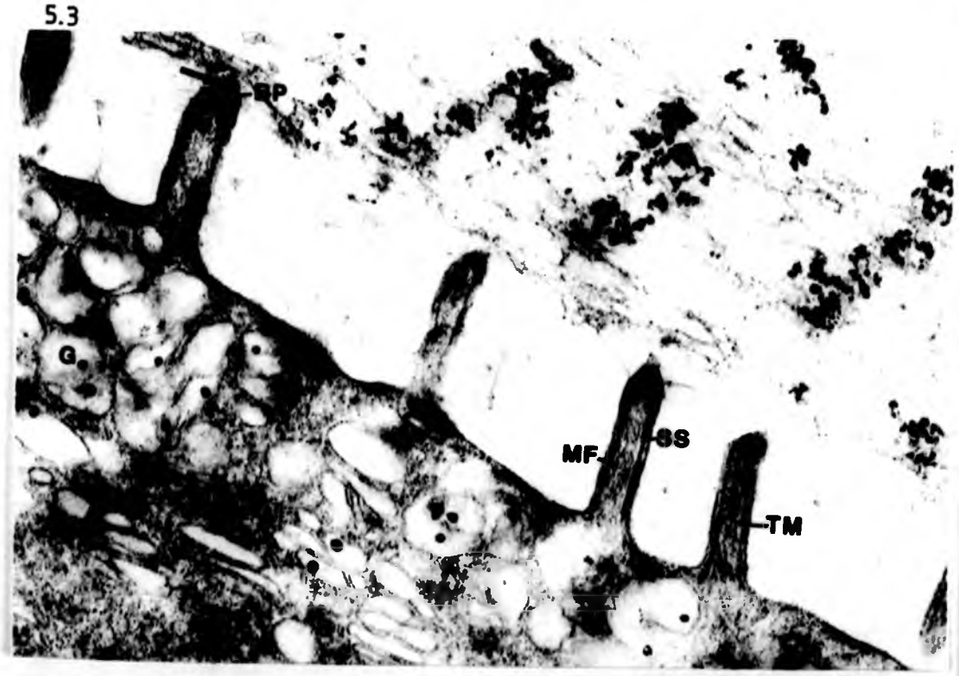

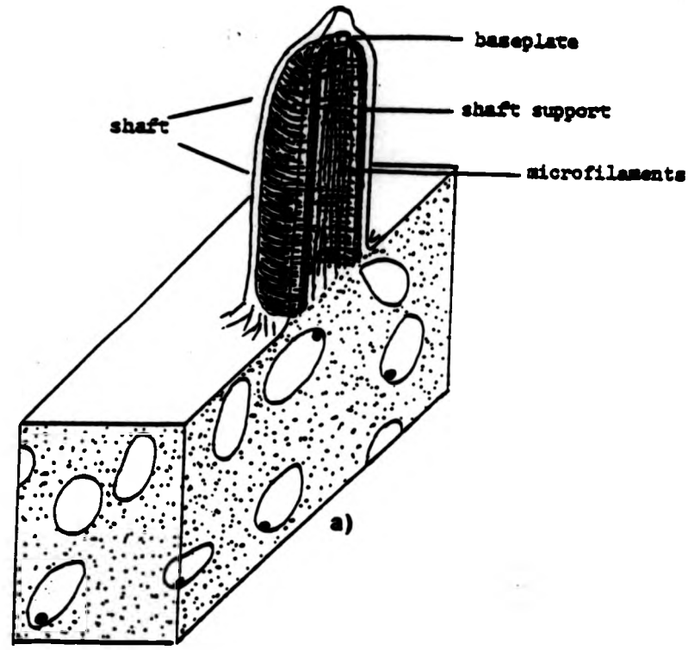

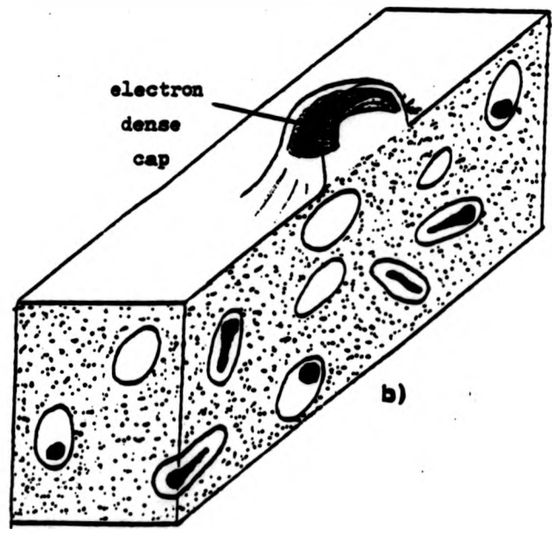

Fig. 5.4 Diagrammatic representation of the tegumentary projections occurring on hydatid cysts and protoscoleces. a) truncated microthrix; b) blunt elevation; c) type 1 sucker microthrix; d) type 2 sucker microthrix; e) rostellar microthrix.

5.4 cont.

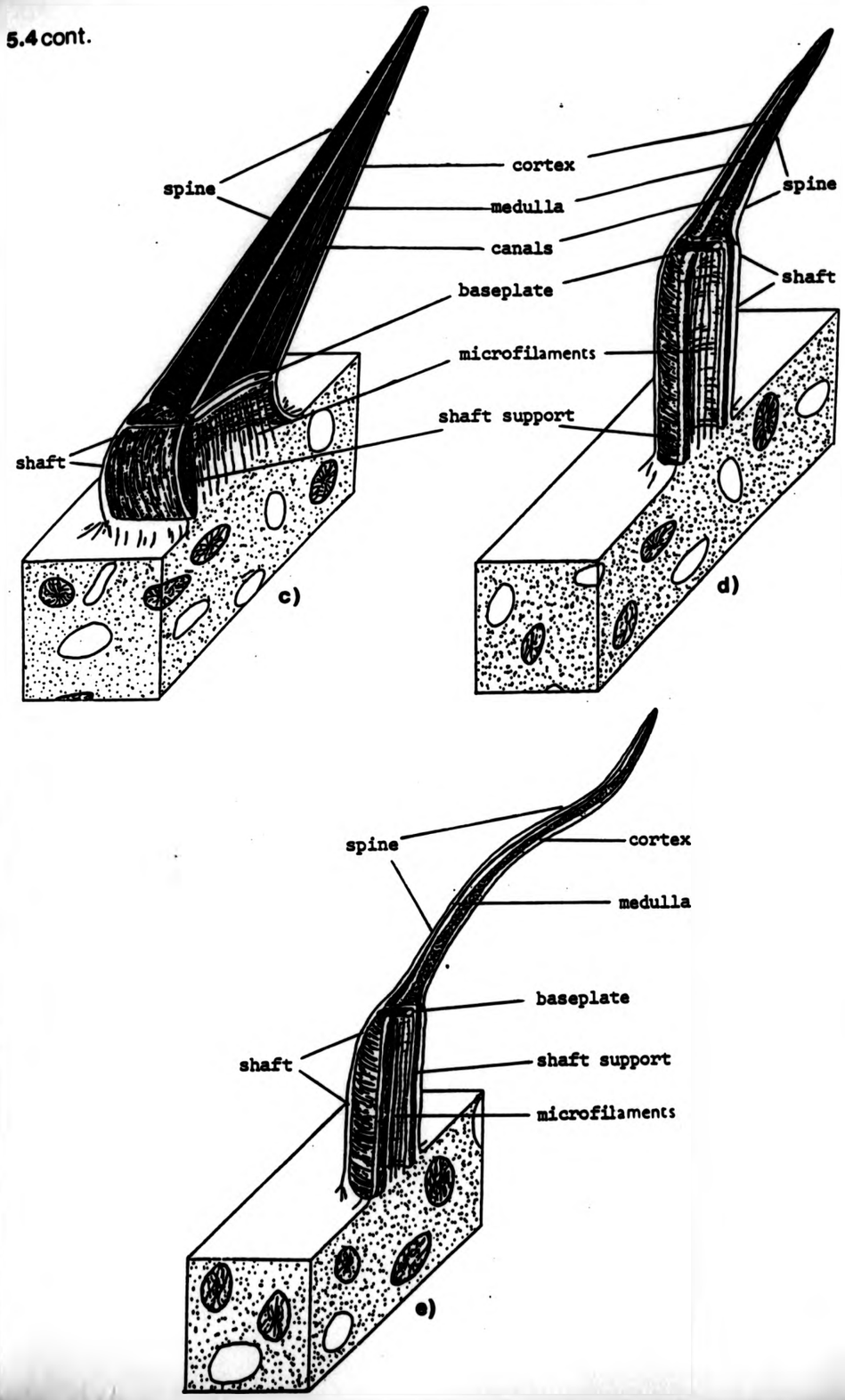
spine
cortex
medulla
canals
baseplate
microfilaments
shaft support
shaft
c)
spine
shaft
d)
spine
cortex
medulla
baseplate
shaft
shaft support
microfilaments
e)

Fig. 5.5 TEM of the laminated layer of a 9 month murein cyst showing the aggregates of electron-dense granules (AG) within the microfibrillate matrix. X136,000

5.5

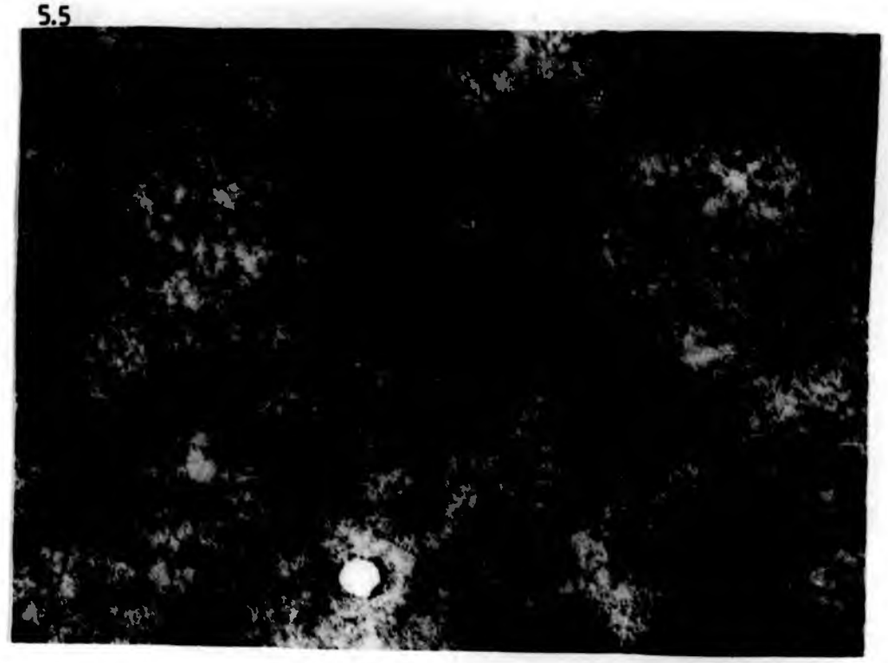

Fig. 5.6 TEM of the cyst wall of a murine hydatid cyst, 4 months p.i. The aggregates of electron-dense granules (G) are present throughout the laminated layer (LL) except in the region immediately adjacent to the tegumentary distal cytoplasm (DC). BL; basement lamina. X39,100.

5.6

Fig. 5.7 TEM of the laminated layer of a murine cyst 12 months p.i. The granule clusters (G) are often present in bands (arrows) which presumably correspond to the laminations observed in LM. X11,000.

5.7

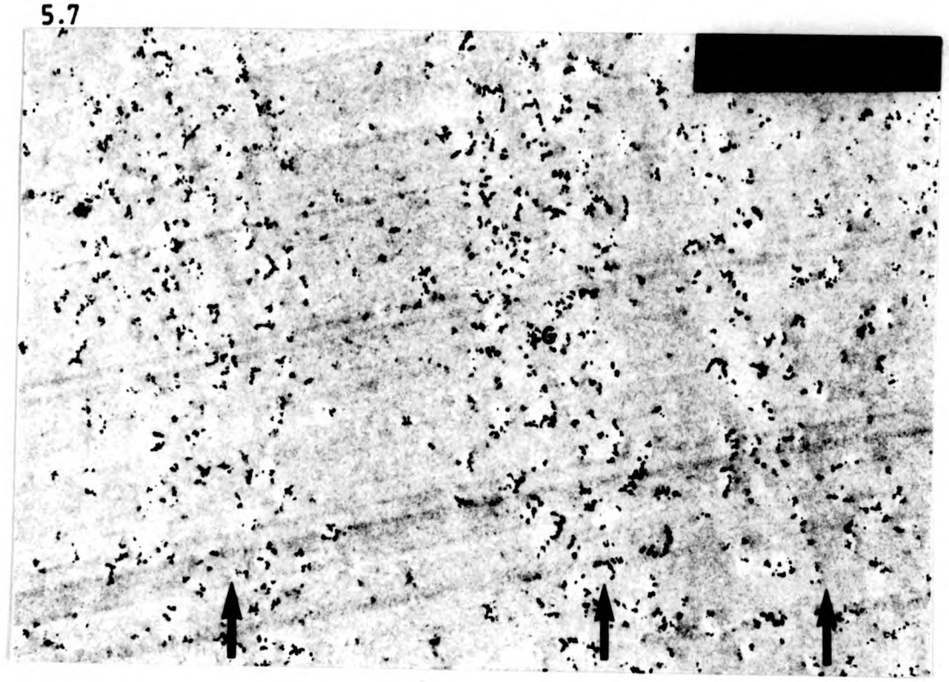

Fig. 5.8 TEM of the tegumentary distal cytoplasm of a murine cyst 10 months p.i. The granules (G) within the tegumentary distal cytoplasm can be seen to have an internal alveolar structure. TM; truncated microtriches. (unstained section) X103,000.

5.8

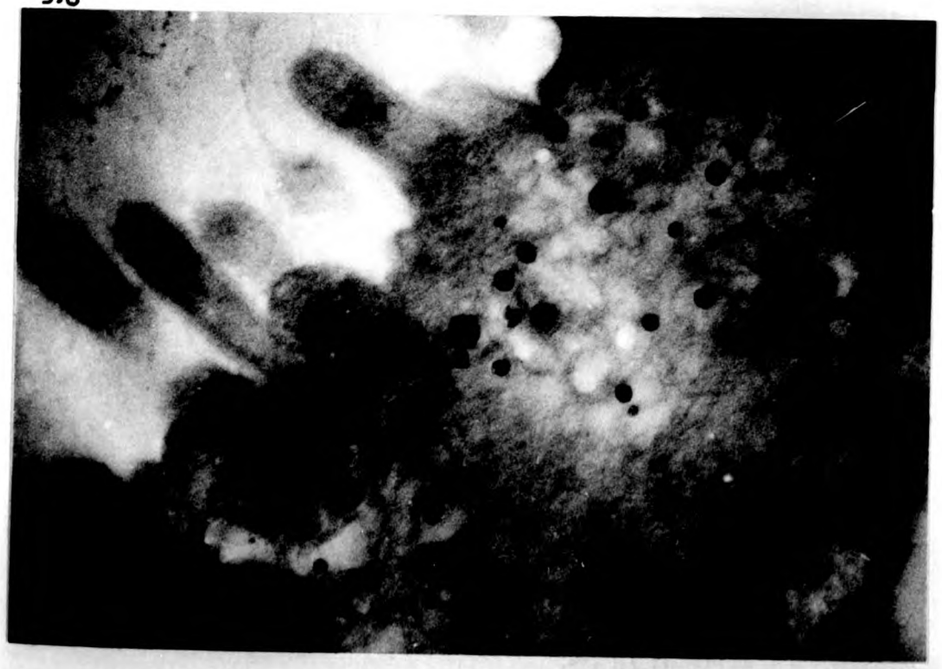

Fig. 5.9 TEM of the laminated layer of a murine cyst 10 months p.i. The electron-dense granules of the laminated layer also have an alveolar structure (arrows) suggesting they are of a similar origin to those occurring in the tegument. (Unstained section) X103,000.

5.9

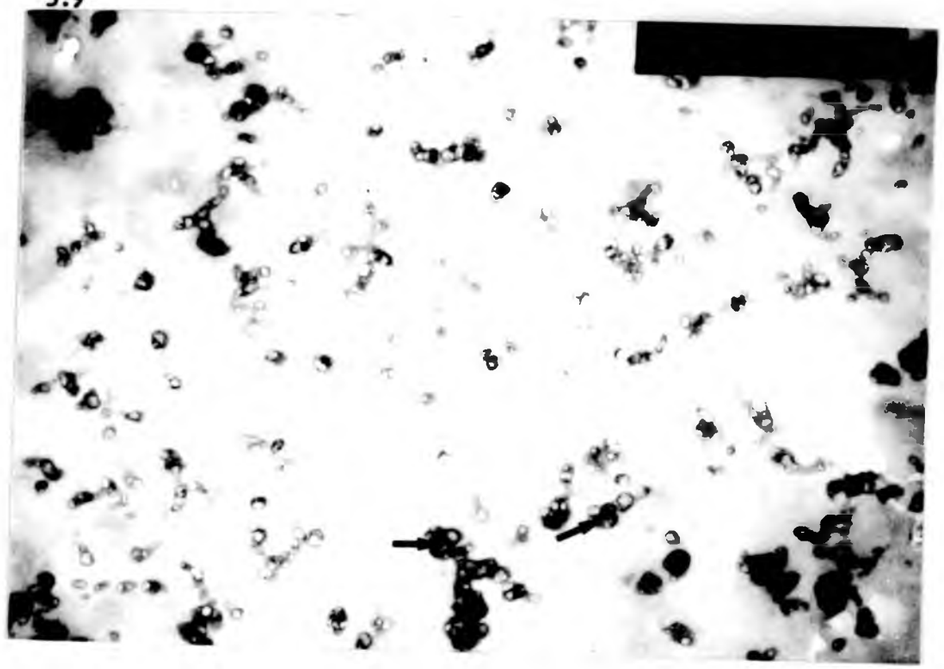

5.10

Fig. 5.10 TEM of the tegumentary distal cytoplasm (DC) of a murine cyst, 15 months p.i. The vesicles of the tegument mainly have a random orientation but occasionally are orientated with their long axis perpendicular to the apical membrane (arrows) M; mitochondria, Ms; muscle. X20,500.

Fig. 5.11 TEM of the distal cytoplasm of a murine cyst 6 months p.i. Portions of the basal plasma membrane extend into the distal cytoplasm to form basal infolds (arrows). Occasional mitochondria (M) are present near the base of the distal cytoplasm. X 42,000

5.11

Fig. 5.12 TEM of a tegumentary cyton from the germinal layer of a murine cyst, 9 months p.i. The perinuclear cytoplasm contains many vesicles with electron-dense granules (G) similar to those of the distal cytoplasm. N; nucleus, No; nucleolus, GC; Golgi complex. X29,200.

5.12

Fig. 5.13 TEM of a tegumentary cyton from the germinal layer of a murine cyst, 6 months p.i. Vesicles with electron-dense granules (G) are present near Golgi complexes (GC) in which other such smaller granules are present (arrows). Ribosome-like bodies (R) are present within the perinuclear cytoplasm and surrounding the nuclear membrane. X44,200.

5.13

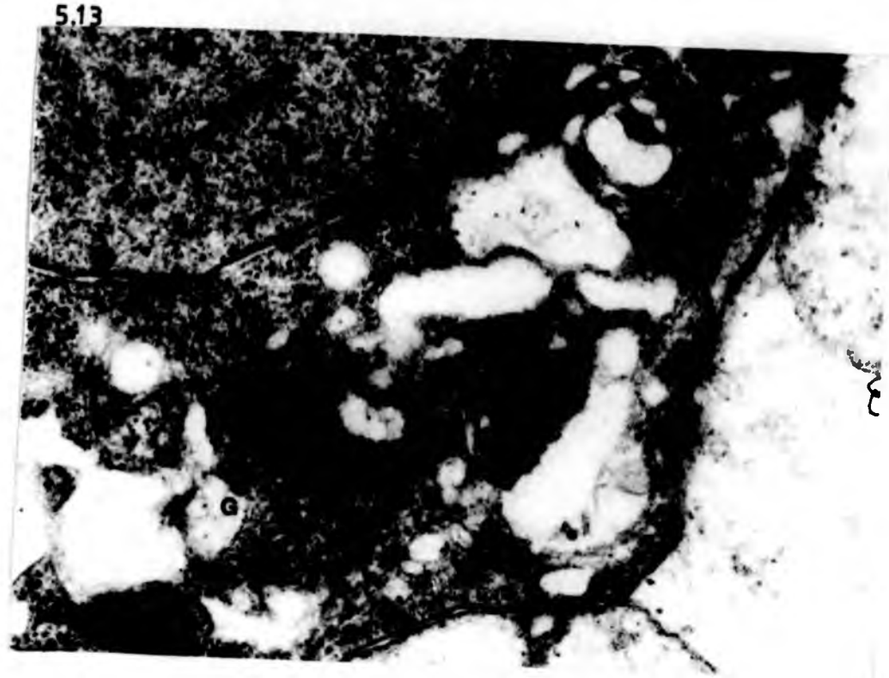

Fig. 5.14 TEM of a cyton from the germinal layer of a murine cyst 4 months p.i. Small vesicles (TV), devoid of granules are also present in the perinuclear cytoplasm and may represent transition vesicles between the endoplasmic reticulum and Golgi complexes. Glycogen reserves (Gl) in the a rosette formation, are present within cytoplasmic processes projecting from the perinuclear cytoplasm. R; Ribosome-like bodies. X39,100

5.14

Fig. 5.15 TEM of a tegumentary cyton from a murine cyst 12 months p.i. The perinuclear cytoplasm possesses granule-containing vesicles (G) Golgi complexes (GC) and additional vesicles with a dense, asymetric peripheries and slightly flocculent contents (F). The endoplasmic reticulum (ER) is limited to single cisternae around the periphery of the cytons. The cytoplasmic processes (P) are occasionally devoid of glycogen reserves and may possess osmophillic lipid droplets (lp). X20,500.

5.15

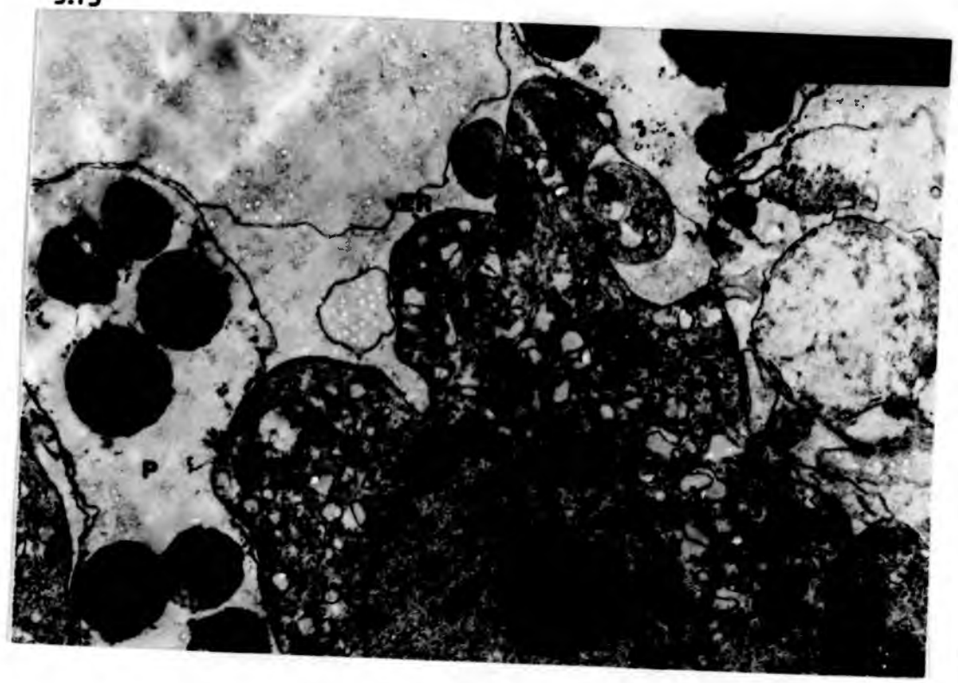

Fig. 5.16 TEM of a tegumentary cyton from a murine cyst 6 months p.i. Peripheral endoplasmic reticulum (ER) is present and in some cases possesses attached ribosomes (arrows). N; nucleus, G; Golgi complex. X12,200.

5.16

Fig. 5.17 TEM of the tegument of a murine cyst 12 months p.i. The glycogen containing processes are packed with glycogen (Gl) in the rosette formation and occasionaly non-osmiophillic lipid droplets (Lp). DC; distal cytoplasm. TM; truncated microtriches. X20,500.

5.17

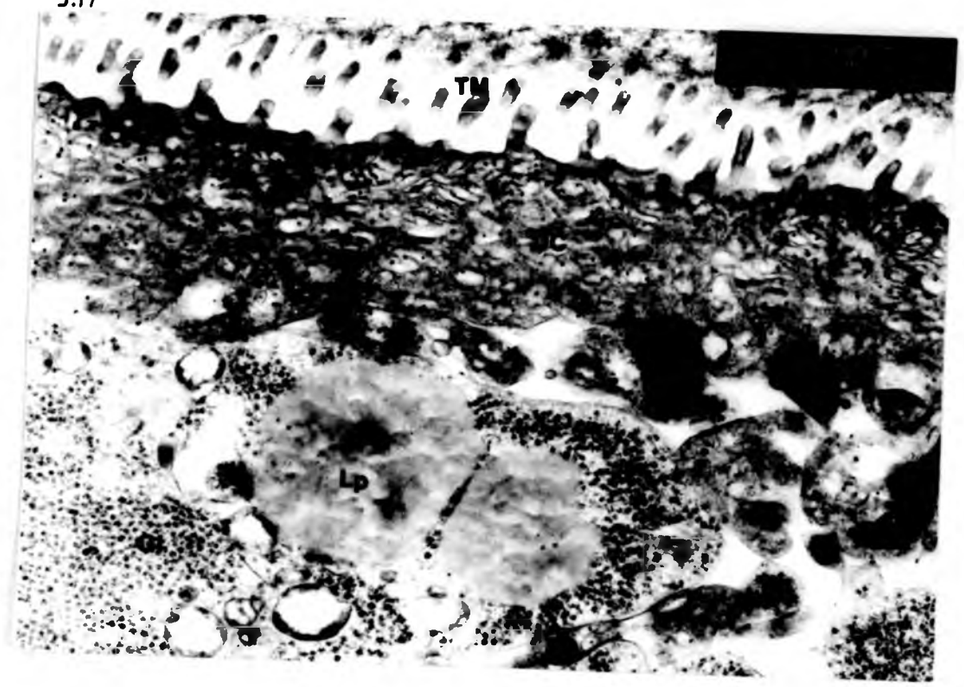

Fig. 5.18 TEM of a tegumentary cyton of a murine cyst 7 months p.i. Occasionaly microtubules (T) are present within the perinuclear cytoplasm. A vacuole (V) which may represent an autophagosome is also present and possesses flocculent contents and an asymetrical periphery of dense lamellar material (L) X63,400.

5.18

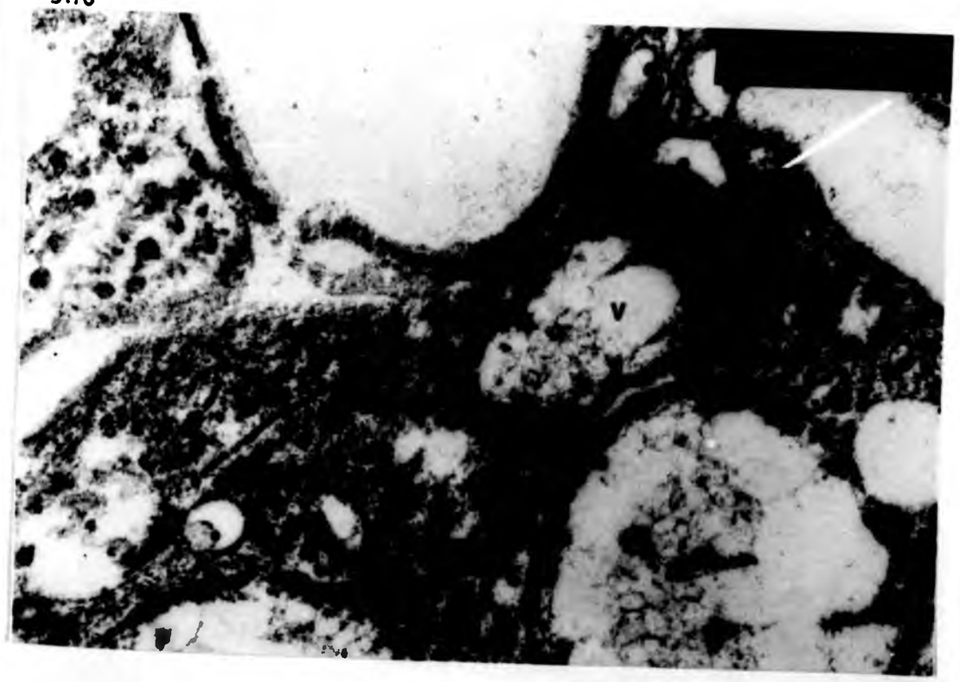

Fig. 5.19 TEM of a tegumentary cyton of a murine cyst 7 months p.i. Two types of vacuole are present in the perinuclear cytoplasm. The first has a moderately dense periphery and flocculent contents and may represent a storage lysosome (L). The second type has an asymetric lamellar periphery and may represent an autophagosome/residual body (P). X29,200.

Fig. 5.20 TEM of a tegumentary cyton of a murine cyst 9 months p.i. The size of the storage lysosomes (L) appears to be affected by fusion with other small vesicles (arrow). N; nucleus. X29,200.

5.19

5.20

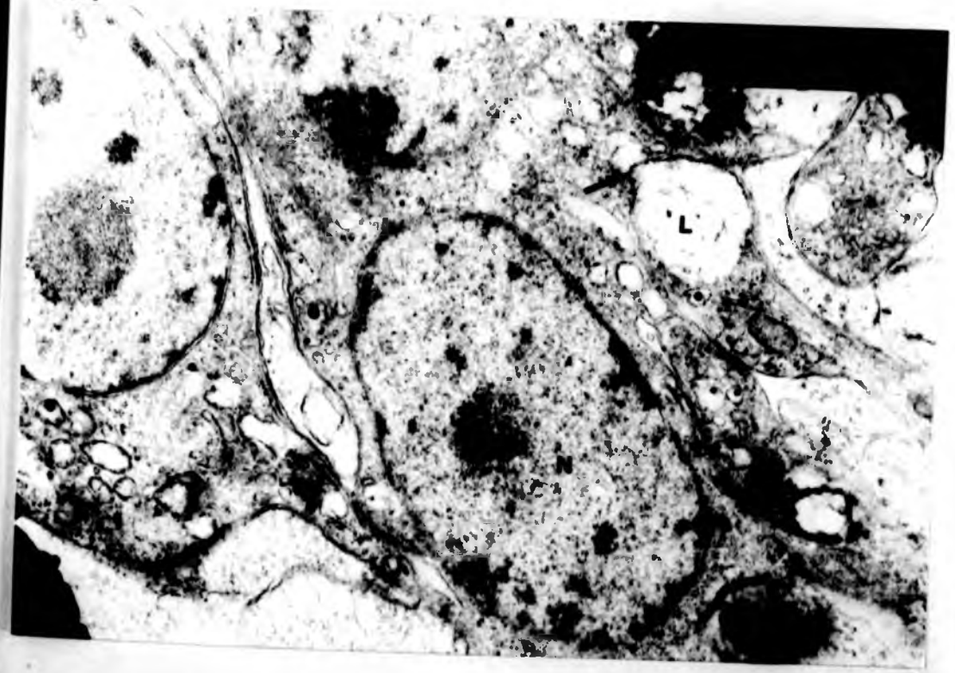

Fig. 5.21 TEM of a tegumentary cyton from a murine cyst 8 months p.i. The periphery of a residual body is shown to have a lamellar appearance (arrow) suggesting a membraneous origin. X79,600.

5.21

Fig. 5.22 TEM of a myocyton from the germinal layer 5 months p.i. Note that these cytons have a paler cytoplasm and narrower mitochondria (M) compared to the tegumentary cytons. X28,200.

5.22

Fig. 5.21 TEM of a tegumentary cyton from a murine cyst 8 months p.i. The periphery of a residual body is shown to have a lamellar appearance (arrow) suggesting a membraneous origin. X79,600.

5.21

Fig. 5.22 TEM of a myocyton from the germinal layer 5 months p.i. Note that these cytons have a paler cytoplasm and narrower mitochondria (M) compared to the tegumentary cytons. X28,200.

5.22

Fig. 5.23 LM of a section of a murine cyst 5 months p.i. incubated with FITC labelled WGA. The lectin has bound strongly to the laminated layer (LL) and to the germinal layer (GL). CC; calcareous corpuscle. X958.

Fig. 5.24 LM of a section of a murine cyst 5 months p.i. incubated with FITC labelled SBA. The lectin has bound to both the laminated layer (LL) and germinal layer (GL). CC; calcareous corpuscle. X958.

Fig. 5.25 LM of a section of a murine cyst 5 months p.i. incubated with FITC labelled PNA. The lectin has bound strongly to the laminated layer (LL) and germinal layer (GL). CC; calcareous corpuscles. X958.

5.23

5.24

5.25

Fig. 5.26 LM of a section of a murine cyst 5 months p.i. incubated with FITC labelled APA. The lectin has neither bound to the laminated layer (LL) nor the germinal layer (GL). X958.

Fig. 5.27 LM of a section of a murine cyst 5 months p.i. unstained. The laminated layer (LL) does not fluoresce but the germinal layer (GL) shows a slight autofluorescence (long camera exposure). X958.

Fig. 5.28 LM of a section of a murine cyst 5 months p.i. incubated with FITC labelled Con A. The lectin does not bind to the laminated layer (LL) but does bind strongly to the germinal layer (GL). CC; calcareous corpuslces. X958

5.26

5.27

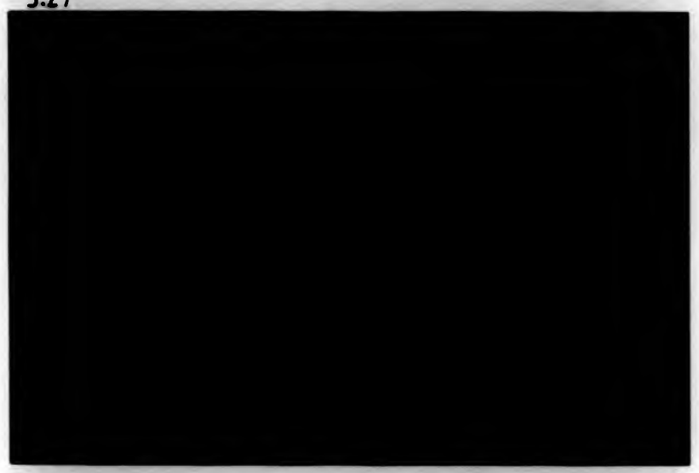

5.28

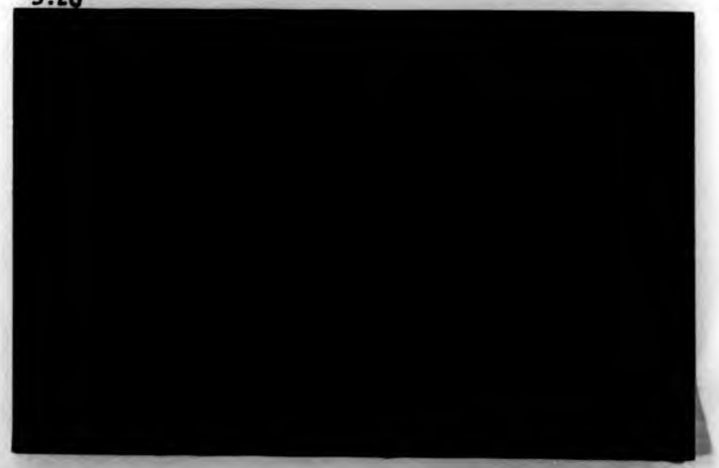

Fig. 5.29 TEM of a murine cyst 9 months p.i. incubated with peroxidase labelled WGA. A strong reaction is present in the laminated layer (LL) although non-specific deposits are present in the germinal layer tegument (T). X14,200.

Fig. 5.30 TEM of a 9 month murine cyst incubated with peroxidase labelled WGA. Non-specific reaction products (arrows) within the distal cytoplasm (DC) make precise localization impossible. LL; laminated layer. 29,200.

5.29

5.30

Fig. 5.31 TEM of the cyst wall of a murine cyst 6 months p.i. stained for carbohydrates using the periodic acid-thiosemicarbazide method. The laminated layer (LL) and glycogen-containing processes (Gl) give a strong reaction whilst the distal cytoplasm (DC) does not react. X5,480.

Fig. 5.32 TEM of the distal cytoplasm of a murine cyst 6 months p.i. stained using the periodic acid-thiosemicarbazide method. Little if any reaction product is present in the tegumentary vesicles (V) although the laminatedlayer (LL) reacts strongly. X63,400.

5.31

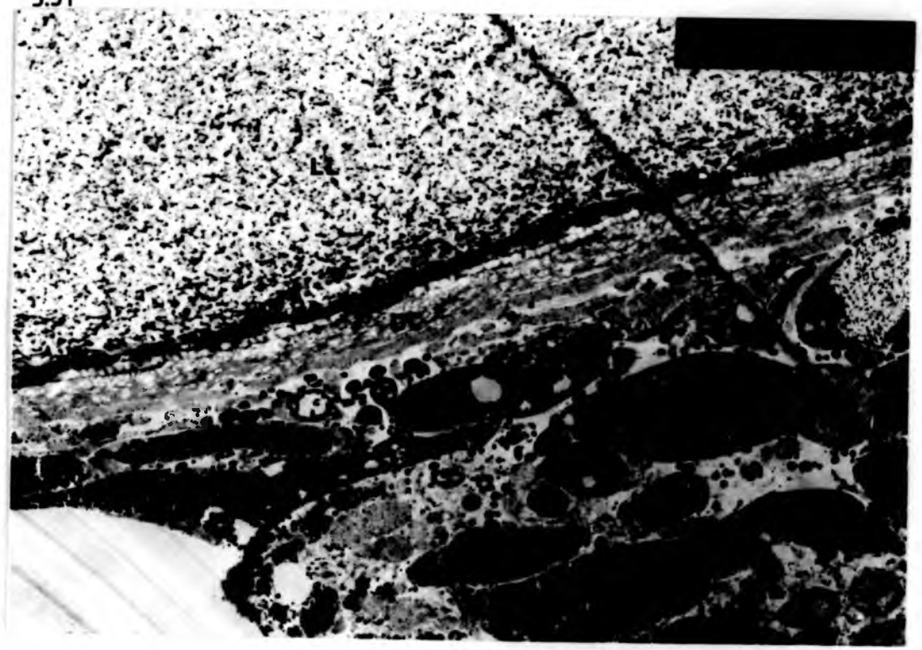

5.32

Fig. 5.33 TEM of the laminated layer of a murine cyst 6 months p.i. incubated in silver proteinate alone (control). Slight deposits are present throughout the layer, particularly within artifactual fissures. G; granule clusters. 63,400.

Fig. 5.34 TEM of a tegumentary distal cytoplasm of a murine cyst 6 months p.i. incubated in a medium lacking periodic acid (control). Slight deposits are present around the granules of the tegumentary vesicles (arrow). TM; truncated microtriches. X79,600.

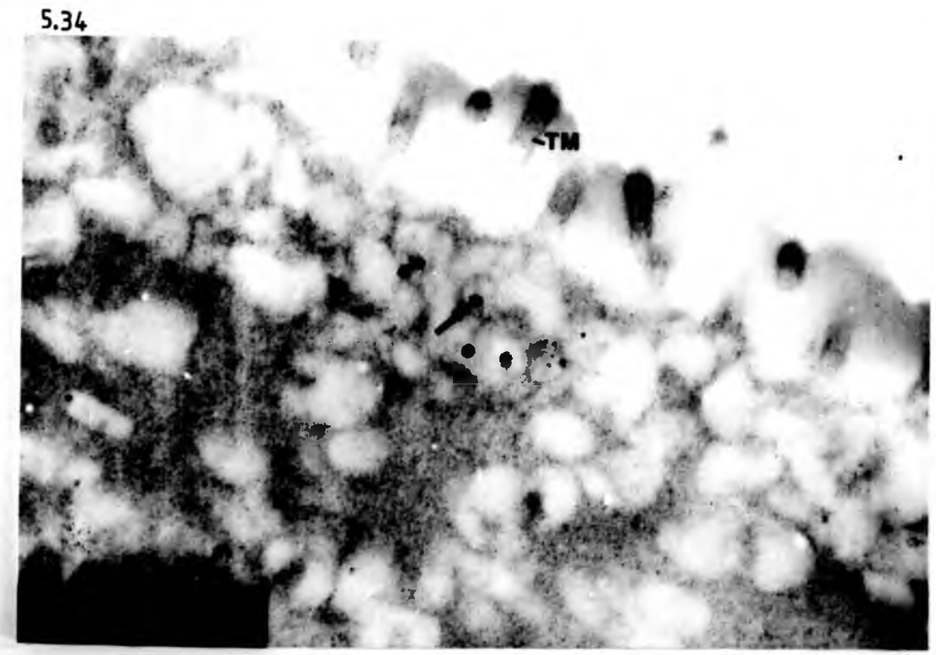

Fig. 5.35 TEM of a tegumentary cyton of a murine cyst 6 months p.i. stained using the period acid - thiosemicarbazide method. Little reaction product is present in the perinuclear cytoplasm except for a single large vacuole (V). N; nucleus, DC; distal cytoplasm. X29,200.

5.35

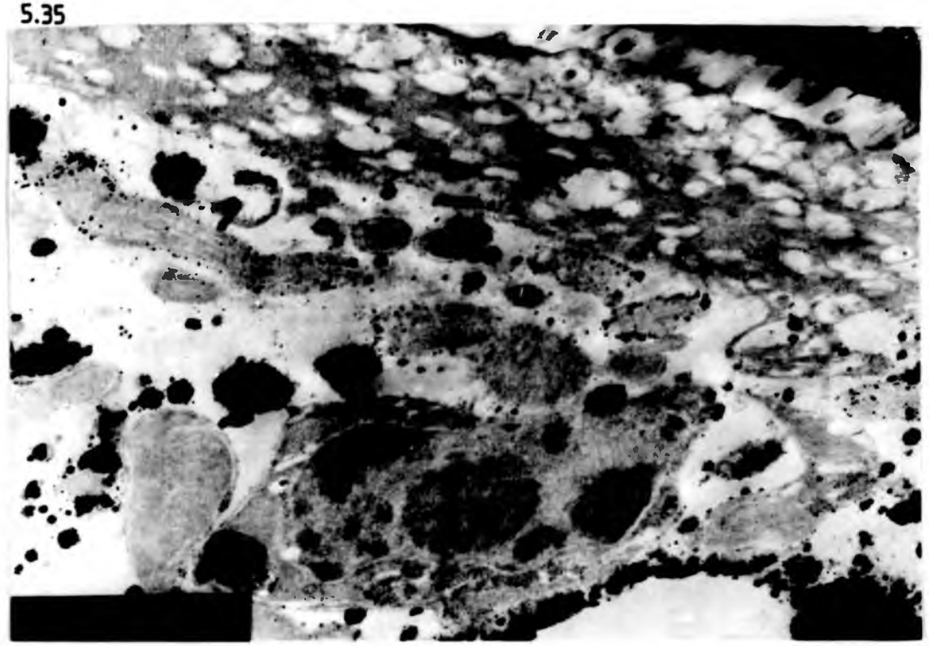

Fig. 5.36 TEM of an autophagic body within a tegumentary cyton of a 6 month murine cyst, stained using the periodic acid-thiosemicarbazide method. Both the contents and lamellar periphery (arrow) of these structures give a positive reaction for carbohydrates. X79,600.

5.36

Fig. 5.37 TEM of a tegumentary cyton from a murine cyst 6 months p.i. stained using the periodic acid - thiosemicarbazide method. A dense product is present within the storage lysosomes (L). X39,100.

5.37

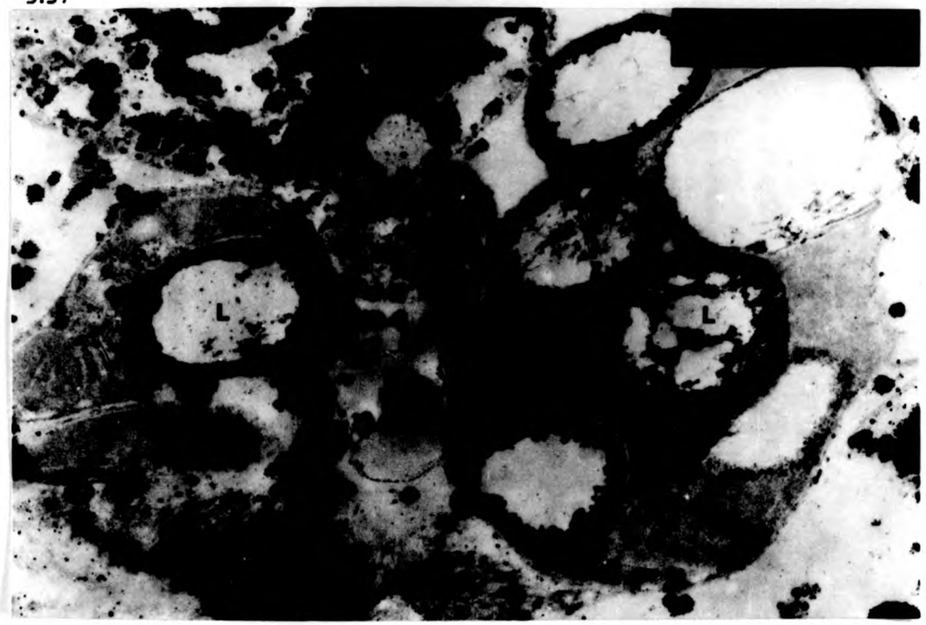

Fig. 5.38

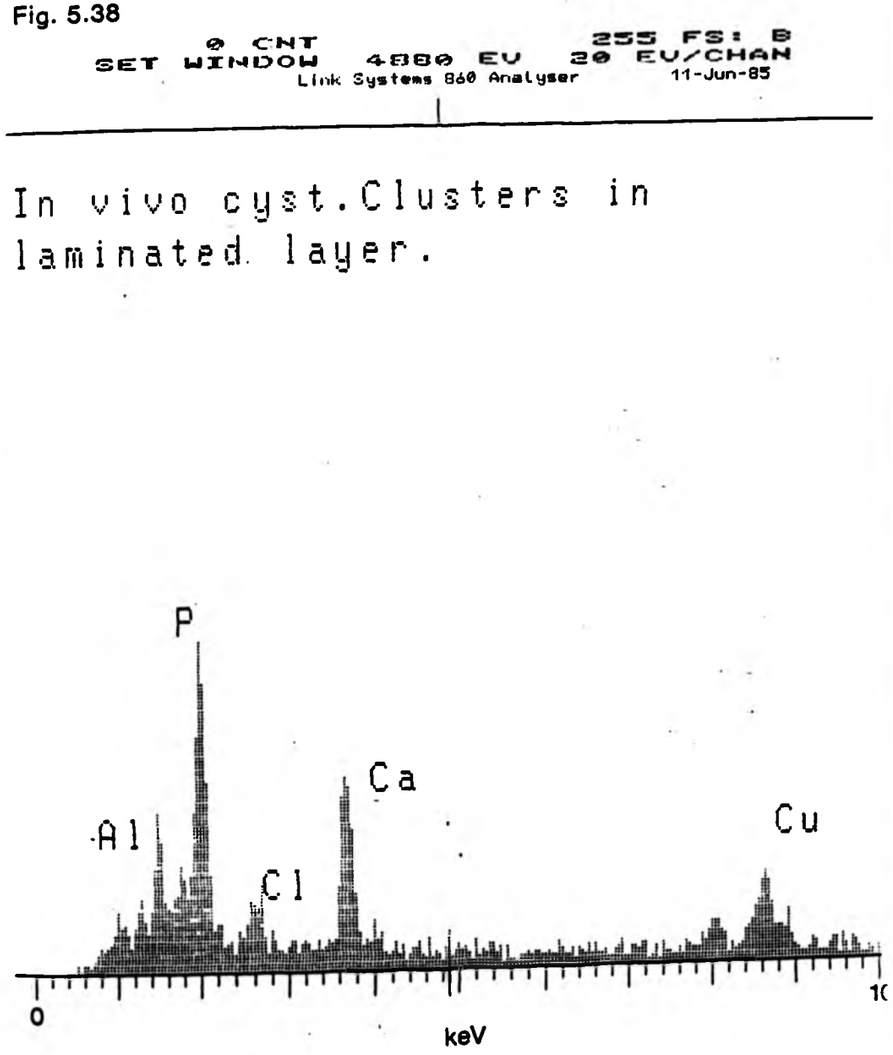

Fig. 5.38 Spectrum for the X-ray microanalysis of the electron-dense granules within the laminated layer of murine cysts. Significant peaks for phosphorus (K emission=2.1 keV) and calcium (K emission=3.7 keV) are present whilst the presence of other elements such as aluminium, chlorine and copper can be linked to the grids, resin or grid holder.

Fig. 5.39 Spectrum from the X-ray microanalysis of the dense granules within the 'G' vesicles of the germinal layer of murine cysts. Significant peaks for phosphorous (K emission=2.1keV) and calcium (K emission=3.7 keV) are present as well as the usual contaminating elements.

Fig. 5.39

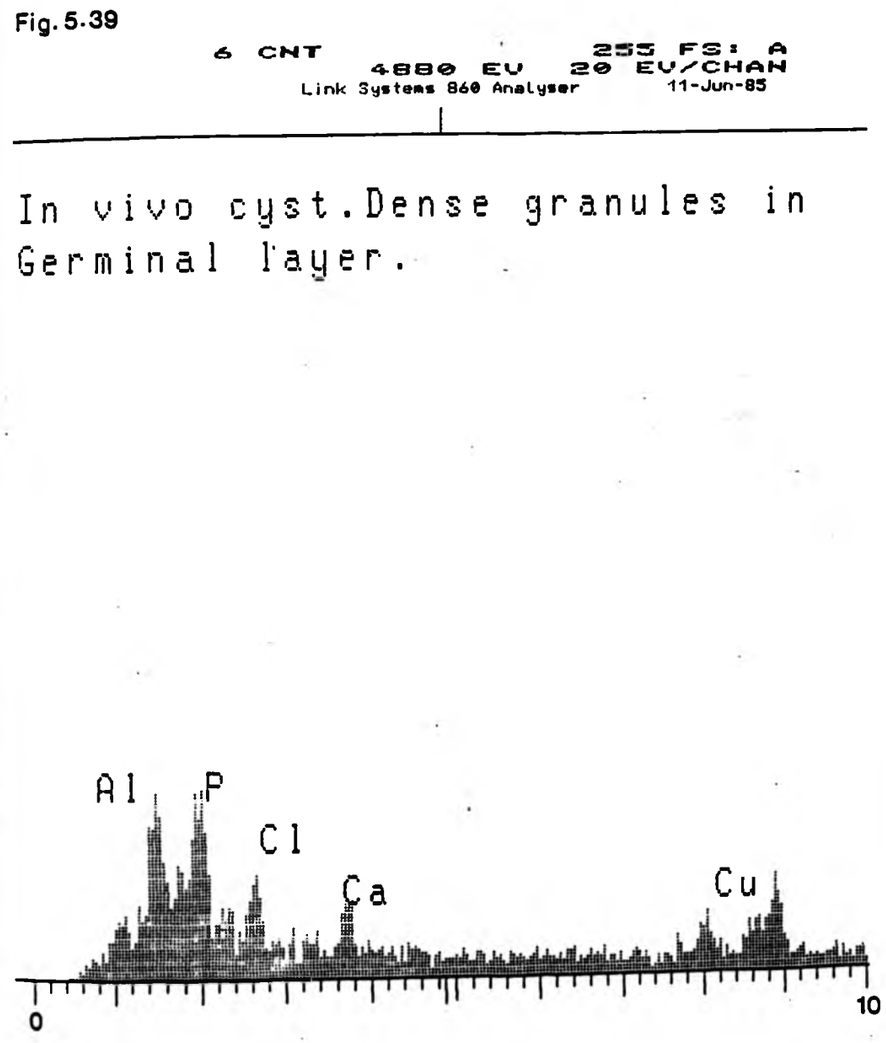

Fig. 5.40 Composite X-ray spectra comparing the analysis of both the laminated layer and 'G' vesicle granules from murine cysts. Both structures appear to contain phosphorous and calcium although the amount of these elements is lower for the 'G' vesicles. This is presumably due to variation in the amount of each structure analysed.

Fig. 5.40

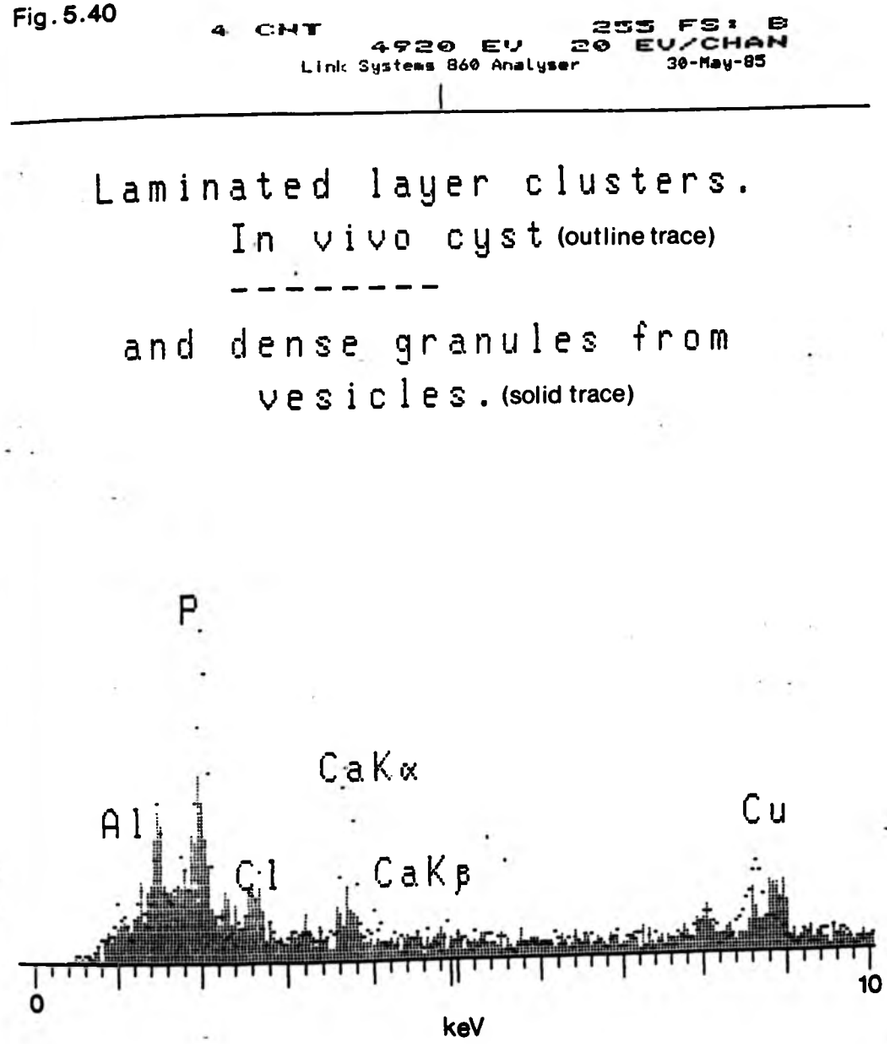

Fig. 5.41 TEM of the brood capsule wall from an equine cyst. The distal cytoplasm (DC) is narrow and possesses lucent membraneous vesicles (V). Truncated microtriches (TM) are occasionally present projecting into the interior of the capsule. X20,500.

Fig. 5.42 TEM of the brood capsule wall from an equine cyst. A tegumentary cyton is present where no internuncial processes occur. The nucleus (N) therefore appears to be in a swollen region of the distal cytoplasm (DC). Truncated microtriches (TM) project inwards towards the protoscoleces (P) and appear to possess a glycocalyx (GX). Glycogen containing cytoplasmic extensions (Gl) are also present and structures which may represent lysosomes or residual bodies (R) occur in the perinuclear cytoplasm. X20,000.

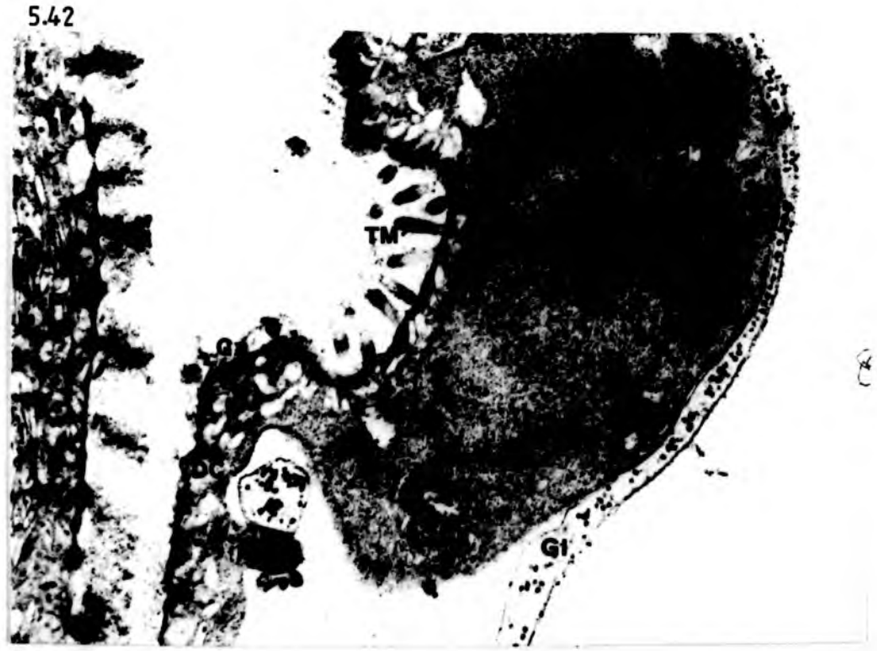

Fig. 5.43 TEM of the brood capsule wall from an equine cyst stained for carbohydrate using the periodic acid - thiosemicarbazide reaction. A slight glycocalyx (arrow) is present on the surface of the distal cytoplasm (DC). C; brood capsule cavity. Cy; cyton. X29,200.

Fig. 5.44 TEM of the brood capsule wall from an equine cyst. The perinuclear cytoplasm possesses ribosomes (Rb) and occasional lucent vesicles (V). DC; distal cytoplasm, IC; internuncial processes. M; mitochondrion. X20,000.

5.43

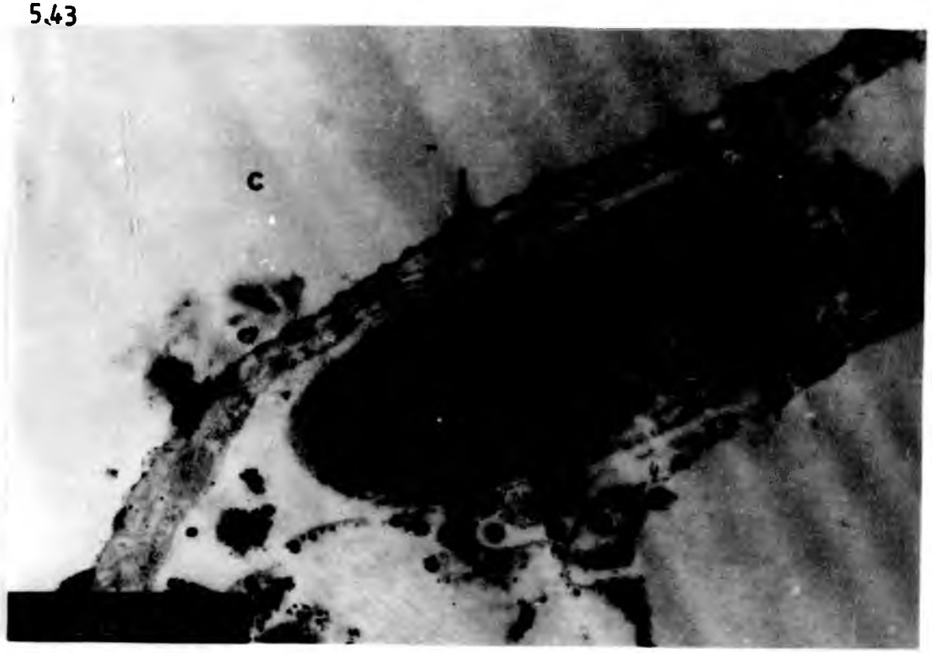

5.44

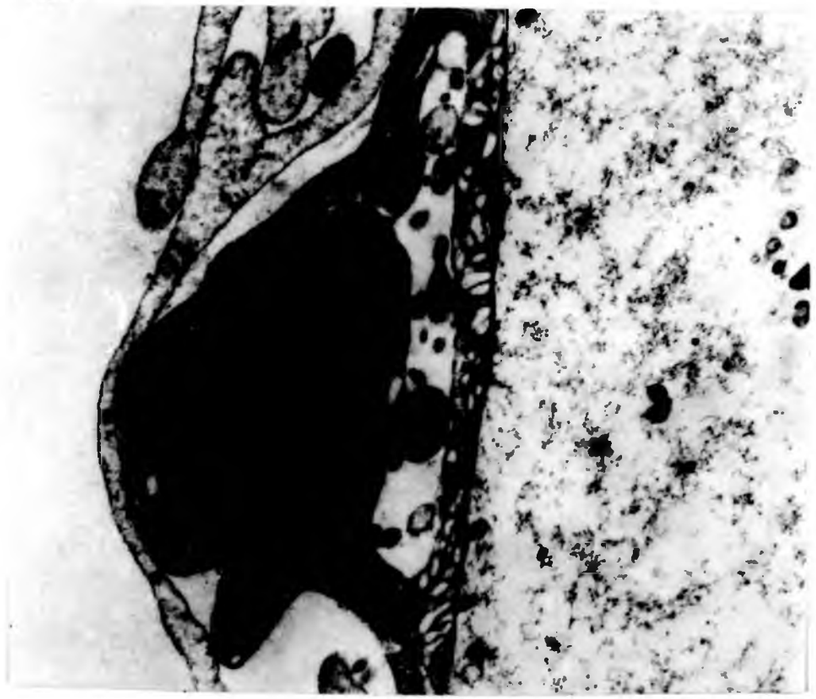

Fig. 5.45 TEM of the protoscolex attachment stalk from an equine cyst. The stalk possesses a significant population of truncated microtriches (TM) and has flame cell ducts (F) within it. P; protoscolex. X63,400.

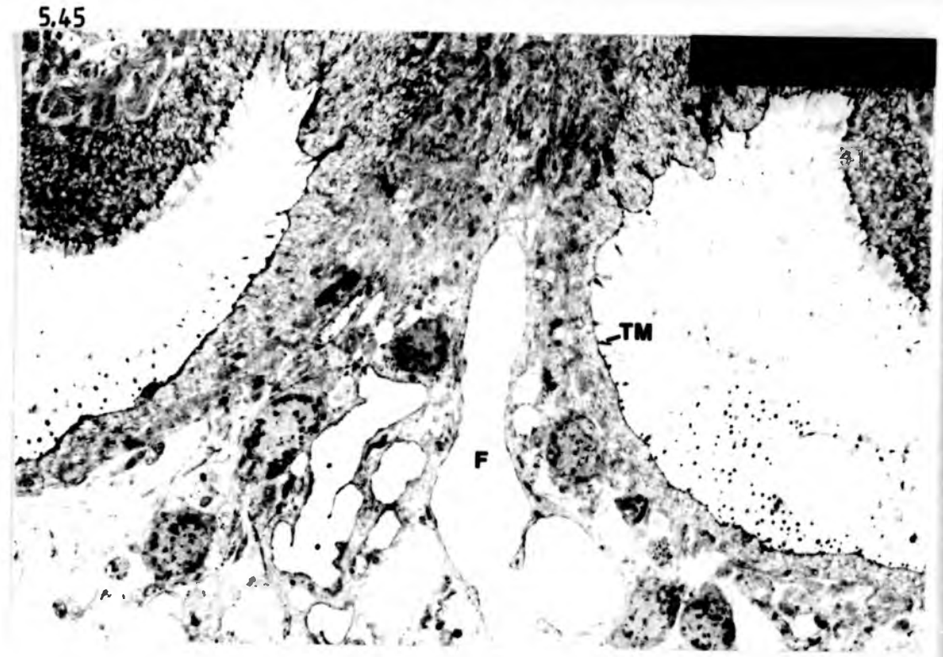

Fig. 5.46 TEM of the protoscolex attachment stalk from an equine cyst. The distal cytoplasm occassionally possesses vesicles with electron dense contents, similar to those of the protoscolex soma tegument (arrows). The interior of the stalk possesses flame cell collecting ducts (F) and muscle tissue (Ms) TM; truncated microtriches, P; protoscolex. X6,590.

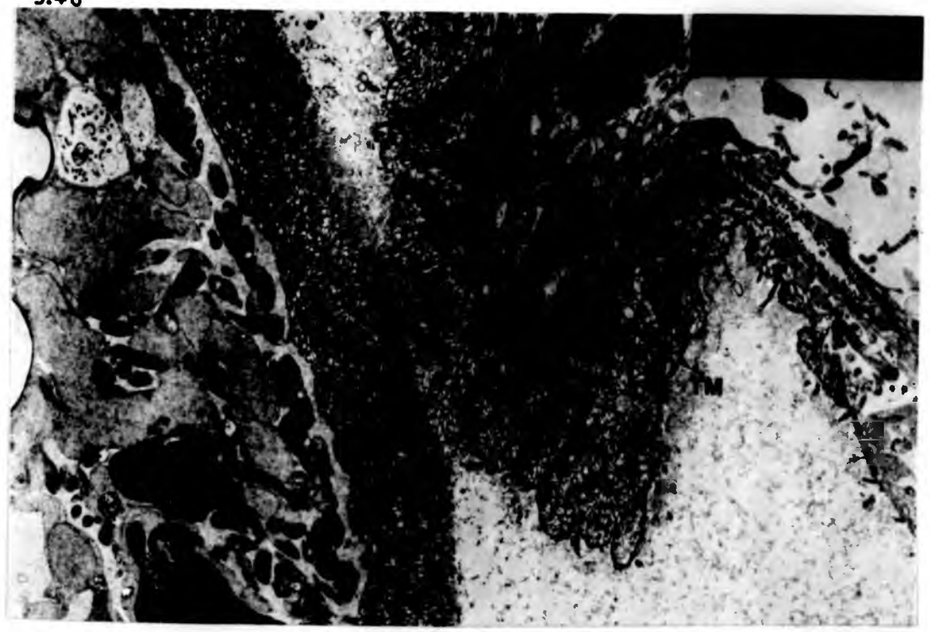

Fig. 5.47 TEM of the protoscolex attachment stalk from an equine cyst. The truncated microtriches are identical to those of the germinal layer in possessing a shaft support (SS), a spherical baseplate (BP) and occasionally an accumulation of electron-dense material (arrow) at the apex. X79,600.

5.47

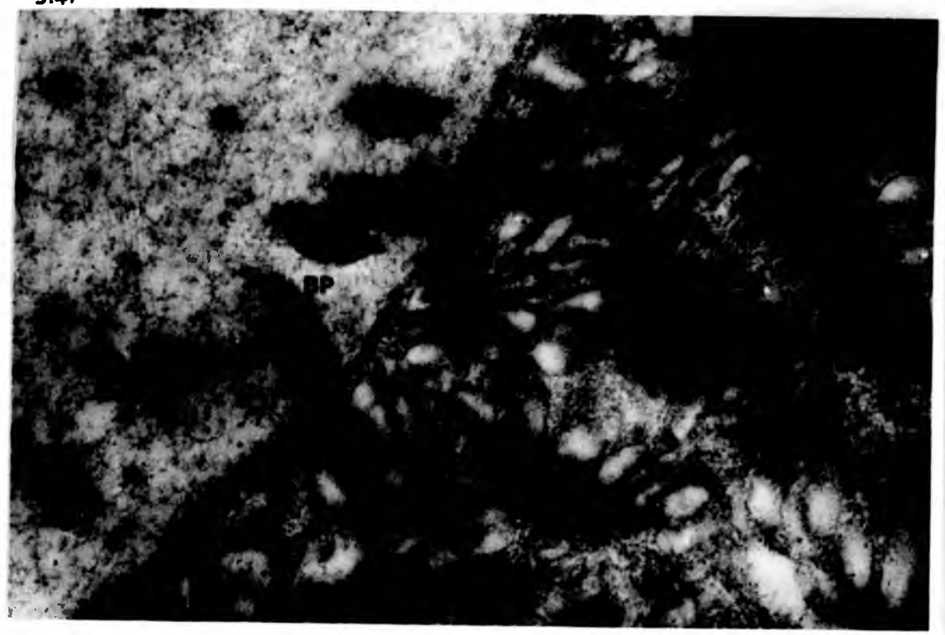

Fig. 5.48 TEM of the brood capsule wall from an equine cyst. Flame cell collecting ducts (F) and muscle tissue (Ms) are present on the outer surface of the capsule. X15,200.

5.48

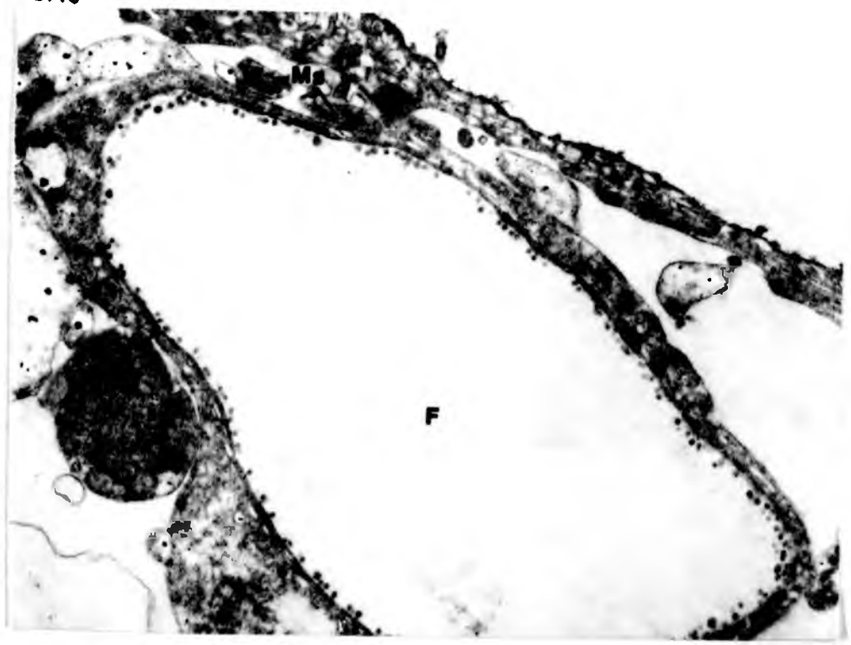

Fig. 5.49 SEM of an intact brood capsule from an equine cyst. Flame cell collecting ducts can be seen crossing the brood capsule in several directions (arrows). X150.

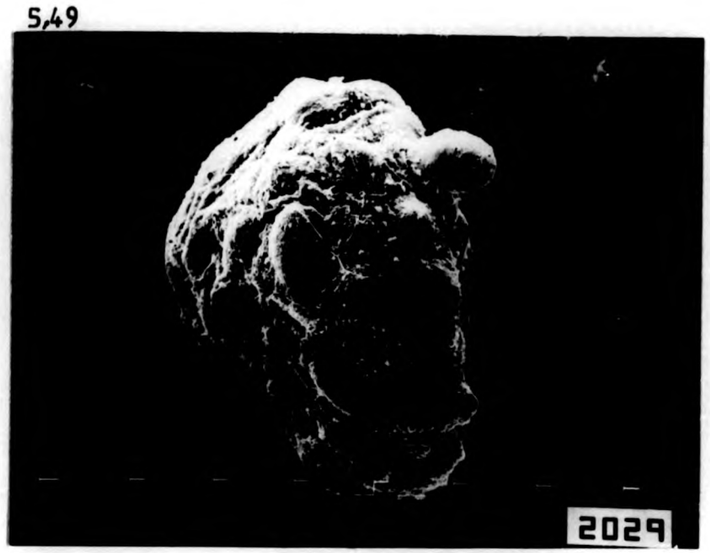

Fig. 5.50 SEM of the outer surface of a brood capsule showing the collecting ducts (D) at higher magnification. X2,000.

Fig. 5.51 SEM of an evaginated protoscolex. The rostellar (R) and sucker (Sk) regions make up the scolex which is anterior to the soma (So). X750.

Fig. 5.52 SEM of a protoscolex in the invaginated condition with the scolex withdrawn into the soma (So). X1,000.

5.51

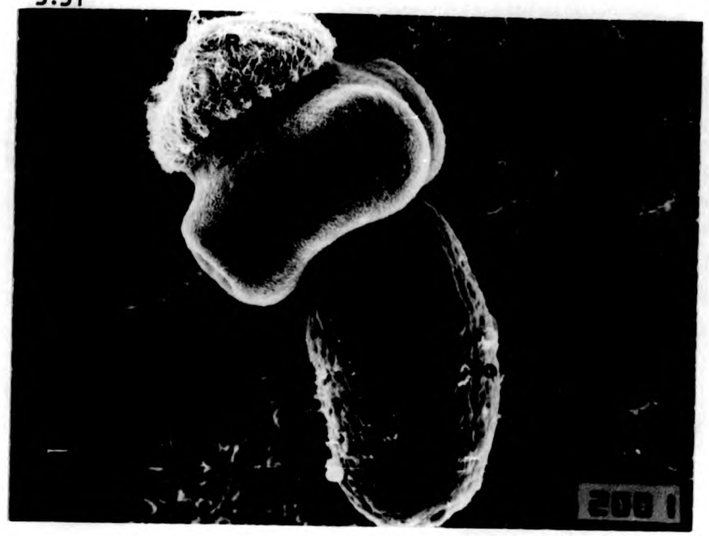

5.52

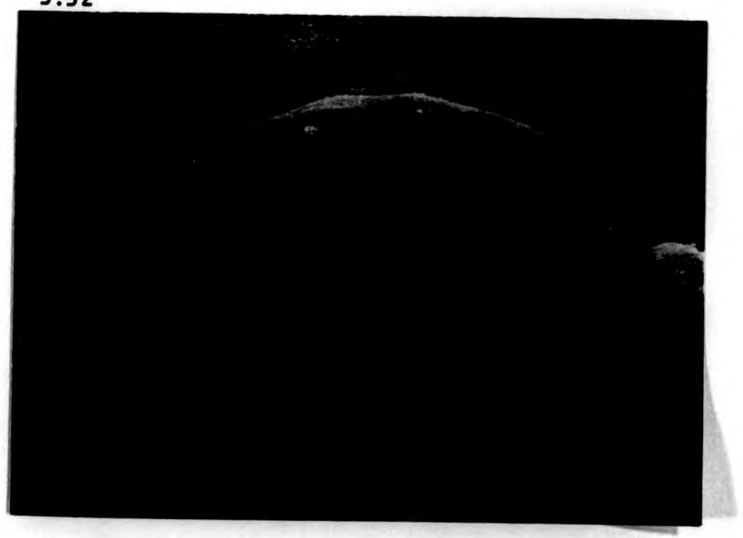

Fig. 5.53 TEM of the soma surface of a protoscolex from an equine cyst. Small blunt elevations (BE) with electron-dense caps are present below a thick glycocalyx (Gx). X44,200.

5.53

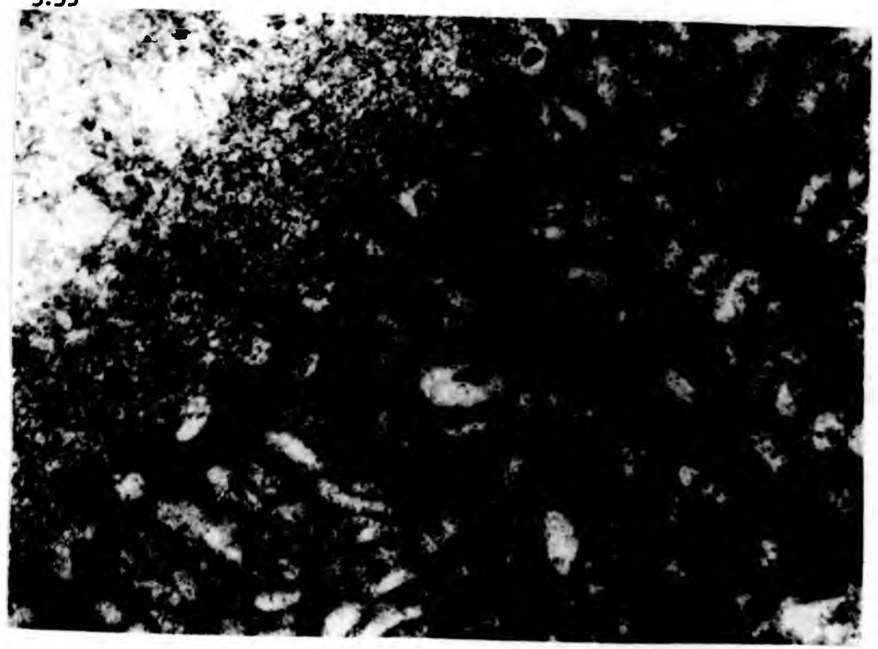

Fig. 5.54 TEM of the distal cytoplasm of the protoscolex soma tegument. Numerous vesicles are present within the distal cytoplasm. The major type (T_1) are ovoid and possess a 'comet' shaped electron dense core. BE; blunt elevations, Gx; glycocalyx, BL, basement lamina, Ms; muscle. X39,100.

5.54

Fig. 5.55 TEM of the anterior soma tegument to T_1 vesicles and electron lucent T_3 vesicles, occasional T_2 vesicles, with dense flocculent contents, are also present. BI; basal infold of the basal plasma membrane. X79,600.

5.55

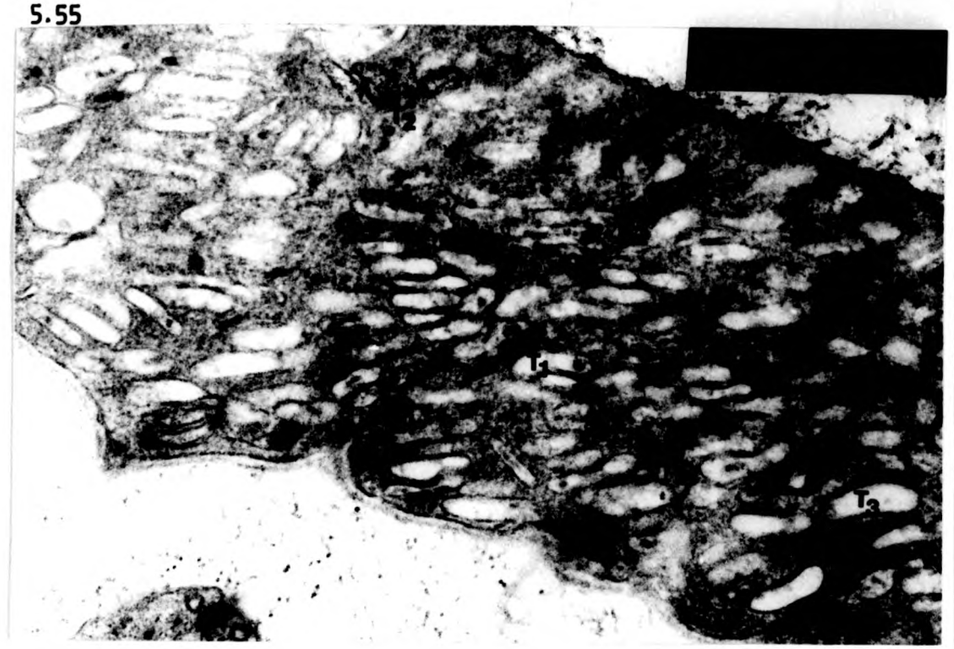

Fig. 5.56 TEM of the anterior soma tegument of the protoscolex. The tegumentary cytons (C) are connected to the distal cytoplasm (DC) by internuncial processes (TP). CM; circular muscle, LM; longitudinal muscle. X20,500.

5.56

Fig. 5.57 TEM of a tegumentary cyton from the soma tegument of a protoscolex. The cytons characteristically possess a dense cytoplasm, a large central nucleus (N) and occassional mitochondria (M). Golgi complexes (G) are small and ribosome like bodies (R) are abundant. No; nucleolus, Gl; glycogen within cytoplasmic processes. X39,100.

5.57

Fig. 5.58 TEM of a cyton from the soma tegument of a protoscolex. Golgi complexes (G) occur within the perinuclear cytoplasm close to peripheral endoplasmic reticulum (ER) which occasionally has associated ribosomes (arrow). X63,400.

5,58

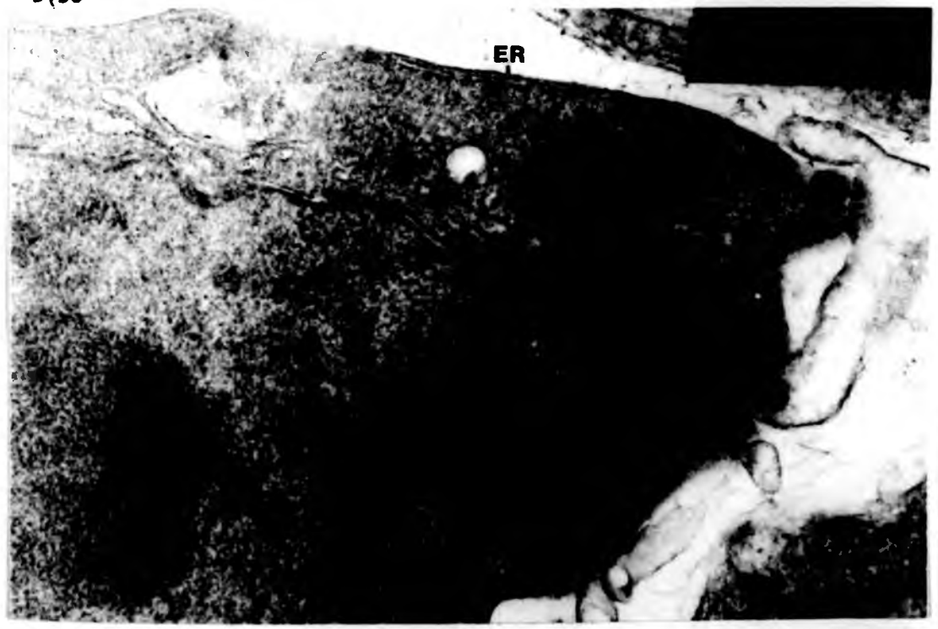

Fig. 5.59 TEM of the protoscolex soma tegument. An active Golgi complex (G) is present in the cyton and possesses cisternae with dense contents (arrow) at the maturing face. The vesicles (V) produced by the Golgi complex eventually contain an electron-dense core. DC; distal cytoplasm. X29,200.

5.59

Fig. 5.60 TEM of the protoscolex soma tegument showing characteristic T_1 vesicles in the cytons and distal cytoplasm. G; Golgi complex, M; mitochondria. X39,100.

5.60

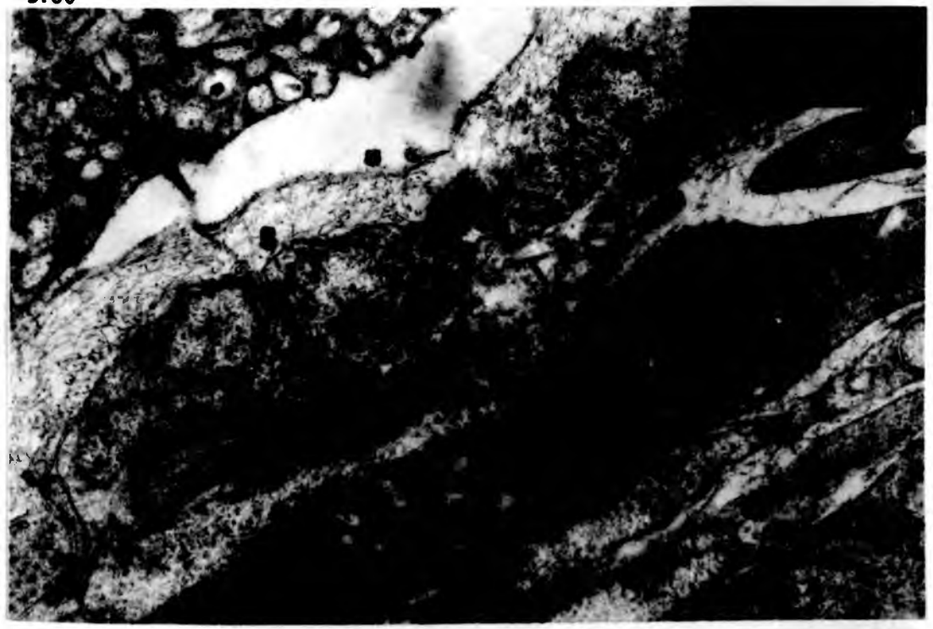

Fig. 5.61 TEM of the protoscolex sucker tegument. Numerous T_2 vesicles (T_2) are present in the distal cytoplasm and spined microtriches are present at the surface. These projections are of two types. Type 1 (Mt_1) have short brood shafts while type 2 (Mt_2) have longer, narrower shafts. X39,100.

Fig. 5.62 TEM of the major microthrix type on the sucker tegument. The spine (Sp) has a medulla (Md), which appears laminated, and a less dense cortical region (C). It is separated from the shaft (Sh) cortical region (C). It is separated from the shaft (Sh) by a base plate (BP). The shaft has an asymmetrical shaft support (SS) and often possesses longitudinal microfilaments (MF - see inset) T_2; T_2 vesicles, T_3; T_3 vesicles. X79,600. (inset, X121,000).

5.61

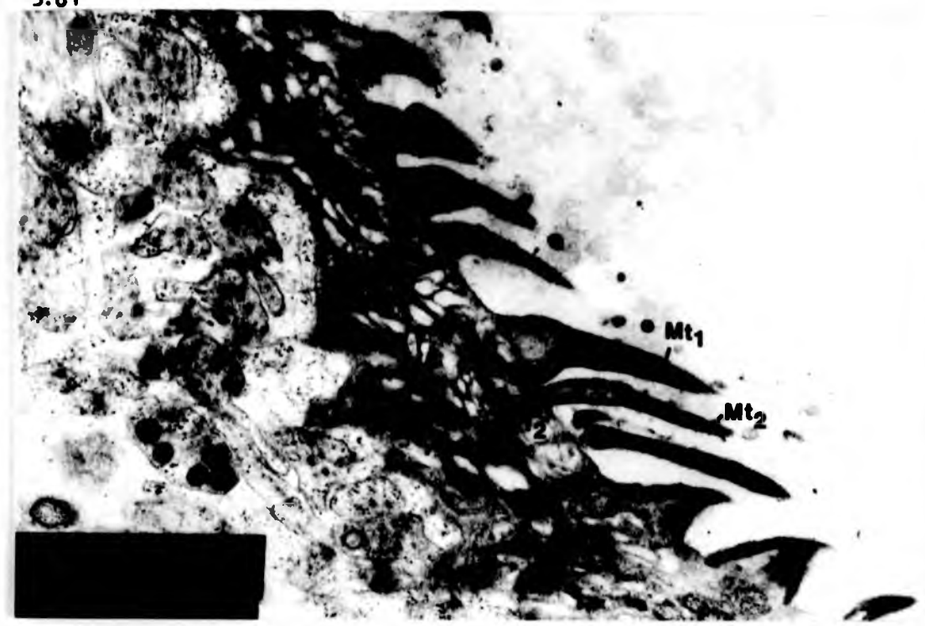

5.62

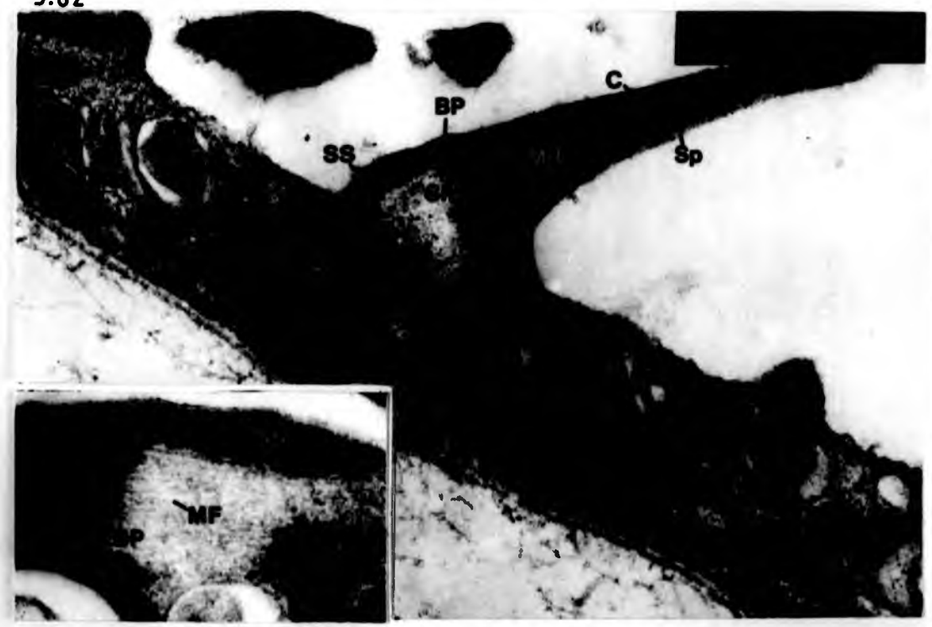

Fig. 5.63 TEM of a scolex microthrix spine in transverse section. Note that tubule-like structures (arrow) are present in the medulla. C; cortex. X214,000.

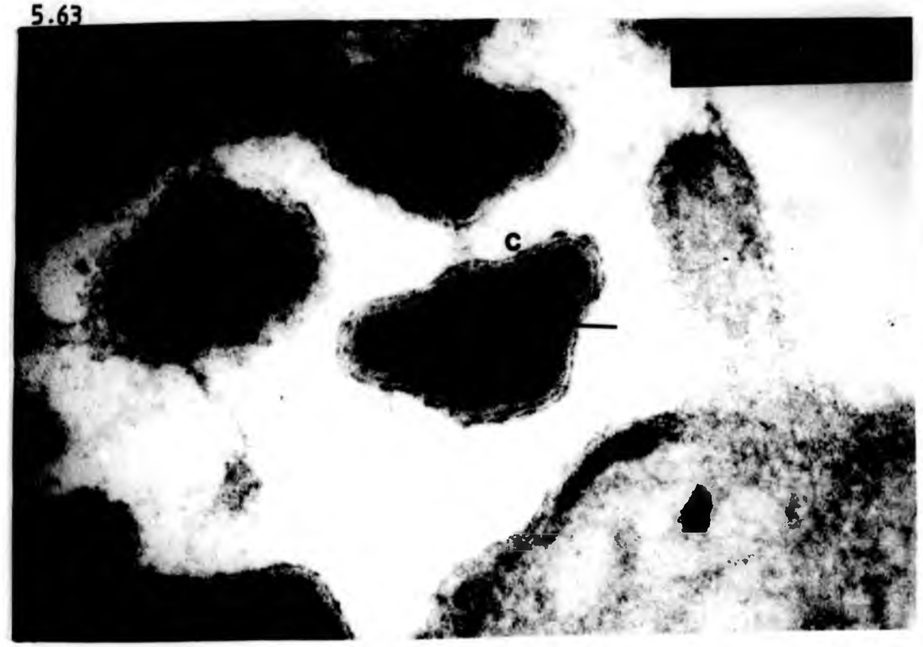

Fig. 5.64 TEM of the rostellar tegument of the protoscolex. The rostellar microtriches possess short narrow shafts (Sh) and long, filamentous spines (Sp). T_2l; T_2 vesicles. X39,100.

Fig. 5.65 TEM of the rostellar microtriches showing the baseplate (BP) as an elongate tubular structure. Sh; shaft, Sp; spine, H; hook. X63,400.

Fig. 5.66 SEM of the scolex of a protoscolex. The rostellar microtriches (R) are long and filamentous and obscure the rostellar hooks (H). Sk; sucker. X1,500.

5.65

5.66

Fig. 5.67 TEM of the rostellum of a protoscolex showing a rostellar hook (H) within the tegumentary distal cytoplasm. X5,480.

Fig. 5.68 TEM of the rostellar, tegumentary distal cytoplasm. The hooks (H) are seen in transverse section and are surrounded by very long infolds of the basal plasma membrane (BI). X79,600.

5.67

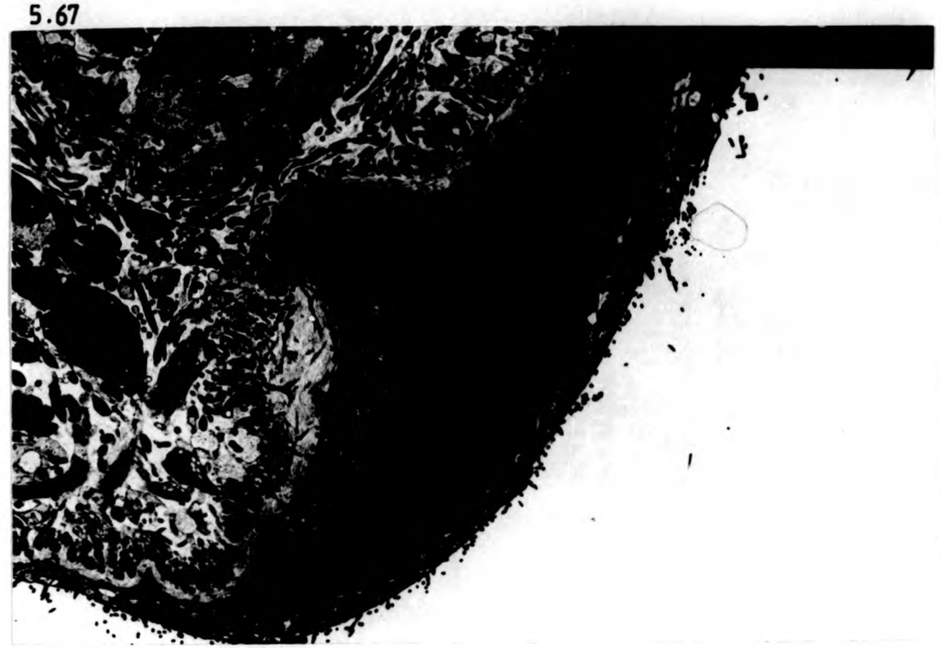

5.68

Fig. 5.69 SEM of the protoscolex rostellar hooks (H) in an extended condition. The hooks are entirely covered by microthrix bearing tegument. Mt; microtriches. X7,500.

5.69

Fig. 5.70 TEM of the protoscolex rostellar tegument. A sensory bulb (B) is present in the distal cytoplasm. The bulb possesses a cilium (C) which extends to the exterior and a large mitochndrion (M). The bulb is held in place by a septate desmosome (arrows) and had an inner electron dense collar (Co). X63,400.

5.70

Fig. 5.71 TEM of a scolex tegumentary cyton. A large prominent nucleus (N) is present and Golgi complexes (G) possessing cisternae with dense contents occur in the perinuclear cytoplasm. X39,100.

Fig. 5.72 TEM of tegumentary cytons from the scolex region of a protoscolex. Dense flocculent T_2 vesicles (T_2) are present in the perinuclear cytoplasm. N; nucleus. X20,500.

5.71

5.72

Fig. 5.73 LM section of an invaginated protoscolex incubated with FITC labelled WGA. The lectin has bound to the surface of the soma tegument (arrow) and various internal structures. CC; calcareous corpuscles. X958.

Fig. 5.74 LM section of an invaginated protoscolex incubated with FITC labelled SBA. The lectin has bound to the surface of the soma tegument (arrow) and around the calcareous corpuscles (CC). X958.

Fig. 5.75 LM section of an invaginated protoscolex incubated with FITC labelled PNA. The lectin has bound to the surface of the soma tegument (arrow). X958.

5.73

5.74

5.75

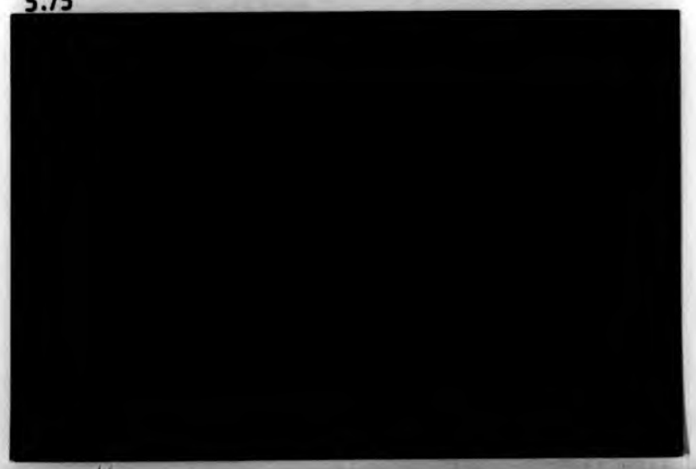

Fig. 5.76 LM section of an invaginated protoscolex incubated with FITC labelled APA. THe lectin has not bound to the parasite and only the autofluorescence of the hooks (H) is evident. X958.

Fig. 5.77 LM section of an invaginated protoscolex incubated with FITC labelled Con A. The lectin has only bound to structures within the body of the protoscolex and not to the tegumentary surface (arrow). X1520.

Fig. 5.78 LM section of an invaginated protoscolex in PNA plus galactose (control). Binding of the lectin has been inhibited by the presence of the sugar and only the autofluorescence of the hooks (H) is evident. X958.

5.76

5.77

5.78

Fig. 5.79 LM whole mount of an invaginated protoscolex incubated in FITC labelled SBA. Bright fluorescence is evident around the soma surface. The hooks (H) and calcareous corpuscles (CC) show autofluorescence. X380.

Fig. 5.80 LM whole mount of invaginated protoscoleces (unincubated control) showing the autofluorescence of the hooks (H) and calcareous corpuscles (CC). X380.

Fig. 5.81 LM whole mount of an evaginated protscolex incubated with FITC labelled SBA. The lectin has bound strongly to the soma surface (So) but not to the scolex (Sc). X380.

5.79

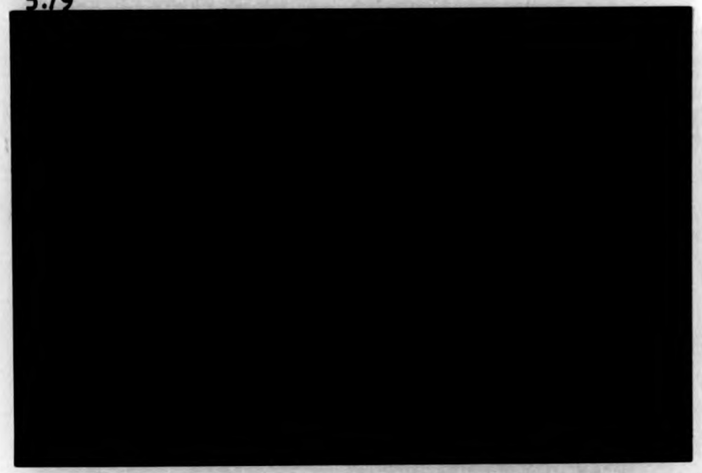

5.80

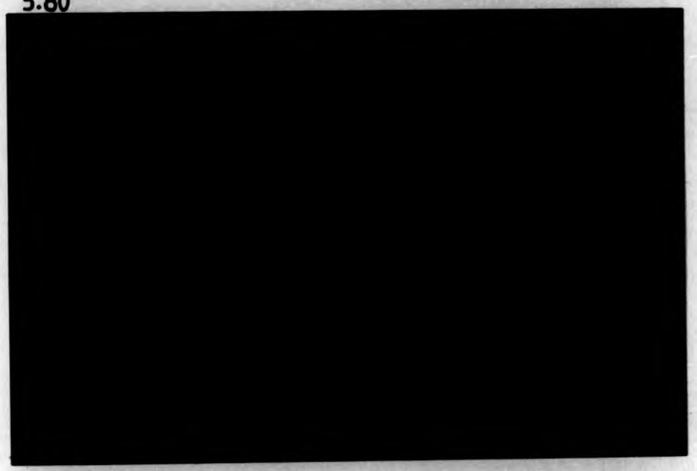

5.81

Fig. 5.82 TEM of the soma tegument of a protoscolex stained for carbohydrate using the periodic acid-thiosemicarbazide reaction. A dense reaction product is present in the glycocalyx (Gx) and the glycogen reserves (Gl). The distal cytoplasm (DC) and cytons (C) are, however, virtually unstained. X11,000.

5.82

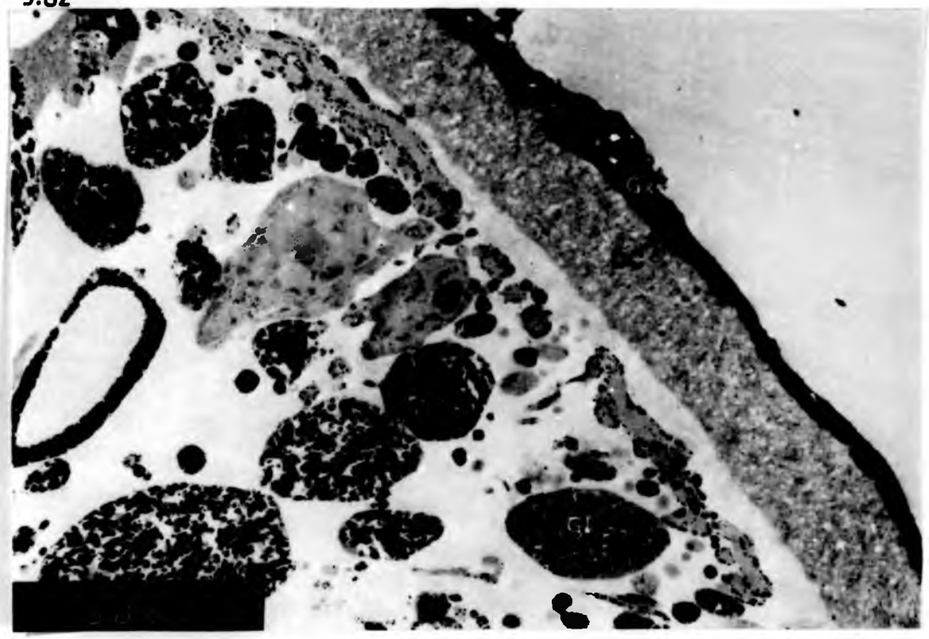

Fig. 5.83 TEM of the anterior soma tegument of a protoscolex stained for carbohydrate using the periodic acid - thiosemicarbazide reaction. A reaction product is present in the glycocalyx (Gx) and in some of the tegumentary vesicles (arrows) which are presumably T_2 in nature. X63,400.

5.83

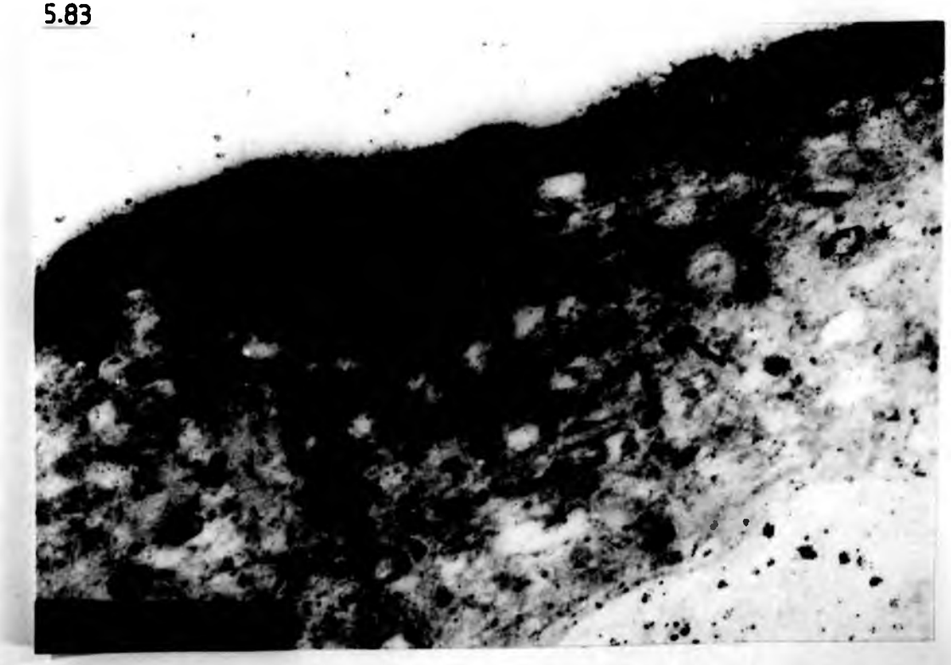

Fig. 5.84 TEM of the scolex tegument of a protoscolex stained for carbohydrate using the periodic acid - thiosemicarbazide reaction. The T_2 vesicles (T_2) in the distal cytoplasm stain densly for carbohydrate whilst a light reaction is observable on the microthrix spines (Sp). X63,400.

Fig. 5.85 TEM of the scolex tegument of a control protoscolex for the periodic acid - thiosemicarbazide reaction (minus periodic acid). The vesicles of the distal cytoplasm do not give a positive reaction. Mt; microthrix. X63,400.

5.84

5.85

Fig. 5.86 TEM of the scolex tegumetn of a control protoscolex for the periodic acid - thiosemicarbazide reaction (minus periodic acid). No reaction product is present in either the tegument or associated glycogen reserves. X20,500.

5.86

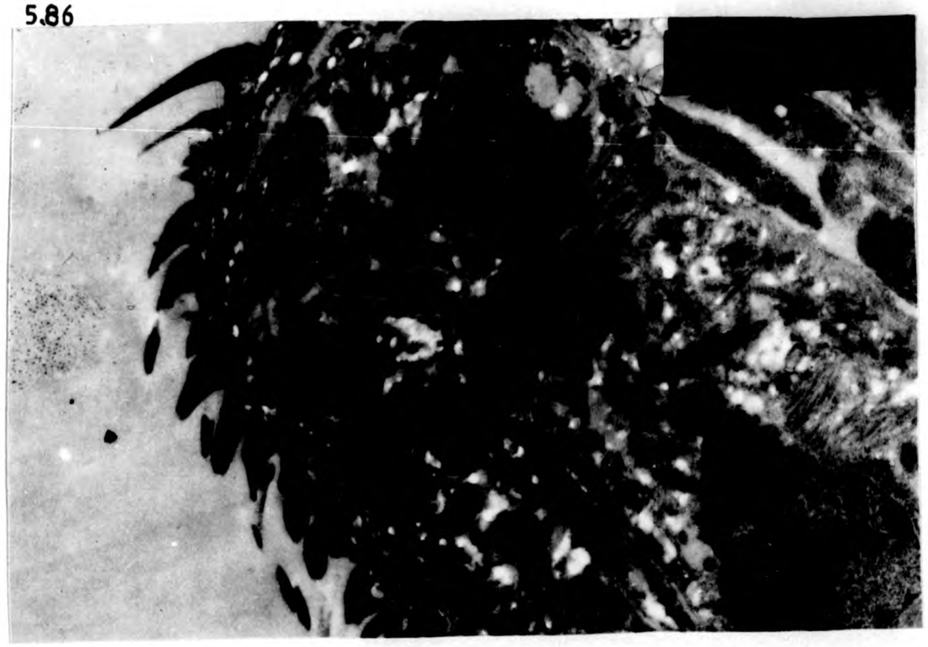

Fig. 5.87 TEM of the scolex tegument of a protoscolex stained for carbohydrate using the periodic acid - thiosemicarbazide reaction. A positive reaction is present in the tegumentary vesicles (V) and the glycogen reserves (Gl). X11,000.

5.87

Fig. 5.88 TEM of a scolex tegumentary cyton stained for carbohydrate using the period acid - thiosemicarbazide reaction. The T_2 vesicles (V) in the perinuclear cytoplasm give a positive reaction. Ms; muscle. X29,200.

5.88

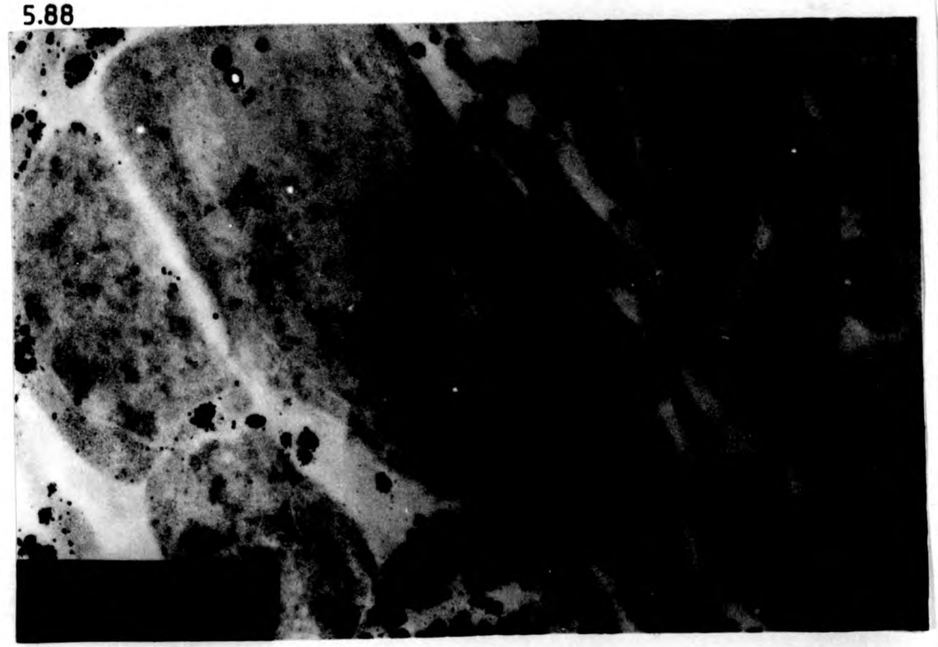

Volume Two

part B

CHAPTER SIX.

ULTRASTRUCTURAL CHANGES OCCURRING IN THE PROTOSCOLEX TEGUMENT DURING CYSTIC DEVELOPMENT IN VIVO AND IN VITRO.

Fig. 6.1 TEM of the parasite surface 4 days p.i. Note the large number of host leucocytes at the surface of the tegumentary distal cytoplasm (DC). THe host cells are mainly of macrophage (Mo) or eosinophil (E) origin. X5,230.

6.1

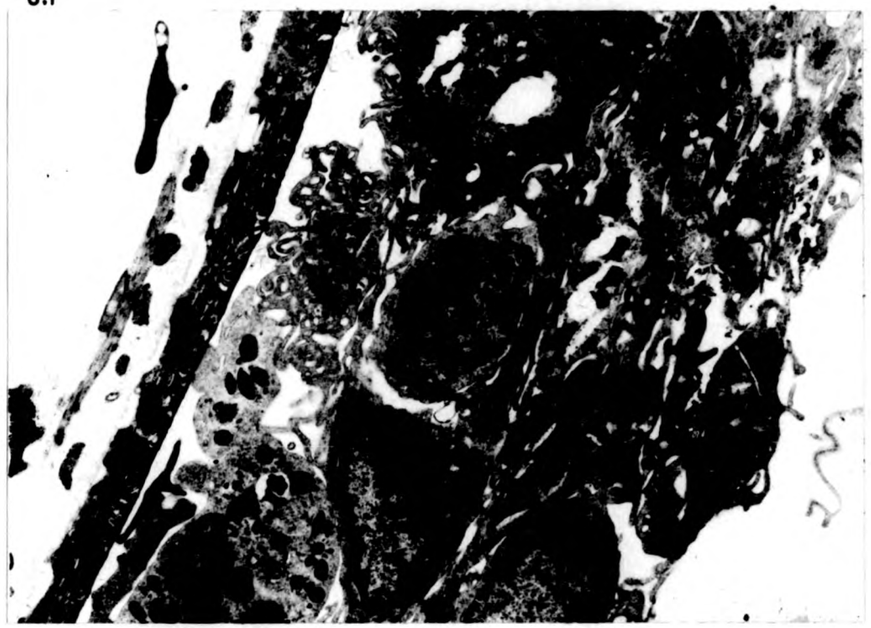

Fig. 6.2 TEM of the host cellular response 4 days p.i. showing macrophages in an activated state possessing large pseudopodia (P) and residual bodies (R) N; nucleus. X15,200.

6.2

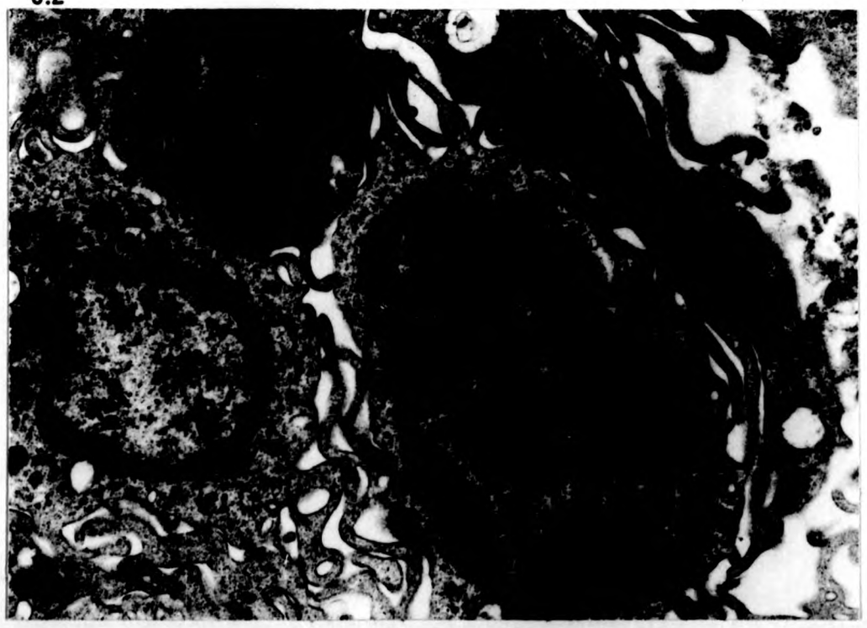

Fig. 6.3 TEM of the soma surface of a protoscolex 4 days p.i. Note that the blunt elevations (arrows) have become flattened and the extensive glycocalyx has been lost. T_2 vesicles (T_2) were becoming more prominent in the distal cytoplasm and existed with T_3 vesicles (T_3). Mo; macrophage. X76,400.

6.3

Fig. 6.4 TEM of the soma surface of a protoscolex 2 days p.i. The blunt elevations (arrows) have become flattened and the glycocalyx has been lost. T_1 ad T_3 vesicles are the most prominent within the distal cytoplasm (DC). Golgi complexes (G) are evident in the cytons and abundant glycogen reserves (Gl) are present. X15,200.

6.4

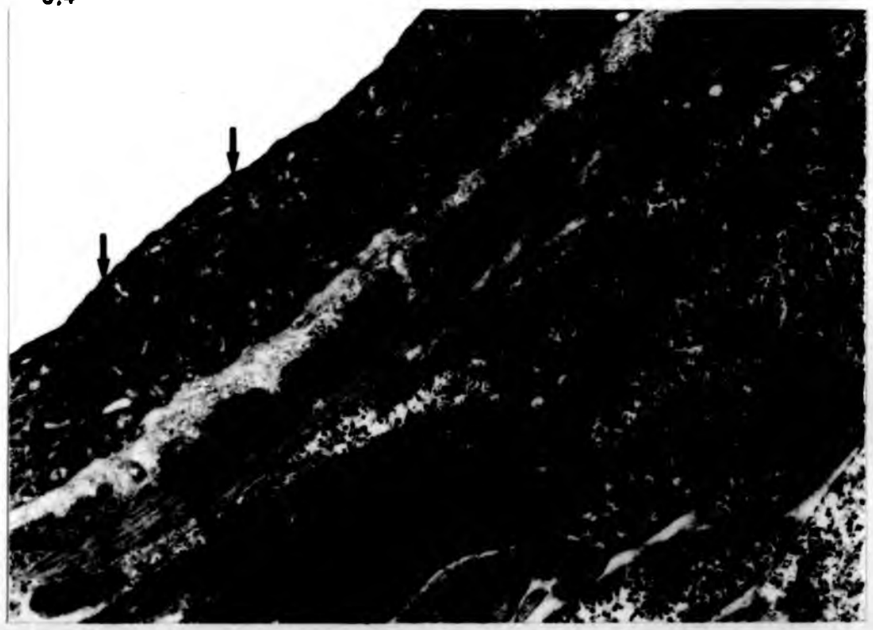

Fig. 6.5 TEM of the soma tegument of a protoscolex 4 days p.i. The number of T_1 vesicles has become reduced in the distal cytoplasm and these structures are outnumbered by T_2 and T_3 vesicles. Mo; macrophages. X44,200.

Fig. 6.6 TEM of the soma tegument of a protoscolex 4 days p.i. Within the cytons large numbers of ribosomes (R) are present, often associated with the peripheral endoplasmic reticulum (ER). Golgi complexes (G) producing T_2 vesicles and mitochondria (M) are also more evident. X15,200.

6.5

6.6

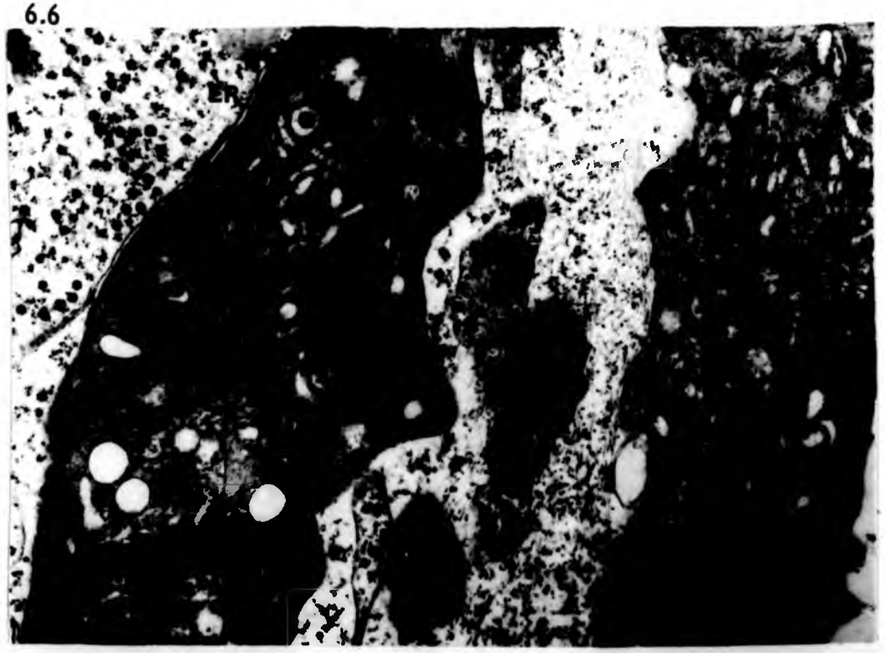

Fig. 6.7 TEM of the soma tegument of a protoscolex 4 days p.i. The distal cytoplasm (DC) has a vacuolated appearance due to detachment from the basement lamina (B) which may be caused by the host cells (Mo). Residual body-like structures (R) are also present in the distal cytoplasm. X20,000.

6.7

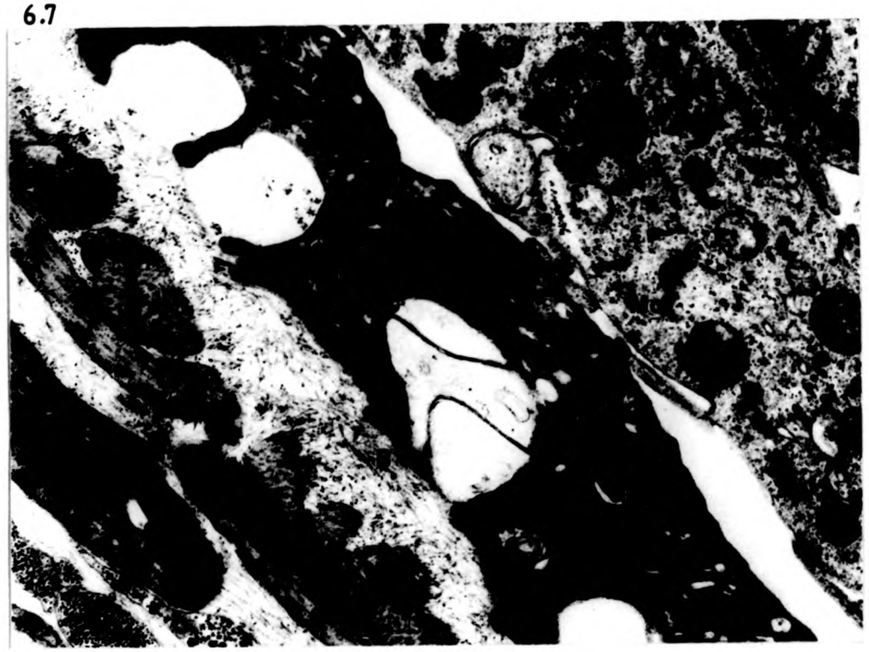

Fig. 6.8 TEM of the soma tegument of a protoscolex 4 days p.i. The distal cytoplasm is detaching severely from the basement lamina (B) in a region where eosinophils (E) are degenerating at the parasite surface. X11,000.

6.8

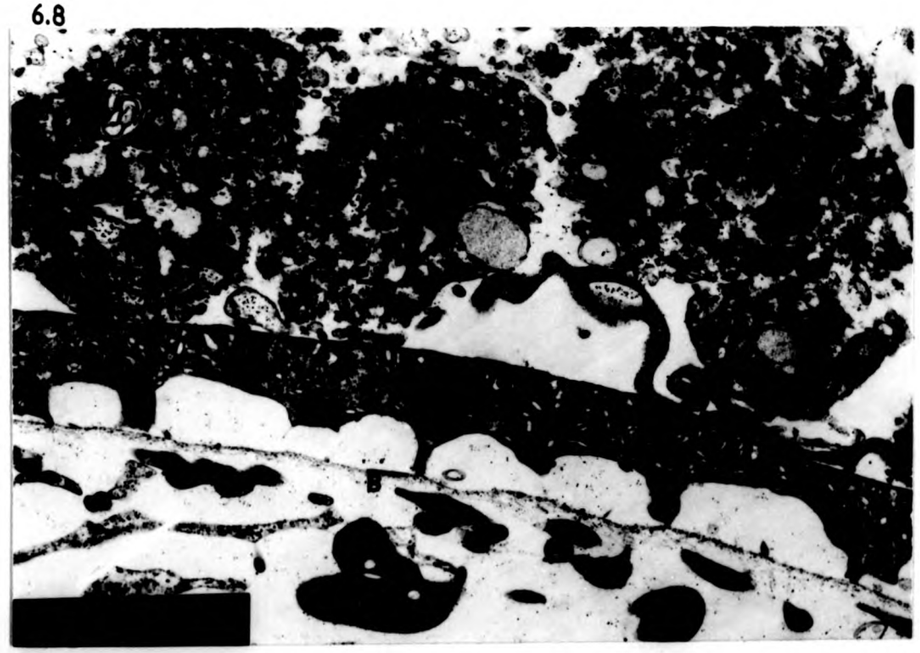

Fig. 6.9 TEM of the scolex region of a protoscolex 2 days p.i. THe entire tegumentary distal cytoplasm has been removed down to the suckers (Sk) and engulfed by host macrophages (Mo). Microthrix spines (Sp) can be seen within residual bodies in the macrophages. X15,200.

6.9

Fig. 6.10 TEM of the soma tegument of a protoscolex 7 days p.i. The number of T_2 vesicles (T_2) has now become dramatically increased in the distal cytoplasm and truncated microtriches (TM) are also becoming evident. X39,100.

6.10

Fig. 6.11 TEM of the soma tegument of a protoscolex 7 days p.i. Large numbers of mitochondria (M) are present in the cytons together with active Golgi complexes (G) and T_2 vesicles (T_2). X29,200. Inset: Golgi complex producing T_2 vesicles. X39,100.

Fig. 6.12 TEM of the soma region of a protoscolex 12 days p.i. stained for carbohydrates using the periodic acid-thiosemicarbazide method. The increased numbers of T_2 vesicles (T_2) in the distal cytoplasm give a strong reaction for carbohydrates. X39,100.

6.11

6.12

Fig. 6.13 TEM of the soma tegument of a protoscolex 12 days p.i. The distal cytoplasm is now packed with T_2 vesicles (T_2) and elongate mitochondria (M) are evident at its base. Truncated microtriches (TM) are becoming uplifted from the tegumentary surface. X29,200.

Fig. 6.14 TEM of the soma tegument of a protoscolex 12 days p.i. The cytons are occasionally packed with mitochondria (M). N; nucleus, DC; distal cytoplasm, G; Golgi complex. X29,200.

6.13

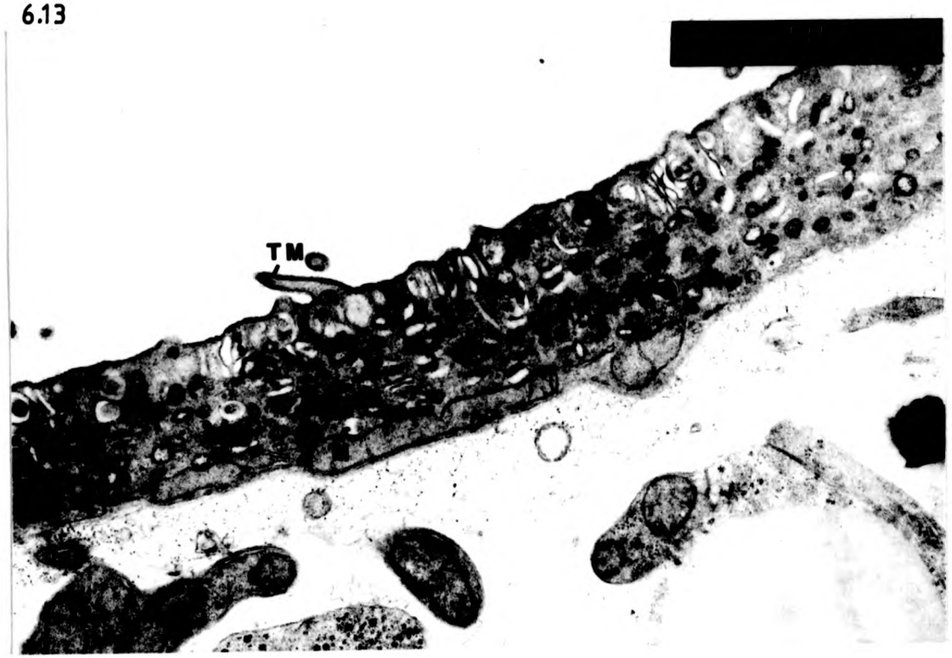

6.14

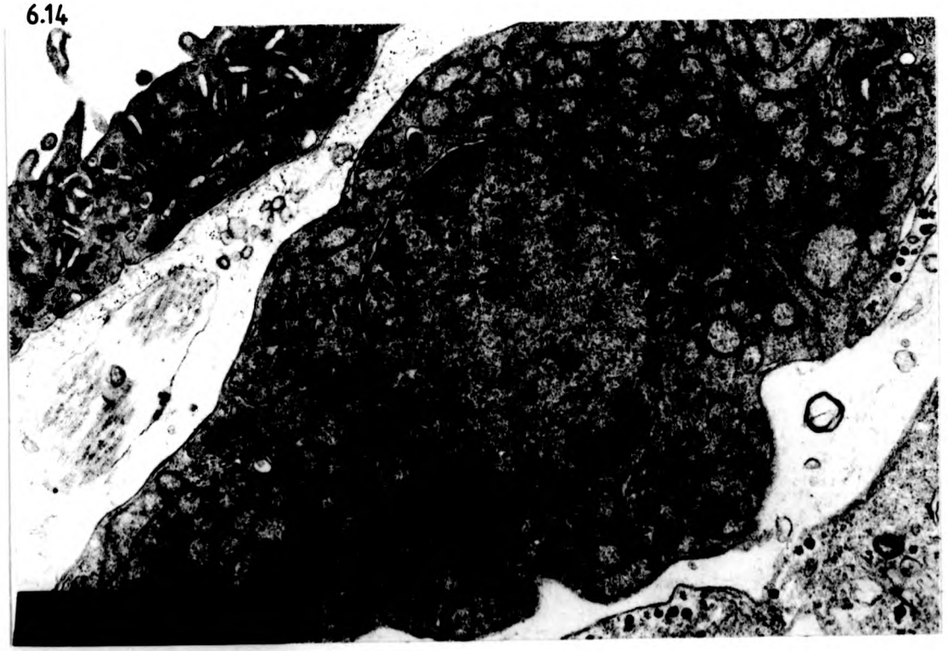

Fig. 6.15 TEM of the soma tegument of a protoscolex 4 days p.i. The distal cytoplasm is starting to produce truncated microtriches (arrows) which are formed by the electron-dense material (E.D.) of the now flattened blunt elevations forming the shaft support of the microthrix. The spherical base plate (BP) is present before elevation of the projections. X63,400.

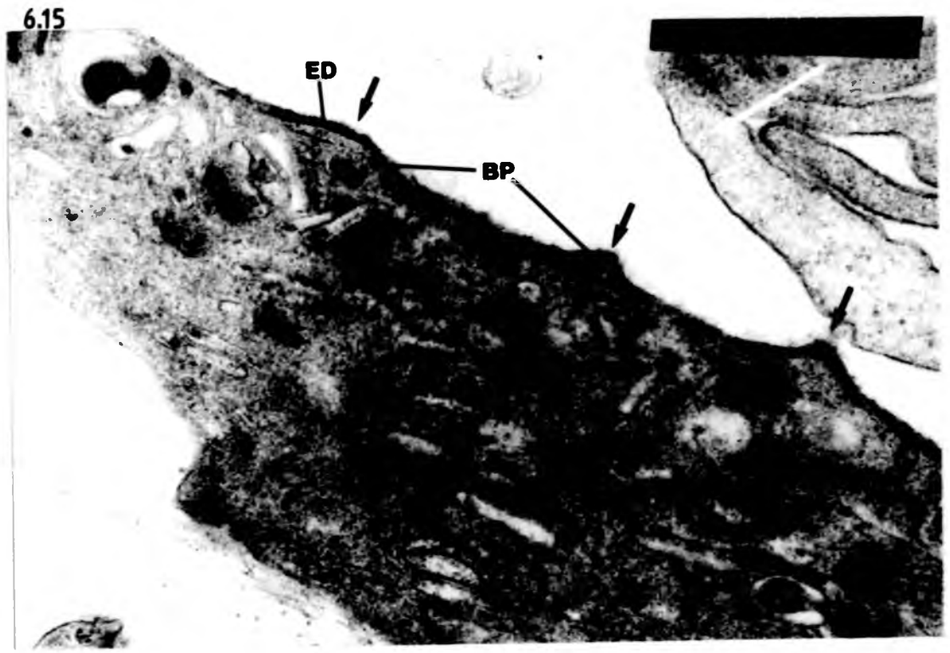

Fig. 6.16 TEM of the soma tegument of a protoscolex 7 days p.i. Truncated microtriches (TM) have become elevated from the tegument surface. Occasional T_2 vesicles (T_2) are seen in close proximity to the forming projections. X76,400.

Fig. 6.17 TEM of the host cellular response 10 days p.i. Most of the cells in the immediate vicinity of the parasites are degenerating. E; eosinophil granules, N; nucleus. X9,250.

Fig. 6.18 TEM of the tegument of a protoscolex 28 days p.i. The entire distal cytoplasm above the basement lamina (B) has been severely disrupted and the mitochondria (M) appear to have abnormal cristae. TM; truncated microthrix. X15,200.

6.17

6.18

Fig. 6.19 TEM of the scolex tegument of a protoscolex 28 days p.i. The distal cytoplasm possesses both T_2 vesicles and 'G' vesicles and also T_2 vesicles which have an electron-dense granule in them (arrows) (see inset). Spined microtriches (Mt) are still present at the surface. X39,100. Inset X121,000

6.19

Fig. 6.20 TEM of a scolex tegumentary cyton from a protoscolex 30 days p.i. Both T_2 vesicles (T_2) and 'G' vesicles (G) are present within the same perinuclear cytoplasm. M; mitochondria, Go; Golgi complex. X63,400.

6.20

Fig. 6.21 TEM of a developing cyst 30 days p.i. The tegument of the original soma region now possesses abundant 'G' vesicles (G) and reduced numbers of T_2 vesicles (T_2). The early laminated layer (LL) appears as strands of amorphous material possessing clumps of electron dense granules (Gr). TM; truncated microtriches. X39,100.

Fig. 6.22 TEM of a developing cyst 30 days p.i. In some cases the laminated layer (LL) possesses membraneous vesicles (Vs) in addition to the electron-dense granules (Gr). G; 'G' vesicles, T_2; T_2 vesicles, TM; truncated microtriches. X63,400.

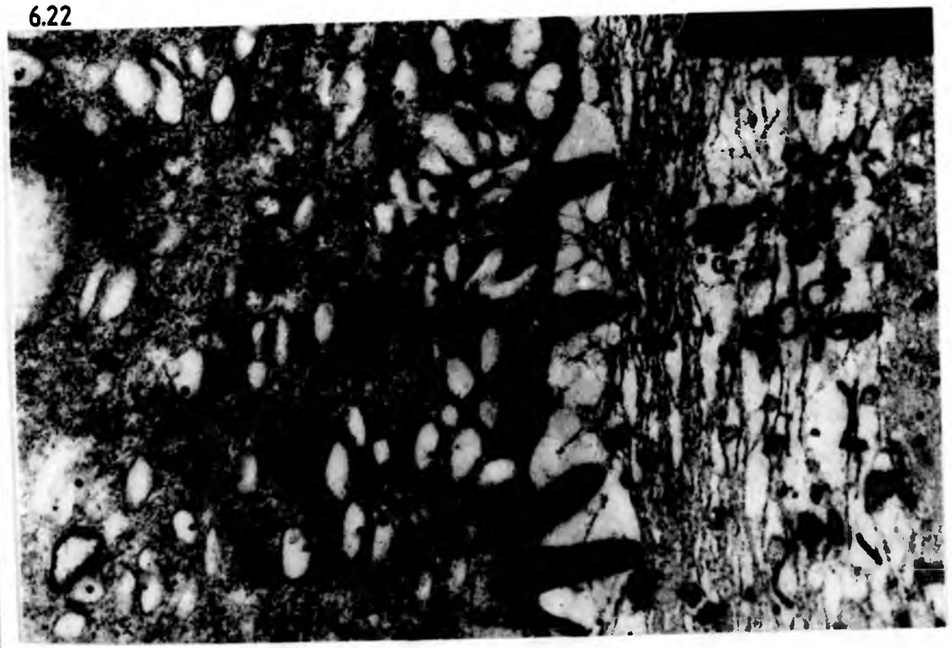

Fig. 6.23 TEM of the tegumentary distal cytoplasm of a developing cyst 30 days p.i. Numerous T_2 vesicles (T_2) are present together with 'G' vesicles (G). The lamianted layer (LL) possesses both aggregates of dense granules (arrow) and membraneous vesicles (Vs). X33,600.

6.23

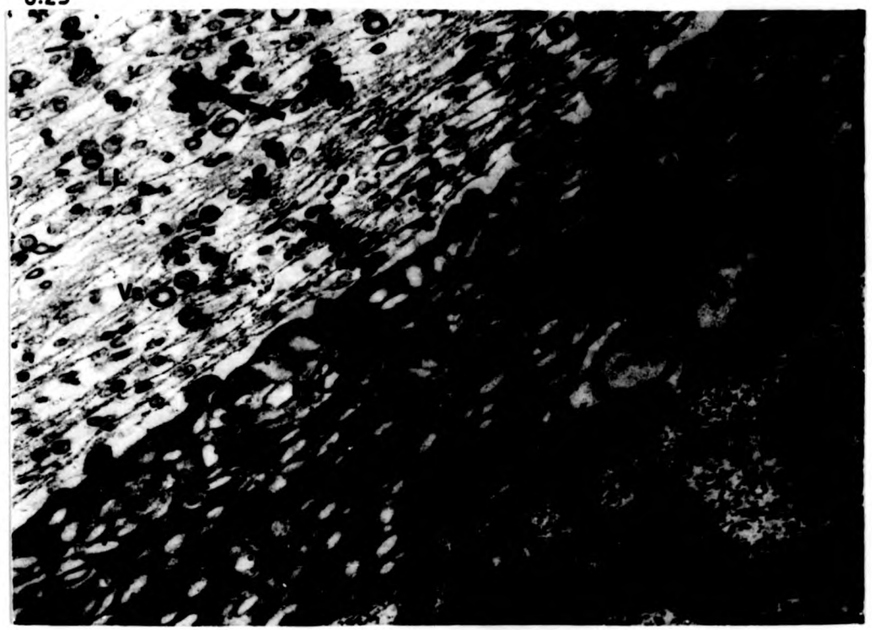

PAGINATION
ERROR

Fig. 6.25 TEM of the tegumentary distal cytoplasm of a developing cyst 54 days p.i. The T_2 vesicles have now disappeared from the tegument and 'G' vesicles (G) predominate. TM; truncated microtriches, LL; laminated layer. X39,100.

Fig. 6.26 TEM of a tegumentary cyton from a developing cyst 30 days p.i. The perinuclear cytoplasm is devoid of T_2 vesicles and 'G' vesicles predominate (G). Smaller granules (arrow) within the Golgi fields appear to contribute to the 'G' vesicles. X33,600.

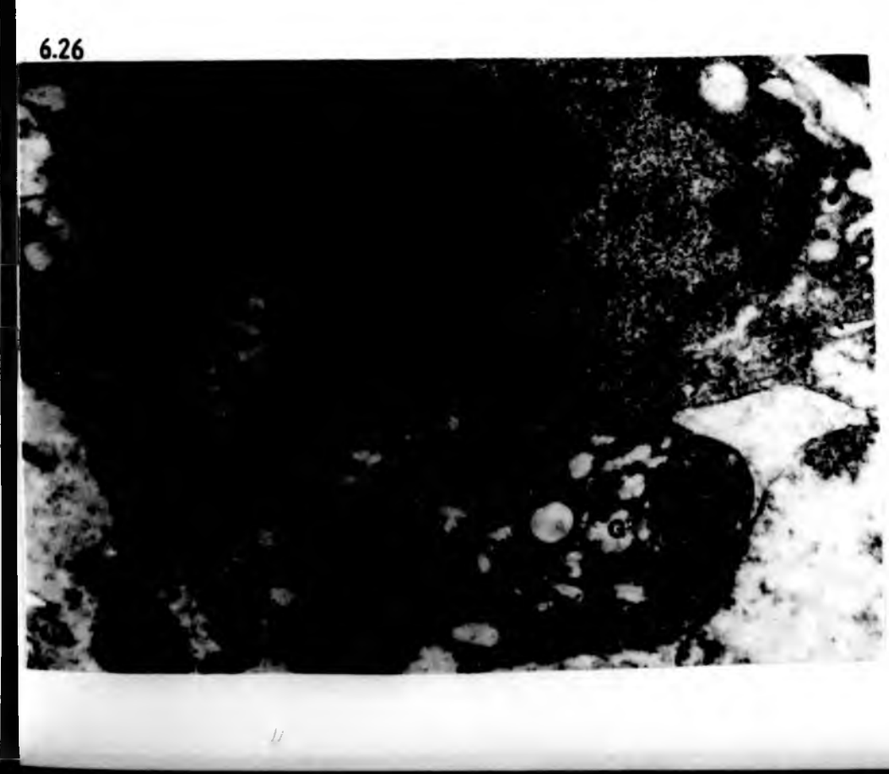

Fig. 6.27 TEM of a tegumentary cyton from a cyst 4 months p.i. A Golgi complex (G) is present and is active in the production of T_4 vesicles (T_4). Note that the cisternae of the maturing face possess flocculent contents (arrow) similar to that of the T_4 vesicles. ER; endoplasmic reticulum, M; Mitochondria. X103,000.

Fig. 6.28 TEM of the tegumentary distal cytoplasm of a cyst 4 months p.i. Occasional T_4 vesicles (T_4) are present together with the 'G' vesicles (G). LL; laminated layer Gl, glycogen reserves. X63,400.

Fig. 6.29 TEM of a sucker within the scolex of a developing cyst 30 days p.i. The sucker contains large bare areas (arrow) and appears to be degenerating. Residual bodies (R) are also present. P; periphery of the sucker. X7,170.

6.29

Fig. 6.30 TEM of the wall of a developing cyst 64 days p.i. The laminated layer (LL) is well developed and contains abundant granule aggregates. DC; tegumentary distal cytoplasm. X2,700.

6.30

Fig. 6.31 TEM of the host cellular response at the periphery of a developing cyst 54 days p.i. The active macrophage (Mo) is in the process of phagocytosing the electron-dense granules of the laminated layer (arrows). St; strands of laminated layer matrix material. X20,500.

Fig. 6.32 TEM of the laminated layer (LL) of a developing cyst 54 days p.i. The aggregates of electron dense granules appear larger (arrow) at the periphery of the laminated layer adjacent to the host cells (C). X9,250.

6.31

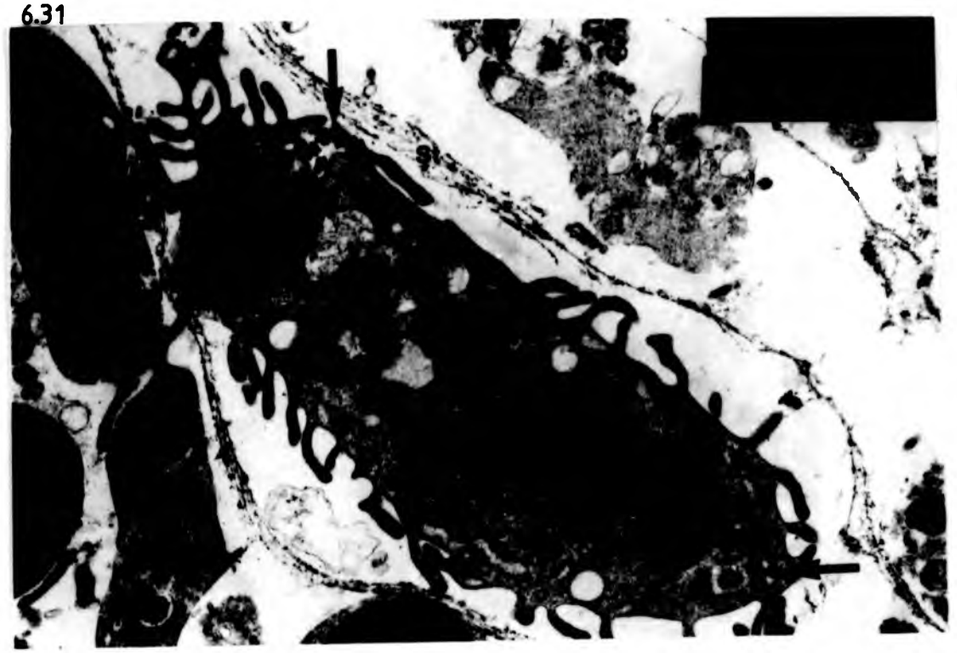

6.32

Fig. 6.33 TEM of the cyst wall of a developing cyst 64 days p.i. The microtriches (Mt) of the former scolex region have been shed into the laminated layer (LL) and replaced by a population of truncated microtriches (TM). X20,000.

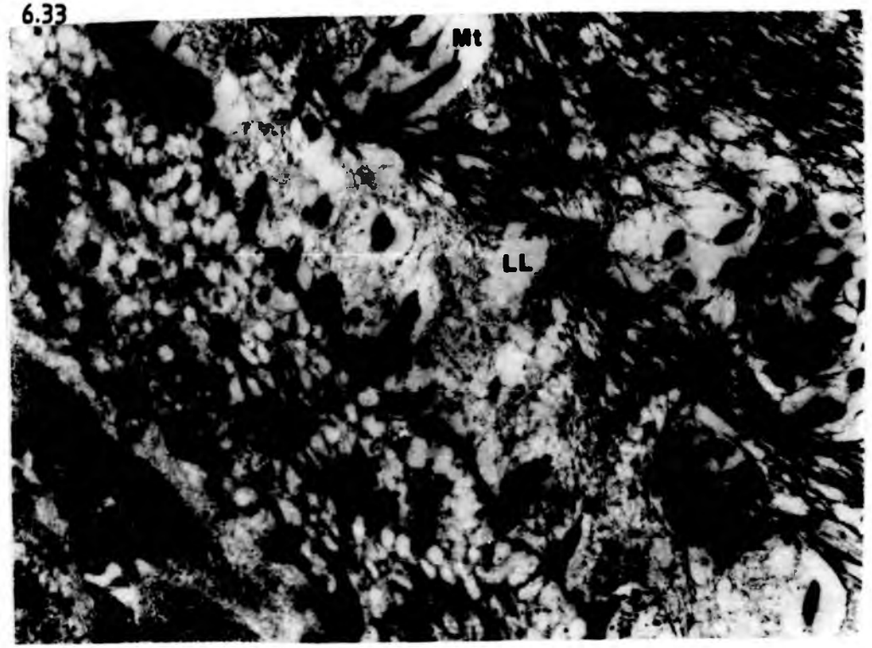

Fig. 6.34 TEM of a hook bud (B) from a developing cyst 54 days p.i. The hooks (H) have become dislodged and incorporated into a bud derived from the scolex distal cytoplasm (DC). LL; laminated layer. X3,570.

Fig. 6.35 TEM of a hook bud (B) released from a developing cyst 54 days p.i. H; hooks, LL; laminated layer. X5,230.

Fig. 6.36 TEM of a fully developed cyst 90 days p.i. Glycogen reserves within the germinal layer are sparse whilst large lipid droplets (Lp) are present. DC; Distal cytoplasm, C; cyton, LL; laminated layer. X7,170.

6.35

6.36

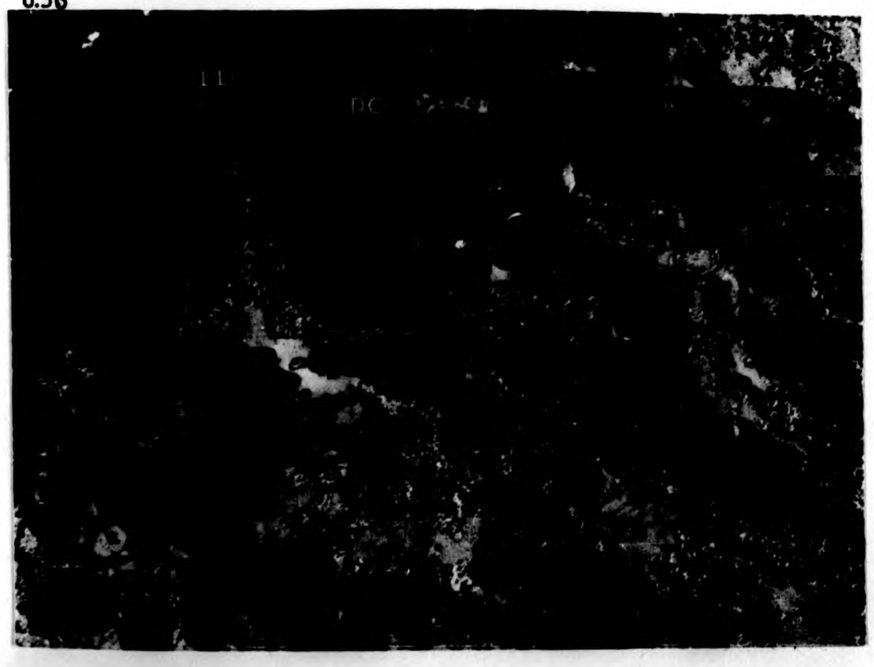

Fig. 6.37 TEM of the germinal layer of a fully formed cyst 6 months p.i. The distal cytoplasm (DC) is now mature and large glycogen reserves (Gl) are present in underlying cytoplasmic processes. LL; laminated layer. X6,590.

6.37

Fig. 6.38 TEM of the soma tegument of a protoscolex cultured in a diffusion chamber, 12 days p.i. There is a slight increase in the number of T_2 vesicles but no loss of the glycocalyx (Gx) has occurred. Not the dense non-specific deposit on the surface of the glycocalyx (arrow). X39,100.

6.38

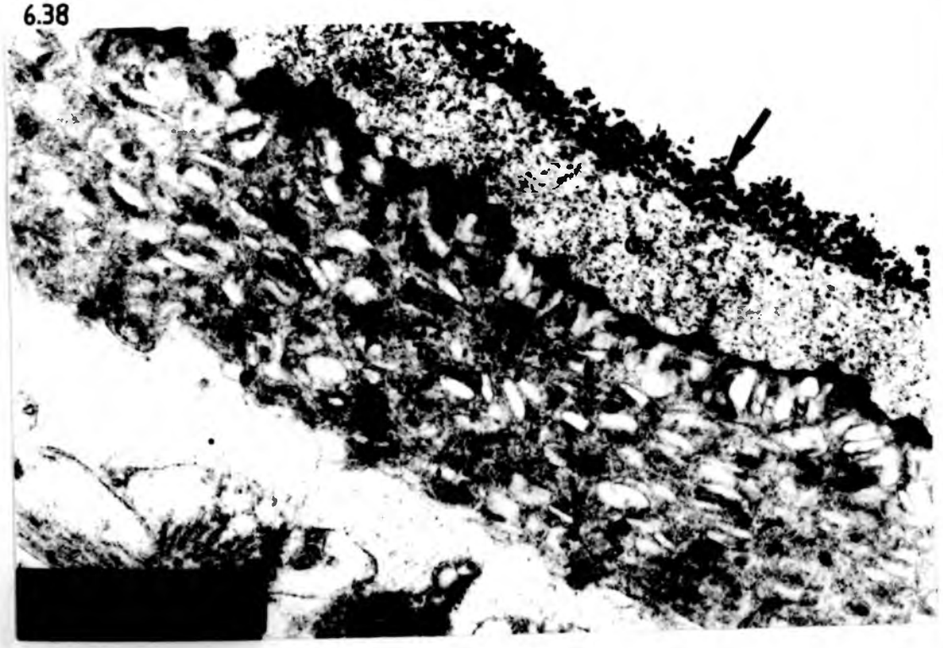

Fig. 6.39 TEM of a protoscolex cultured in a diffusion chamber, 4 days p.i. Note that severe lysis and stripping of the tegumentary distal cytoplasm (DC) has occurred in the scolex region. X8,960.

Fig. 6.40 TEM of the soma tegument of a protoscolex cultured in a diffusion chamber, 12 days p.i. Truncated microtriches (TM) are beginning to form as the blunt elevations (BE) become flattened. The glycocalyx (Gx), although less dense, is still evident at this stage. X39,100.

6.39

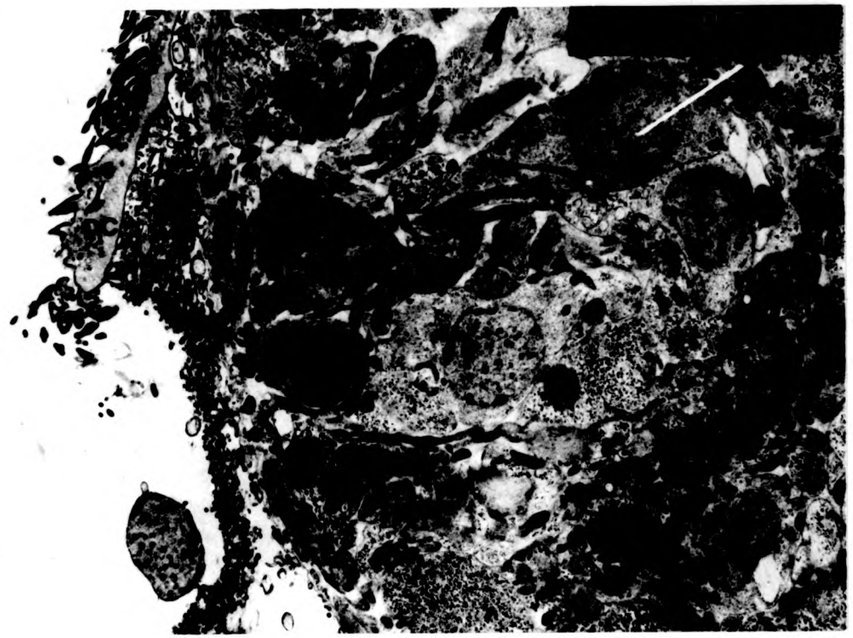

6.40

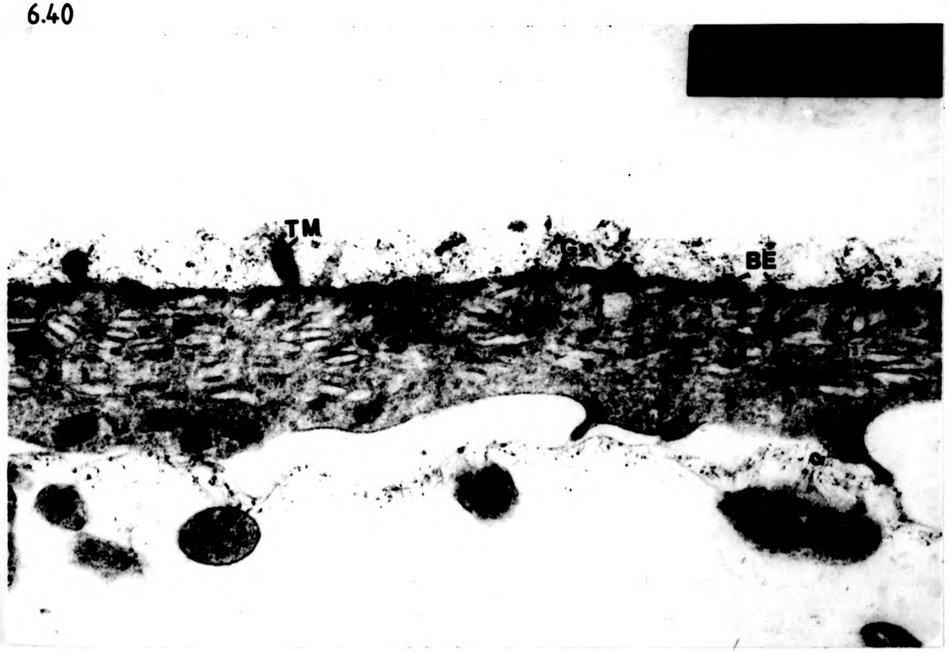

Fig. 6.41 TEM of the soma tegument of a protoscolex cultured in a diffusion chamber, 35 days p.i. Truncated microtriches (arrow) can be seen uplifting from the tegumentary surface at a time when the laminated layer (LL) is just forming. Note that this layer does not possess aggregates of electron-dense granules. BP; baseplate G; 'G' vesicles. X63,400.

6.41

Fig. 6.42 TEM of a tegumentary cyton of a developing cyst cultured in a diffusion chamber, 35 days p.i. 'G' vesicles (G) and T_4 vesicles (T_4) are present in the vicinity of the Golgi complexes (GC). M; mitochondrion. X63,400.

6.42

Fig. 6.43 TEM of a tegumentary cyton from a developing cyst cultured in a diffusion chamber, 35 days p.i. Carbohydrate-containing storage lysosomes (L) are increasingly evident and occasionally occur in close proximity to each other, presumably prior to coalescence (arrow). X39,100.

6.43

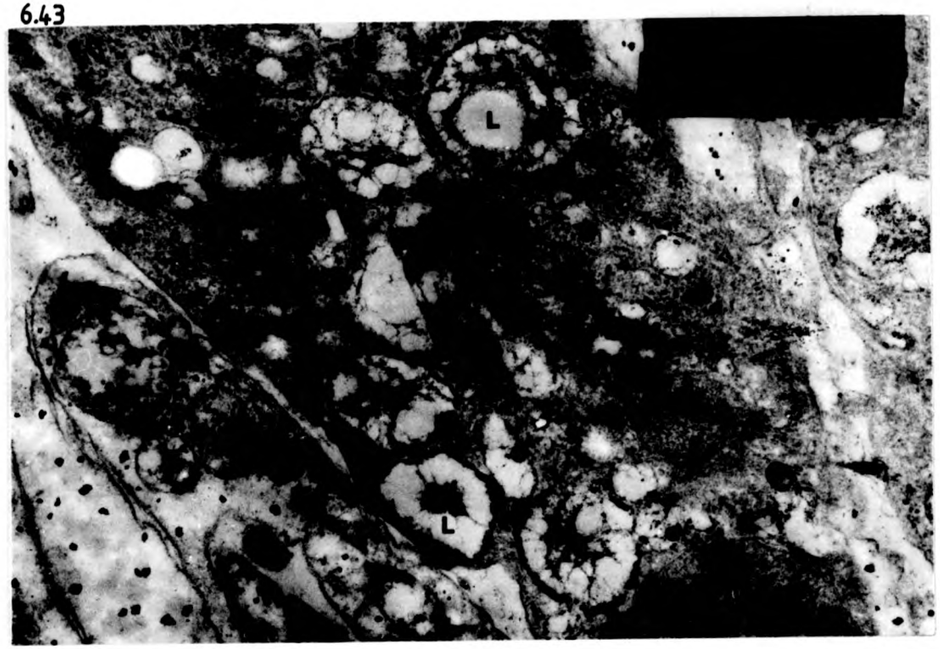

Fig. 6.44 TEM of the tegument of a developing cyst cultured in a diffusion chamber, 35 days p.i. Occasional cysts possessed host cells (HC) which had penetrated the chamber and become entrapped in the laminated layer (LL). Aggregates of electron dense granules were most evident near the entrapped cells (arrow). DC; Distal cytoplasm, C; cyto. X3,450.

6.44

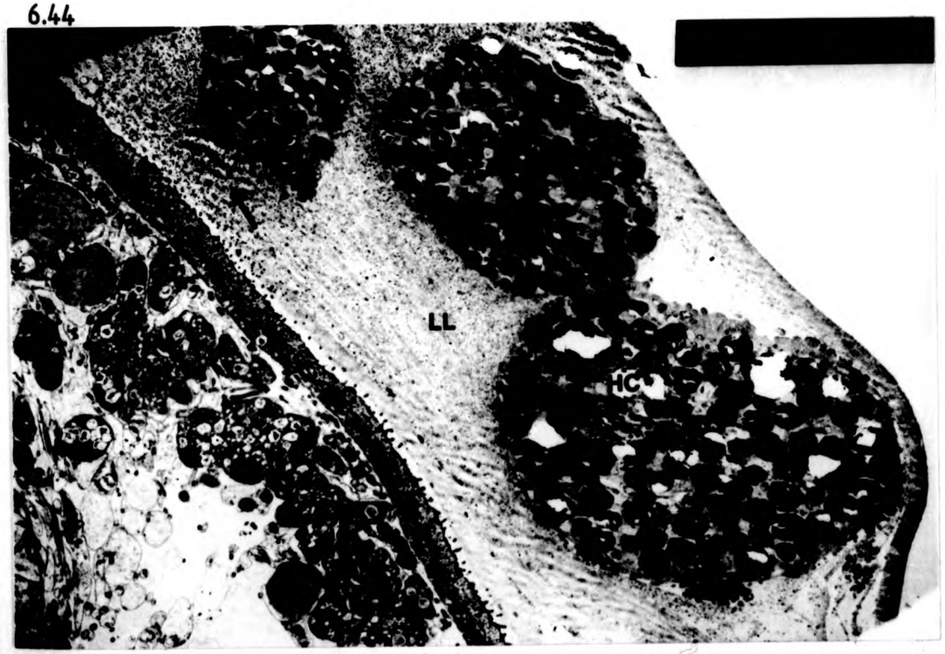

Fig. 6.45 TEM of the tegument of a developing cyst cultured in a diffusion chamber, 35 days p.i. 'G' vesicles (G) are present in both the distal cytoplasm and cytons but the laminated layer (LL) is generally devoid of electron dense aggregations. Membraneous vesicles (V) may, however, occur in the laminated layer. L; carbohydrate containing storage lysosomes. X11,000.

6.45

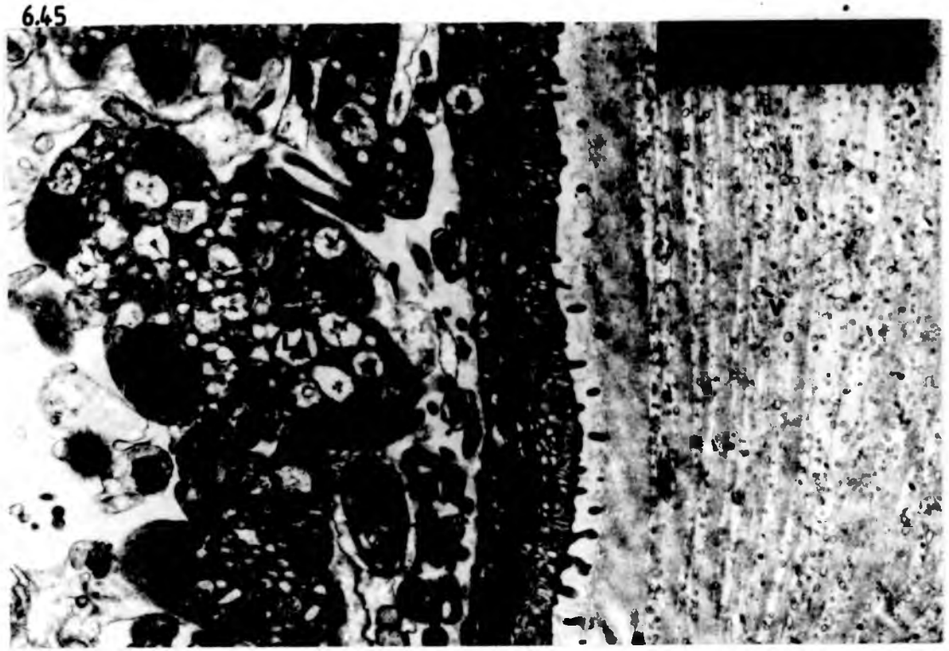

Fig. 6.46 TEM of the laminated layer of a cyst cultured in a diffusion chamber, 7 months p.i. Regional variations exist in the layer and aggregates of electron-dense granules (G) are present only in certain areas. In the remainder, the matrix is condensed into denser fibrillae (F). X29,200.

6.46

Fig. 6.47 TEM of the laminated layer of a cyst cultured in a diffusion chamber, 7 months p.i. The distribution of electron-dense granule aggregations (G) is 'patchy' and occurs between regions where denser fibrillae occur. X6,590.

6.47

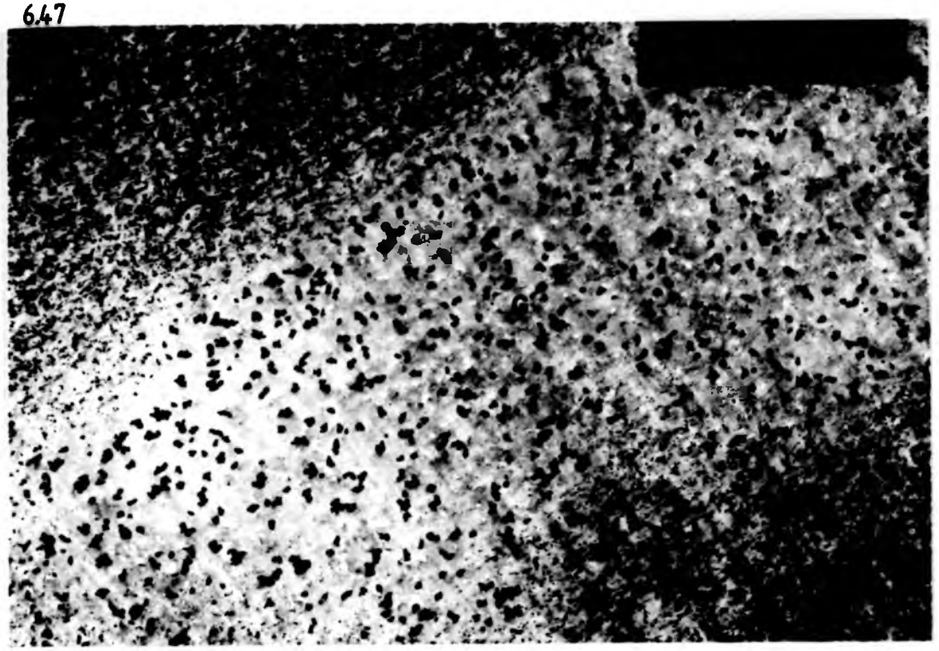

Fig. 6.48 TEM of the soma tegument of a protoscolex after 4 days in culture. The blunt elevations (BE) remain upright and the glycocalyx (Gx) is still evident. T_1; T_1 vesicles, T_2; T_2 vesicles. X58,000.

6.48

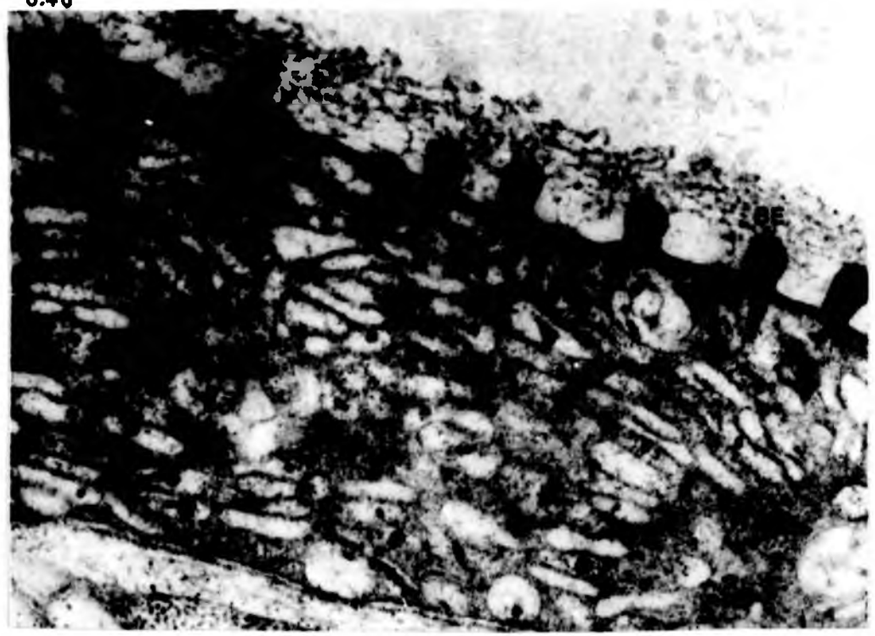

Fig. 6.49 TEM of a soma tegumentary cyton from a protoscolex after 9 days in culture. Golgi complexes (G) are present and active in the production of T_2 vesicles (T_2). M; mitochondrion, ER; endoplasmic reticulum, Gl; glycogen containing extension. X33,600.

6.49

Fig. 6.50 TEM of the scolex tegument of a protoscolex after 9 days in culture. Golgi complexes (G) within the cytons are active in the production of T_2 vesicles (T_2). LM; longitudinal muscle CM; circular muscle. X20,000.

6.50

Fig. 6.51 TEM of the soma tegument of a protoscolex cultured *in vitro* for 14 days. The glycocalyx (Gx) has become reduced in depth but is still evident. The blunt elevations (BE) have also become reduced in height and increased T_2 vesicles are present in the distal cytoplasm. X39,100.

6.51

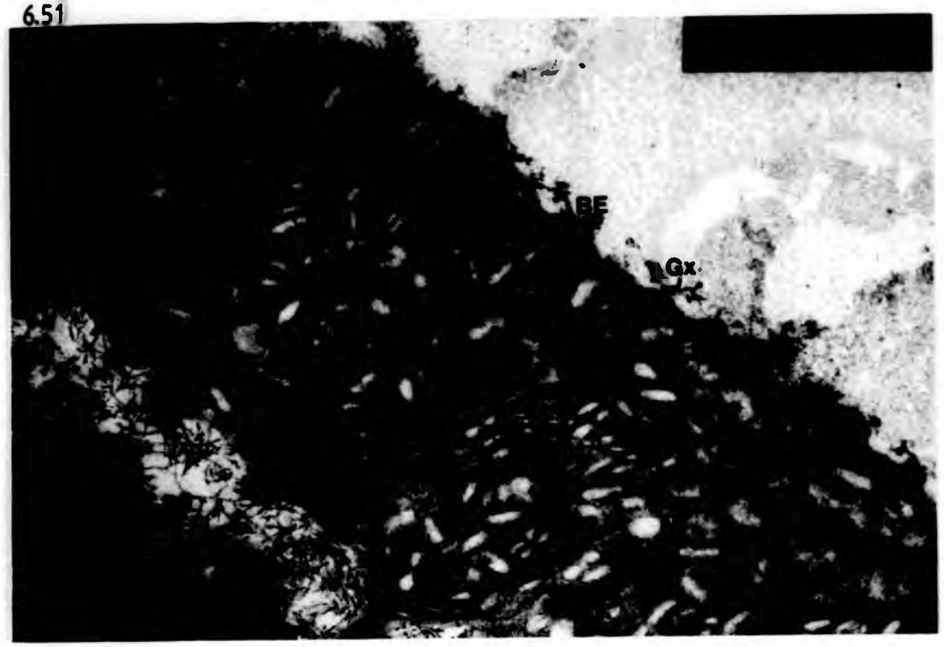

Fig. 6.52 TEM of the soma tegument of a protoscolex cultured *in vitro* for 21 days. The protoscolex has vesiculated and the tegumentary distal cytoplasm (DC) has become narrower. Cytons are not numerous and widely spaced appart leaving 'bare' areas of distal cytoplasm. X8,960.

6.52

Fig. 6.53 TEM of the soma tegument of a protoscolex cultured *in vitro* for 28 days. Truncated microtriches (TM) are beginning to form although a small amount of glycocalyx material (Gx) is still present. The cytons contain abundant mitochondria (M) some of which appear swollen (arrow). X14,200.

6.53

Fig. 6.54 TEM of the soma tegument of a protoscolex cultured *in vitro* for 14 days. The truncated microtriches (TM) form parallel to the tegumentary surface and are subequently uplifted into an upright position. X14,200.

6.54

Fig. 6.55 TEM of the soma tegument of a protoscolex cultured *in vitro* for 28 days. The distal cytoplasm contains both T"2: vesicles (T_2) and 'G' vesicles (G). TM; truncated microtriches. X44,200.

6.55

Fig. 6.56 TEM of a tegumentary cyton from a developing cyst cultured *in vitro* for 40 days. 'G' vesicles (G) and T_4 vesicles (T_4) are present in the perinuclear cytoplasm. X28,200.

6.56

Fig. 6.57 TEM of the soma tegument of a developing cyst cultured *in vitro* for 30 days. The laminated layer (LL) has just started to appear and T_4 vesicles (T_4) are present in the distal cytoplasm storage lysosomes (L) are present in the cytons. X15,200.

Fig. 6.58 TEM of the scolex tegument of a protoscolex cultured *in vitro* for 40 days. 'G' vesicles (G) are present in the distal cytoplasm and cytons but the early laminated layer (LL) lacks electron-dense aggregations and consists only of a microfibrillate matrix. X11,000.

6.57

6.58

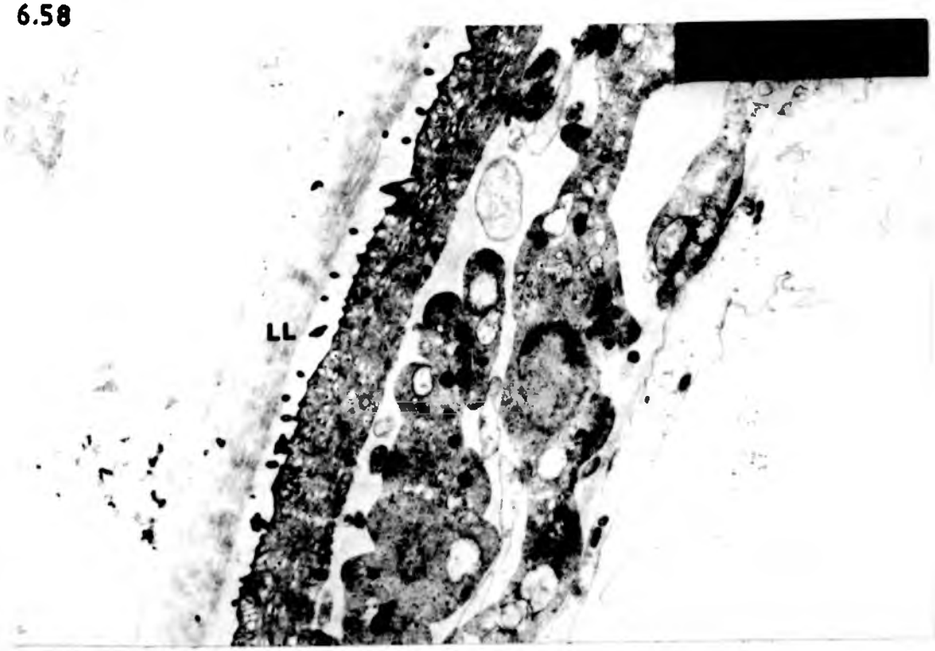

Fig. 6.59 TEM of the cyst wall of a cyst cultured *in vitro* for 84 days. The laminated layer possesses dense fibrillate components (arrow) which appear different to the granule accumulations present *in vivo* (see inset). G; 'G' vesicles, TM; truncated microtriches. X63,400.

6.59

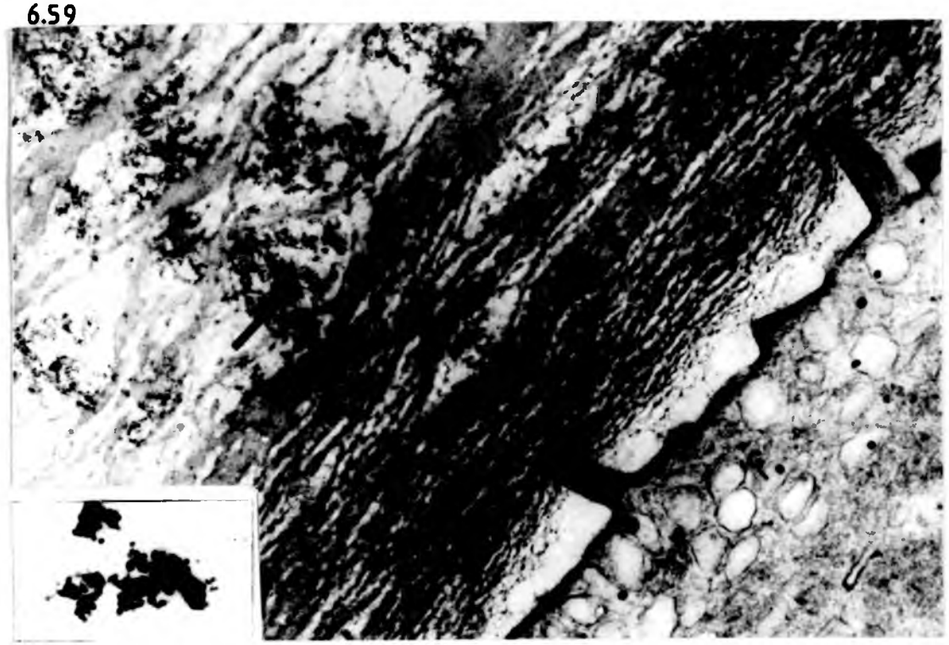

Fig. 6.60 TEM of the scolex tegument of a developing cyst cultured *in vitro* for 84 days. Spined microtriches (Mt) are only occasionally present beneath the laminated layer (LL) and are being replaced by a population of truncated microtriches (TM). T_4 vesicles (T_4) are present some of wich contain dense granules (arrow). X20,000.

6.60

FIG. 6.61 TEM of a tegumentary cyton from a developing cyst cultured for 120 days *in vitro*. Large residual bodies (R) with lamellated peripheries are present in the perinuclear cytoplasm. N; nucleus, T_4; T_4 vesicle. X28,200.

6.61

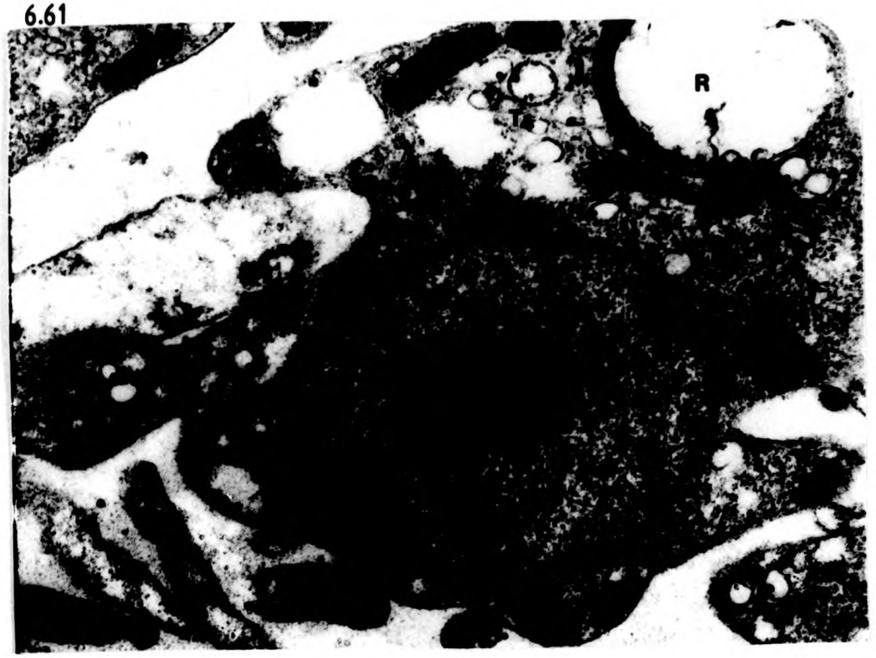

Fig. 6.62 TEM of the former scolex tegument of a developing cyst cultured *in vitro* for 120 days. Residual bodies with lamellated peripheries (R) are present in the distal cytoplasm. Mt; spined microthrix, LL; laminated layer. X28,200.

6.62

Fig. 6.63 TEM of the germinal layer of a cyst cultured *in vitro* for 110 days. The laminated layer (LL) has become considerably thicker and large lipid droplets (Lp) are evident in the germinal layer. Many of the mitochondria (M) are swollen. N; nucleus. X6,590.

6.63

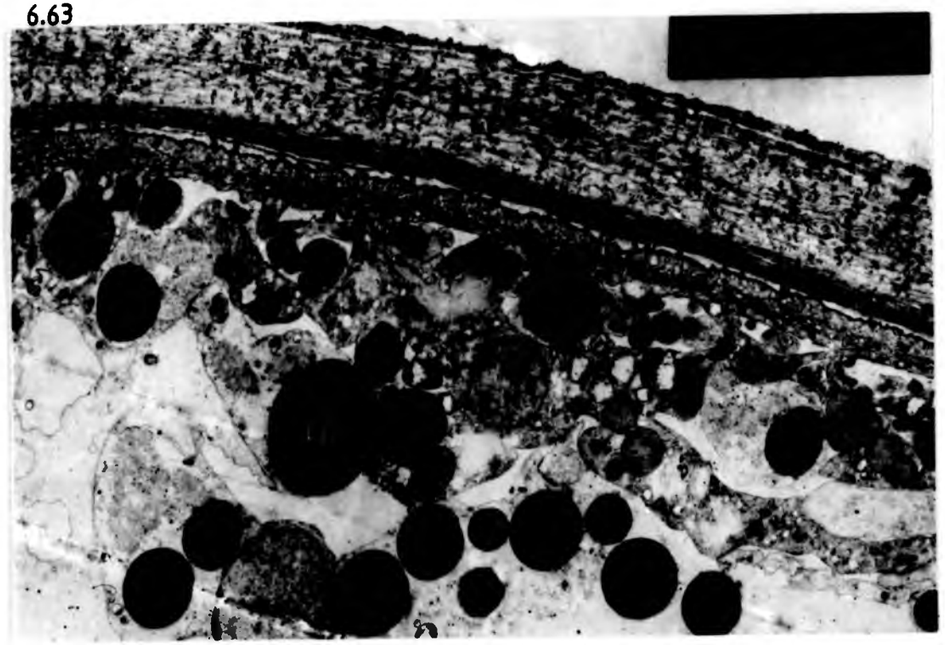

Fig. 6.64 TEM of a posterior bladder on a protoscolex cultured *in vitro* for 14 days. The distal cytoplasm (DC) is narrow and possesses T_3 vesicles (T_3). The cytons have a large nucleus (N) but few other organelles. X20,000.

6.64

Fig. 6.65 TEM of a posterior bladder on a protoscolex cultured *in vitro* for 14 days. A flame cell collecting duct (CD) is present on the inside of the bladder. X20,000.

6.65

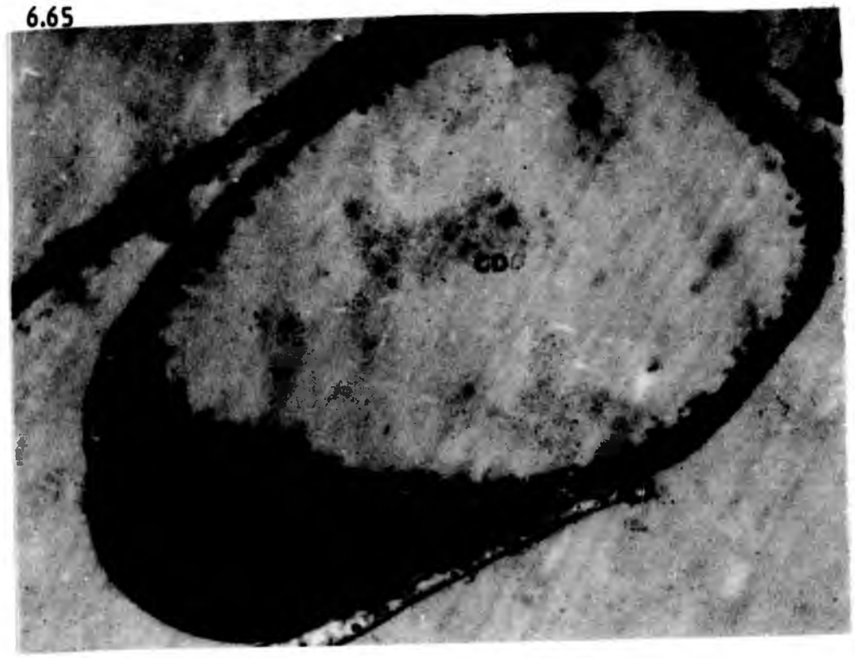

Fig. 6.66 TEM of the distal cytoplasm of a posterior bladder on a protoscolex cultured *in vitro* for 6 days. A number of truncated microtriches (TM) project outwards from the bladder. M; Mitochondria. X58,000.

6.66

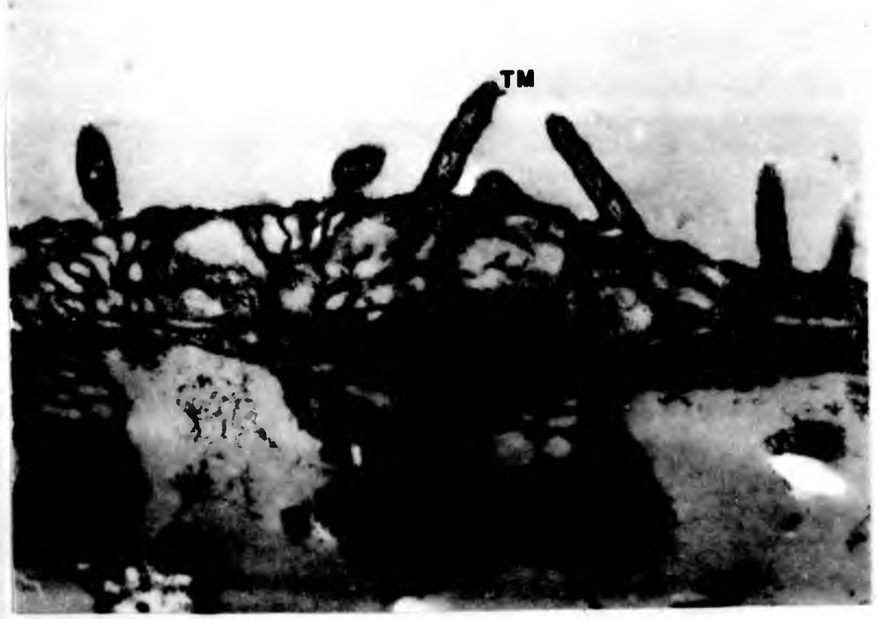

Fig. 6.67 TEM of the soma tegument of a protoscolex showing adult-like development during *in vitro* culture for 54 days. Note that spined microtriches (Mt) are present at the surface and active Golgi complexes (G) are evident within the cytons. N; nucleus. X20,500.

6.67

Fig. 6.68 TEM of the soma distal cytoplasm of a protoscolex undergoing adult-like development during *in vitro* culture for 48 days. Spined microtriches (Mt) are forming parallel to the surface prior to uplifting. T_2; T_2 vesicles. X39,100.

6.68

Fig. 6.69 TEM of the soma tegument of a protoscolex showing adult-like development during *in vitro* culture for 54 days. Spined microtriches are forming initially parallel to the surface before subsequent uplifting. The T_2 vesicles (T_2) occasionally appear less flocculent and occur close to the developing microtriches. Sp; spine, Sh; shaft, SS; shaft support. X103,000.

6.69

Fig. 6.70 TEM of the soma tegument of a protoscolex showing adult-like development during *in vitro* culture for 60 days. T_2 vesicles (T_2) with their dense flocculent contents are present in large numbers in the distal cytoplasm. LM; longitudinal muscle, CM; circular muscle. X63,400

6.70

Fig. 6.71 TEM of a tegumentary cyton in the soma region of a protoscolex showing adult-like development during *in vitro* culture for 54 days. Golgi complexes (G) are active and large numbers of T_2 vesicles (T_2 are present. X29,200.

6.71

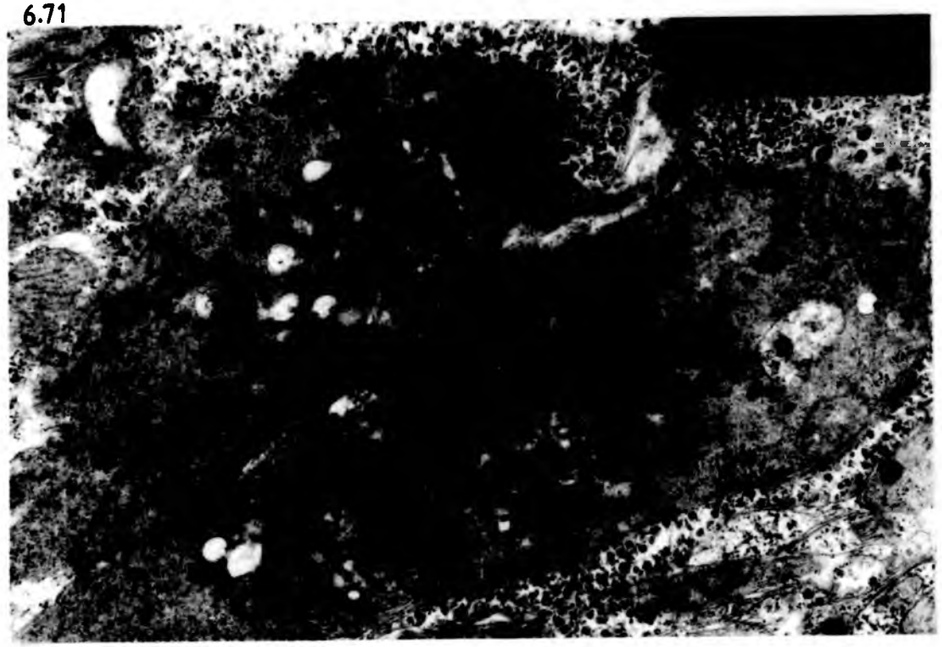

Fig. 6.72 TEM of a soma tegumentary cyton of a protoscolex showing adult-like development during *in vitro* culture for 54 days. High power micrograph of a Golgi complex. Note that the cisternae of the maturing face (arrow) possess flocculent contents similar to that of the T_2 vesicles (T_2). X121,000.

6.72

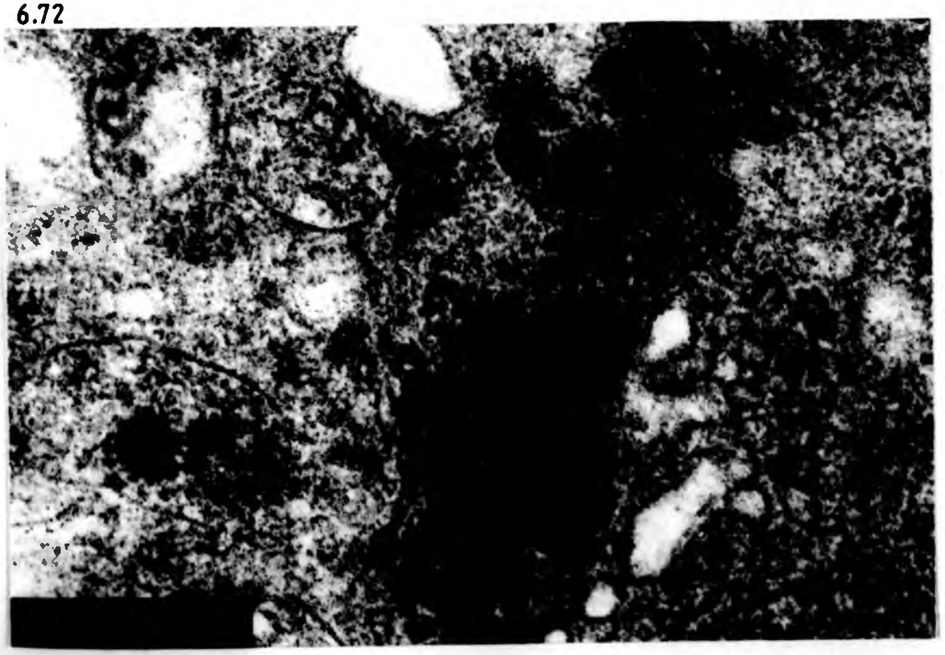

Fig. 6.73 TEM of a tegumentary cyton of a protoscolex showing adult-like development during *in vitro* culture for 60 days. Note the close association between the Golgi complexes (G) and the peripheral rough endoplasmic reticulum (ER). Transition vesicles (TV) can also be seen between these two organelles. N; nucleus. X39,100. (O_sO_4 fixation only). X39,100.

6.73

CHAPTER SEVEN

ULTRASTRUCTURAL DEVELOPMENT OF THE TEGUMENT ASSOCIATED WITH THE MATURATION OF PROTOSCOLICES IN BROOD CAPSULES.

Fig. 7.1 SEM of the internal surface of a fertile, murine cyst showing immature brood capsules appearing as small papillae (P). X35.

Fig. 7.2 SEM of immature brood capsules, at different stages of development, on the internal surface of a fertile murine cyst. X500.

7.1

7.2

Fig. 7.3 SEM of an immature brood capsule showing its bulbous tip attached to the germinal layer (GL) by a narrower stalk (S). Note the cells with many cytoplasmic processes covering the surface of the capsule (arrow). X1,000.

7.3

Fig. 7.4 LM whole mount of an early brood capsule prior to protoscolex formation. C; capsule cavity. X540.

7.4

Fig. 7.5 LM whole mount of developing brood capsules in the process of protoscolex formation. Note the multiplication of cells (arrow) at the distal end of the capsule cavity which subsequently form the early protoscolex bud (B). X340.

7.5

Fig. 7.6 LM whole mount of a developing brood capsule with more advanced protoscolex formation. The sucker (Sk) and rostellar (R) regions are delimited and the hooks are visible (arrow). Note that the presumptive soma region (So) has not yet protruded into the cavity. X540.

7.6

Fig. 7.7 LM whole mount of a brood capsule with a complete single, invaginated protoscolex. H; hooks. X540.

Fig. 7.8 LM whole mount of a more avanced brood capsule possessing two fully formed protoscoleces. H; hooks. X540.

7.7

7.8

Fig. 7.9 SEM of a murine brood capsule which has ruptured and everted so that protoscoleces, at various stages of development protrude outwards from the brood capsule wall. X200.

7.9

Fig. 7.10 TEM of an early brood capsule, prior to protoscolex formation. Note the numerous cells surrounding the brood capsule cavity (C). LL; laminated layer, GL; germinal layer. X1,200

7.10

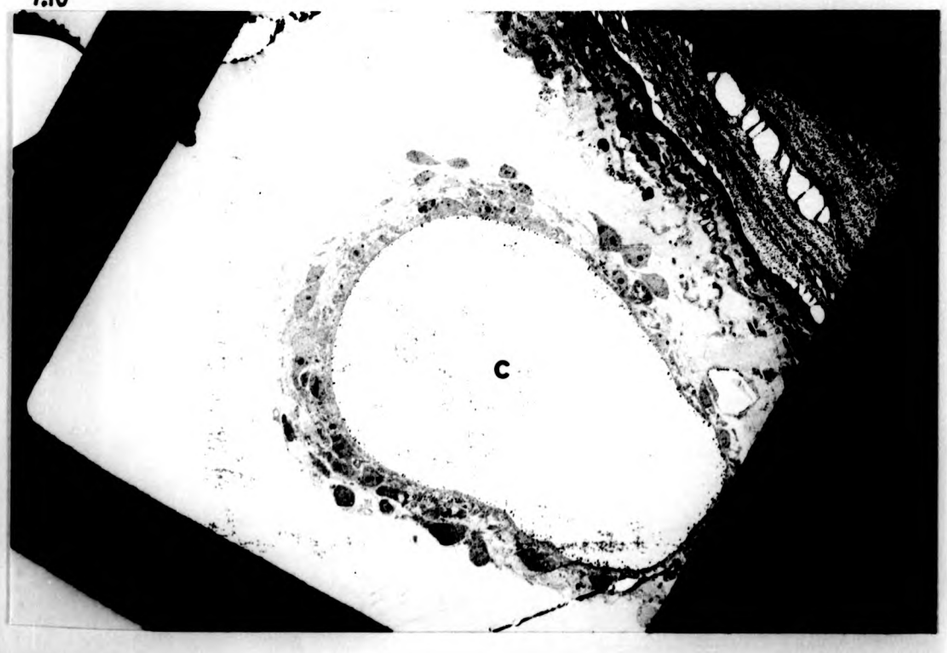

Fig. 7.11 TEM of the brood capsule tegument prior to protoscolex formation. The distal cytoplasm (DC) possesses mainly T_3 vesicles (arrows) and a scant population of truncated microtriches (T.M.). Note the population of undifferentiated cells surrounding the tegument. N; nucleus, M; mitochondria. X1,370.

7.11

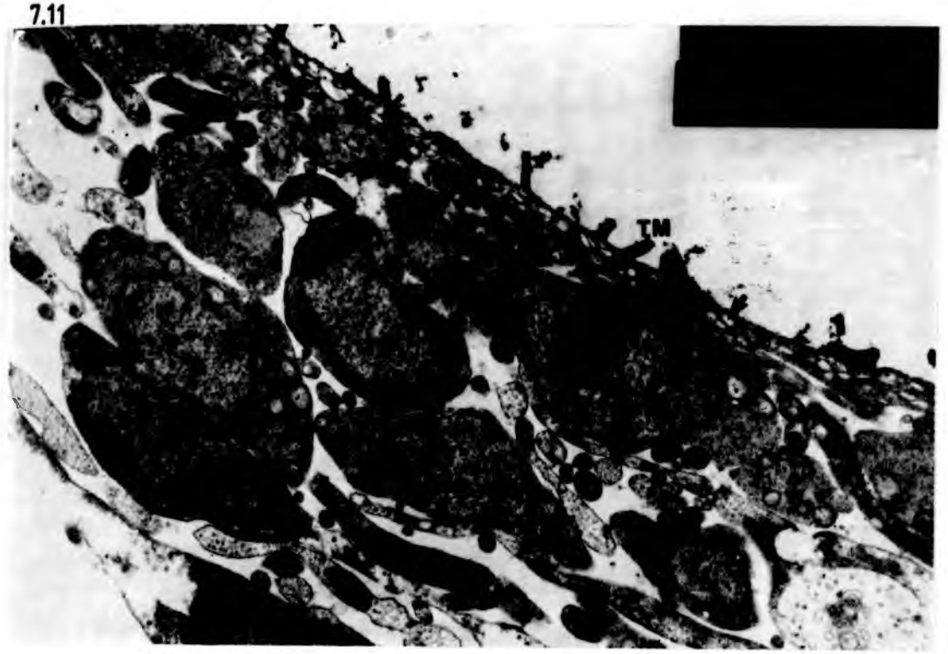

Fig. 7.12 SEM of early (stage 1) protoscolex bud projecting from the brood capsule wall (BC). The bud possesses a distal portion (D) and a proximal portion (P) which in intact capsules, projects slightly to the exterior. X750.

7.12

Fig. 7.13 TEM of a stage 1 development protoscolex showing the distal portion (D) projecting into the capsule cavity. Note the large number of undifferentiated cells within the protoscolex bud. DC; tegumentary distal cytoplasm. X3,450.

Fig. 7.14 TEM of a stage 1 developing protoscolex showing the proximal region (P) projecting slightly to the exterior of the capsule. X3,450.

7.13

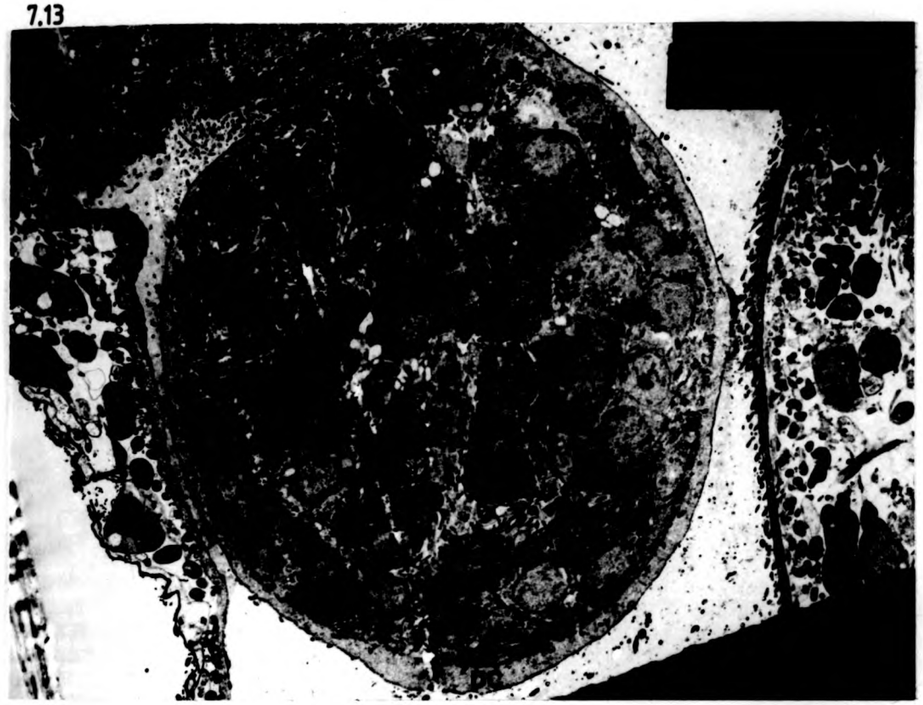

7.14

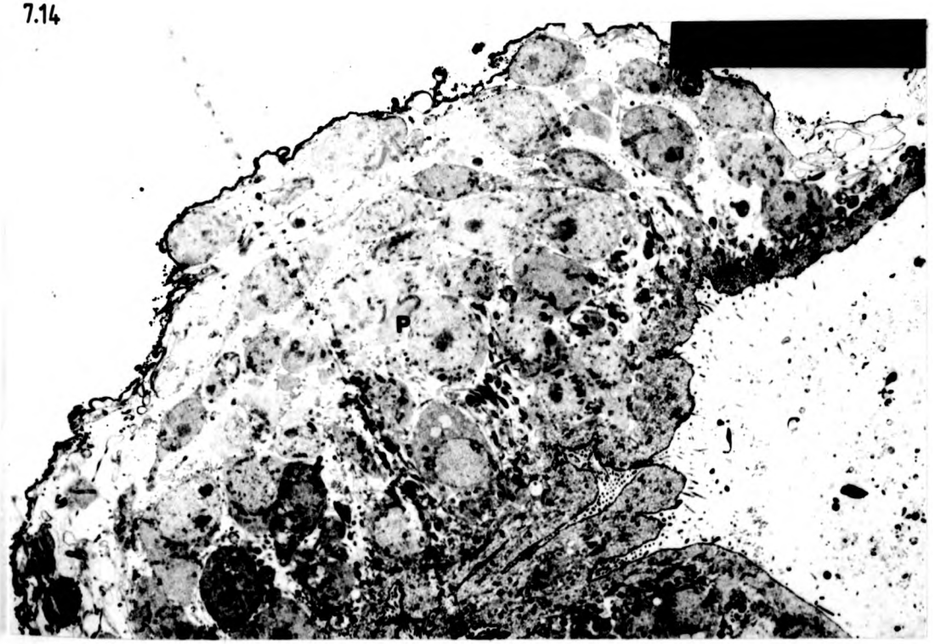

Fig. 7.15 TEM of the tegumentary distal cytoplasm (DC) of the distal region of a stage 1 protoscolex bud. Note the general lack of complex structure within the tegument. Occassional T_3 vesicles (arrows) and small truncated microtriches (T.M.) are present together with small mitochondria (M). X20,500

Fig. 7.16 TEM of the distal tegument of a stage 1 protoscolex bud showing microvilli (Mv) present together with truncated microtriches (TM). Note the presence of a shaft support (arrow) in the truncated microtriches which is absent from the microvilli. X63,400

7.15

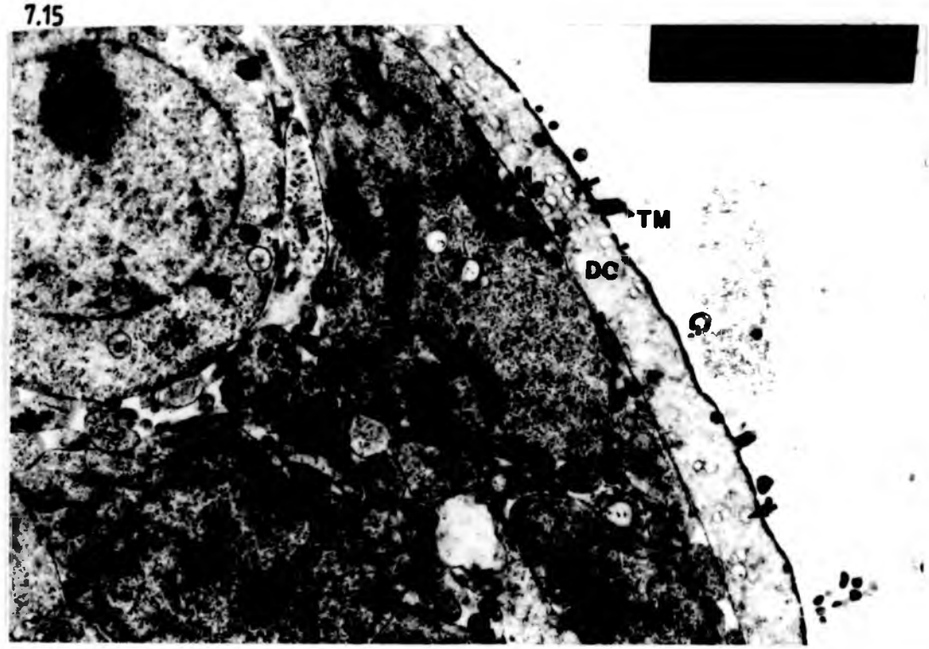

7.16

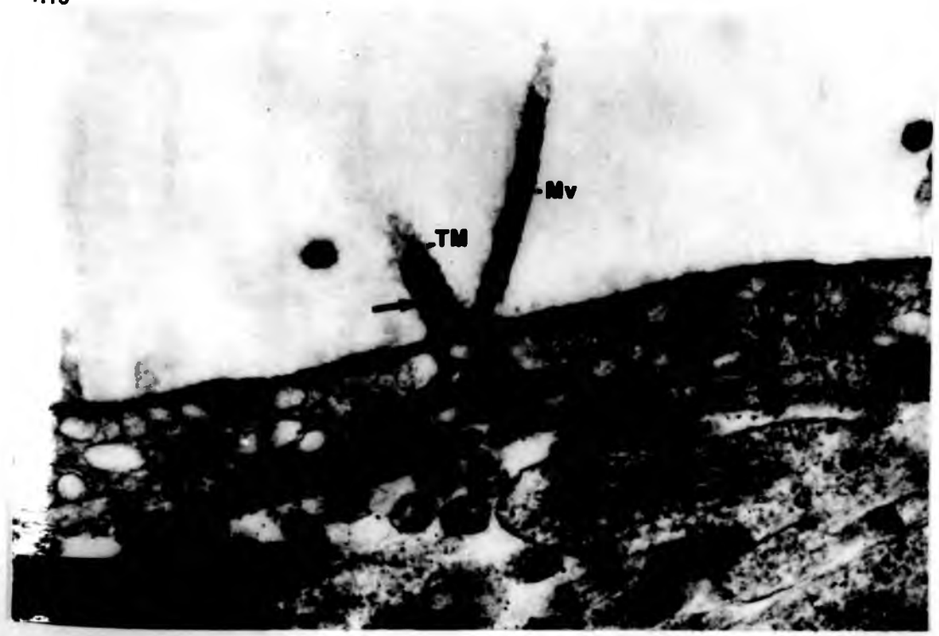

Fig. 7.17 TEM of the proximal tegument of a stage 1 protoscolex possessing truncated microtriches (TM) and numerous long microvilli (Mv). The vesicles of the distal cytoplasm are mainly of T_3 origin although occasional vesicles contain rod like bodies (arrow). X39,100.

Fig. 7.18 SEM of the proximal region of a stage 1 protoscolex showing the numerous long microvilli (Mv) present on the surface. X7,500.

7.17

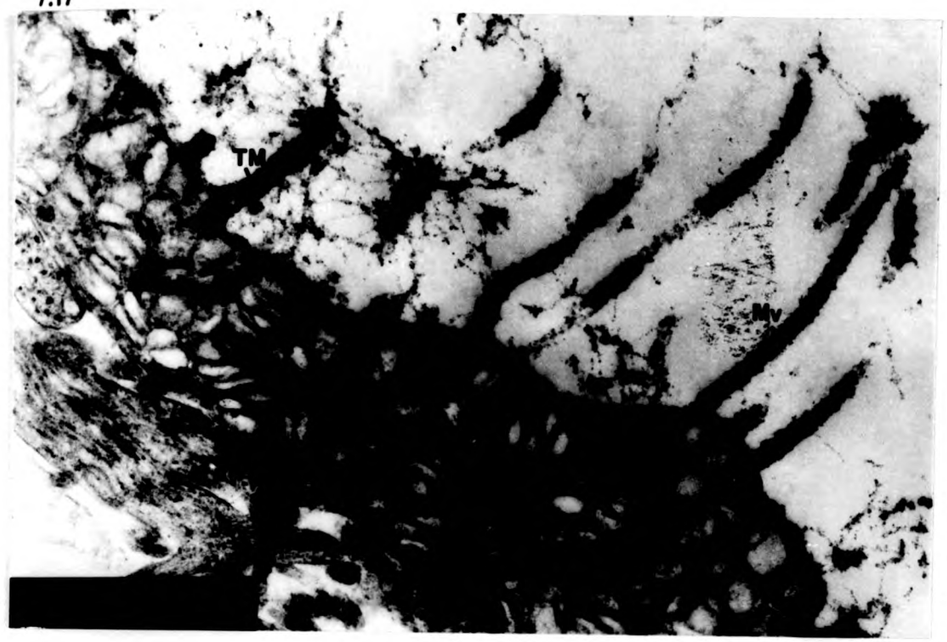

7.18

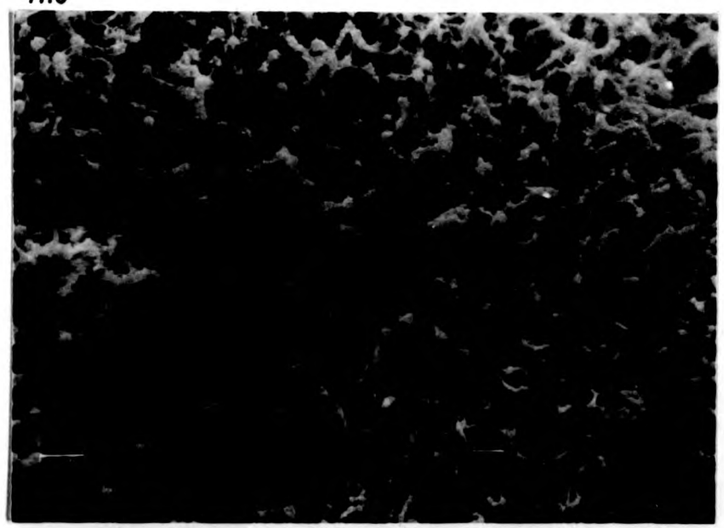

Fig. 7.19 SEM of a stage 2 protoscolex bud. The rostellum (R) and sucker regions (Sk) are now delimited within the distal region whilst the proximal region (P) remains unchanged. X750.

7.19

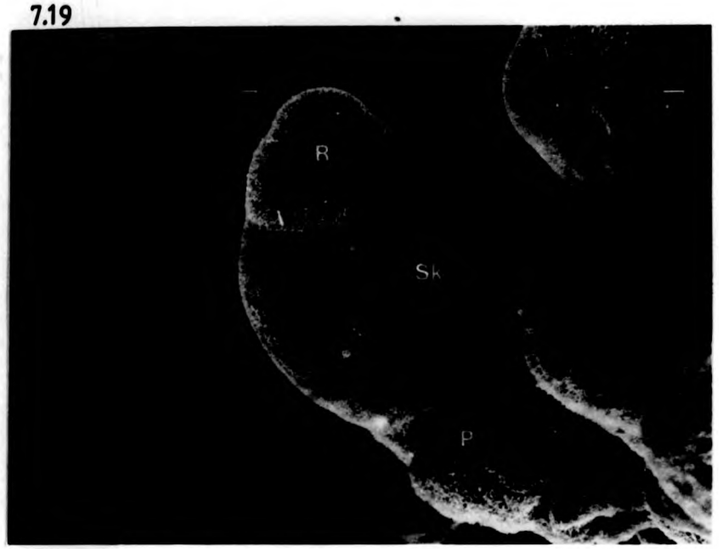

Fig. 7.20 SEM of the scolex of a stage 2 protoscolex bud showing the presence of truncated microtriches (TM) and short microvilli (Mv) the latter being recognised by their brighter appearance. X7,500.

7.20

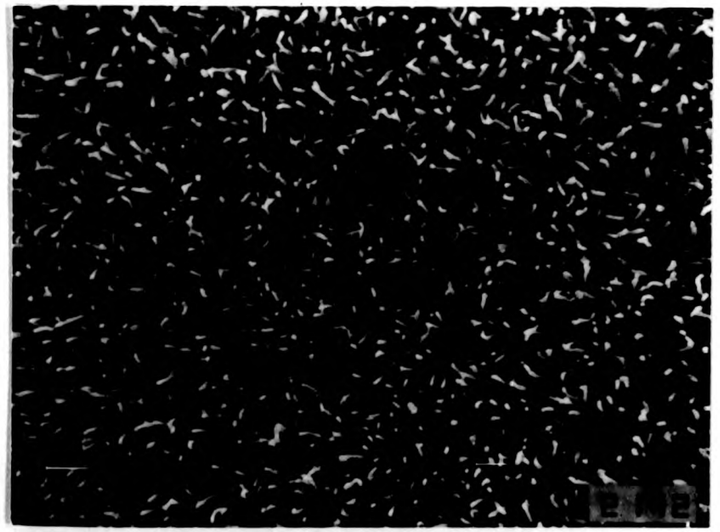

Fig. 7.21 TEM of the scolex tegument of a stage 2 developing protoscolex showing the presence of truncated microtriches (TM) and short microvilli (Mv). X63,400.

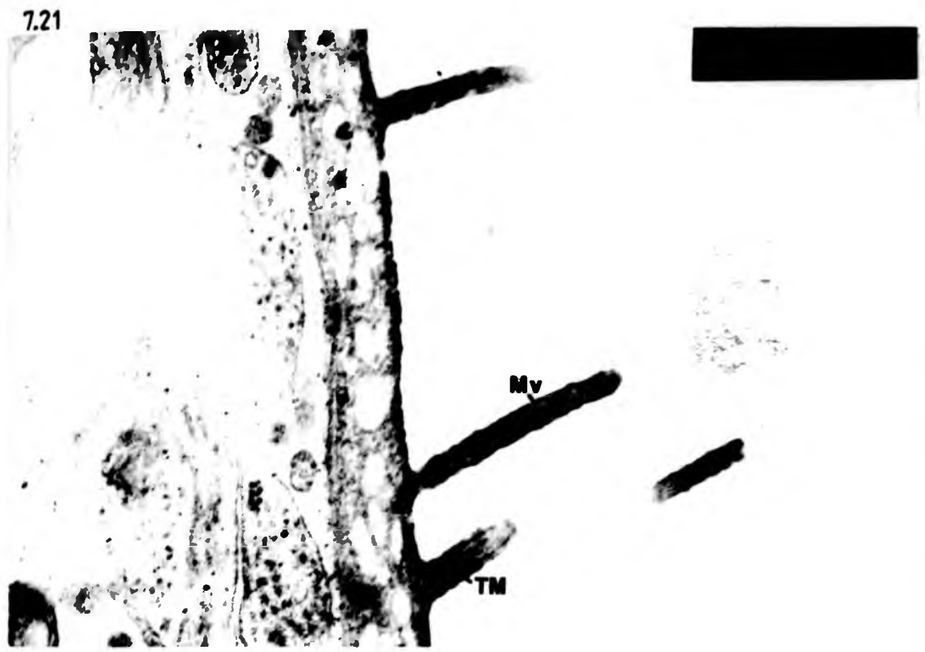

Fig. 7.22 TEM of the distal cytoplasm of the presumptive soma (proximal) region of a stage 2 developing protoscolex. Note the numerous T_3 vesicles (T_3) and vesicles with electron dense cores which are presumably T_1 in nature (T_1). Dense, flocculent T_0 vesicles are also evident (T_0). X39,100.

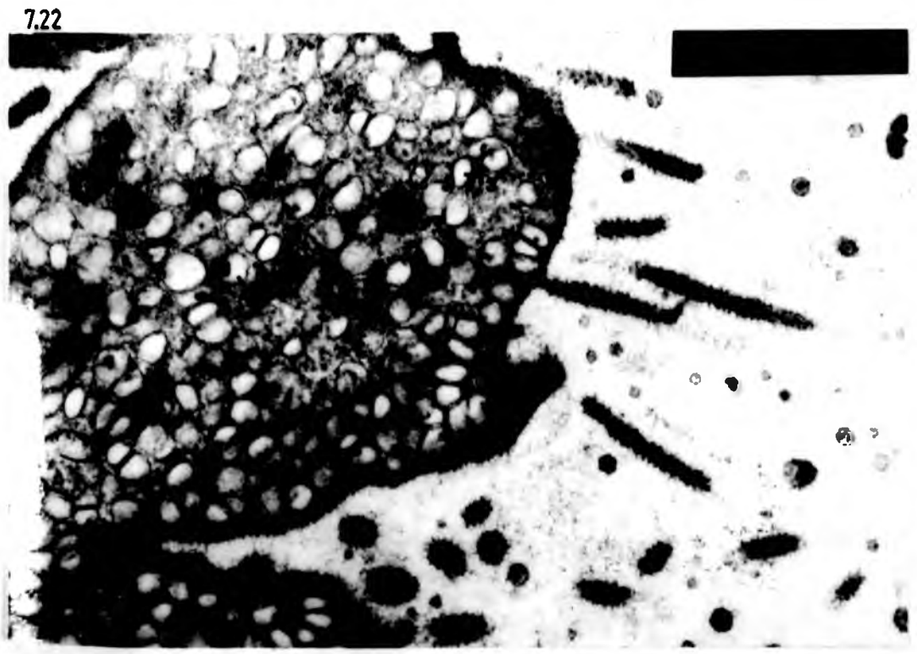

Fig. 7.23 TEM of the distal cytoplasm of the presumptive soma (proximal) region of a stage 2 developing protoscolex, stained for carbohydrate using the periodic acid-thiosemicarbazide method. The contents of the T_0 vesicle (T_0) and the surface glycocalyx material (G) give a positive reaction whilst other vesicles are negative. X63,400.

7.23

Fig. 7.24 TEM of the distal cytoplasm of the presumptive soma showing a T_0 vesicle (T_0) in close association with the apical membrane. Note the continuity of the apical and vesicle membranes (arrow). X103,000.

7.24

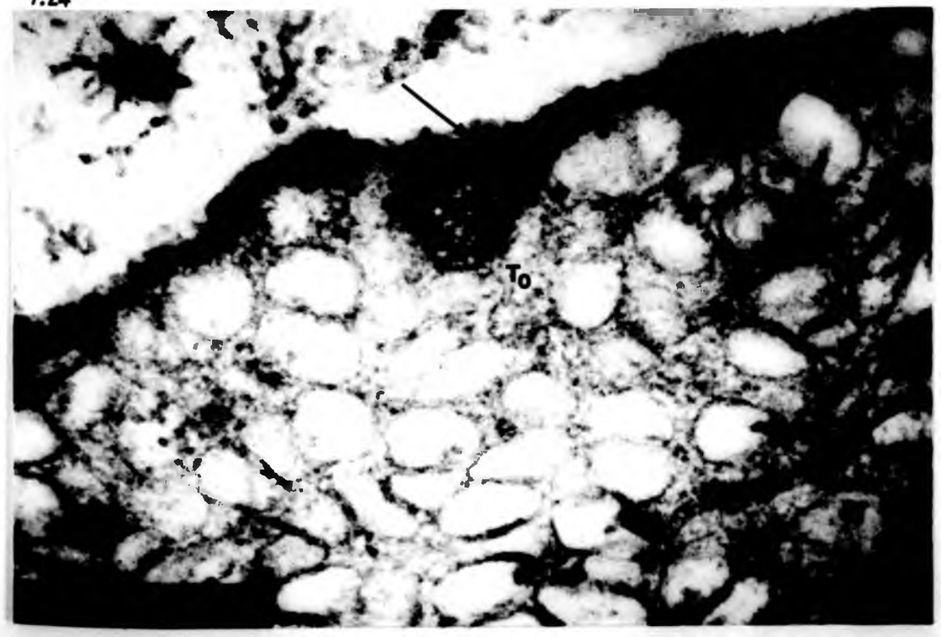

Fig. 7.25 TEM of the tegument of the presumptive soma region of a stage 2 developing protoscolex showing the presence of T_0 and T_1 vesicles in both the distal and perinuclear cytoplasm. N; nucleus, G; Golgi complex, Mv; microvilli. X14,200.

7.25

Fig. 7.26 SEM of a stage 3 developing protoscolex. The rostellum (R) is now more cone shaped whilst there is a broadening of the sucker region (Sk). So; presumptive soma. X750

7.26

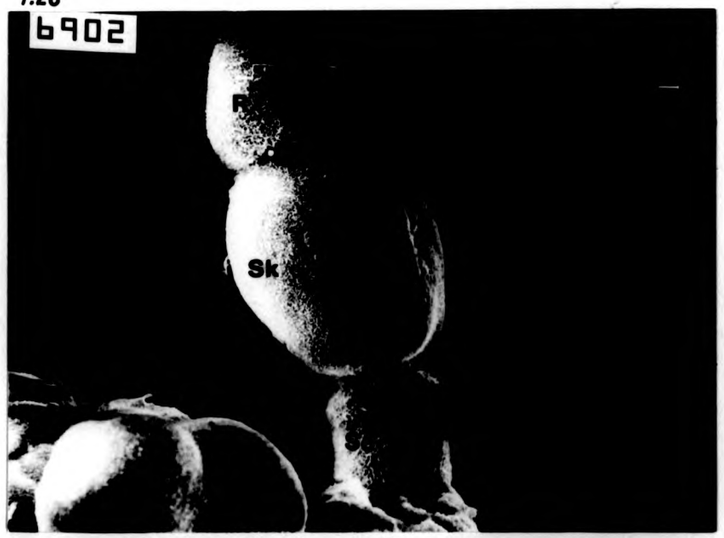

Fig. 7.27 SEM of the rostellar region of a stage 3 developing protoscolex showing the presence of increased numbers of microvilli (Mv). Also present are broad, triangular shaped M_1 large microtriches (M_1). X7,500.

Fig. 7.28 TEM of the rostellar region of a stage 3 developing protoscolex showing the presence of broad M_1 large microtriches (M_1). Note the conspicuous shaft support material (arrow) along the longest side of the projections. Sp; spine, BP; base plate, Mv; microvilli. X39,100.

7.27

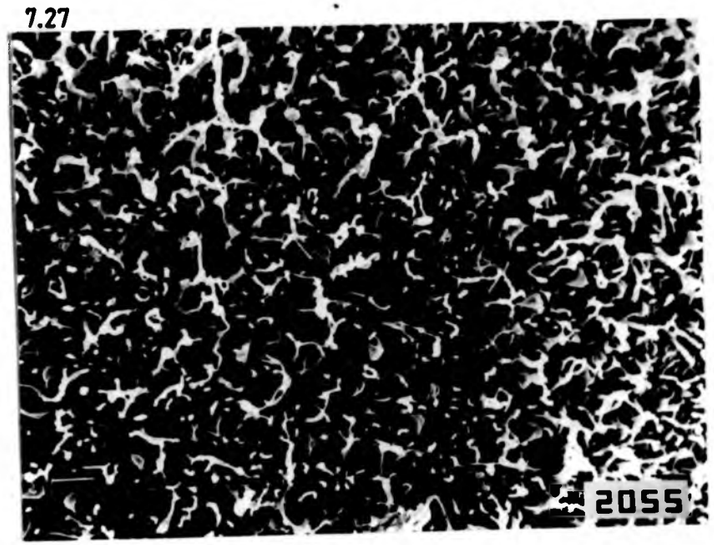

7.28

Fig. 7.29 TEM of the sucker tegument of a stage 3 developing protoscolex showing the presence of spined microtriches (Mt) which appear to have formed by transformation from existing truncated microtriches. Note the presence of a large amount of shaft support material (arrows) which presumably contributes to the spine. Mv; microvillus. X39,100.

7.29

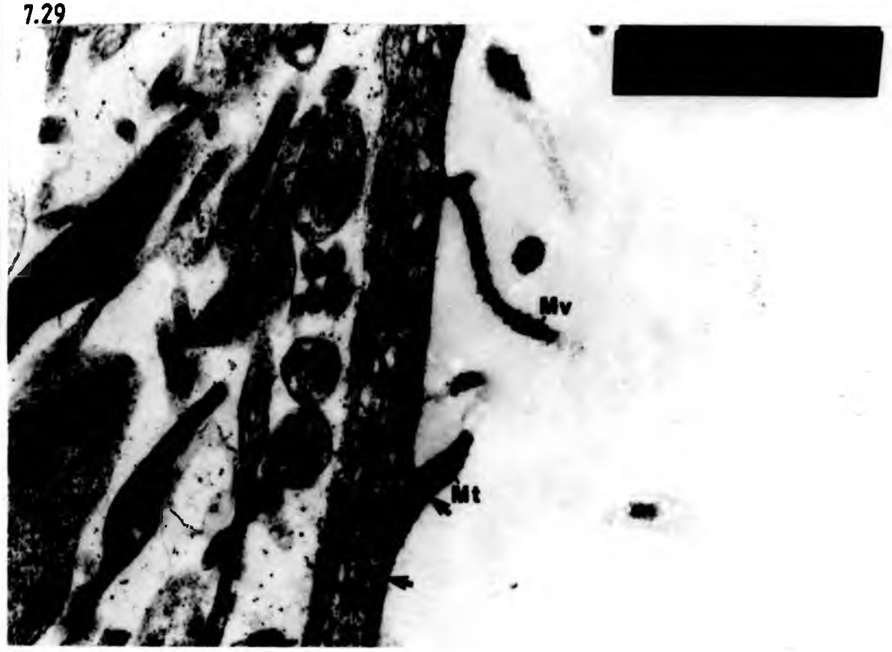

Fig. 7.30 TEM of the sucker tegument of a stage 3 developing protoscolex showing spined microtriches (Mt) shortly after *de novo* formation and uplifting. Note that the shaft support material (arrow) is not as extensive as in the microtriches in Fig. 7.29. X39,100.

7.30

Fig. 7.31 SEM of a stage 4 developing protoscolex. The rostellum now possesses a rostellar ridge (RR) and the suckers (Sk) are more clearly outlined. X750.

7.31

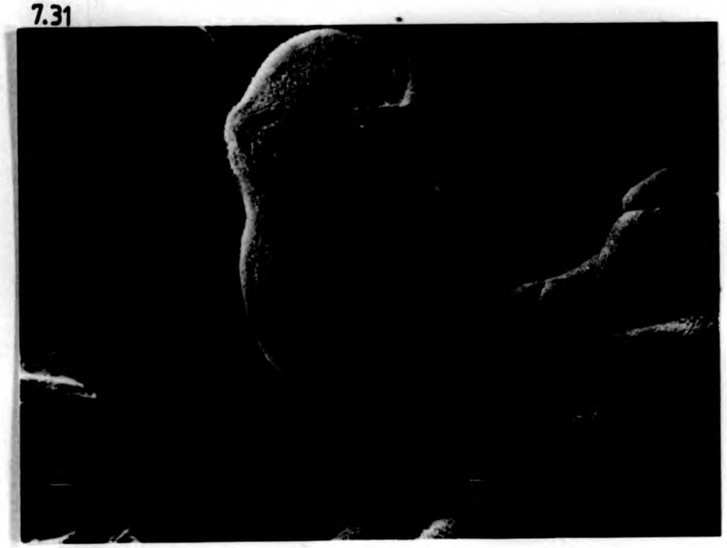

Fig. 7.32 SEM of the rostellar ridge of a stage 4 developing protoscolex showing enlarged M_1 microtriches (M_1) in the vicinity of the ridge. Mv; microvilli. X7,500

7.32

Fig. 7.33 SEM of a stage 4 developing protoscolex showing M_1 large microtriches (M_1) becoming more pronounced at the base of the rostellum. X7,500.

7.33

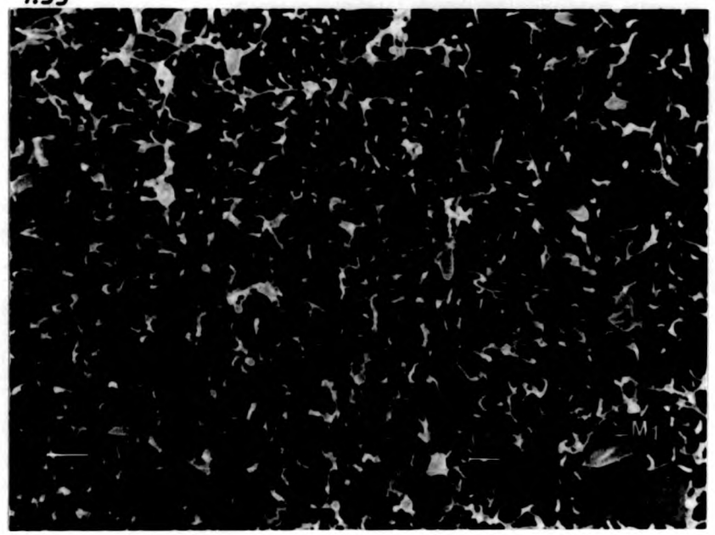

Fig. 7.34 TEM of the rostellar tegument of a stage 4 developing protoscolex showing M_1 large microtriches which have now become greatly enlarged. Sp; spine, Sh; shaft, Mv; microvillus. X30,750.

7.34

Fig. 7.35 SEM of a stage 5 developing protoscolex. The rostellar hooks (H) are now evident projecting from the base of the rostellum and long microvilli are present over the entire surface. X1,500.

7.35

Fig. 7.36 SEM of the rostellar hooks (H) of a stage 5 developing protoscolex. Note that the hooks appear ridged and are now covered by tegument. Mv; microvilli. X7,500.

7.36

Fig. 7.37 TEM of a rostellar hook (H) of a stage 5 developing protoscolex. Note that the hook still has a microthrix configurations and is not covered by the tegumentary distal cytoplasm. Mv; microvilli. X11,000.

7.37

Fig. 7.38 SEM of the sucker region of a stage 5 developing protoscolex showing the presence of spined microtriches (Mt) and numerous long microvilli (Mv). X7,500.

7.38

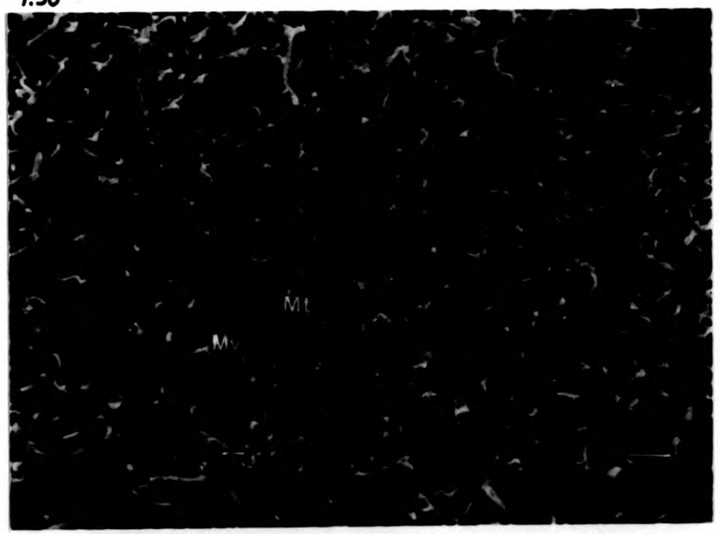

Fig. 7.39 TEM of the scolex tegument of a stage 5 developing protoscolex showing numerous T_2 vesicles (T_2) in the distal cytoplasm (DC) and internuncial processes. (IP). M; muscle. X39,100.

7.39

Fig. 7.40 SEM of a stage 5 developing protoscolex showing a band of enlarged M_2 microtriches (M_2) immediately below the rostellar hooks (H). Mv; microvilli, Mt; normal spined microtriches. X7,500.

7.40

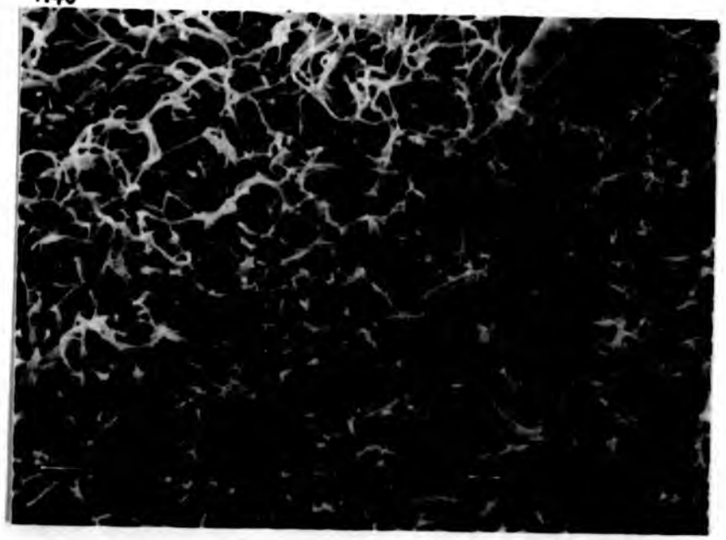

Fig. 7.41 TEM of the M_2 large microtriches (M_2) in a fold between the rostellum and the sucker regions (Sk). Note the increase in size of the microtriches from posterior to anterior. X14,200.

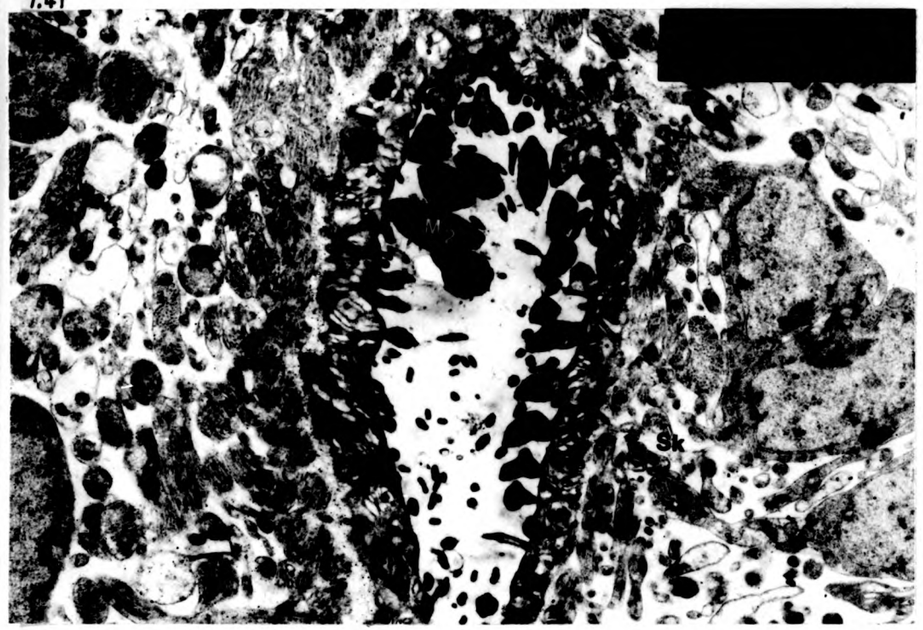

Fig. 7.42 TEM of the M_2 large microtriches appearing to result from the fusion of two smaller microtriches. Note the two baseplates (BP) present in each M_2 microthrix and an internal electron dense region representing adjacent shaft supports (arrow). X79,600.

Fig. 7.41 TEM of the M_2 large microtriches (M_2) in a fold between the rostellum and the sucker regions (Sk). Note the increase in size of the microtriches from posterior to anterior. X14,200.

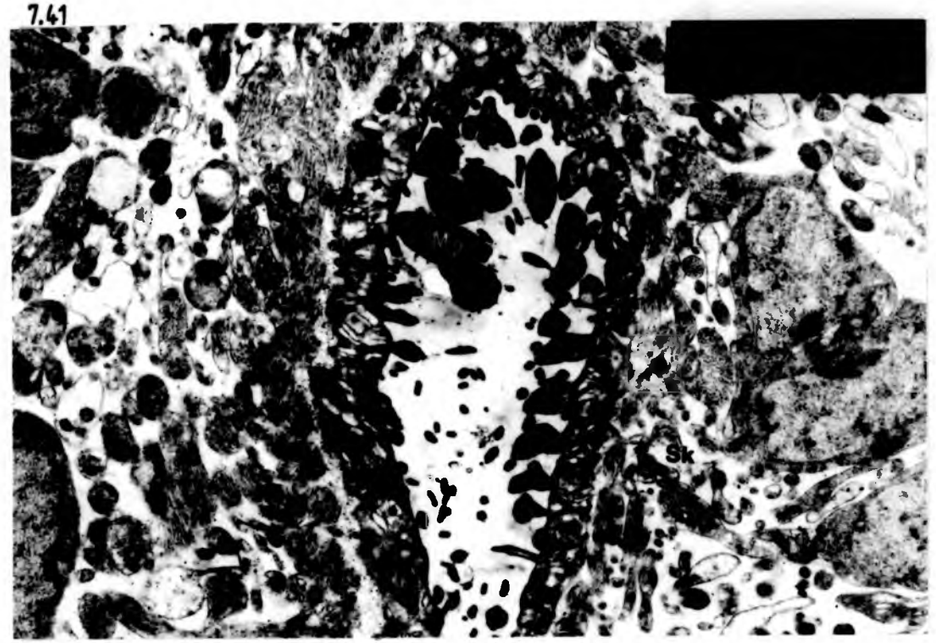

Fig. 7.42 TEM of the M_2 large microtriches appearing to result from the fusion of two smaller microtriches. Note the two baseplates (BP) present in each M_2 microthrix and an internal electron dense region representing adjacent shaft supports (arrow). X79,600.

Fig. 7.43 TEM of the M_2 large microtriches and the abundant T_2 vesicles (T_2) present in the tegument. Note that some of the T_2 vesicles are present within the shaft of the M_2 microtriches. X63,400.

7.43

Fig. 7.44 SEM of a stage 6 developing protoscolex showing the presumptive soma (So) becoming elevated. H; hooks, Sk; suckers. X750.

7.44

Fig. 7.45 SEM of the sucker region of a stage 6 developing protoscolex showing a reduction in the size and number of microvilli (Mv) present. Spined microtriches (Mt) now predominate. X7,500.

7.45

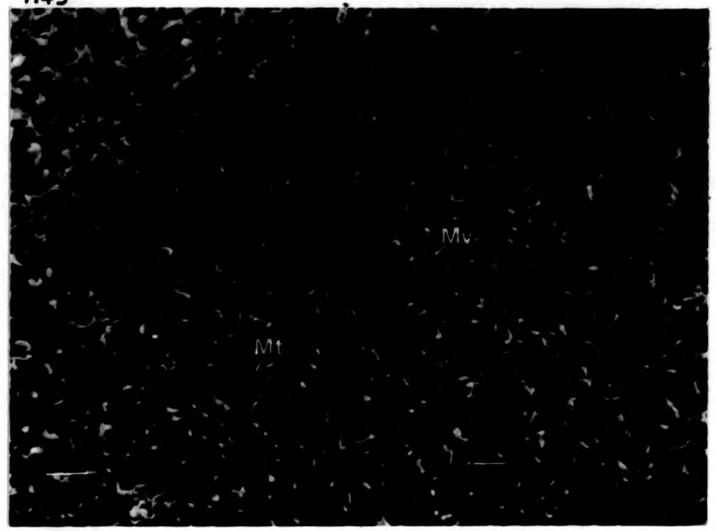

Fig. 7.46 SEM of the rostellar/sucker junction of a stage 6 developing protoscolex showing the band of M_2 large microtriches (M_2) as being still evident. Microvilli (Mv) are still present on the rostellum but are reduced over the suckers. X7,500.

7.46

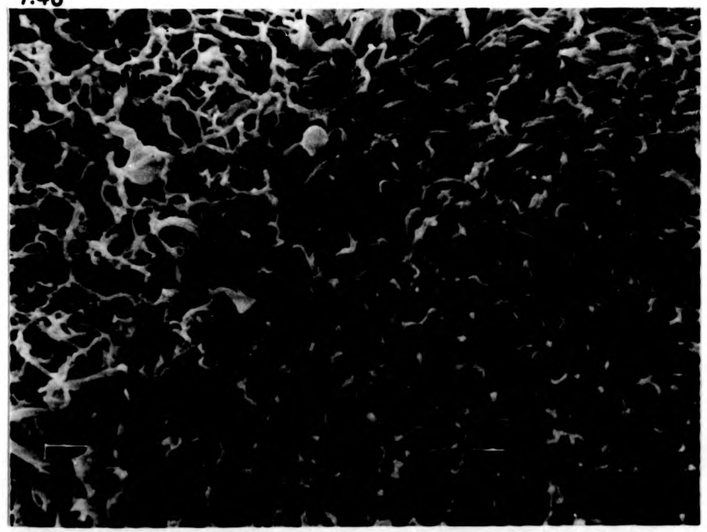

Fig. 7.47 TEM of the scolex region of a stage 6 developing protoscolex. The M_2 large microtriches (M_2) are still present at the base of the rostellum but are not associated with the rostellar hooks (H). X5,480.

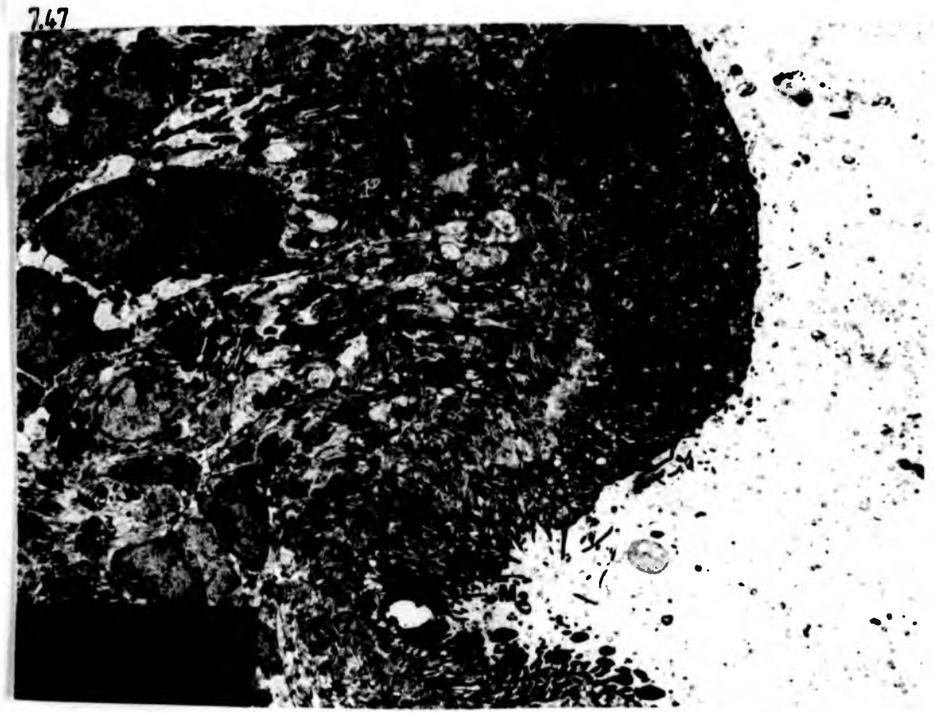

Fig. 7.48 TEM of the soma region of a stage 6 developing protoscolex. Microvilli (Mv) and truncated microtriches (TM) are still evident but are now outnumbered by blunt elevations (BE). Note that in some cases the blunt elevations appear to be forming under the microvilli. T_1; T_1 tegumentary vesicles, G; glycocalyx. X63,400.

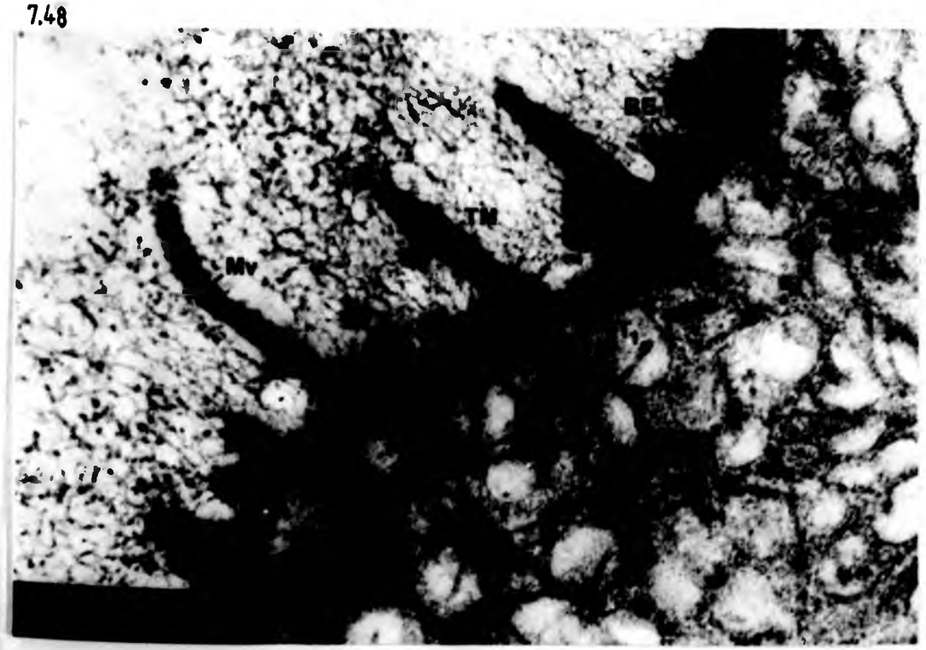

Fig. 7.49 TEM of the soma tegument of a stage 6 developing protoscolex showing tegumentary cytons active in the production of T_1 vesicles (T_1) DC; distal cytoplasm, N; nucleus. X11,000.

Fig. 7.50 SEM showing subsequent development of protoscoleces involving further elevation of the soma (So) and loss of the microvilli and truncated microtriches. Sk; suckers. X750.

7.49

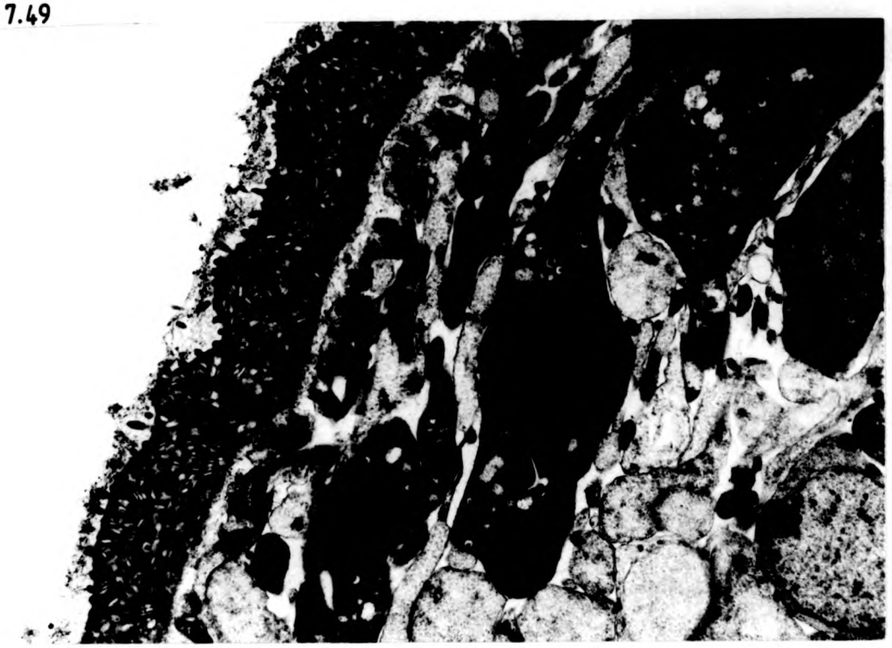

7.50

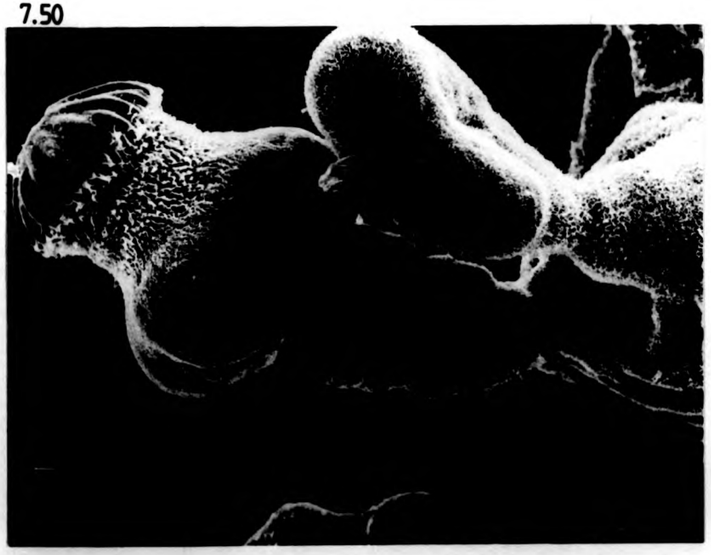

Fig. 7.51 TEM of the sucker region of a protoscolex late in development after the microvilli have been lost while the spined microtriches predominate. Sp; spine, Sh; shaft, T_2; T_2 tegumentary vesicle, M; muscle. X39,100.

7.51

Fig. 7.52 TEM of enlarged microthrix spines which have been shed from the protoscoleces during development. X39,100.

7.52

Fig. 7.53 SEM of the rostellum of a stage 5 developing protoscolex showing the rostellar tegument covered with long microvilli (Mv) and the hooks (H) uncovered by the tegument. X2,000.

Fig. 7.54 SEM showing subsequent development of the rostellum. Note that the hooks (H) are now covered by the tegument and that the microvilli (Mv) are disappearing. X2,000.

Fig. 7.55 SEM of an almost fully developed protoscolex showing the hooks being totally covered by the rostellar tegument. The microvilli have now totally been replaced by long filamentous microtriches (Mt). X2,000.

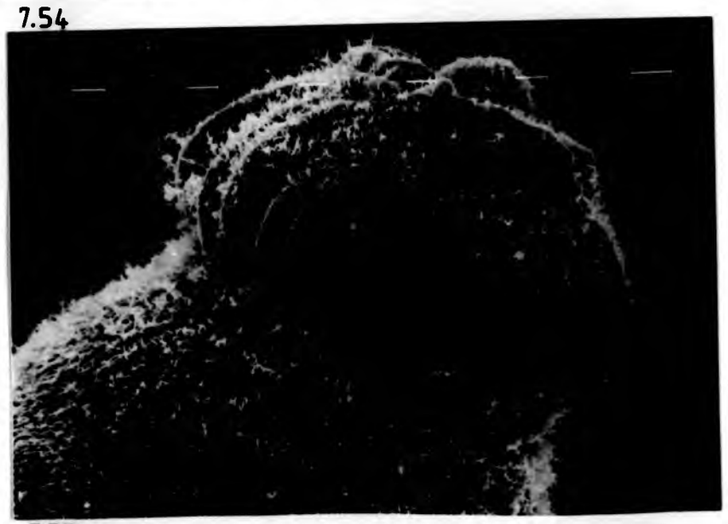

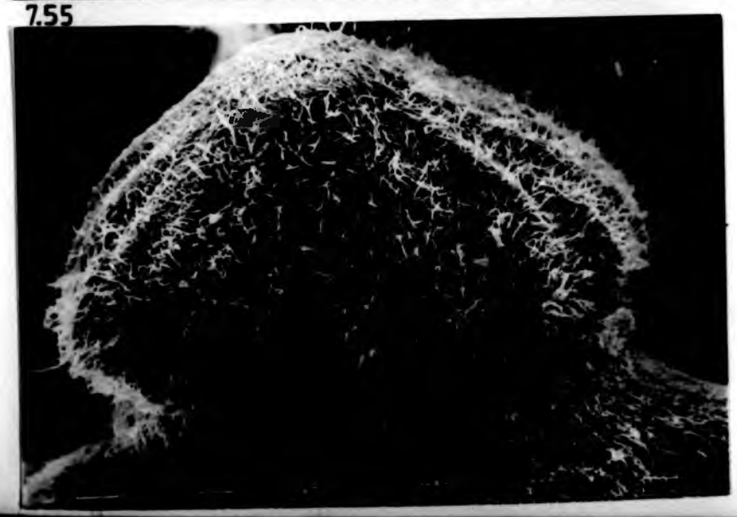

Fig. 7.56 TEM of filamentous microtriches forming parallel to the surface of the rostellar tegument (arrow). T_2; T_2 vesicle. X63,400. Inset. Fully uplifted rostellar microtriches. X39,100.

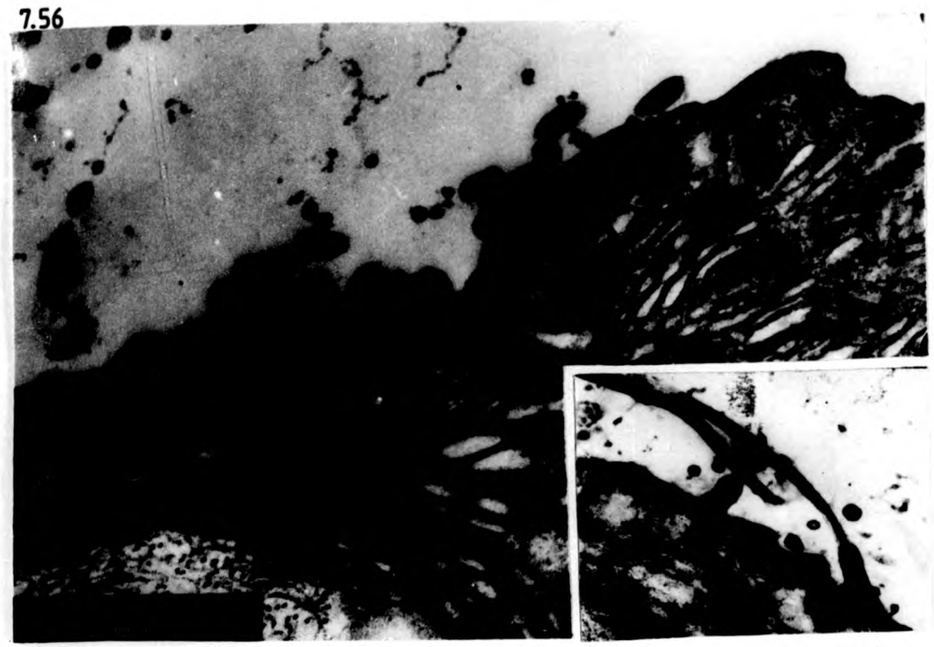

Fig. 7.57 TEM of a fully formed rostellar hook now composed of the characteristic blade (B), guard (G) and handle (H) portions. Note that the hook is completely enclosed in the rostellar tegument. X6590.

Fig. 7.58 SEM of the rostellar hooks of a fully formed protoscolex. The hooks are fully extended but are still covered by microthrix (Mt) bearing tegument. X7,500.

7.58

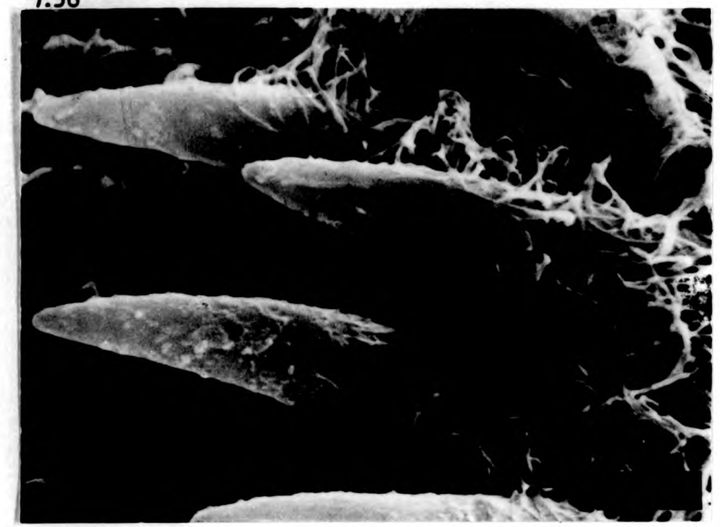

Fig. 7.59 SEM of a fully formed protoscolex undergoing invagination. Note the suckers (Sk) being withdrawn into the soma region (So). X750.

7.59

Fig. 7.60 Diagrammatic summary of the surface development of protoscoleces within brood capsules.

Truncated microtriches

Microvili

Sucker microtriches

Type I large microtriches

Type II large microtriches

Hook

Rostellar microtriches

Blunt elevations

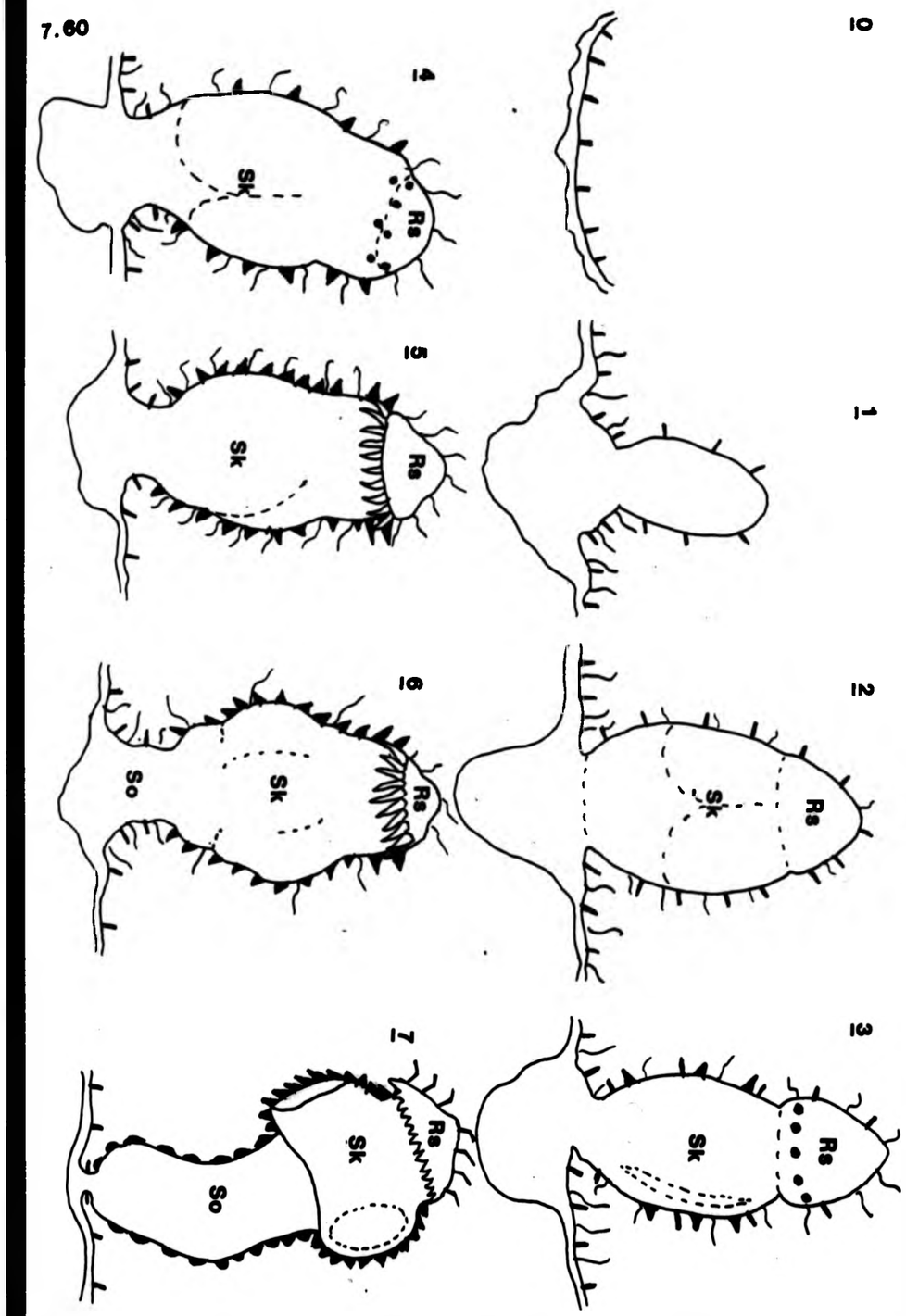

Fig. 7.61 LM of an early developing brood capsule with a single protoscolex (P) forming on the outside. H; hooks. X540.

Fig. 7.62 SEM of a mature brood capsule with two protoscoleces (P) forming on the outside. X350.

7.61

7.62

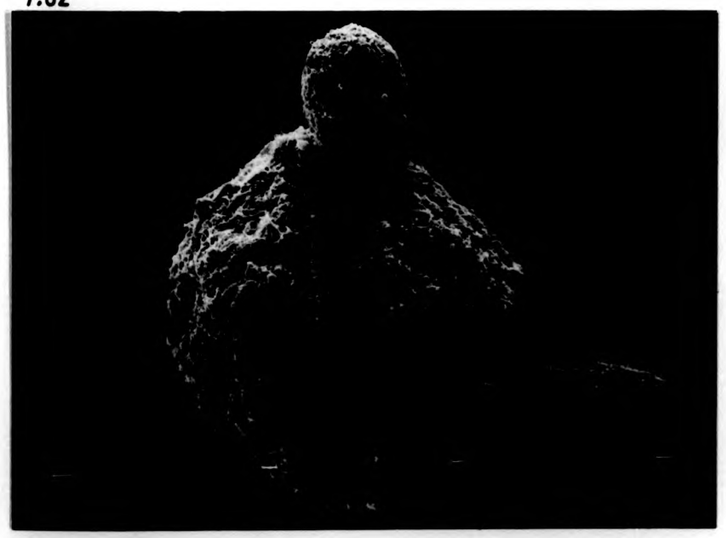

Fig. 7.63 TEM of a protoscolex developing on the outside of a brood capsule. A portion of the protoscolex is projecting into the capsule whilst the remainder projects outwards. Note the presence of well formed hooks (H) and M_2 large microtriches (M_2 on the tegument lined interior of the protoscolex. The exterior of the protoscolex (arrow) is cellular and not tegumentary. BC; brood capsule wall. X1,200.

7.63

Fig. 7.64 Diagrammatic representation of the possible way in which external developing protoscoleces could continue development inside the brood capsule.

Fig. 7.64

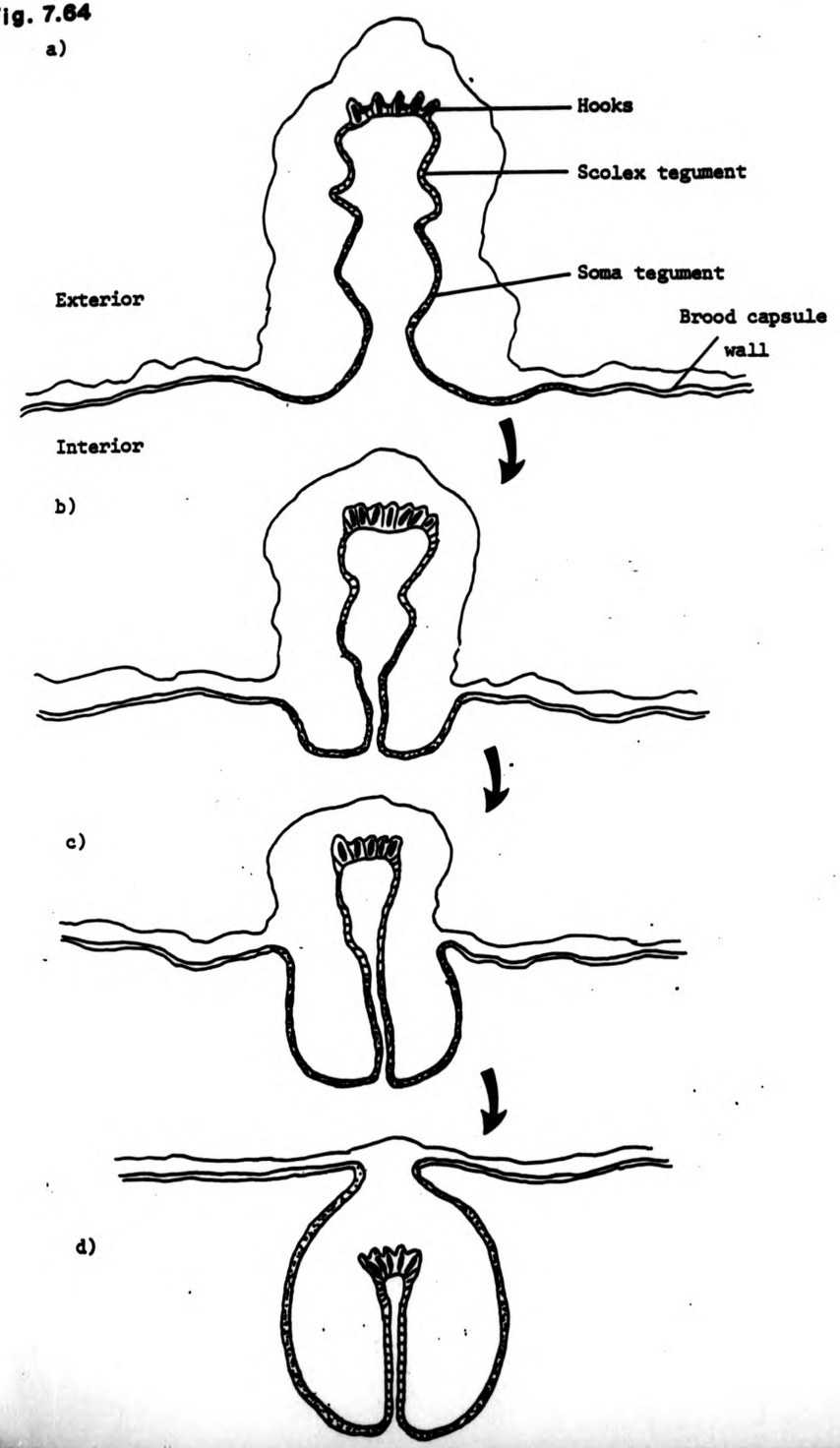

CHAPTER EIGHT

INVESTIGATIONS ON ATTEMPTED DISRUPTION OF CYSTIC DEVELOPMENT USING NONIDET P.

Fig. 8.1 TEM of a Golgi complex (G) in the soma region of an untreated protoscolex. Note that the cisternae are narrow and that few mitochondria (M) are present. ER; endoplasmic reticulum. X39,100.

8.1

Fig. 8.2 TEM of a soma tegumentary cyton of a protoscolex after 15 min in 10µM monensin. Note the swollen cisternae of the maturing face (MF) whilst those of the forming face (FF) remain narrow. X63,400.

8.2

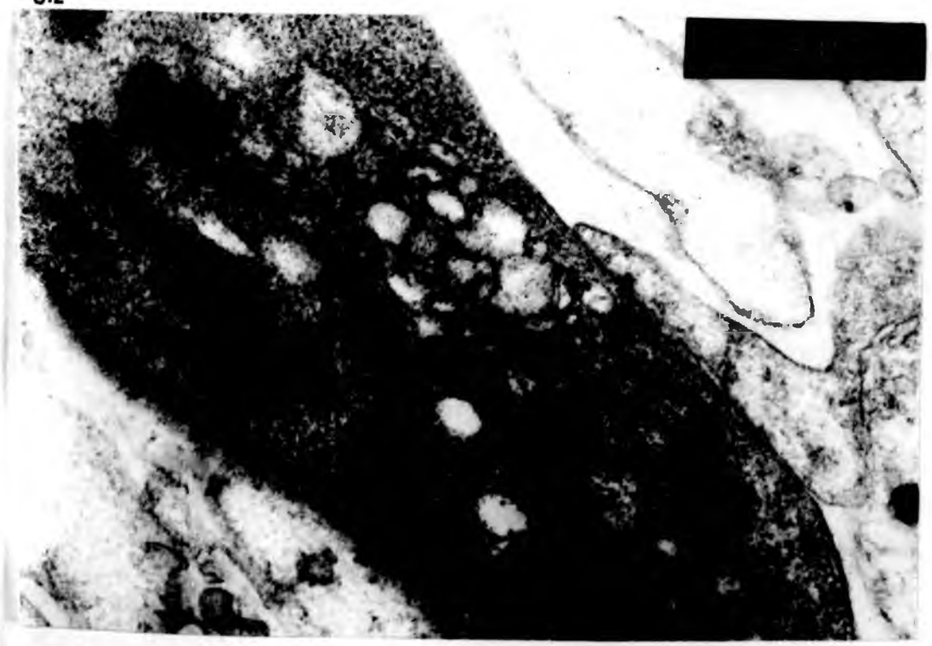

Fig. 8.3 TEM of a soma tegumentary cyton after 1 hour in 10μM monensin. Note the swollen cisternae of the Golgi complex occur in both the maturing (MF) and forming faces (FF). Swollen electron-lucent vesicles (V) are also present near the complexes although the single cisternae of endoplasmic reticulum (ER) remain unaffected. Occasional mitochondria (M) are also swollen whilst others remain unchanged. X63,400.

Fig. 8.4 TEM of a soma tegumentary cyton after 1 hour in 10μM monensin. Increased electron-lucent vesicles (V) are present in the vicinity of the Golgi complexes, together with increased mitochondrial profiles (M). Two types of residual bodies are also present. The first type (R_1) has multilaminate stacks of electron dense material (MS) (inset); the second type (R_2) contains general debris. N; nucleus, DC; distal cytoplasm. X14,200 (inset X79,600).

8.3

8.4

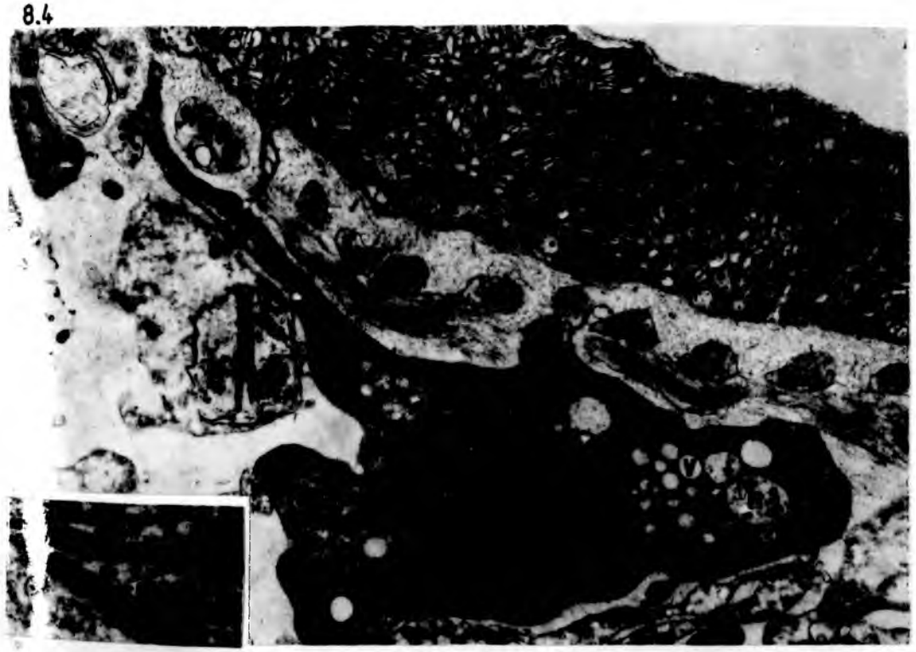

Fig. 8.5 TEM of a tegumentary cyton of an un-incubated control protoscolex stained for acid phosphatase. Occassional reaction deposits can be seen around presumed Golgi vesicles (arrow) and in areas which may represent transition vesicles (curved arrow) between the Golgi and endoplasmic reticulum. X79,600.

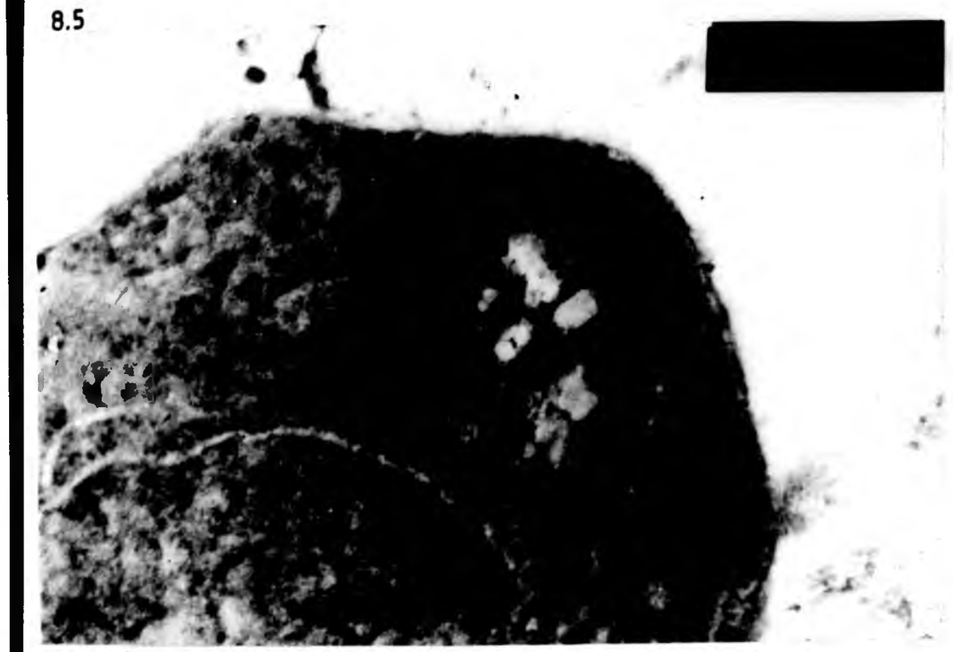

Fig. 8.6 TEM of a soma tegumentary cyton of an un-incubated control protoscolex stained for thiamine pyrophosphatase. Note the occasional reaction deposits around some of the Golgi derived vesicles (arrows). X63,400.

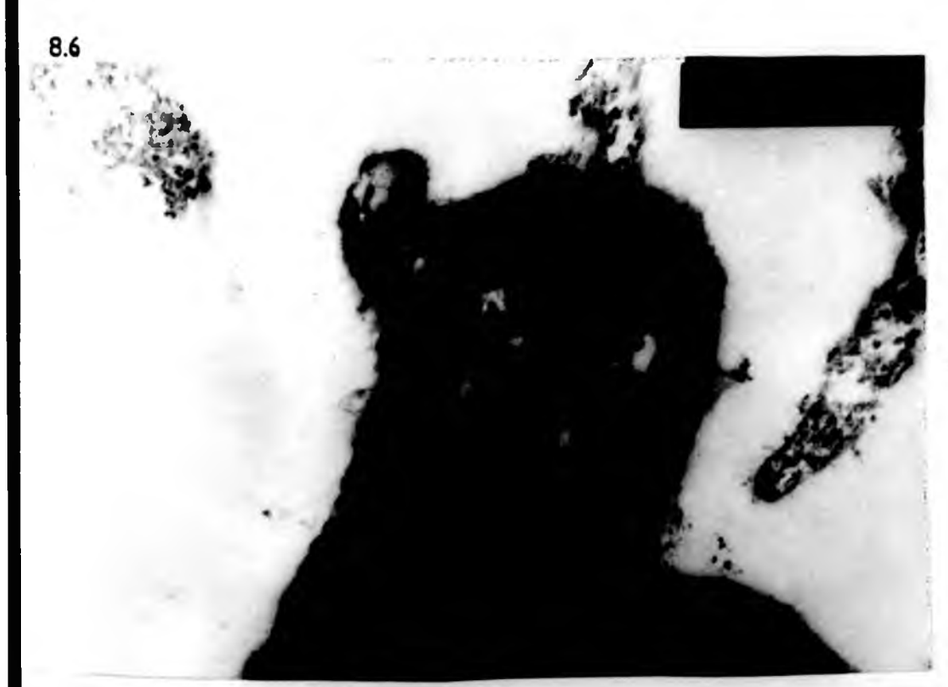

Fig. 8.7 TEM of a tegumentary cyton of a protoscolex incubated in 10μM monensin for 1 hour and stained for acid phosphatase. No reaction deposits are present. G; Golgi complex. X79,600.

Fig. 8.8 TEM of a tegumentary cyton of a protoscolex incubated in 10μM monensin for 1 hour and stained for thiamine pyrophosphatase. No reaction deposits are present. G; Golgi complex. X79,600.

8.7

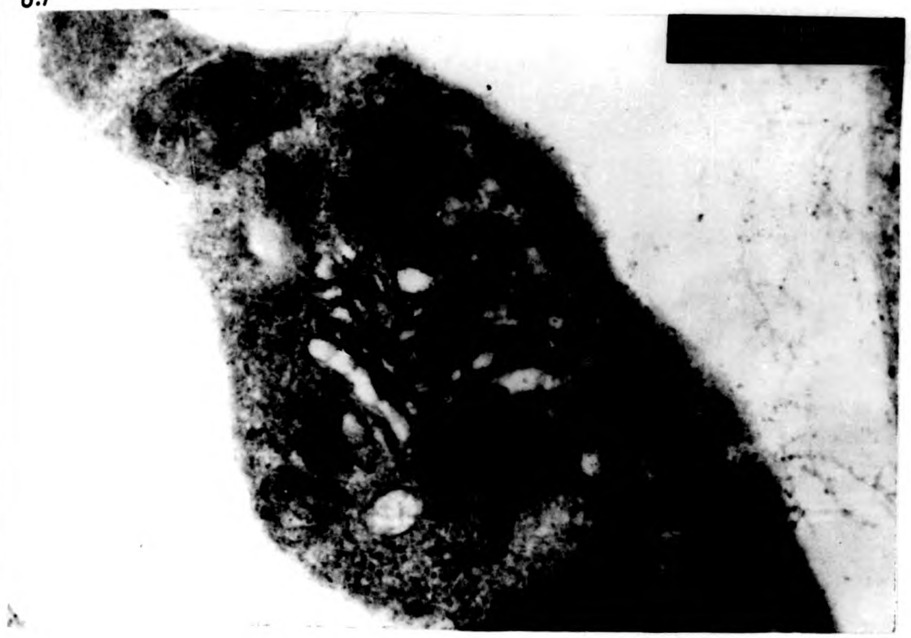

8.8

Fig. 8.9 TEM of a tegumentary cyton of a protoscolex incubated in 10μM monensin for 3 hours. Numerous large electron-lucent vesicles (V) characterize the cytons although the endoplasmic reticulum (ER) remains unchanged. N; nucleus. X29,200.

Fig. 8.10 TEM of the distal cytoplasm of a protoscolex incubated in 10μM monensin for 3 hours. A large vacuole (V) and both types of residual body (R_1, R_2) are present. X29,200.

8.9

8.10

Fig. 8.11 TEM of the tegument of a protoscolex incubated in 10μM monensin for 3 hours showing severe vacuolation of the distal cytoplasm at the base of the scolex. Abundant debris (D) and shed microtriches (Mt) suggest that disruption of the distal cytoplasm has taken place out of section plane. X8,960.

8.11

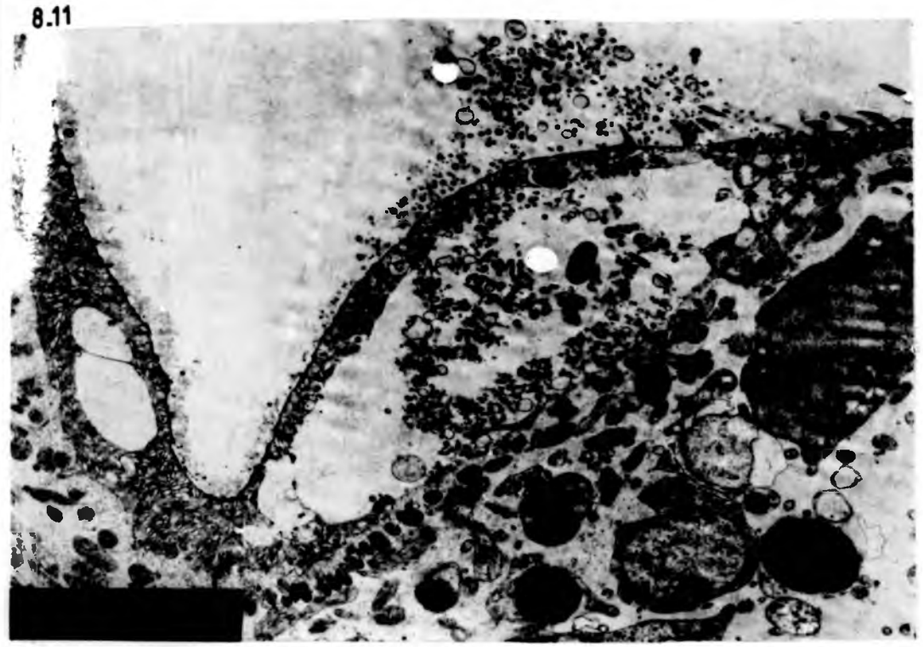

Fig. 8.12 TEM of the soma tegument of a protoscolex incubated in 10μM monensin for 12 hours. The cytons contain numerous large vesicles (V) and the mitochondria (M) also are swollen, possessing dilated cristae (arrowheads). The vesicles of the distal cytoplasm (DC) appear turgid. X20,500.

8.12

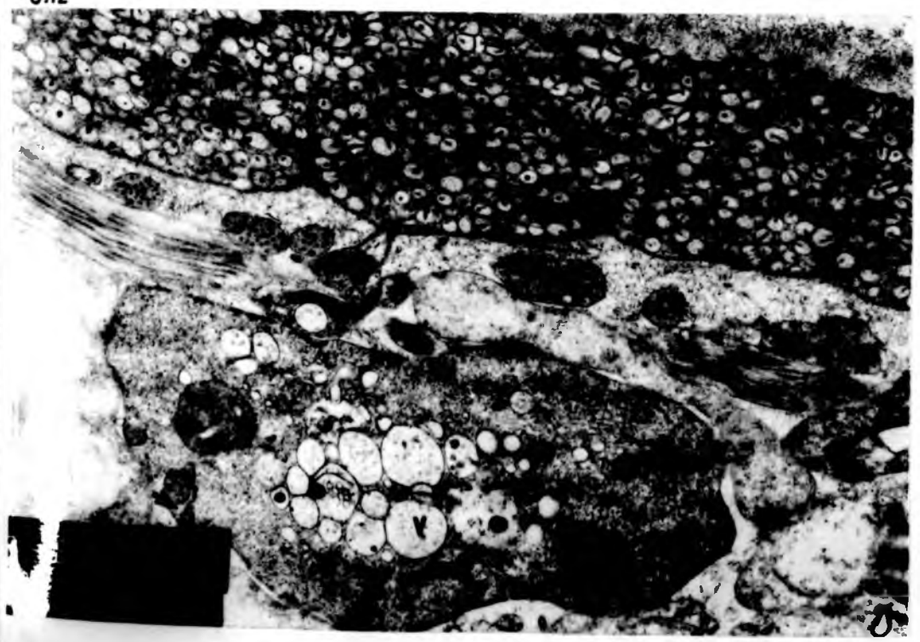

Fig. 8.13 TEM of the tegument of a protoscolex incubated in 10μM monensin for 12 hours. note that the cytons are highly vacuolated and occasionally multinucleate. N; nucleus. X11,000.

8.13

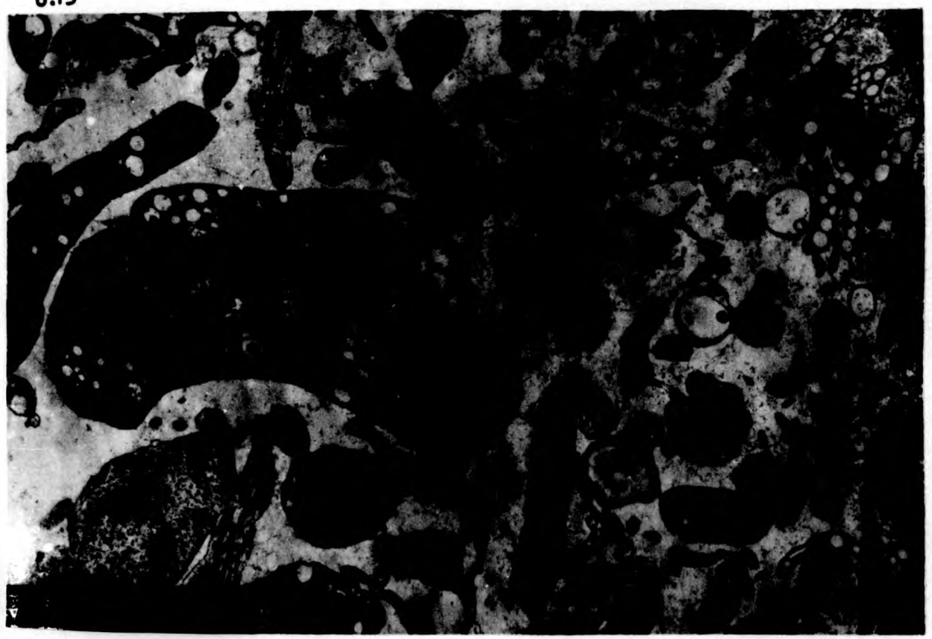

Fig. 8.14 TEM of the tegument of a protoscolex incubated in 10μM monensin for 12 hours. The cytons (C) are highly vacuolated as is the distal cytoplasm (DC). X5,480.

Fig. 8.15 TEM of the tegument of a protoscolex incubated in 10μM monensin for 24 hours. Note that the tissue is pale and lacks contrast. DC; distal cytoplasm, C; cyton, Ms; muscle. X14,200.

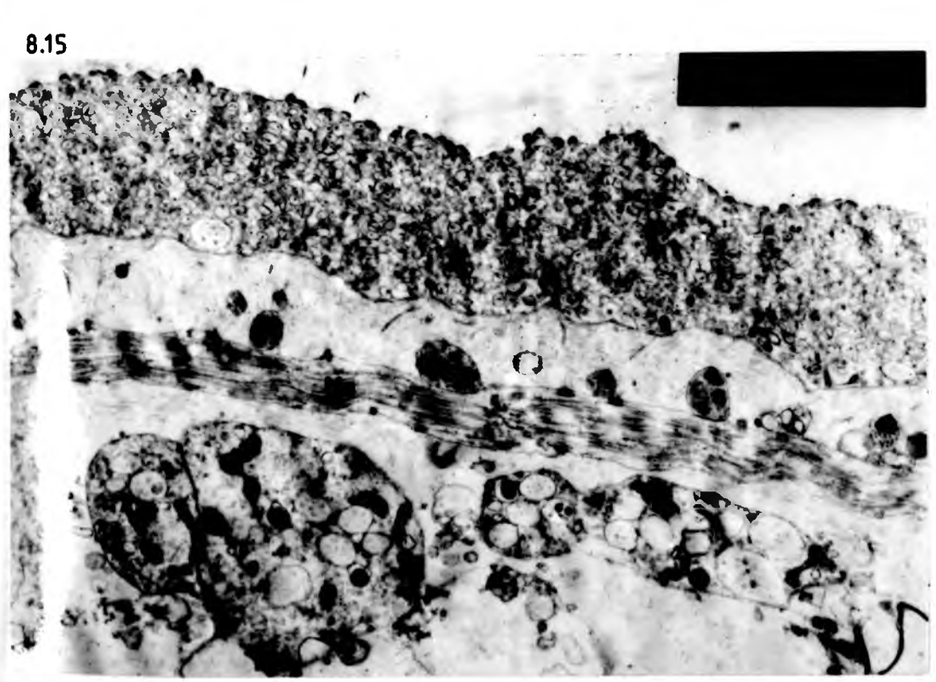

Fig. 8.16 TEM of a tegumentary cyton of a protoscolex incubated in 10μM monensin for 24 hours. The tissue is necrotic and numerous vesicles (V), debris (D) and mitochondrial remnants (M) are present. N; nucleus. X20,500.

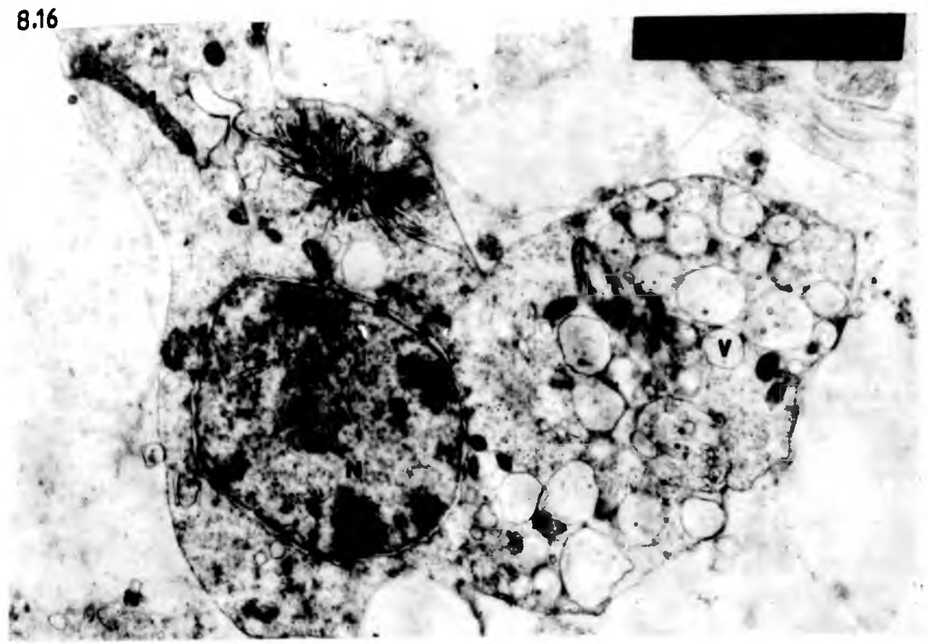

Fig. 8.17 TEM of the scolex tegument of a protoscolex incubated in 10μM monensin for 24 hours. The distal cytoplasm (DC) is again necrotic and highly vacuolated. X20,500.

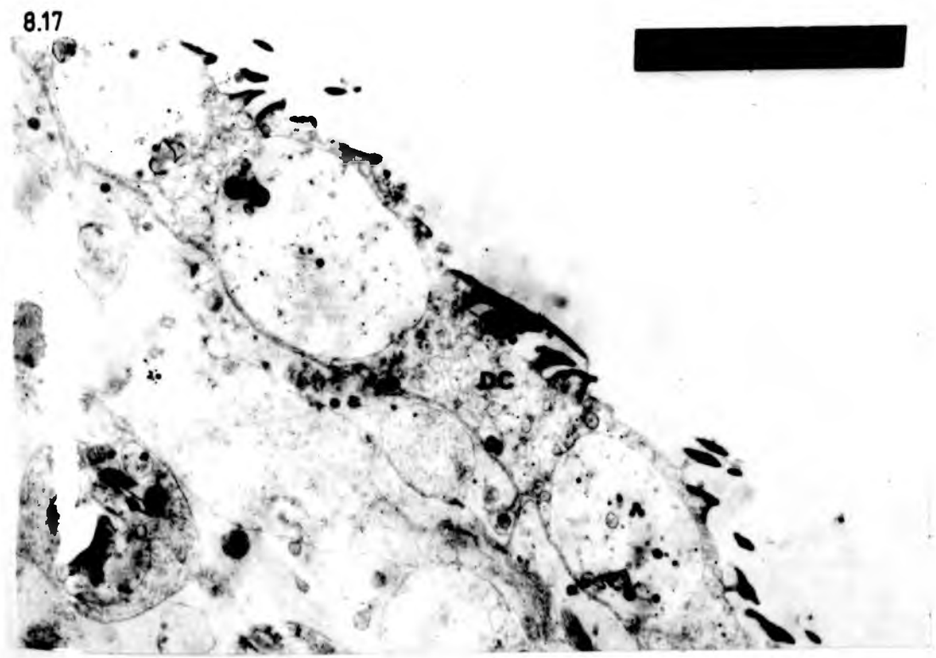

Fig. 8.18 TEM of the tegument of a protoscolex incubated in 10μM monensin for 24 hours. Note that the distal cytoplasm (DC) is contorted into many folds (arrows). X3,450.

8.18

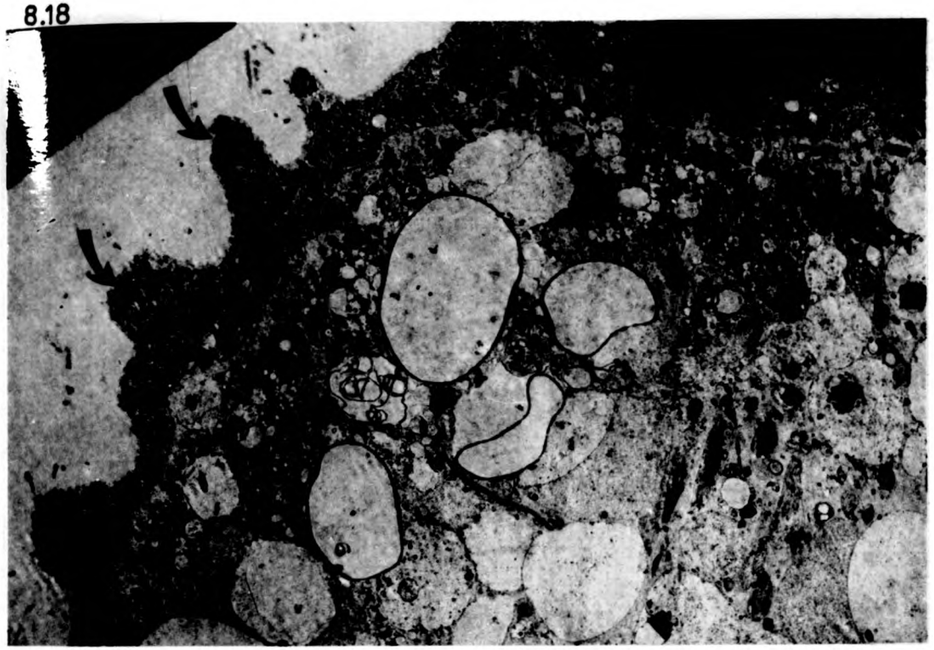

Fig. 8.19 TEM of the distal cytoplasm of a protoscolex incubated in 10μM monensin for 24 hours. Numerous vacuoles (V) are present and a large cytoplasmic bleb (B) extends from the tegumentary surface. X6,590.

8.19

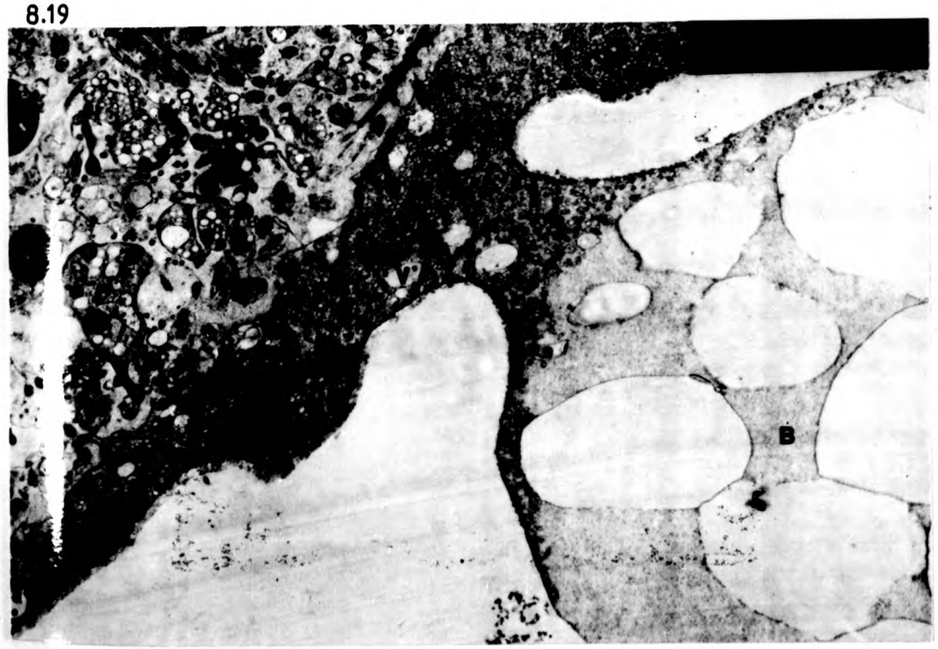

Fig. 8.20a SEM of a protoscolex incubated in 10μM monensin for 24 hours. Note the highly profiled suckers (Sk) and the folded nature of the soma (So). X750.

Fig. 8.20b SEM high power of the folded nature of the soma region. X3,500.

8.20a

8.20b

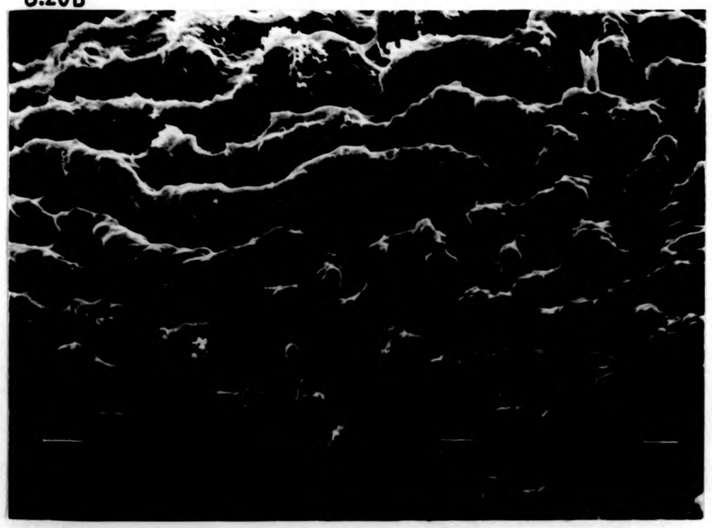

Fig. 8.21a SEM of a protoscolex incubated in 10μM monensin for 24 hours. The protoscolex is necrotic and possesses numerous cytoplasmic blebs (B). Sc; scolex, So; soma. X750.

8.21a

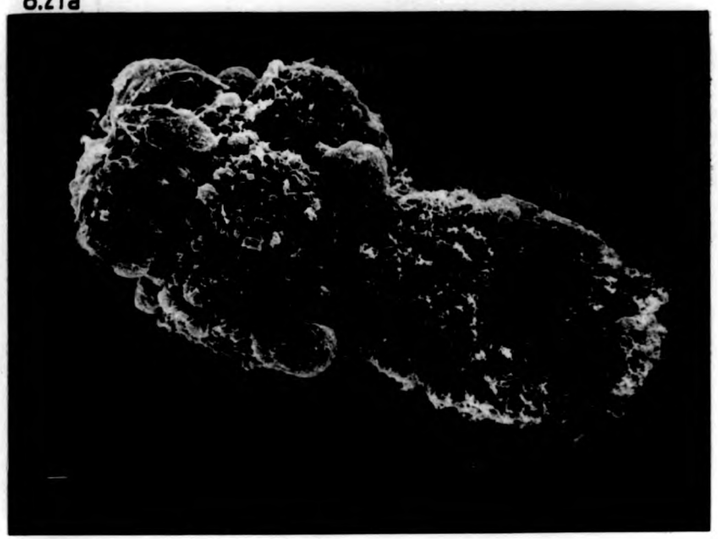

Fig. 8.21b SEM high power of a tegumentary bleb on the scolex showing the microtriches (Mt) in disarray. X3,500.

8.21b

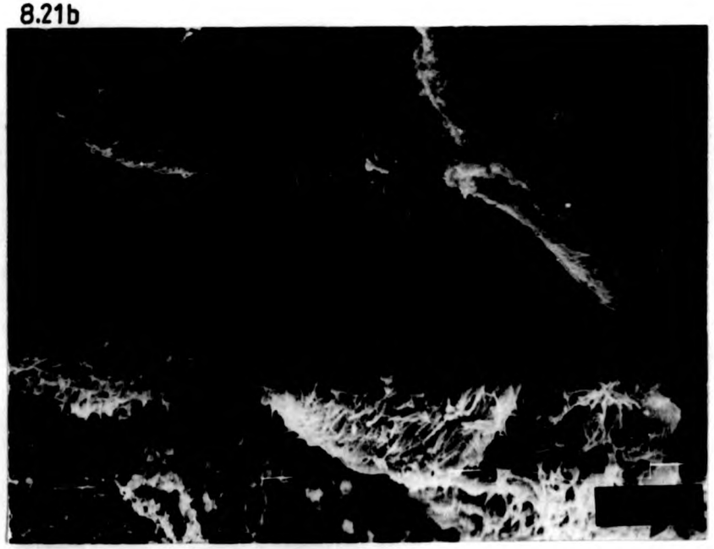

Fig. 8.22 SEM of a control incubated protoscolex showing the normal appearance of the scolex (Sc) and soma (So) regions. X750.

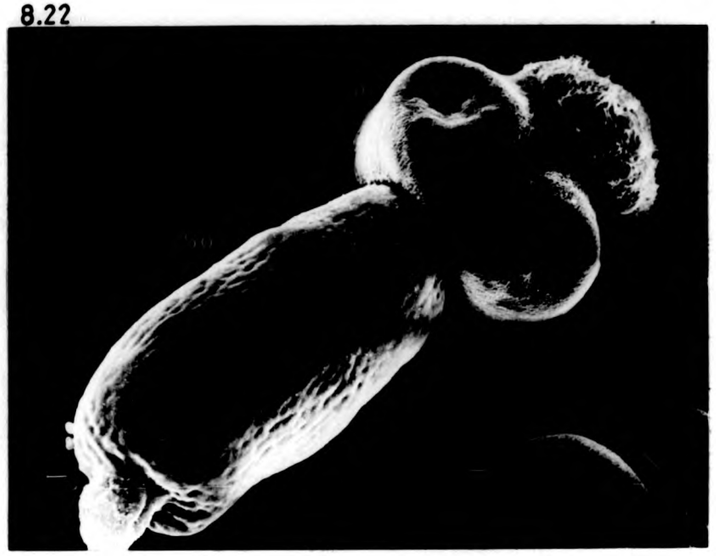

Fig. 8.23 TEM of a tegumentary cyton from a control incubated protoscolex showing the normal compressed form of the Golgi cisternae (G). X63,400.

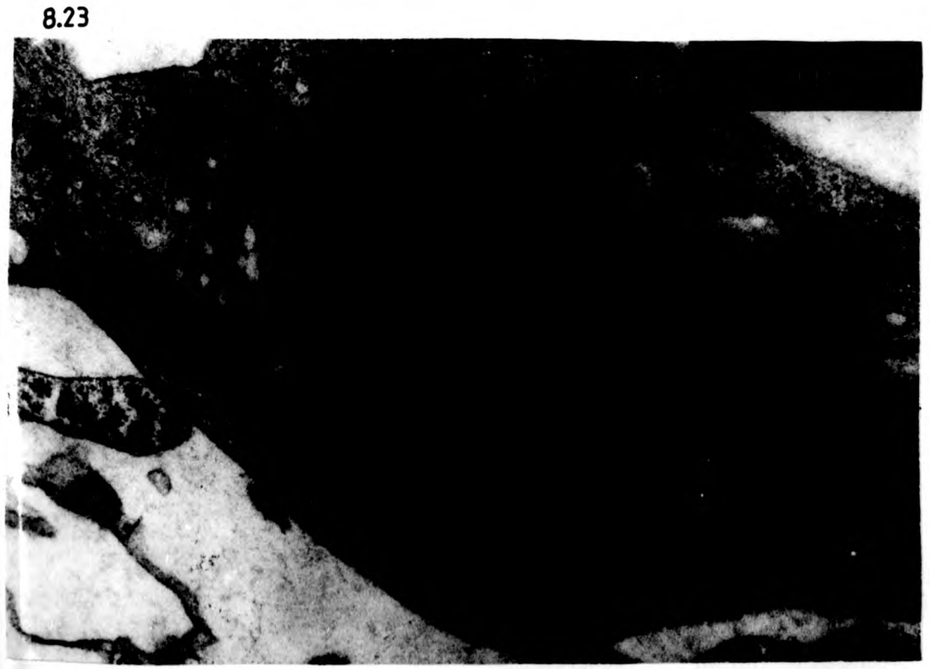

Fig. 8.24 TEM of a tegumentary cyton of a protoscolex incubated in 10μM monensin for 24 hours. The tissue is only slightly affected and the Golgi cisternae (G) are in the first stages of swelling. X63,400.

Fig. 8.25 TEM of a 9 month murine cyst incubated in 10μM monensin for 15 min. Increased numbers of electron lucent vesicles (V) are present together with very large storage lysosomes (L). DC; distal cytoplasm, LL; laminated layer. X14,200.

8.24

8.25

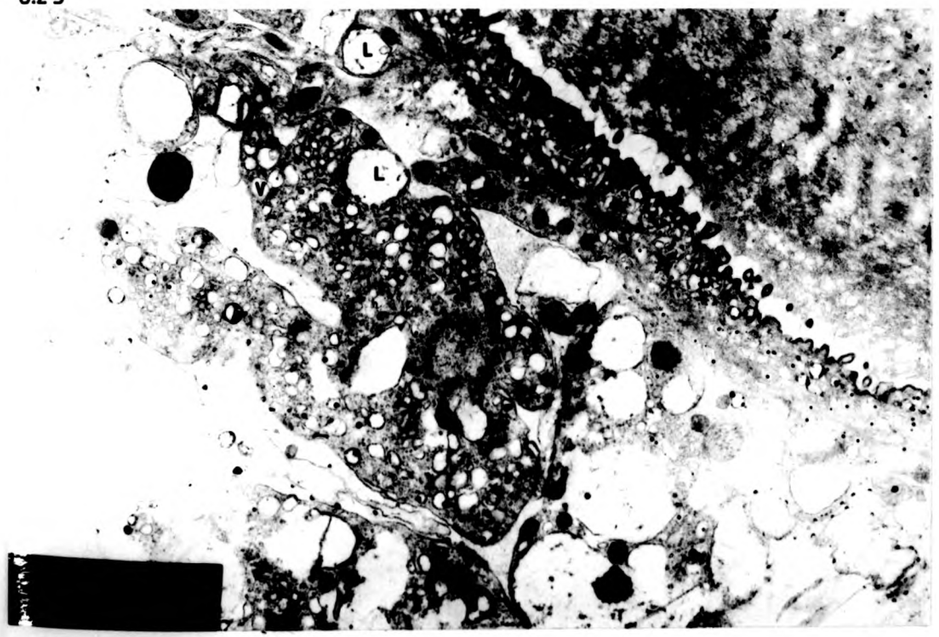

Fig. 8.26 TEM of a 9 month murine cyst incubated in 10μM monensin for 15min. Many of the 'G' vesicles of the distal cytoplasm have an electron-dense periphery and enlarged dense granules (arrows). LL; laminated layer. X39,100.

8.26

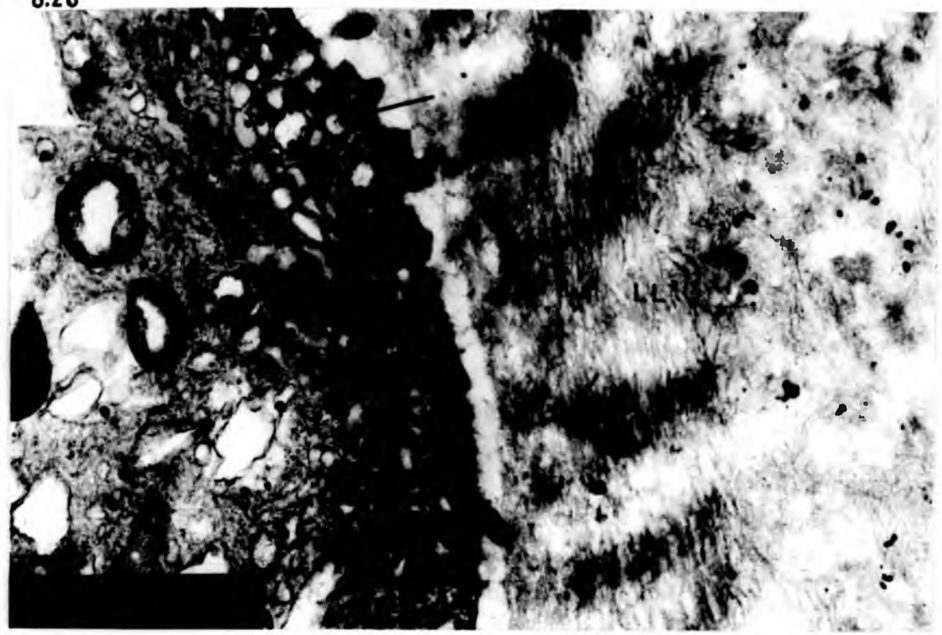

Fig. 8.27 TEM of a 9 month murine cyst incubated in 10μM monensin for 15min. Note the enlarged granules (arrows) of the 'G' vesicles in the distal cytoplasm and cytons and also the large storage lysosomes (L). X29,200.

8.27

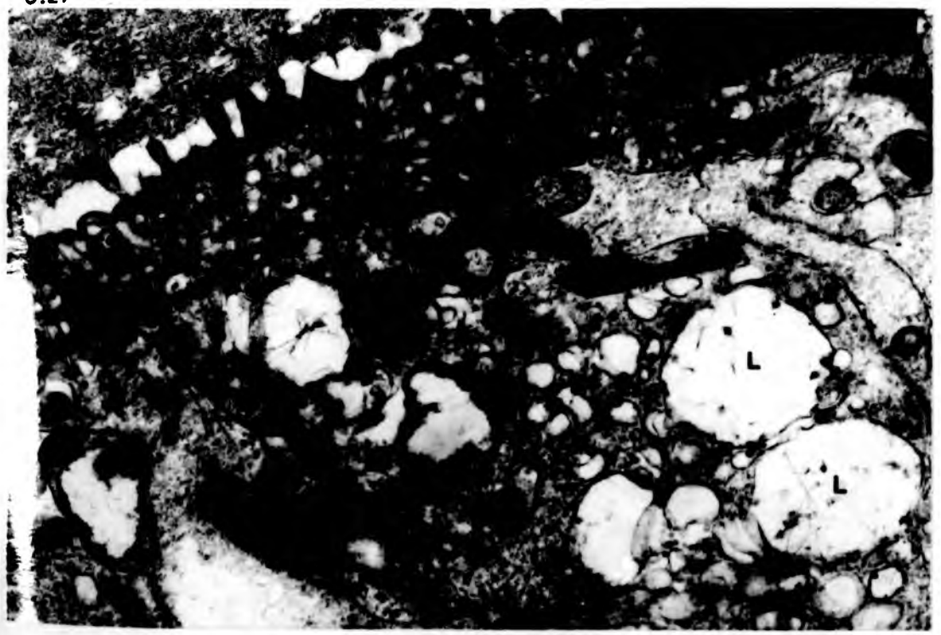

Fig. 8.28 TEM of a 9 month murine cyst incubated in 10μM monensin for 1 hour. Note the increased size and number of the storage lysosomes (L) and also the mitochondria (M) which appear more numerous. DC; distal cytoplasm, LL; laminated layer, N; nucleus. X14,200.

8.28

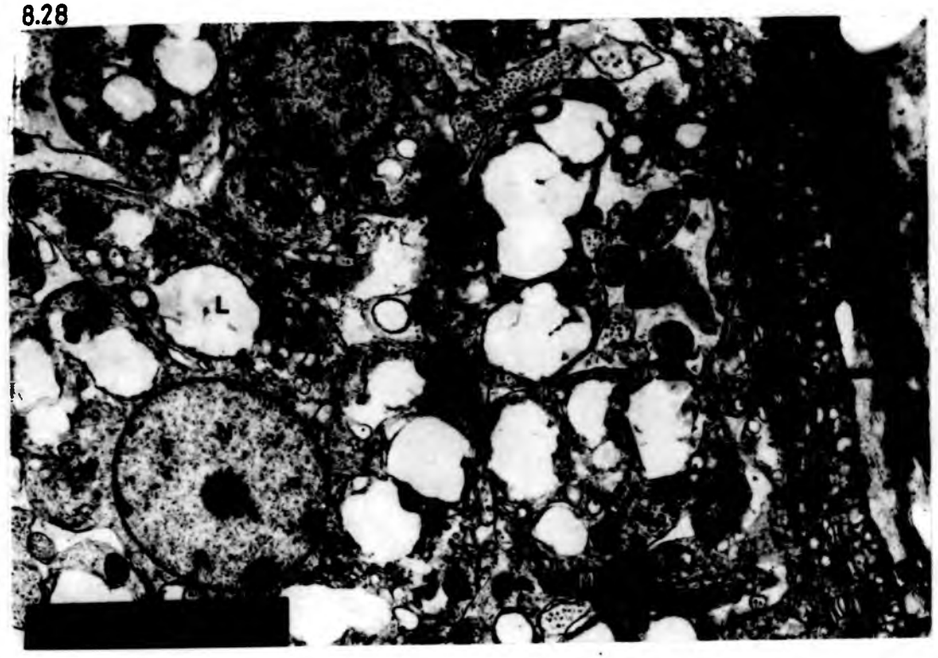

Fig. 8.29 TEM of a 9 month murine cyst incubated in 10μM monensin for 1 hour. Note the very elongate mitochondria (M) in the tegumentary tissue. These organelles possess a dense matrix with occasional transverse cristae (C). X29,200.

8.29

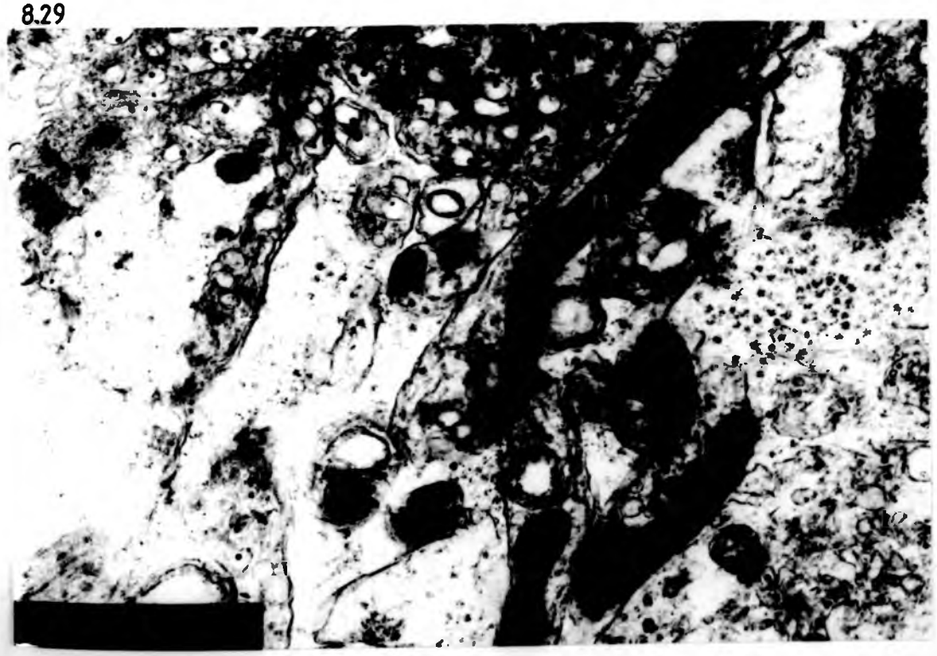

Fig. 8.30 TEM of a 9 month murine cyst incubated in 10μM monensin for 1 hour. The vesicles of the tegumentary cytons apper to be bounded by membranes which have lost thier integrity and appear convoluted (arrows). Mitochondria (M) and other cytoplasmic components appear to be becoming incorporated into autophagic vacuoles (Vc). X39,100.

8.30

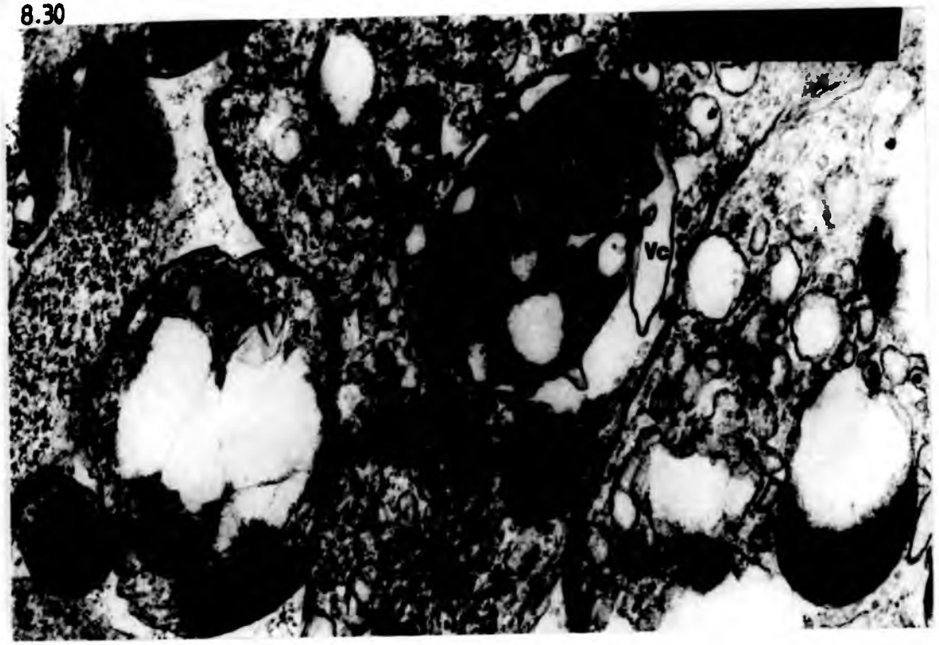

Fig. 8.31 TEM of a 9 month murine cyst incubated in 10μM monensin for 1 hour. Occasional myocytons possess nuclei (N) of whch the outer membrane appears to be 'blown out' (arrows). X20,500.

8.31

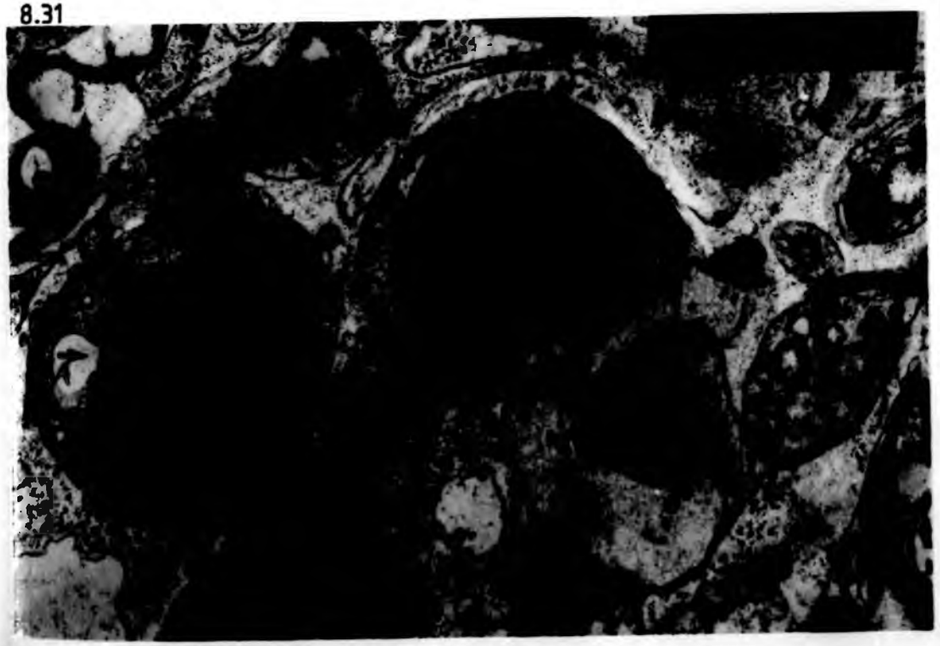

Fig. 8.32 TEM of a 12 month murine cyst incubated in 10μM monensin for 3 hours. Large clusters of mitochondria (M) are present in the internuncial processes just below the distal cytoplasm. The cristae (C) of the mitochondria appear very obvios within the matrix of the organelles. X29,200.

8.32

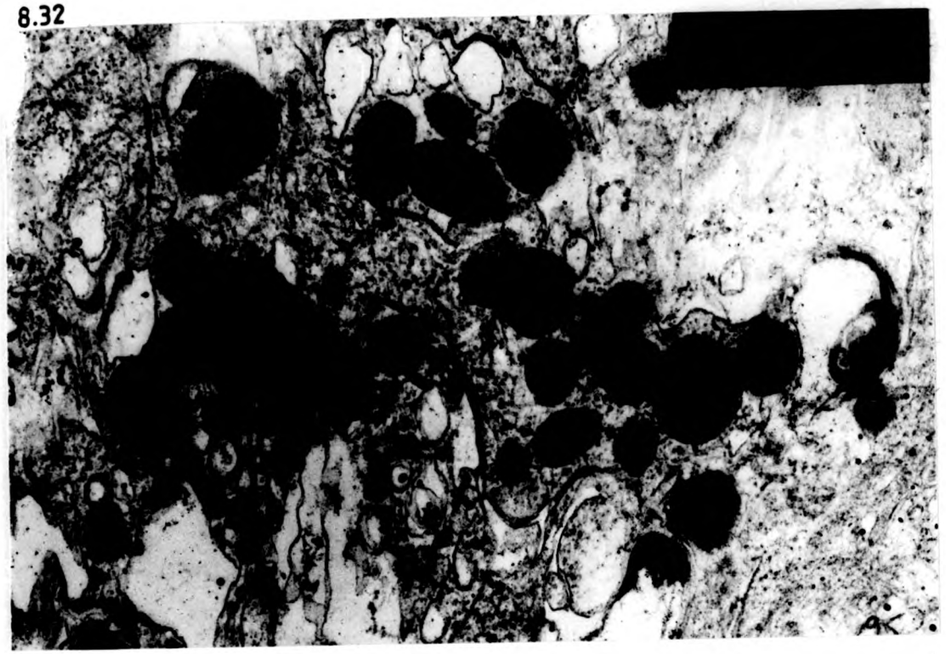

Fig. 8.33 TEM of a 12 month murine cyst incubated in 10μM monensin for 3 hours. High power micrograph showing mitochondria in which the cristae (C) appear dilated. X63,400.

8.33

Fig. 8.34 TEM of a 12 month murine cyst incubated in 10μM monensin for 3 hours. Increased membraneous whorls (W) are present within the cytons in close proximity to large mitochondria (M). X39,100.

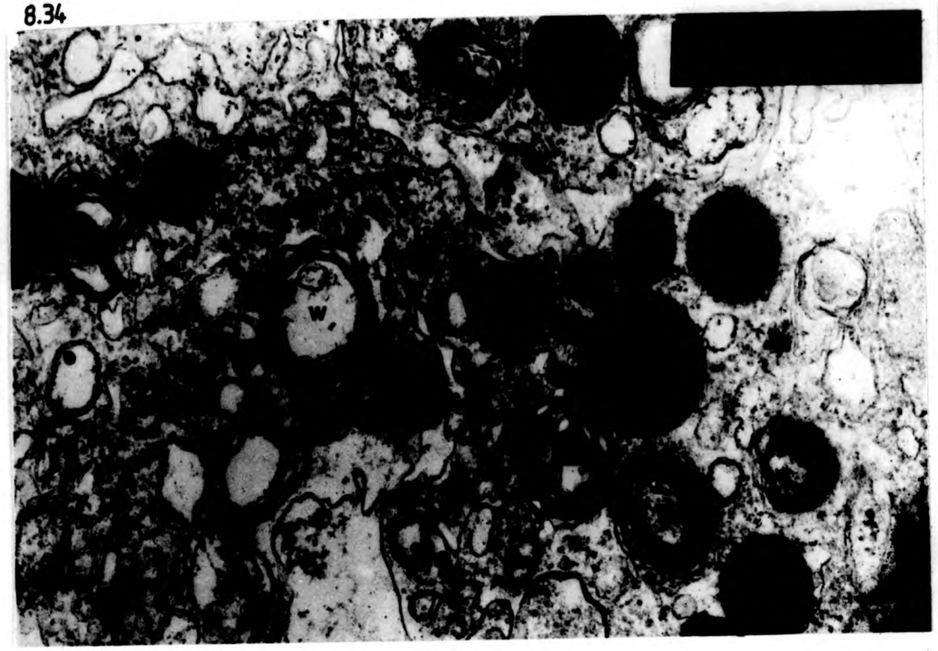

Fig. 8.35 TEM of a 12 month murine cyst incubated in 10μM monensin for 8 hours. The tegumentary tissue now appears pale and the cytons possess large vacuoles (V) mitochondria (M) and membraneous whorls (W). The nuclei (N) are also pale in appearance. DC; distal cytoplasm. X14,200.

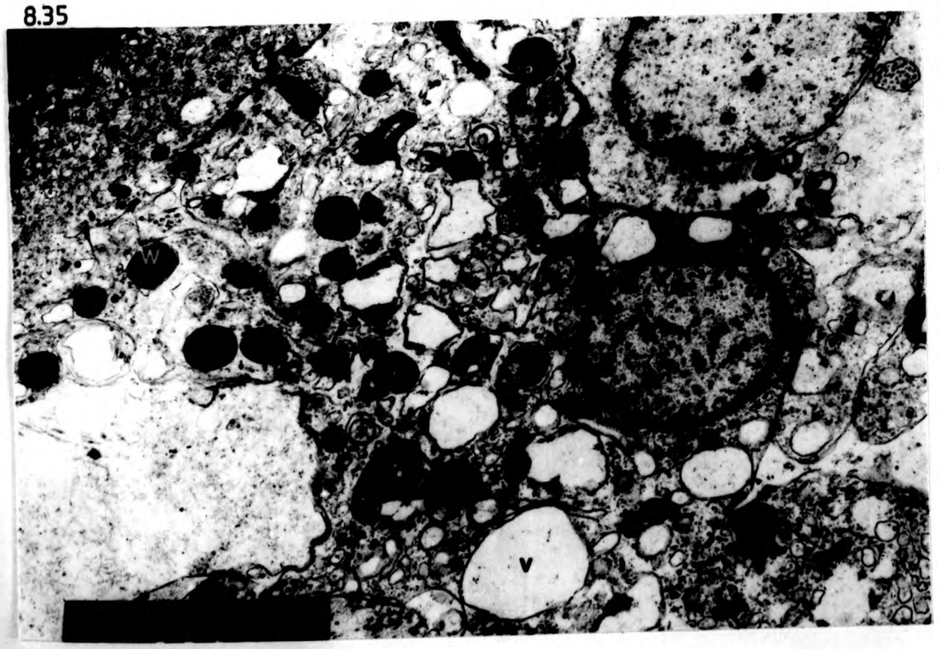

Fig. 8.36 TEM of a 12 month murine cyst incubated in 10μM monensin for 8 hours. The tegumentary mitochondria often possess dilated cristae (C) which often appeared circular. X79,600.

8.36

Fig. 8.37 TEM of a 12 month murine cyst incubated in 10μM monensin for 8 hours. Some of the tegumentary mitochondria (M) are surrounded by a series of membranes (arrow) suggesting encapsulation and breakdown. Others possess dilated cristae (C). X39,100.

8.37

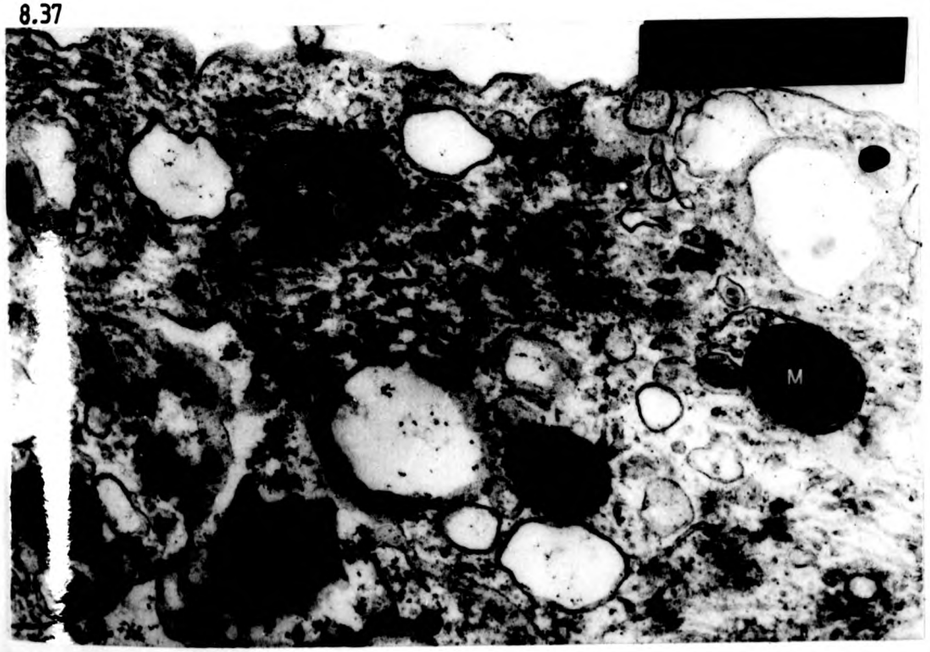

Fig. 8.38 TEM of a 12 month murine cyst incubated in 10μM monensin for 8 hours. The distal cytoplasm (DC) of the tegument although pale in appearance is relatively unaffected compared to the cytons and internuncial processes where numerous membraneous whorls (W) and abnormal mitochondria (M) are present. X29,200.

8.38

Fig. 8.39 TEM of a 12 month murine cyst incubated in 10μM monensin for 24 hours. The tegumentary cytons consist of a mass of large membraneous vacuoles and the tissue is clearly dead. X14,200.

8.39

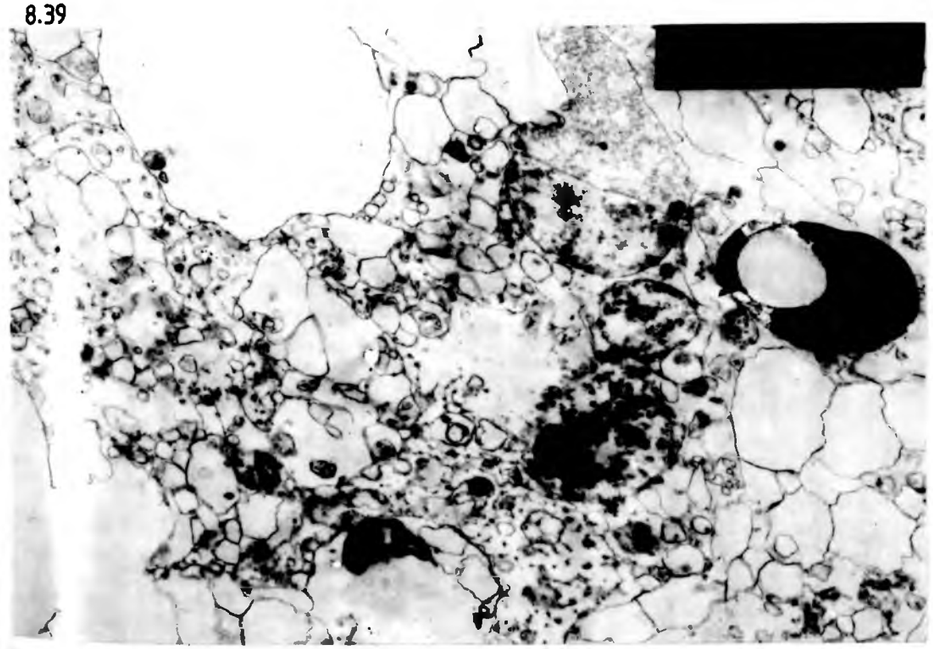

Fig. 8.40 TEM of a 12 month murine cyst incubated in 10μM monensin for 24 hours. The distal cytoplasm (DC) also appears necrotic and is composed of a series of large vacuoles lying adjacent to the laminated layer (LL). X11,000.

8.40

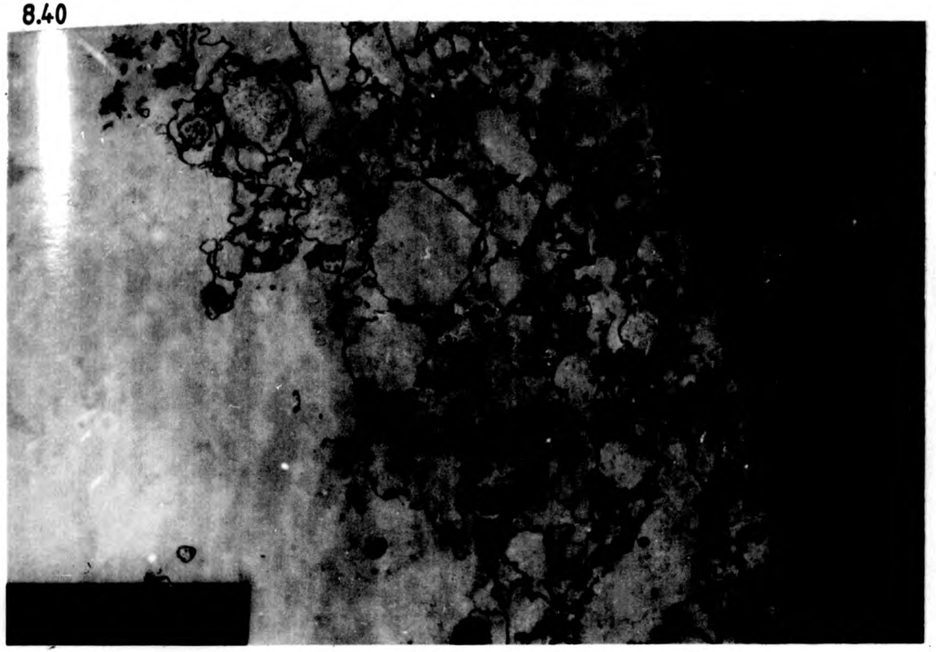

Fig. 8.41 TEM of a 12 month murine cyst incubated in control medium for 56 hours. The tegumentary cytons appear unaffected and possess occasional mitochondria (M) normal vesicles and Golgi complexes (G). N; nucleus, ER endoplasmic reticulum. X20,500.

8.41

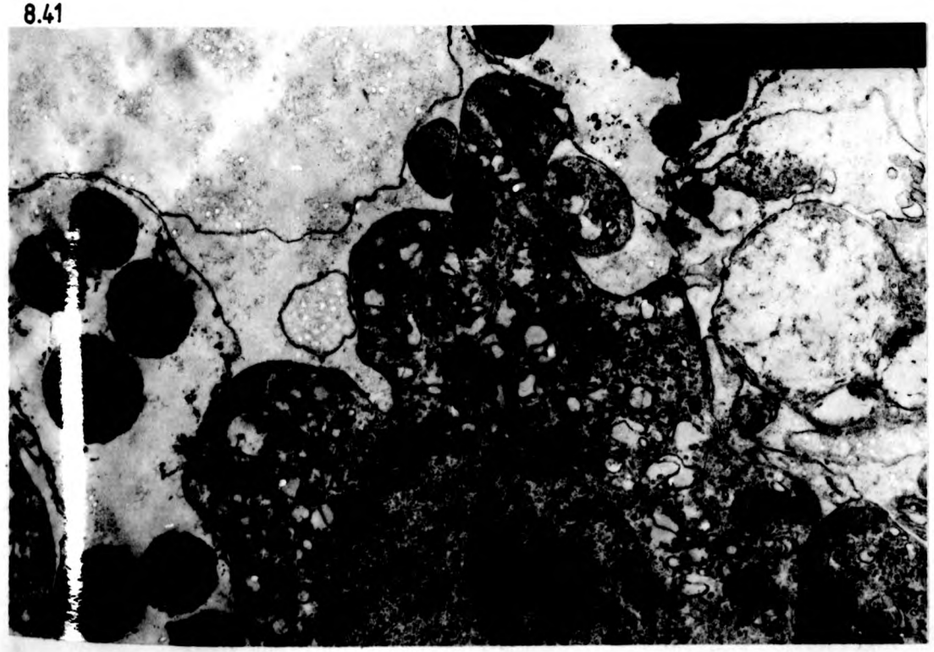

Fig. 8.42 TEM of a 12 month murine cyst incubated in 10μM monensin for 56 hours. The distal cytoplasm (DC) also appears unaffected although clusters of mitochondria (M) are sometimes evident just below the basal membrane. L; storage lysosomes. X29,200.

8.42

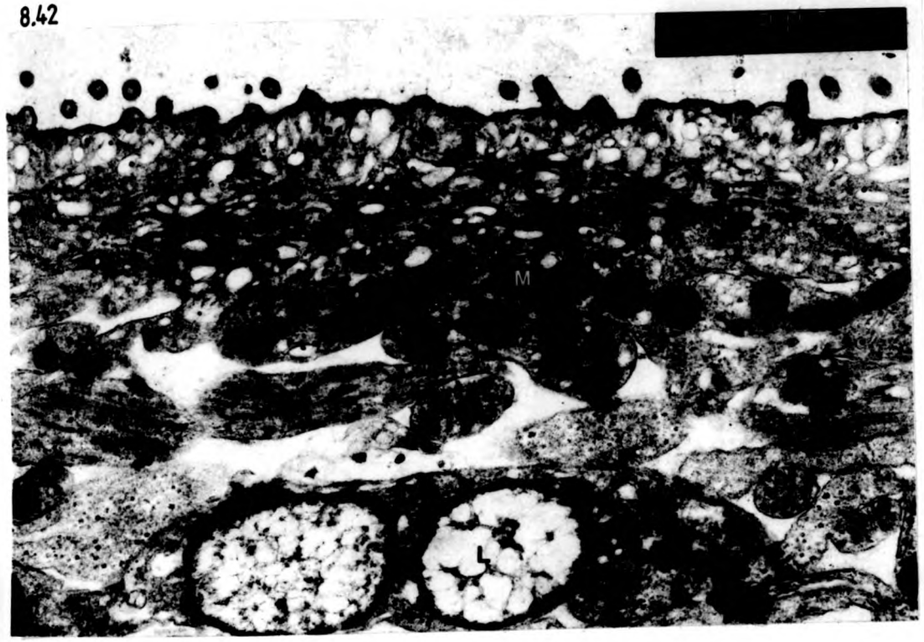

Fig. 8.43 LM of a 12 month murine cyst (unincubated control) showing a normal structure with the germinal layer (GL) in contact with the laminated layer (LL). Calcareous corpuscles (CC) can also be seen within the cyst. X45.

8.43

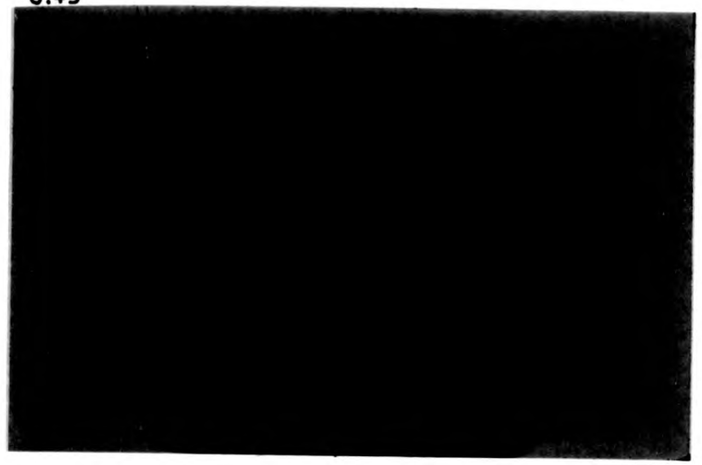

Fig. 8.44 LM of a 12 month murine cyst incubated in 10μM monensin for 8 hours. The germinal layer (GL) is darker and has a pitted appearance (arrows). LL; laminated layer. X152.

8.44

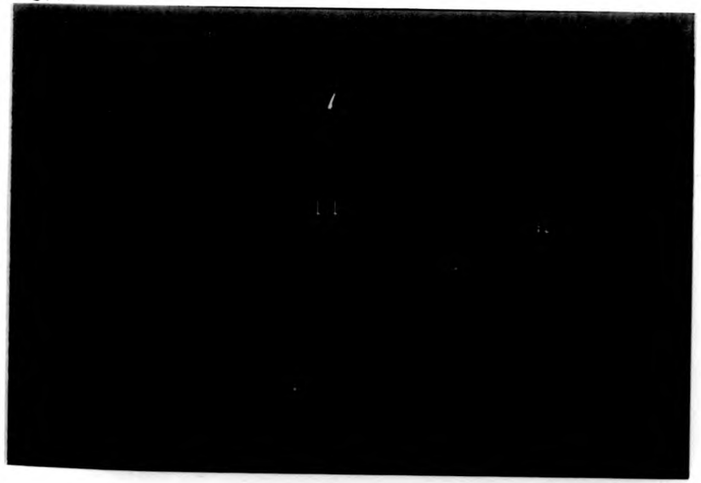

Fig. 8.45 LM of a 12 month murine cyst incubated in 10μM monensin for 12 hours. The germinal layer (GL) has now detached from the laminated layer (LL) in places. X152.

8.45

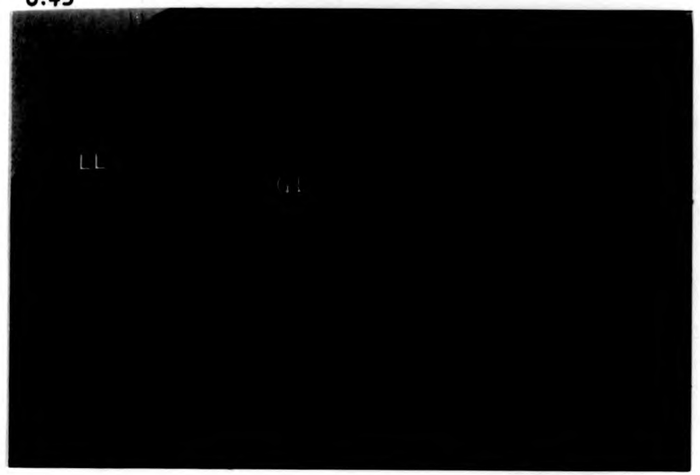

Fig. 8.46 LM of a 12 month murine cyst incubated in 10μM monensin for 24 hours. The germinal layer (GL) has now completely detached from the laminated layer (LL) and has collapsed into the centre of the cyst. X95.

8.46

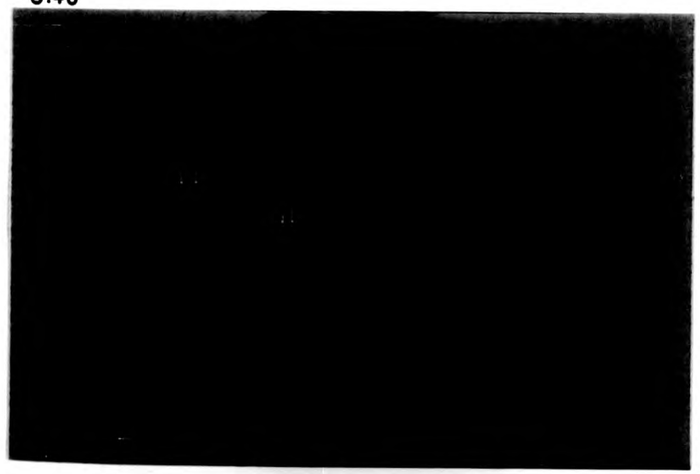

Fig. 8.47 TEM of a 32 day *in vitro* cultured cyst incubated in 10μM monensin for 1 hour. The tegumentary cytons contain numerous swollen vesicles (V). N; nucleus. X20,500.

Fig. 8.48 TEM of a 32 day *in vitro* cultured cyst incubated in 10μM monensin for 1 hour. The distal cytoplasm also possesses numerous enlarged vesicles (V). X39,100.

8.47

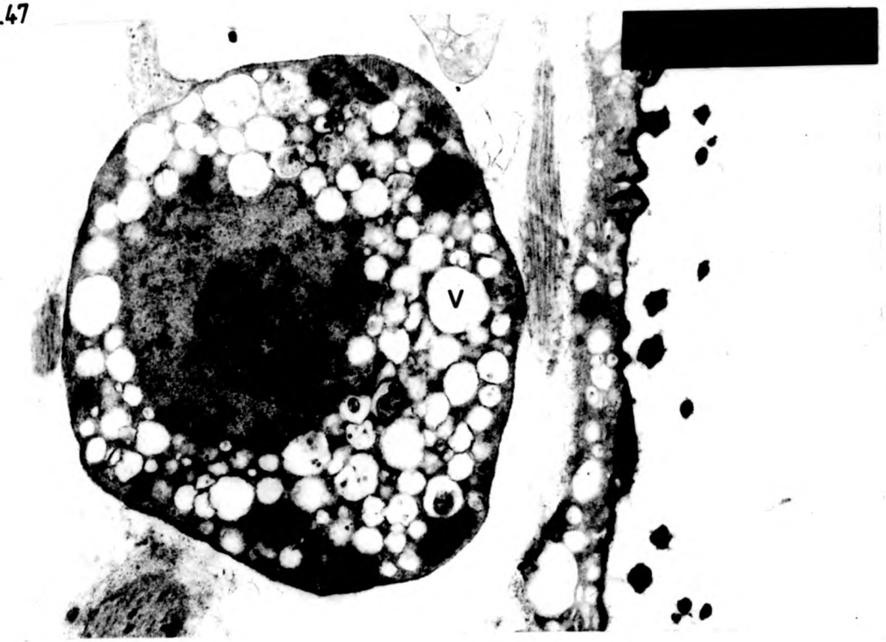

8.48

Fig. 8.49 TEM of a 108 day *in vitro* cultured cyst incubated in 10μM monensin. The distal cytoplasm of the former scolex region possesses abnormal mitochondria (M) and residual bodies (R). LL; laminated layer. X39,100.

8.49

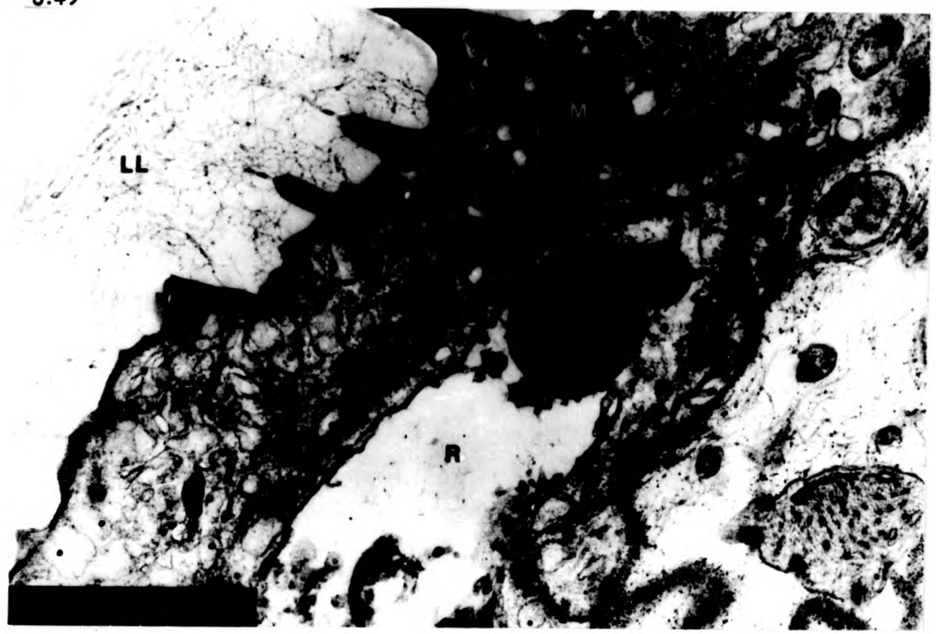

Fig. 8.50 TEM of a 10 month cyst from a mouse injected with 0.2ml of 10μM monensin daily 21 days. Tegumentary distal cytoplasm possessing some enlarged granules (arrows) within the 'G' vesicles. TM; truncated microtriches, LL; laminated layer. X39,100.

8.50

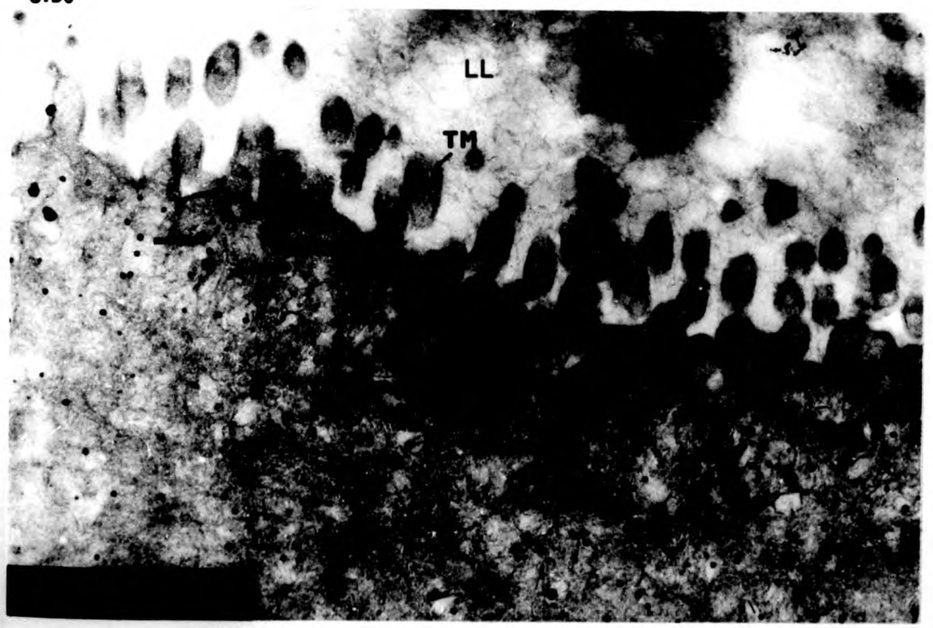

Fig. 8.51 TEM of a 10 month murine cyst from a mouse injected i.p. with 0.5ml of 20μM monensin daily. 21 days. The tegumentary tissue appears relatively unaffected even though the cyst was slightly pitted. Increased numbers of mitochondrial profiles (M) are, however, evident. DC; distal cytoplasm, N; nucleus. X14,200.

8.51

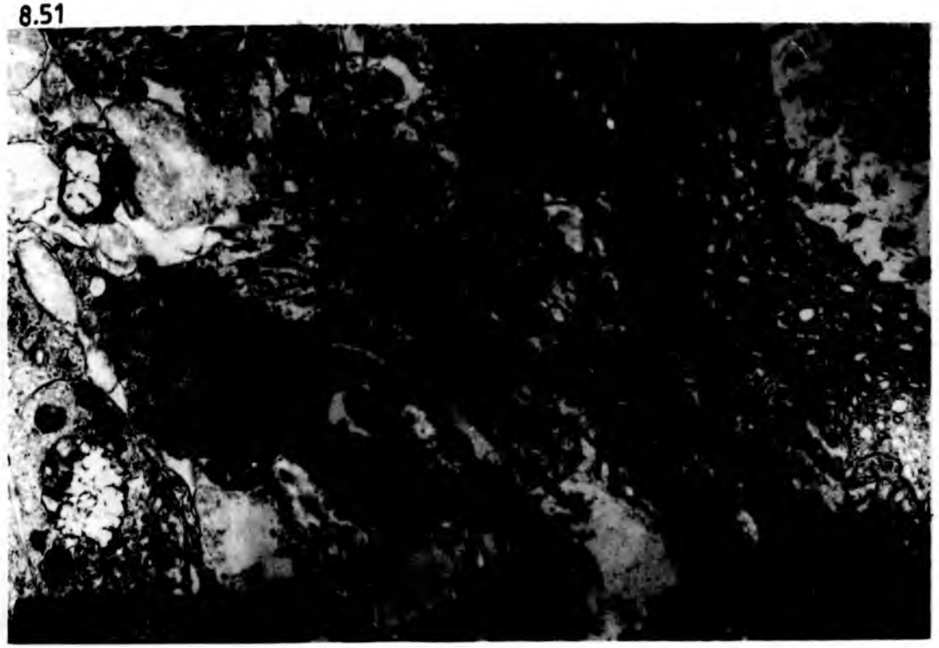

Fig. 8.52 TEM of a 10 month murine cyst from a mouse injected i.p. with 0.5ml of 20μM monensin daily. 30 days - pitted cyst. Increased mitochondrial profiles are present with some mitochondria appearing swollen (M). Occasional membraneous whorls (W) are also present. Lp; lipid droplet. X20,500.

8.52

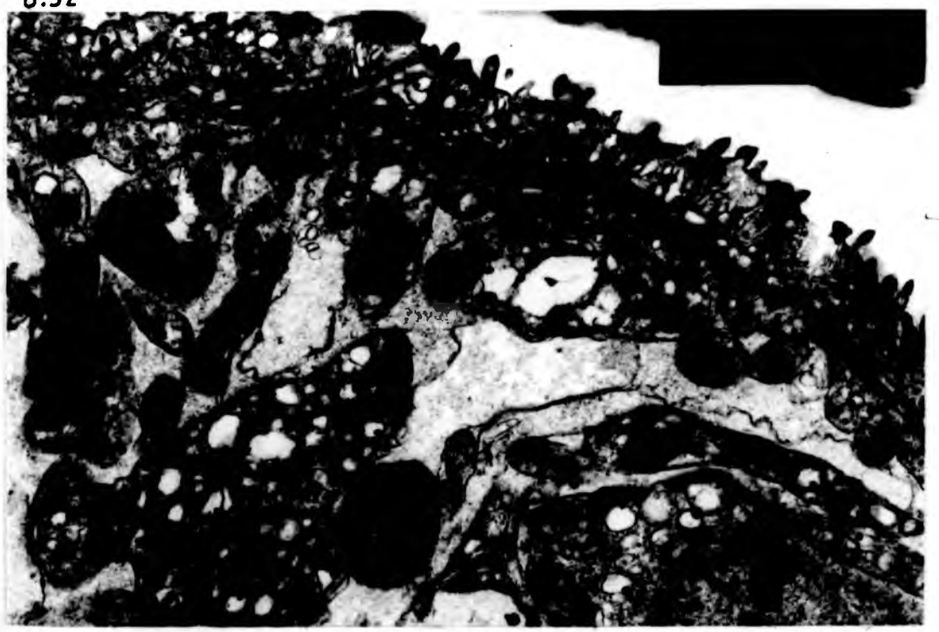

Fig. 8.53 TEM of a 10 month murine cyst from a mouse injected i.p. with 0.5ml of 20μM monensin daily. 60 days - detaching germinal layer. The tegumentary distal cytoplasm is considerably vacuolated possessing large swollen vesicles (V). LL; laminated layer. X29,200.

8.53

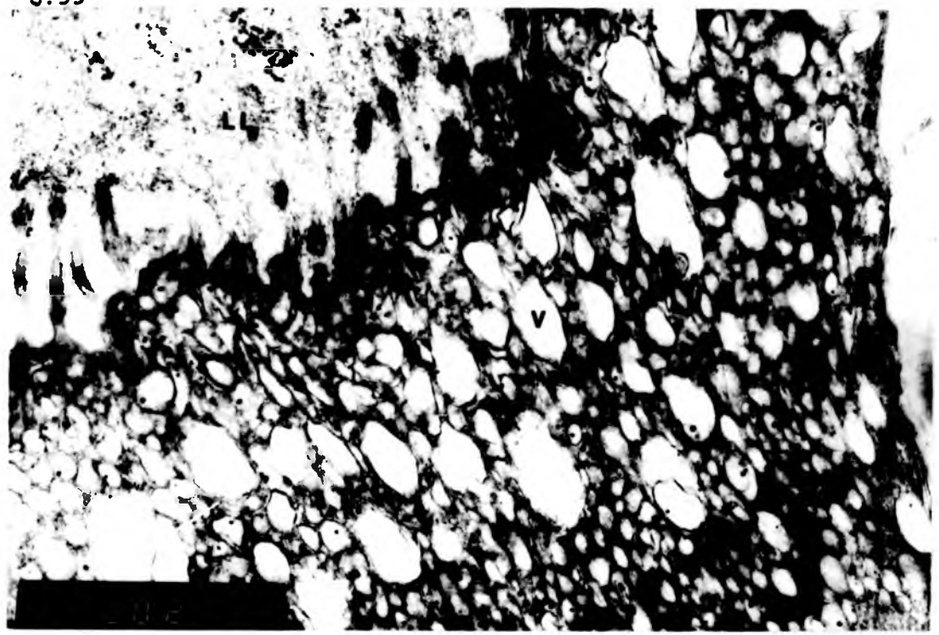

Fig. 8.54 TEM of a 10 month murine cyst from a mouse injected i.p. with 0.5ml of 20μM monensin daily. 60 days - detaching germinal layer. The tegumentary cytons possess large vacuoles (V) membraneous whorls (W) and mitochondria with abnormal cristae (M). N; nucleus, D.C.; distal cytoplasm. X14,200

8.54

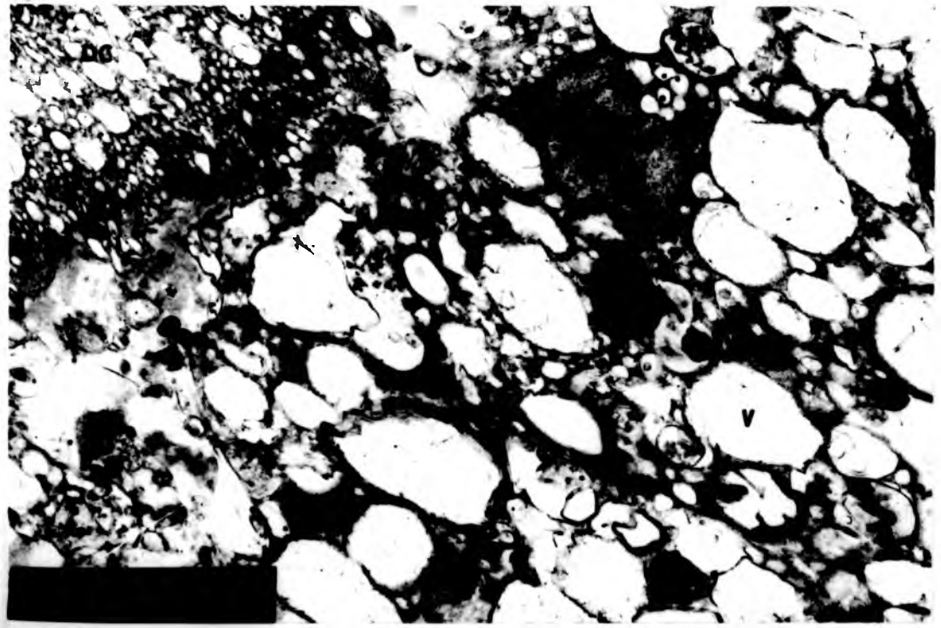

Fig. 8.55 TEM of a 7 month murine cyst from a mouse gavaged with 0.25mg monensin daily. 10 days - pitted cyst. The vesicles (V) of the distal cytoplasm are irregular in shape and enlarged mitochondria (M) are present at the base of the distal cytoplasm. Note the pitted region (star) where the germinal layer has detached from the laminated layer (LL). X39,100.

8.55

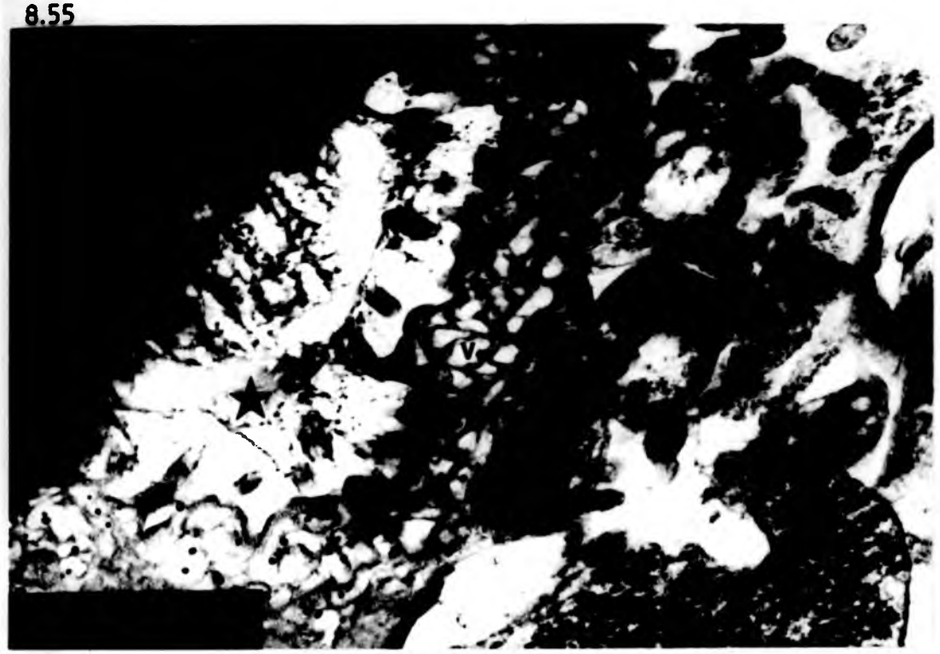

Fig. 8.56 TEM of a 7 month murine cyst from a mouse gavaged with 0.25mg monensin daily. 10 days - pitted cyst. Tegumentary cytons showing large areas of degenerated tissue (D) and enlarged mitochondria (M). X20,500.

8.56

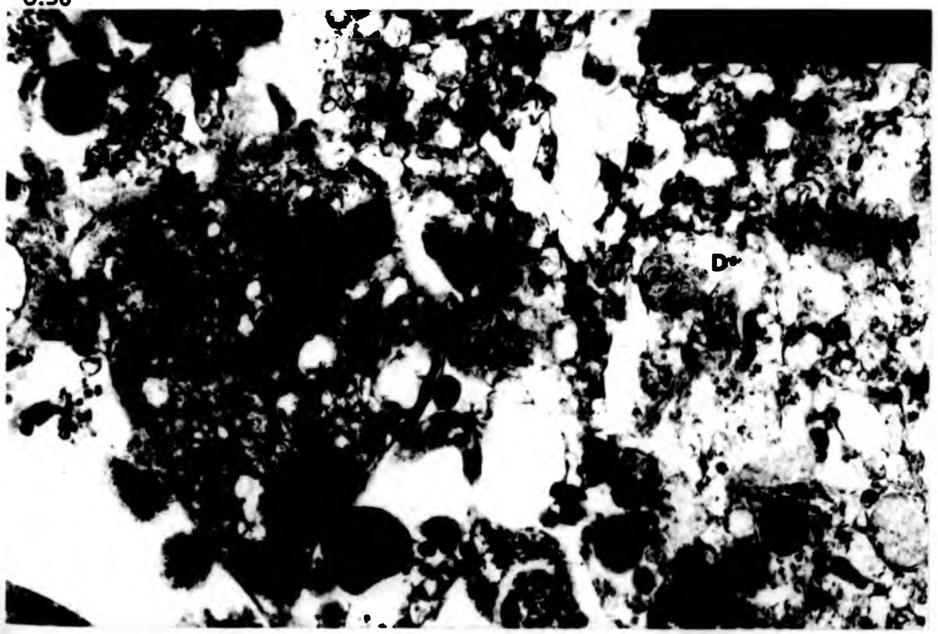

Fig.8.57 TEM of a 12 month murine cyst given 1.5-3.0mg monensin daily in feed. 25 days - pitted cyst. The distal cytoplasm is relatively normal but possesses some swollen vesicles (V). LL; laminated layer. X14,200.

Fig. 8.58 TEM of a 12 month murine cyst given 1.5-3.0mg monensin daily in feed. 49 days - cyst with detached germinal layer. The tegumentary tissue is clearly degenerated and possesses large vacuoles (V) membraneous whorls (W) and swollen mitochondria (M). Note that the distal cytoplasm (DC) is no longer attached to the laminated layer. N; nucleus. X11,000.

8.57

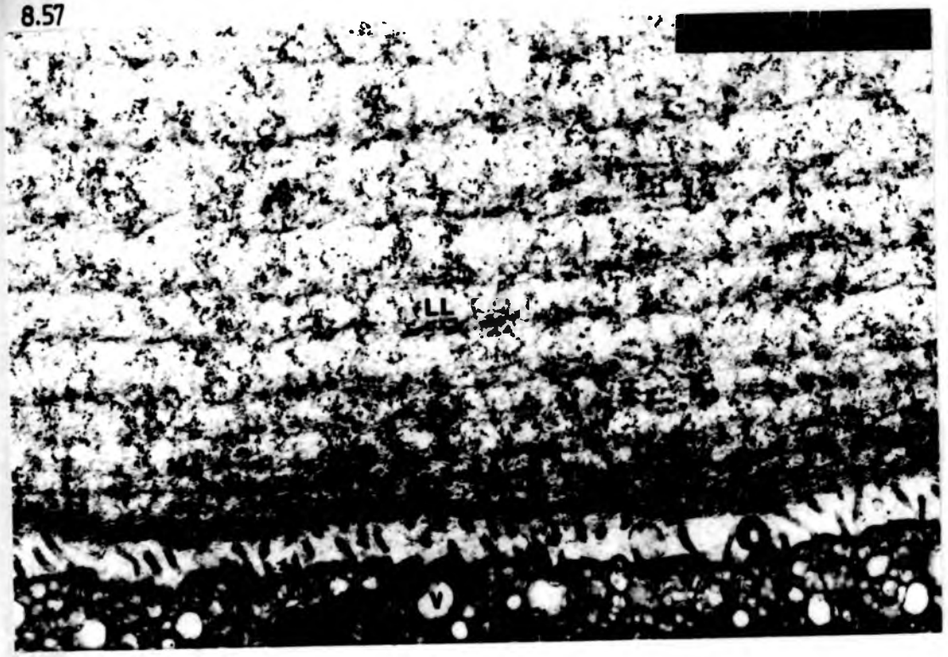

8.58